Australian Government

Australian Grape and Wine Authority

THE UNIVERSITY OF ADELAIDE AUSTRALIA

Integrating the carbon and water economies of grapevine for optimal management in challenging environments

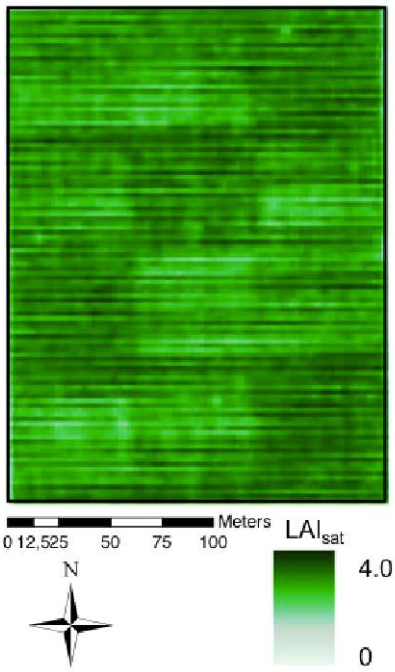

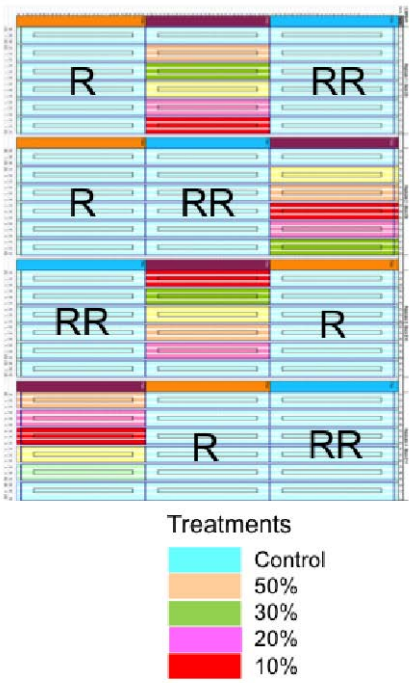

FINAL REPORT to

AUSTRALIAN GRAPE AND WINE AUTHORITY

Project Number: **UA 08-03**

Principal Investigator: **Professor Stephen D. Tyerman**

Research Organisation: **University of Adelaide**

Date: 21 December 2015

Report on:

Integrating the carbon and water economies of grapevine for optimal management in challenging environments

Project UA 08-03

2008-2013

Prepared by: Professor Stephen D. Tyerman

21 December 2015

School of Agriculture, Food and Wine
Plant Research Centre
Adelaide University, Waite Campus
PMB #1, Glen Osmond
SA 5064
P: +618 8303 6663
steve.tyerman@adelaide.edu.au

Cover image: (a) Growth distribution map, depicting Leaf Area Index (LAI_{sat}) obtained from satellite imagery (World View 2) (season 2010-11). (b) Corresponding irrigation trial design at the Oxford Landing estate for season 3 (2010-11). Light blue = Control irrigation (5 ML/ha/year), orange= 50% of control, green= 30% of control, yellow= 30% of control with deficit, pink= 20% of control, red= 10% of control, R = vines in recovery for one year after being submitted to two years of irrigation treatments, RR = vines in recovery for two years after being submitted to one year of irrigation treatments.

Table of Contents

1. Abstract

Chardonnay on Ramsey rootstock was studied for its long-term responses in physiology and productivity to prolonged sustained deficit irrigation (SDI) and recovery for various periods in a warm climate at Yalumba's Oxford Landing Estate near Qualco, South Australia. Irrigation rates (varied frequency or depth in one case) were 10%, 20%, 30%, 30%D (reduced depth), 50% and 100% of normal industry rates corresponding to between 12% and 82% of ETc on average over four seasons. SDI of 10% resulted in moderate effects on leaf physiology, with net CO_2 assimilation dropping by about 50% and closely linked to stomatal conductance. This was independent of the consecutive year of SDI, and recovery in most cases occurred within the subsequent season of full irrigation. Stomatal conductance and midday stem water potential were good measures of the degree of vine water stress. Prolonged SDI and recovery resulted in a moderate decrease in yield (about 50% at 10% SDI) largely due to reduced berry weight. This shifted vine balance into a state of overcropping based on the ratio of yield:pruning weight. Increased juice pH with increasing deficit would potentially reduce wine quality. These changes were independent of the number of seasons of deficit. Recovery of yield after one year of 10% SDI could take up to three seasons and after longer periods of SDI, vines had smaller trunks and therefore reduced total carbohydrate reserves that may compromise resilience. Trunk carbohydrate concentration at budburst was correlated to yield across seasons and in response to SDI, but there was no effect on trunk carbohydrate concentration in dormancy. Despite up to four seasons of SDI as low as 10% of control irrigation, only very limited effects were seen on the vine root systems. As SDI increased, from 50% to 10%, fine root surface area decreased to approximately 60% at 10% SDI. New methods of measuring vine water stress were developed using near infrared reflectance spectroscopy (correlated to vine water potential) and thermal imaging of canopies (correlated to stomatal conductance). Canopy leaf area index and porosity are shown to be accurately measured using a cover photography method that has recently been developed into an iPhone app.

Abbreviations: SDI sustained deficit irrigation**; LWP** midday leaf water potential; **SWP** midday stem water potential; **PDWP** pre-dawn leaf water potential; **g** leaf conductance; $\mathbf{g_s}$ stomatal conductance; **A** leaf net CO_2 assimilation; **E** leaf transpiration rate; **NIR** near infrared; **PCA** principal component analysis; **PC** principal component; **PLS** partial least squares regression; **PRESS** prediction residual error sum of squares; **R** coefficient of correlation in validation; **RWC** relative water content; **SECV** standard error in cross validation; **SD** standard deviation; **WUE** water use efficiency; $\mathbf{WUE_i}$ instantaneous water use efficiency = $\mathbf{A/g_s}$ **; NSC** non-structural carbohydrate; **LAI** Leaf area Index; $\mathbf{ET_c}$ crop evapotranspiration; **ANOVA** analysis of variance; **TSS** total soluble solids; **TA** titratable acidity; **GDD** growing degree days (taken with base ten degrees centigrade); **MJT** mean January temperature

2. Executive summary

Changes in global climate and decreased water availability over the past 20 years in Australia have prompted research into the short and long term effects of environmental stresses on grapevines and their resilience to those stresses. The long-term effects of water stress on grapevine physiology and productivity and in particular on the way carbohydrates are assimilated and stored in the plant are still not well understood. Furthermore there are no studies to date that have examined in detail the recovery process after long term deficit irrigation. The main objectives of this project were to: i) characterise the impact of significant reductions in irrigation on vine physiology and productivity over a 3-4 year time frame, ii) determine the way water and carbon economies of the grapevine are integrated under these conditions, iii) obtain information on the physiology of vines in recovery after severe water stress has been applied and conditions revert to normal, iv) develop new vine stress monitoring tools.

The main field study comprised six irrigation regimes imposed on mature Chardonnay vines on Ramsey rootstock, growing in a warm to hot semi-arid environment. The irrigation regimes consisted of Control (100%) (approx. 5ML ha^{-1} $season^{-1}$ typical for the region) and reductions to 50%, 30%, 20% and 10% from the control, which constitute sustained deficit irrigation (SDI). The reduction consisted of reduced frequency of irrigation rather than reduced depth at each irrigation event. Normal irrigation was provided up until fruit-set. One treatment included a reduced irrigation depth but same frequency as controls (30%D). After the 2008-09 season, one section of each irrigation treatment was restored to control irrigation levels in order to study the recovery after reduced irrigation. Vine water stress and gas exchange were monitored at key stages in addition to standard berry development, berry composition, yield and yield components during the trial. Trunk, leaf and root samples were collected at key stages to be analysed for non-structural carbohydrate (NSC) concentration. Mini-rhizotron tubes were installed to examine the dynamics of root growth.

Over the course of four seasons the 10% and 30%D treatment caused the greatest degree of physiological stress, and when recovery was not attained in the first season of full irrigation, it was more likely to be observed within the following season or after more consecutive seasons of SDI i.e. more than one season of deficit resulted in longer recovery times. Stomatal conductance was generally the most sensitive parameter. With respect to the levels of SDI and their absolute effects on vine physiology, often the 50% and occasionally the 30% treatments showed only small reductions in leaf water potential and leaf gas exchange. This would indicate that this level of SDI would have only minimal effects on vine physiology. Of all the SDI treatments, the 20% treatment appeared to give the optimum stomatal conductance and net carbon dioxide assimilation suggested by previous research for optimal grape quality, but leaf water potentials were often more negative than observed in the other treatments, suggesting that the 30% treatments may be a safer option as a target based on leaf physiology.

For vine yield there was a trend over three seasons of SDI for yield to recover towards that of the control. After return to 100% irrigation there appeared to be an over-compensation effect with higher yields in the fourth season of recovery. Recovery was not as evident in the pruning weights for the low SDI (10%, 20%, 30%D) but may occur for the 30% and 50% SDI. A conservative estimate for complete recovery of yield after one year of SDI would be in the third season of full irrigation, but recovery can occur earlier for less extreme SDI. Leaf area index (LAI) did not fully agree with pruning weight in that LAI did not show any difference in recovery kinetics between 10%, 20%, 30% and 30%D SDI, however for 10% SDI both LAI and pruning weight recoveries were in agreement. It should be noted that the 2008-09 season had a low effective rainfall during the growth season compared to the following three seasons in which recovery after one year of SDI was examined. Therefore, we have examined one scenario where the SDI year was more extreme and the recovery years less extreme in terms of total water applied.

For three out of four seasons (2008-09, 2010-11, 2011-12) the linear relationship between yield and irrigation plus effective rain were not significantly different and across all years the slope of the regression lines are not significantly different, providing a common slope of 0.014 kg vine^{-1} mm^{-1}. This translates to 21.1 kg ha^{-1} mm^{-1} or 2,108 kg ha^{-1} ML^{-1} gained in yield per hectare for every mm or ML total water (rain plus irrigation) applied respectively. Note that this is the incremental water productivity and not the absolute water productivity since the regression lines do not intercept at the origin. So for example, for 2008-09, 2010-11 and 2011-12 seasons the absolute water productivity at 200 mm of total water applied was 7.2 tonne ML^{-1} ha^{-1}. This probably indicates that vines had access to a stored water source perhaps deeper in the profile or from winter rainfall. However, the main determining factor for yield was the total water applied in any season, irrespective of the number of seasons prior where water applied was above or below the average. The main yield components affected by SDI were berry weight and bunch weight, with bunches per vine and berries per bunch generally not affected by SDI. The recovery information may suggest a strategy for handling reduced irrigation allocations, i.e. one year at 10% SDI followed by one year at 50%, potentially allowing reasonable yields and quality over a several-year time frame. This "year-to-year pulsed-SDI" strategy may also condition vines for SDI in the future.

Generally there was no effect of SDI on the rate of evolution of berry weight, TSS, pH or TA despite there being significant differences between treatments in initial and final levels of these parameters. For the first two seasons comprising one and two years of SDI, there were significant interactions between time and treatment for sugar accumulation on a per berry basis indicating that sugar accumulation per berry was decreased under increased deficit. Overall, juice pH (increased with deficit) and sugars per berry (decreased with deficit) were the most sensitive berry compositional characters that in some cases revealed a carry-over effect from previous years of SDI into the recovery seasons. However, it was surprising that successive seasons of reduced irrigation gave the same characteristics of the effects of total water applied on pH, indicating that if carry-

over occurred from previous deficits this did not change significantly the response in juice pH to total water received by the vines.

Reduced irrigation had a significant impact on trunk carbohydrate storage in the immediate post-harvest period, and sugar concentration in the trunk was negatively correlated with the previous yield both across seasons and within a season. There was no effect of SDI on NSC at dormancy, yet yield could be predicted from the NSC concentrations in vine trunks at budburst that responded both to SDI and other variables. Recovery of NSC concentration in the trunk appeared to be complete after one season after successive seasons of the 10% SDI, but total trunk capacity to store carbohydrate is reduced substantially due to reduced growth under SDI over four years. There was an interesting asymmetry in trunk growth with larger diameter in the direction of the vine row that was associated with the 10% SDI that could indicate the direction that roots grow within the row. Fine roots had higher carbohydrate storage than trunks but data were limited due to measurement difficulties. Leaf carbohydrate was dependent on phenological stage but was not affected by SDI.

Taking advantage of the expertise we gained in the project using near infrared (NIR) spectroscopy (see below) we also investigated whether NIR could be used to predict starch and NSC concentration in freeze-dried and ground grapevine trunk and leaf tissues. We demonstrated that a robust universal model could be applied to the prediction of TNC in both leaves and trunks, making it a practical tool for a rapid screening of TNC concentration in grapevine tissues at given phenological stages. The advantages of this method are the speed of the analysis (less than 30 seconds required for the spectrum to be collected) and the elimination of the use of chemical reagents. Monitoring the spatio-temporal distribution of TNC concentration with NIR will help management decisions based on the data we provide on critical stages for measurement.

We also examined the dynamics of root growth in the major field trial. Mini-rhizotron tubes were installed in three of the irrigation treatments (30%, 50% and 100%) and imaging was undertaken for the final three years of the five, providing data for a) the third year of SDI, b) the first year of full irrigation following three years of SDI, c) a fourth year of SDI, d) the second year of full irrigation following three years of SDI and e) the first year of full irrigation following four years of SDI. Mini-rhizotron imaging was matched with bi-annual soil coring, from which roots were extracted and root length and dry mass determined. Fine root dry mass (0.6 to 0.8 kg m^{-3}) demonstrated intra- and inter-seasonal differences. Root length density was not significantly different between seasons, averaging 4.5 km m^{-3} at veraison from the same samples. Over-wintering fine root length and biomass were reduced by SDI, with the effect increasing with increasing deficit. The impact at veraison was less, with reductions not significant. The data also indicated a greater proportion of new roots was present each season under SDI than under control irrigation, which matched the observation from the cores that SDI effects on root length were present in winter, but not during the growing season. Despite up to four seasons of deficit irrigation as low as 10% of control irrigation, only very limited effects were seen on the vine root systems. These results demonstrate the resilience of

the root system when faced with soil water stress and the ability of the vine to increase the resource allocation to the root system under these circumstances. The mini-rhizotron system also demonstrated the remarkable longevity of fine roots in this vineyard of Ramsey rootstock in sandy soils in a hot climate.

For tools to rapidly monitor vine water stress we focussed on three techniques: Near infrared (NIR) spectroscopy, infrared (Thermal or IR) imaging and canopy imaging to measure leaf area index. These are expanded upon below:

NIR spectroscopy was evaluated as a method to estimate water potential of grapevines. Cabernet Sauvignon, Chardonnay and Shiraz leaves were scanned using an Integrated Spectronic or an ASD FieldSpec® 3 (350-1850 nm) spectrophotometer and then measured to obtain leaf and stem water potentials using a pressure chamber. Calibrations were built and NIR showed good prediction ability for stem water potential for the three grapevine varieties and for the two seasons studied. The best calibration was obtained for the prediction of stem water potential in Shiraz (R= 0.92 and a SECV= 0.09 MPa). Differences in the NIR spectra were related to the leaf surface from which the spectra were collected, and this had an effect on the accuracy of the calibration results for water potential. However we demonstrated that NIR can be used as a simple and rapid method to detect grapevine water status. The advantages of this new approach are speed and low cost of analysis. It would be possible for NIR to be used as a non-destructive, in-field tool for irrigation scheduling.

Thermal imaging of crop canopies has been proposed more than a decade ago as a sensitive methodology to determine water status of different crops. However, this technique has not been fully applied for irrigation scheduling purposes mainly due to a lack of consensus in the adequate use of the technique for different crops. We developed an automated methodology using MATLAB® programming techniques to analyse infrared thermal images taking into consideration the pitfalls pointed out previously in the literature. The proposed method was tested in the reduced irrigation and recovery trial for Chardonnay in the 2010-11 season, and in the 2009-10 season from seven varieties. There was a clear separation (assessed by principal component analysis) between control and recovery compared to stress treatments using stomatal conductance and stem water potential, and indices derived from canopy temperatures measured by infrared imaging. High and significant correlations were found between canopy temperature indices and other measures of water stress obtained in the same vines that were independent of leaf area index. Results have shown that the automated analysis of infrared thermal images is a suitable method to rapidly obtain critical information of grapevine water status for irrigation scheduling purposes.

Monitoring of canopy vigour is an important tool in vineyard management to obtain balanced vines (vegetative vs reproductive organs) and to monitor seasonal water deficits. Leaf area index is the main parameter representing canopy vigour. We tested an automated computational method to obtain leaf area index and canopy vigour parameters from grapevines with digital photography and video analysis using MATLAB programming techniques for

rapid data uptake and gap size analysis. A temporal and spatial assessment of the method was tested in the sustained deficit and recovery experiment and these data were geo-referenced and compared to the normalised difference vegetation index extracted from the WorldView-2 satellite images at a 2 m^2 per pixel resolution. The maximum leaf area index data obtained with cover digital photography and video analysis are an accurate, cost-effective and easy-to-use method to estimate spatial and temporal canopy LAI and structure when compared to standard measurements (allometry and plant canopy analyser). We demonstrated that the method proposed is an accurate and inexpensive tool for application in experiments and by the industry to monitor spatio-temporal distribution of vigour.

This project has met all the primary objectives and has provided:

- Valuable information on vine water relations and leaf gas exchange during prolonged SDI and recovery indicating that despite moderate effects on leaf physiology, recovery from SDI is relatively rapid and that stomatal conductance is a good measure of the degree of vine water stress.
- Yield, yield components and berry composition as affected by prolonged SDI and recovery indicate that Chardonnay on Ramsey rootstocks growing in a warm dry climate can tolerate down to 10% of normal industry irrigation rates (average of 12% of ETc) for up to four seasons (depending on rainfall) and still survive and be potentially recovered for normal productivity. However, recovery of productivity could take up to three seasons after one year of SDI at 10% and prolonged SDI resulted in poor vine balance towards overcropping.
- A better indication of rates of irrigation that could save significant quantities of water. For example, 50% SDI showed little difference to 100% and could be used more routinely without significant effects on productivity for Chardonnay on Ramsey rootstock.
- Information on the best strategy for saving water during periods of water shortage or increased water costs. For example, it would not be recommended to reduce the depth of irrigation since this option resulted in greater vine stress and greater reduction in vine productivity compared to the equivalent amount of irrigation at reduced frequency.
- Vine carbohydrate dynamics that can be predictive of yield across seasons and in response to SDI.
- Root growth dynamics under SDI and recovery that indicate their important role in the overall response of the vine and the remarkable resilience of Ramsey rootstock to water deficits.
- New methods for rapidly assessing vine water stress in a field context using NIR, IR imaging, and canopy digital imaging.

3. Background

The Australian wine industry was facing an unprecedented challenge to maintain wine production and quality in the millennium drought from 1995-2009. This was a severe, immediate challenge, but climatic prediction indicates that such events will become more frequent and will occur against a backdrop of increasing temperature and evaporative demand, and quantitative and qualitative deterioration of water resources (http://www.bom.gov.au/climate/updates/articles/a010-southern-rainfall-decline.shtml). There has been considerable R&D to improve crop water use efficiency that accounts for secondary effects such as soil degradation and salinisation, but a major gap in our knowledge restricting our ability to offer clearer alternatives to industry under current conditions and future scenarios is in the longer term effects of such stresses on vines. This is critical to decision making and is determined by the ways in which carbohydrate is allocated in the vine under a range of environmental stresses. Water and carbohydrate are closely linked through photosynthesis and transport within the vine. How carbohydrate is allocated for storage, root growth and fruit production ultimately determines the resilience of the vine and its ability to recover and produce a crop in the subsequent years. This was highlighted in a GWRDC funded workshop on carbohydrate allocation (Walker and Winter, 2006, GWRDC Report). Carbohydrate allocation determines the future production capability of vines that have been induced into survival mode and the exploitation of soil water reserves through changes in root architecture. This project sought to address these shortcomings by developing new tools to help in assessing vine performance under stress and determining the way water and carbon economies of the grapevine are integrated.

Key elements in the success of survival mode strategies is to have (i) excellent vine monitoring tools and better knowledge of vine carbohydrate allocation, and (ii) models linking carbohydrate allocation, survival and future performance. The project focused on developing better tools for vine stress measurement using Near Infrared Reflectance spectroscopy (NIR), thermal imaging (Infra Red, IR) techniques and sap flow sensors that allow more integrated whole of vine block measurements. Modeling the associations of plant physiological status, including amount and distribution of reserve carbohydrates, and its consequences for survival and future performance is a very complex issue, as many interacting factors would contribute to the final outcome (e.g. variety, rootstock, irrigation method used for crop establishment, water quality). Nonetheless, the circumstances towards the end of the millennium drought offered a unique opportunity to assess survival mode options under restricted irrigation and subsequent recovery and this has allowed us to develop some of the fundamental building blocks for future models, and better tools and strategies to minimise the impact of low water applications.

This report is comprised of nine main results chapters, some of which are published papers, that address the carbon and water economy of vines subjected to long term reduced irrigation and recovery (Chapters 6.1 to 6.5), and new tools for monitoring vine carbohydrate status, water status and canopy growth

(Chapters 6.6 to 6.9). Chapters 6.7, 6.8 and 6.9 are presented as the published papers.

Thus the two major components of this project were:

1. The *Reduced Irrigation and Recovery Trial* was largely undertaken at the Yalumba Oxford Landing site in the Riverland on mature Chardonnay vines (details below in Methods). Here measures of vine productivity (yield and yield components), carbohydrate dynamics, root growth and physiology (photosynthesis, water use and water relations) were made in order to determine the impacts of different deficit irrigation levels and the effects of duration (seasons) on recovery.

2. *New tools for monitoring vine function under water stress and recovery using NIR and IR technology* was undertaken at a number of sites including preliminary experiments at the Coombe vineyard (34°58'3.47"S; 138°38'0.43"E) at the University of Adelaide, then mainly at the Oxford Landing site in the *Reduced Irrigation and Recovery Trial*, and in the Project Extension, more commercially oriented trials were begun with Treasury Wine Estates (TWE) at Wynns Coonawarra Estates.

4. Project Objectives, Outputs and Performance targets

4.1 Objectives

Initial project (2008-2011)

1. Develop and refine new NIR and thermal imaging (IR) techniques to monitor vine and berry health and response to stress. This will help further development and practical implementation of our findings to assist with both crop management under extreme drought and crop management for yield, berry and wine quality under recovery from stress.
2. Characterise the impact of severe water stress on vine physiology, with emphasis on whole grapevine transpiration, carbohydrate allocation and roots development. Integration of genetic, environmental and management drivers of crop survival and future production are required for effective management of crops during and after severe stress episodes.

Extension (2012-2013)

3. The principal objective is to quantify irrigated grapevine response and recovery to various durations and degrees of water stress. The project extension will provide knowledge on longer-term effects of both deficit and recovery that will greatly enhance the range of scenarios to which the project outcomes can be applied. This will enable effective decision making by grapegrowers faced with changing irrigation allocations and policy makers faced with determining those irrigation allocations.

4. Characterise the recovery of vine physiology, growth and production from severe water stress, with an emphasis on integration of whole grapevine transpiration, carbohydrate allocation and root system development. Integration of genetic, environmental and management drivers of crop survival and future production are required for effective management of crops during and after severe stress episodes.
5. Develop and refine new Near Infrared Reflectance Spectroscopy methods to rapidly measure vine water stress and carbohydrate allocation.
6. Develop multi-seasonal irrigation strategies for grapegrowers on managing reduced irrigation allocations in conjunction with policy recommendations on drought allocations.

4.2 Outputs and Performance Targets (2008-2011)

Outputs and Performance Targets 2008-09

Outputs	Performance Targets
1. Industry advisory group formed	Industry representatives agreed to collaborate with the project on an advisory role
1. Research staff appointed	2 x research staff appointed, in addition to UA postdoc and CSIRO PhD studentship
2. Field sites and trials fully established	At least two contrasting field sites established with vines on rootstocks.
3. NIR equipment, sap flow sensors plus dataloggers and mini-rhizotron equipment specified.	Equipment purchased.
4 Assess the feasibility of NIR for the determination of water potential and other parameters in leaves and continue the development of IR for determination of canopy conductance. Conduct trials of those applications determined to be feasible for vineyard application.	Calibrations available for key varieties.
5. Information on vine health indicators in 2 year stressed vines at key phenological stages after one year of recovery	Results on vine health indicators available
6. 2-3 yrs field data available	Industry update on trial outcomes from first 2 years.

Outputs and Performance Targets 2009-10

Outputs	Performance Targets
1. Information on physiology of vines in recovery	Data available
2. Information on correlations between carbohydrate storage, vine health indicators and phenology and fertility related to past water stress history.	Correlation data examined and available
3. Prepare technical notes on the application of NIR and IR techniques as plant performance indicators, with details on standard procedures for processing and sample handling.	Technical notes available
4. Dynamics of root growth for water stressed vines and estimation of carbohydrate allocation to roots and other vine components.	First season of data available
5. Wine made from 2 –year stressed vines.	Wine available for sensory analysis
6. 3 yrs field data available	Industry update on trial outcomes from first 3 years.

Outputs and Performance Targets 2010-11

Outputs	Performance Targets
1. Publications on vine carbohydrate dynamics and stress history	Publications in refereed journals
2. Development of relationship between carbohydrate storage, berry sugar accumulation and water stress history.	Model components identified
3. Publish and communicate (e.g. refereed journal/ industry journal), papers describing the application of NIR and IR for measurement of water potential and conductance in leaves.	Second season of calibration data, combined with water stress monitoring
4. Information available to industry on scenarios arising from drought induced vine stasis.	Presentation to industry forums

4.3 Project Extension Outputs and Performance Targets (2011-2013)

Outputs and Performance Targets 2011-12

Output	*Activities*
Knowledge on long-term effects of water deficit and 1 yr recovery on vine physiology.	*Leaf gas exchange, water potentials, sap flow and carbohydrate allocations measured at key phenological stages.*
Knowledge on long-term effects of water deficit and 1 yr recovery on growth and production.	*Leaf area index measures and trunk diameter during season 2011-2012. Berry maturity rate and yield components for harvest 2012.*
Knowledge on long-term effects of water deficit and 1 yr recovery on root system development.	*Mini-rhizotron measures of root development at key phenological stages in season 2011-2012.*

Outputs and Performance Targets 2012-13

Output	*Activities*
Integration of 4 years of field data during water stress and various periods of recovery.	*Data analysis across all 4 years of physiology, growth and yield measurements to extract treatment effects from seasonal differences.*
Near Infrared Reflectance Spectroscopy methods to rapidly measure vine water stress and carbohydrate allocation.	*Calibrations for NIRs for carbohydrate analysis on extracted vine material and other indices of water stress/gas exchange in leaves.*
Industry update on trial outcomes from 4 years.	*Technical article written for industry journal.*
Knowledge on long-term effects of water deficit and 2 yr recovery on vine physiology.	*Leaf gas exchange, water potentials and carbohydrate allocations measured at key phenological stages.*
Knowledge on long-term effects of water deficit and 2 yr recovery on growth and production.	*Leaf area index measures and trunk diameter during season 2012-2013. Berry maturity rate and yield components for harvest 2013.*

Outputs and Performance Targets 2013-14

Output	*Activities*
Integration of 5 years of field data during water stress and various periods of recovery.	*Data analysis across all 5 years of physiology, growth and yield measurements to extract treatment effects from seasonal differences. Analysis of relationships between carbohydrate storage, berry sugar accumulation and water stress history.*
Industry update on final trial outcomes from 5 years.	*Presentations and workshop at 15th AWITC, plus publications in wine industry journals.*
Innovators Network material developed.	*Innovators Network material on 'recovery from drought' developed in consultation with the GWRDC.*
Final report to GWRDC	*Final analysis of outcomes and options for multi-seasonal irrigation strategies for grapegrowers on managing reduced irrigation allocations. Policy recommendations on drought allocations.*

5. Methods: *Main field trial site*

Detailed methods will be provided in each Chapter. Here we provide a description of the primary trial site for the study.

5.1 Yalumba Oxford Landing: Reduced Irrigation and Recovery Trial Structure

In collaboration with Yalumba Nurseries a restricted volume irrigation trial was established in mature Chardonnay grapevines grown at Oxford Landing near Qualco, SA (34° 6'0.76"S; 139°50'55.76"E). The soil consists of 5-25 cm topsoil of a loamy-sand, and the subsoil is sandy loam to loamy-sand. There has been no water table within 3.5 m of the surface, and irrigation water salinity at nearby Hogwash Bend ranged from 160-673 dS/m.

Chardonnay vines (nine years old) grafted on Ramsey rootstock were trained on a two wire vertical trellis system with a vine spacing of 1.8 m between vines and 3.05 m between rows. Cordon height was 1.1 m and row orientation was aligned East-West. The irrigation reductions were applied for 1, 2, 3 and 4 irrigation seasons after which point the irrigation reverted to normal practice (Control) to assess grapevine recovery. In the 2007-08 irrigation season before the trial began, all vines in the trial received 4.77 to 4.83 ML/ha of irrigation.

The whole trial was established in 60 rows made of 92 vines each, covering a total area of 3.68 ha. The trial design was 'strip-plot', with four blocks (replicate), each containing six irrigation treatments that covered three entire rows, each block consisting of 18 rows in total. Within a replicate, each treatment consisted of three rows and the rows were divided in three sections of 30 vines each. In the middle row of each treatment, the middle vine in each section was generally selected for measurements. The blocks were then split into three subplots, to allow irrigation treatments to be applied for one, two or three seasons before reverting to standard irrigation (referred to as 'year 1', 'year 2' and 'year 3' respectively). After three seasons each 'year 3' plot was split into two, to create a 'year 4' treatment, with a fourth season of irrigation treatments. For the fifth season, all sections were provided with standard irrigation. Figure 1 provides a diagram of the trial layout for year 1 (2008-09), year 2, year 3, and year 4.

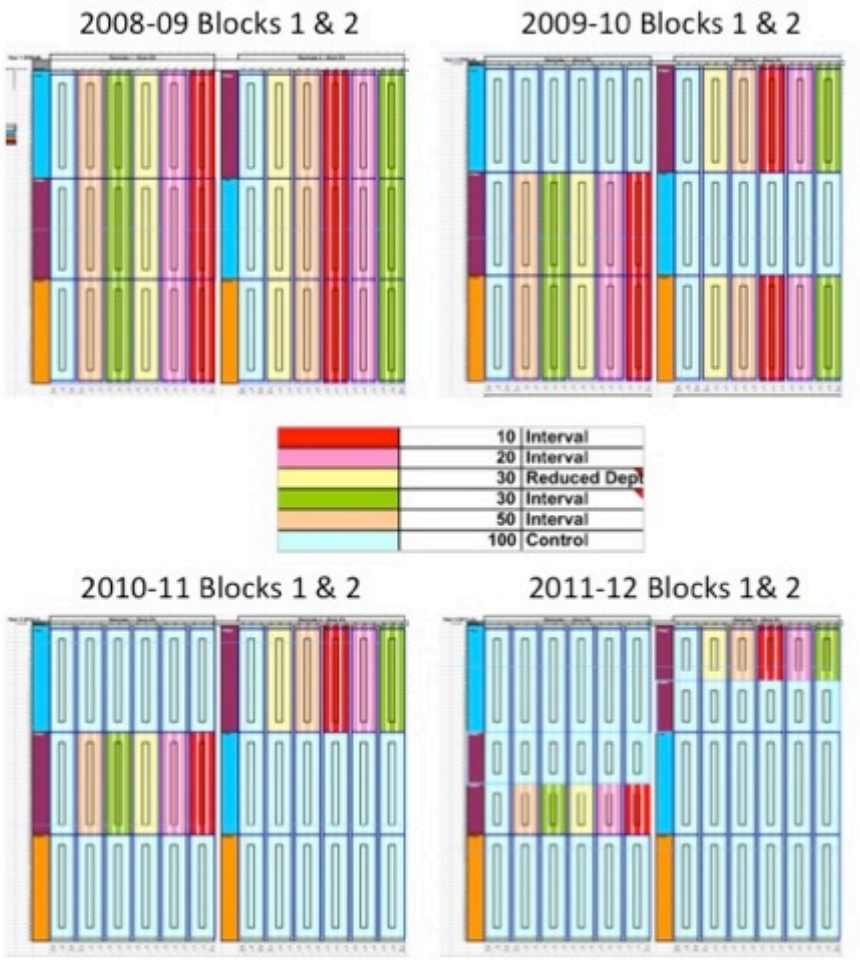

Figure 1 Trial design showing Block 1 and 2 only and illustrating how the sustained deficit irrigation (SDI) vines were returned to full irrigation over the four years. For the 2012-13 season all vines returned to full irrigation. The colour code in the middle of the diagram shows the SDI levels used.

The irrigation treatments were: Control (normal irrigation practices) and reductions to 50%, 30%, 20% and 10% of the Control. The irrigation volume applied at each irrigation event in these five treatments was the same hence to apply the reductions in irrigation, the interval between irrigation events was increased to achieve the lower amounts. All treatments were fully irrigated until fruitset. To further elucidate the best irrigation strategies under low irrigation conditions such as was current in the Riverland region of SA in 2008, an additional 30% irrigation treatment was included (30% D). This treatment was applied at the same frequency as the Control but for only 30% of the irrigation run time. This will determine if there was benefit in applying small irrigations at high frequency (30% D) or deeper irrigations at low frequency (30% I).

To deliver the six irrigation treatments totally independently of each other, a remotely accessed irrigation controller, five new submains and seven pulse flowmeters were installed at the site (Figure 2). All irrigation treatments were delivered in three row blocks and were separately programmable in the controller. Seven pulse flowmeters were installed to verify the irrigation

volumes applied were similar to those calculated in the irrigation schedule. All treatments were irrigated with Netafim Dripmaster pressure compensated in-line drippers with a 2.3 L h^{-1} of flow. All irrigation events were scheduled to apply 6 mm in 4 hr.

Figure 2 Installation of the irrigation controller, five new submains and pulse flowmeters.

An irrigation schedule was calculated by SARDI using the ICMS (Irrigated Crop Management Service) Seasonal Water Budgeting Tool. Yalumba staff scheduled the irrigation controller using this with minor modifications throughout the irrigation season. Each week, both SARDI and Yalumba staff were able to download and monitor the applied irrigation volumes calculated from scheduled hours and pulse flowmeter outputs. SARDI have entered the irrigation data into the ICMS, IRES (Irrigation Recording and Evaluation System) v3.0 to generate irrigation volumes per treatment. Two test-well sites were installed within the high and low contours of the trial site. Since installation in August 2008, both test-wells have remained dry to the bottom of the test-wells at 3.6m (low point) and 5.07m (high point).

5.2 Climate across seasons and irrigation rates

Table 1 provides a summary of the season climate data, rainfall, calculated ETc and treatments total irrigation for each season. Climate data were collected from an automatic weather station at the vineyard and from a SA Murray Darling Basin Natural Resources Management Board automatic weather station approximately 2km east of the trial site (SAMDBNRMB 2011). Rainfall was considered effective if >5mm was recorded within a 24-hour period.

5.3 Phenology

Table 2 provides dates for each season of key phonological stages.

Table 1 Summary of seasonal climate data, rainfall and calculated ETc and treatments total irrigations for each season.

Season	[a]GDD (°C day)	[b]MJT (°C)	[c]Effective Rain (mm, 1st Sept – 1st May)	[d]Total ETc (mm, 1st Sept – 1st May)	Treatment (% full irrigation)	[e]Irrigation (mm)
2008-2009[f]	2129	24.4	38.6	665.5	10 20 30D 30 50 100	90 131 185 176 262 525
2009-2010[f]	2331	23.8	169.2	649.1	10 20 30D 30 50 100	73 123 186 222 271 613
2010-2011[f]	1849	24.0	287.2	525.41	10 20 30D 30 50 100	88 109 166 223 276 509
2011-2012[g]	2084	23.6	144.2	596.325	10 20 30D 30 50 100	37 65 126 117 187 365
2012-2013[h]	2285	23.6	36		100	492

[a] Growing degree days subtracting a base temperature (10°C) from the average temperature recorded each day from 1 October to 30 April and then summating all values above zero.
[b] Mean January temperature.
[c] Effective rain is summation of rainfall between 1 Sept. and 1 May discounting all daily rainfall events less than 10 mm.
[d] Total crop evapotranspiration based on ETo (Tall) which is a recalculation for tall crops in arid environments and with the following crop coefficients: Sep. 0.3, Oct. 0.3, Nov. 0.5, Dec. 0.7, Jan. 0.7, Feb. 0.7, Mar. 0.7, Apr. 0.45. Note that ETc is probably underestimated for the lower rates in later years.
[e] Irrigation divide by 100 to get ML/ha
[f] Irrigation between 1 September and 1 May
[g] Irrigation between 1 September and harvest at end January
[h] Irrigation between 1 September and harvest at end February

Table 2 Dates for key phenology stages in each season of the study

Phenology stage	Season 1	Season 2	Season 3	Season 4
Budburst	8-Sep-08	6-Sep-09	30-Aug-10	3-Sep-11
Flowering	4-Nov-09	29-Oct-09	11-Nov-10	1-Nov-11
Veraison	7-Jan-09	30-Dec-09	3-Jan-11	29-Dec-11
17 °Brix	25-Jan-09	19-Jan-11	9-Feb-11	14-Jan-12

6.0 Results and Discussion

6.1 Effect of SDI and recovery on vine water relations and gas exchange.

Introduction

Alternative approaches to irrigation scheduling are based on the physiological knowledge of grapevine response to water stress. The most common direct sensing methods are of midday leaf water potential (Ψ_{leaf}), and stomatal conductance (Flexas et al., 2010). The pressure chamber technique of measuring Ψ_{leaf}, which is a destructive method, has been assessed in several cases for grapevine as a relatively simple and rapid measurement (Cifre, et al. 2005,Naor, et al. 1997,Sibille, et al. 2007,Tregoat, et al. 2002,Williams and Araujo 2002). Another method to assess water status is pre-dawn leaf water potential ($\Psi_{pre-dawn}$), which is thought to be a surrogate for soil water potential. Physiological thresholds in water potential and gas exchange characteristics have previously been suggested as being able to indicate the optimum level of deficit irrigation to achieve good water use efficiency, reasonable yields and good quality grapes for winemaking (Flexas, et al. 2010,Romero, et al. 2010). In this chapter we explore these characteristics that to date have not been examined over such a long duration of stress and during recovery.

We assess the more traditional aspects of gauging vine water stress over long periods of seasonal continuous deficit and recovery. In addition, the basic water relations and gas exchange responses provide us with potential physiological causes of yield reduction and reallocation of carbohydrates within the vine. This forms a backdrop to the following chapters on vine productivity responses to long-term deficits and recovery. There are no comparable studies that we are aware of that have investigated leaf water relations and gas exchange during recovery over seasons after long-term deficits. Short-term recovery experiments on potted vines are more common e.g. (Pou, et al. 2012). Though a long term recovery experiment has been conducted for saline irrigated vines (Stevens and Partington 2013) gas exchange data are not available. Another study investigated long-term deficits on Chardonnay productivity, but there are no data on leaf physiology (Williams 2014) or recoveries from deficit. The data presented here provide for the first time a comprehensive analysis of the long-term effects of drought and recovery on the physiology of field grown Chardonnay on Ramsey rootstock. It provides critical information on the physiological responses and key indicators of stress responses over the long term that can guide researchers and viticulturists in future drought response assessments.

Methods

Leaf and Stem water potential
Measurements of water potential (LWP midday leaf water potential; SWP midday stem water potential; PDWP pre-dawn leaf water potential); were performed on each vine studied using a Scholander type pressure chamber (PMS Instruments, Model 1005, Albany, OR. USA). For this purpose, a fully expanded

mature leaf was selected from each plant and bagged for at least 30 minutes for SWP before each measurement with a plastic bag coated with aluminium foil. No more than 30 sec elapsed between the leaf cutting and measurement of bagged leaves.

Gas exchange and leaf conductance measurements
Stomatal conductance (g_s), transpiration rate (E) and photosynthesis (A) were obtained using a portable Li-Cor 6400 gas exchange system (Li-Cor Environmental, Lincoln, Nebraska, USA). All Li-Cor measurements were obtained from two or more mature and fully expanded leaves from each plant per replicate. Photosynthetically active radiation (PAR) was set at a saturating level (2000 μmol m^{-2} s^{-1}) using the internal light emitting diode system and CO_2 concentration was regulated close to 400 ppm. The relative humidity of the sample stream and the cuvette air temperature were maintained at ambient values. Leaf g_s was also measured on some occasions using a non-steady state porometer (AP4, Delta-T Devices, Cambridge, UK) calibrated on site using the manufacturer's standard protocol.

Sap flow
Sap-flow probes were installed at 30 cm from the ground surface and wrapped with bubble wrap and aluminium foil to avoid influence from ground heat during the day. The sampling frequency was every 30 min. Sapflow measurements were performed using the compensated heat-pulse method. Heat-pulse sap flow sensors were supplied by Tranzflo New Zealand Ltd. (Palmerston North, NZ) and were connected to a CR23X data logger (Campbell Scientific, Logan, Utah, USA).

Vapour pressure Deficit (VPD) was measured using and aspirated psychrometer using wet and dry bulb temperatures to calculate VPD

Results and Discussion

A total of four seasons of measurements were made. These were Season 1 (2008-09), Season 2 (2009-10), Season 3 (2010-11), and Season 4 (2011-12). The trial was designed so that deficits were applied for up to four continuous seasons and in each season a subset of vines would be returned to control (normal) irrigation. Thus in Season 1 all vines (except control) were subjected to the deficits. Season 2 had some vines in recovery after one year of deficit, season 3 had some vines in recovery for either 2 years (after 1 year of deficit) or 1 year of recovery after 2 years of deficit and so on. The results for gas exchange and water relations presented below will therefore be examined in order of each season of measurement. Subsequently combined data for all seasons will be analysed.

Season 1
In this season the primary aim was to ensure that the deficit irrigation treatments were having the desired effect on vine physiology and that we could detect changes in leaf and stem water potential, and gas exchange that would reflect the water stress treatments.

Figure 1 shows assimilation (A, Figure 1a), stomatal conductance (g_s, Figure 1b), evaporation (E, Fig 1c), and A/gs (intrinsic water use efficiency, WUEi, Figure 1d) measured on two occasions using IRGA on leaves during 2008 when the deficits were imposed. The left hand panels show all the treatments early in the season, while the right hand panels are measured near flowering for the 20%, 50% and Control treatments. Even at this very early stage in the trial g_s and E decline with reduced irrigation and more significantly than A, and consequently there is an increase in WUEi with deficit irrigation (bottom panels). WUEi is very stable in controls across the season. Measurements on a subset of the treatments on three occasions during the season (Figure 2a, b, c, d for A, g_s, E and A/gs respectively) showed that the 30% D (reduced depth of irrigation but same frequency as controls) treatment showed a greater degree of physiological stress (lower g_s) later in the season compared to 30% (reduced frequency of irrigation). WUEi is again shown to increase in the 30%D and 10% especially later in the season (bottom right hand panel).

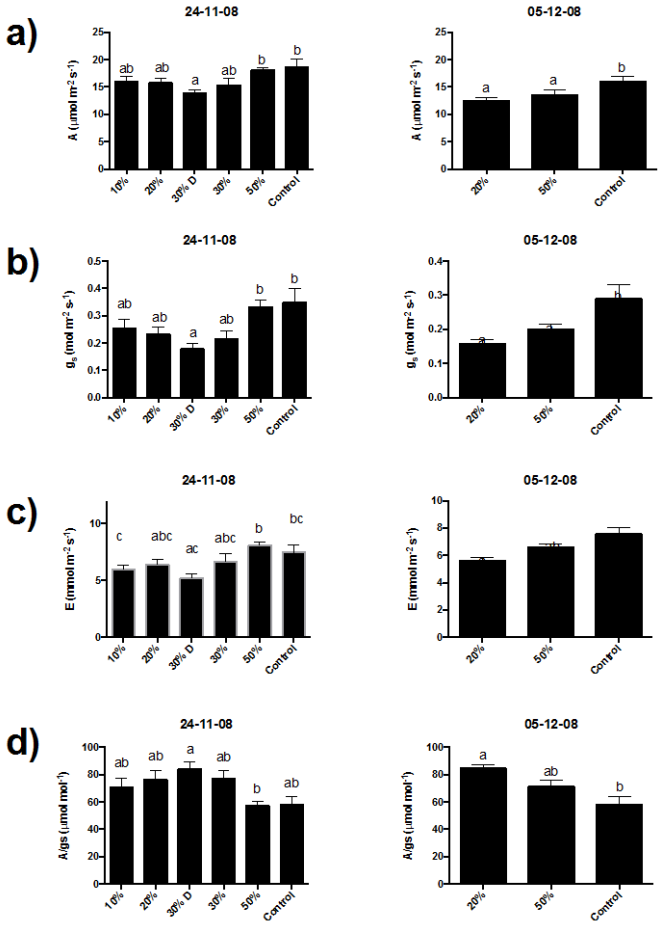

Figure 1 Gas exchange characteristics for the first year of the deficit irrigation trial at Oxford Landing. a) Net Assimilation (A), b) stomatal conductance (g_s), c) transpiration (E) and d) intrinsic water use efficiency WUEi (A/gs) are shown from top to bottom. All treatments were measured on one occasion early in the season (10 days after flowering), and then on a subset of the treatments pre-veraison (dates indicated). Different letter combinations indicate significant differences ($P<0.05$, ANOVA, Holm-Sidak's multiple comparisons test). Error bars = mean +/- SEM.

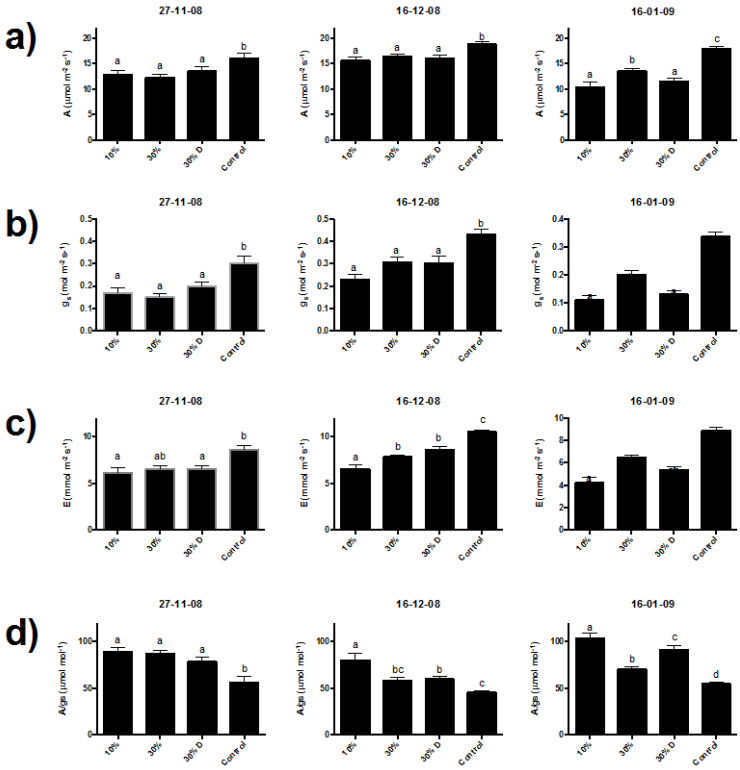

Figure 2 Gas exchange characteristics for the first year of the deficit irrigation trial at Oxford Landing focusing on the 10%, 30%, 30% D and Control treatments on three separate occasions. 27-11-08 was 23 days after flowering, 16-12-08 was pre veraison, and 16-12-08 was nine days after veraison. a) Net Assimilation (A), b) stomatal conductance (g_s), c) transpiration (E) and d) intrinsic water use efficiency WUEi (A/gs) are shown from top to bottom. Different letter combinations indicate significant differences ($P<0.05$, ANOVA, Holm-Sidak's multiple comparisons test). Error bars = mean +/- SEM.

We observed that leaf water potential measured near midday became more negative (more stress) with increasing vapour pressure deficit (VPD) (Figure 3) on two occasions. This might be expected since greater evaporative demand would cause higher transpiration through the hydraulic resistance of the vine resulting in more negative leaf water potentials. Generally the trend was that the differences between the deficit treatments were more evident when VPD was high (Figure 3a, 3c).

We also examined three different ways that water potential can be measured in order to determine the degree of water stress. Figure 4 shows predawn water potential (PDWP), midday stem (after bagging leaves, SWP) and midday leaf water potentials (LWP) as a function of the actual amount of water applied up to the date of measurements. As would be expected for each treatment the leaf water potential was more negative than stem water potential, which was more negative than predawn water potential. The difference between leaf and stem water potential reflects the draw-down in gradient required to move water from the stem to the leaf, while the difference between stem water potential and pre-dawn water potential reflects the draw-down required to bring water from the roots (and soil) to the stem. The difference between stem and leaf water potential is constant for each treatment (0.276 MPa) since the slope of the linear fit to SWP and LWP was not significantly different and equalled 0.187 MPa ML^{-1}

ha^{-1}. However the difference between pre-dawn and stem water potential becomes larger with more deficit, i.e. from 0.45 MPa in controls to 1.2 MPa in the 10% treatment. This may indicate an increase in hydraulic resistance somewhere in the pathway from soil to the stem with water deficit (see later results on vine conductance). Also of note is that leaf and stem water potential reflect the degree of deficit irrigation (linear dependence) much more precisely than pre-dawn water potential. This has been noted by other research on the effect of deficit irrigation on grapevines (Williams and Trout 2005).

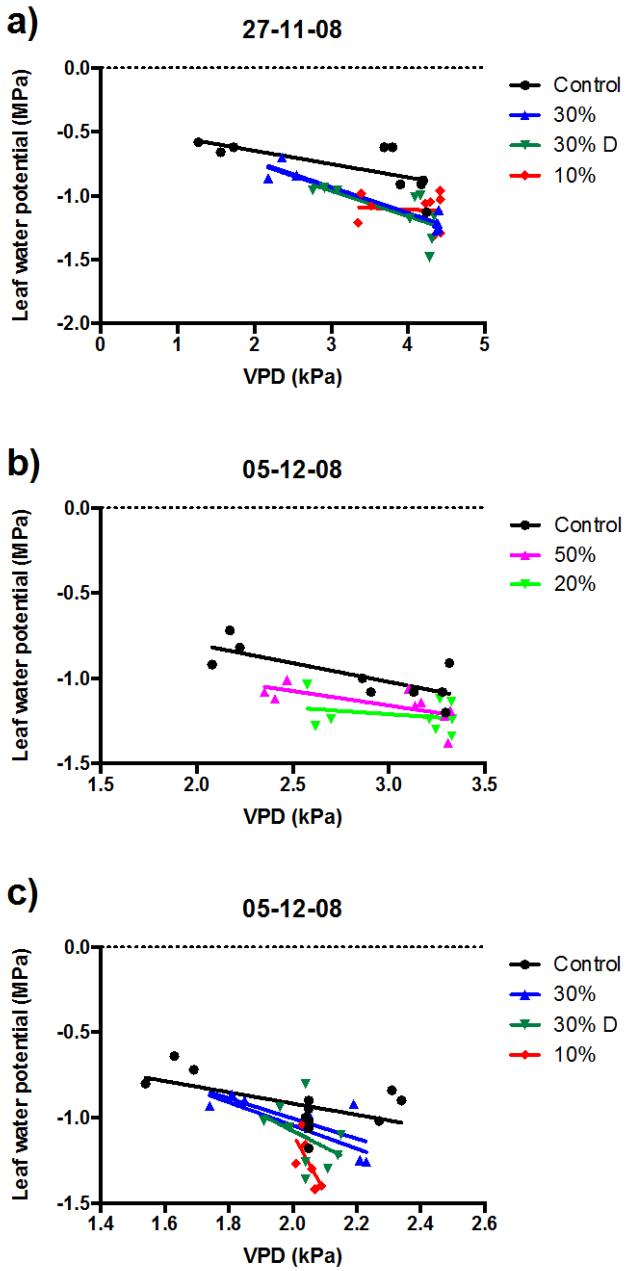

Figure 3 Leaf water potentials for the first season of deficit irrigations plotted as a function of atmospheric vapour pressure deficit (VPD) on two occasions (for dates of phenology see Fig 1 & 2). In most cases the regressions with VPD were significant and the fitted lines differed between irrigation treatments. (a) 30% and 30% D were not significantly different. (b) All treatments differed ($P<0.0068$). (c) 30% and 30% D were not significantly different.

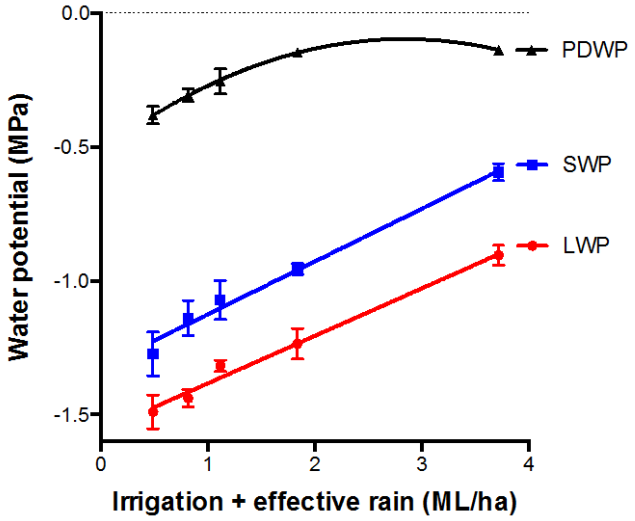

Figure 4 Water potentials (pre-dawn PDWP, midday stem SWP, midday leaf LWP) as a function of actual water applied including effective rainfall during the season. Measurements were made on 7 and 8 Jan. 2009. All regressions are significant ($p<0.05$). Error bars = mean +/- SEM.

Clearly irrigation treatments were having the desired effects physiologically, where water potentials declined with reduced irrigation and this reduced gas exchanged caused by reduced stomatal conductance (largely) and this increased WUEi. The difference between 30% and 30% D was not evident in the leaf water potential measurements having almost identical relationship with VPD (Figure 3). At the lowest applied water, leaf water potentials were close to the permanent wilting point (-1.5 MPa) on some occasions.

In summary, the deficit treatments showed the expected declines in leaf and stem water potential, A, g_s and E as would be expected from previous water stress experiments on grapevines (Chaves, et al. 2007, Romero, et al. 2010, Stevens, et al. 2008, Williams 2012).

Season 2

In Season 2 it was possible to examine the degree of recovery in the physiological parameters to one year of stress followed by almost a full season of full irrigation. Figure 5 shows gas exchange parameters (Figure 5a, b, c, d for A, g_s, E and A/gs respectively) measured late in the season for control, 30% and 10% treatments. Consistent with Season 1 the 30% D showed a greater degree of physiological stress than 30% with more significant reductions in A, g_s and E than controls. This was also reflected in a high WUEi for the 30% D treatment. As is evident from Figure 5 there was complete recovery of the gas exchange parameters after one year with no significant differences detected between control vines and those on full irrigation after one year of deficit at the various levels.

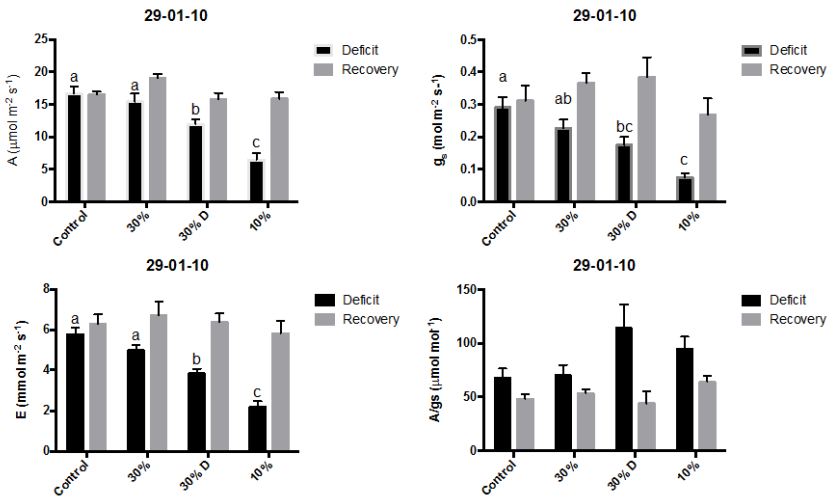

Figure 5 Gas exchange characteristics; a) Net assimilation (A), b) stomatal conductance (g_s), c) transpiration (E), and d) WUEi (A/g_s) for season 2 (09-10), where comparison is made between two years of deficit at various levels (10%, 30%, 30% D, Control) and recovery (first season) after one year of deficit. Measurements were taken on 29-01-10, which was just before harvest. Different letter combinations indicate significant differences ($P<0.05$, ANOVA, Holm-Sidak's multiple comparisons test). No letters across a set of treatments indicates that there was no significant difference. For WUEi there was a significant difference between sustained deficit and recovery. Note that for all treatments there was complete recovery of gas exchange after one season. Error bars = mean +/- SEM.

We also examined the time course of recovery in leaf water potential during season 2 with measurements taken on four occasions during the season (Figure 6). Figure 6a shows the continuous deficit treatments for Control, 30%, 30%D and 10% in which it is evident that towards the end of the season the differences between the treatments became more apparent, particular 10% versus control. For the recovering vines, no significant differences could be detected (Figure 6b). This indicates that as soon as full irrigation is applied, the vines respond by increasing water potential and that there is no carry-over effect from the previous season's deficit. A two way ANOVA showed that there was no effect of time of measurement during the season (Figure 6c).

a)

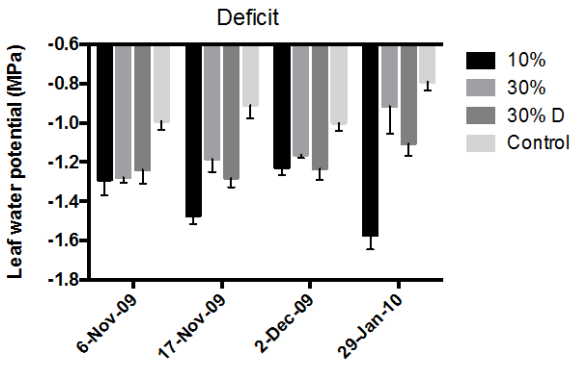

b)

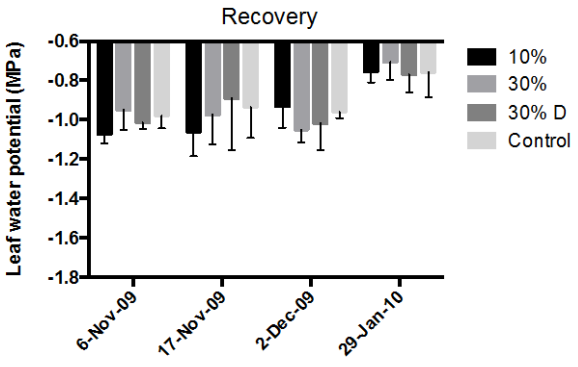

c)

Source of Variation	% of total variation	P value	P value summary	Significant?
Interaction	16.63	0.0001	***	Yes
Time	3.336	0.0539	ns	No
Treatment	46.55	< 0.0001	****	Yes

Holm-Sidak's multiple comparisons test	Mean Diff.	Significant?	Summary
10% vs. 30%	-0.2550	Yes	****
10% vs. 30% D	-0.1758	Yes	***
10% vs. Control	-0.4668	Yes	****
30% vs. 30% D	0.07925	No	ns
30% vs. Control	-0.2118	Yes	****
30% D vs. Control	-0.2910	Yes	****

Figure 6 Leaf water potential for season 2 (09-10) at four time points during the season. Comparison is made between two years of deficit at various levels (10%, 30%, 30% D, Control) a), and recovery (first season) after one year of deficit b). c) Significance summary (2-way ANOVA) on the sustained deficit treatments in a). Note that the effect of time of measurement during the season was not significant but there was a significant interaction with treatment. c) Significance summary between treatments for 29/10/2010. For recovery there was no significant difference between treatments. Error bars = mean +/- SEM.

Season 3

For season 3 we were able to examine 1, 2 and 3 years of deficit treatments and their recoveries respectively of 2 years and 1 year. Figure 7a,b,c,d (A, g_s, E, A/g_s) shows comparison of three years of continuous stress with 2 years + 1 year of recovery. The continuous stress treatment showed reduced A, g_s and E, and increased WUEi for 30% and 10% treatments as would be expected from previous years' measurements. Interestingly, recovery was not complete in g_s and E (Figure 7b,c) for the 2 year deficit + 1 year of recovery, and the degree of recovery decreased with the previous degree of deficit.

Figure 8a,b,c,d (A, g_s, E, A/g_s) allows comparison of gas exchange parameters for the 10% treatment across the three years for each of the recovery periods, i.e. 1 year deficit + 2 year recovery, 2 year deficit + 1 year recovery and 3 year of deficit. In this case, where the measurements were taken later in the season compared to Figure 7, there was complete recovery in the gas exchange parameters. The difference between the data in Figure 7 and 8 could be due to the extra time for recovery during Jan. 2011, since the data for Figure 8 were recorded later in the season compared to the data in Figure 7.

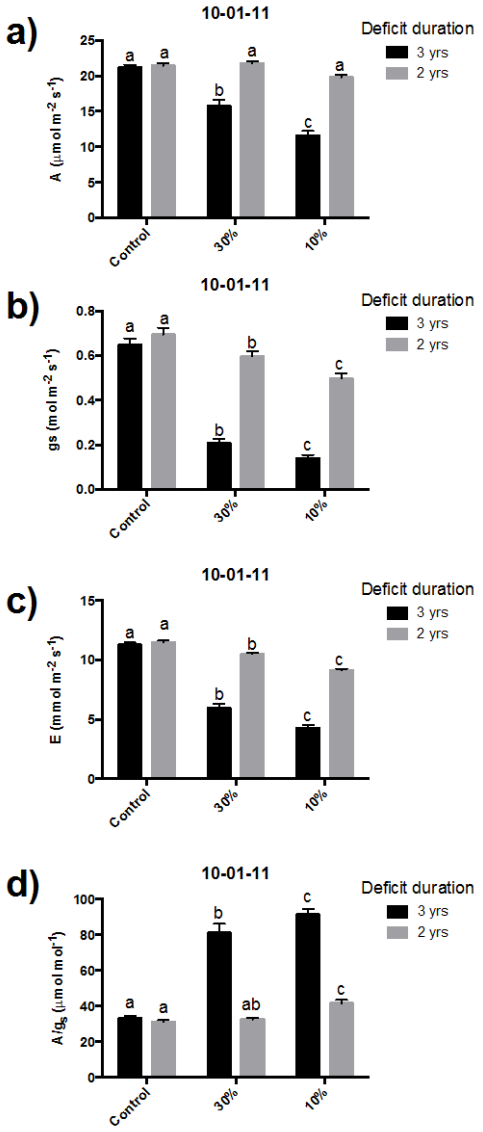

Figure 7 Season 3 gas exchange showing: a) Net assimilation (A), b) stomatal conductance (g_s), c) transpiration (E), and d) WUEi (A/g_s) for vines measured in January 2011, and comparing three years of continuous deficit compared to two years of deficit and one season of recovery. For g_s (b) and E (c) there was incomplete recovery after two years of deficit at both 10% and 30% of normal irrigation (2-way ANOVA with Holm-Sidak's multiple comparisons test, different letter indicates significant difference $P<0.05$). This was not evident for A (a). Error bars = mean +/- SEM.

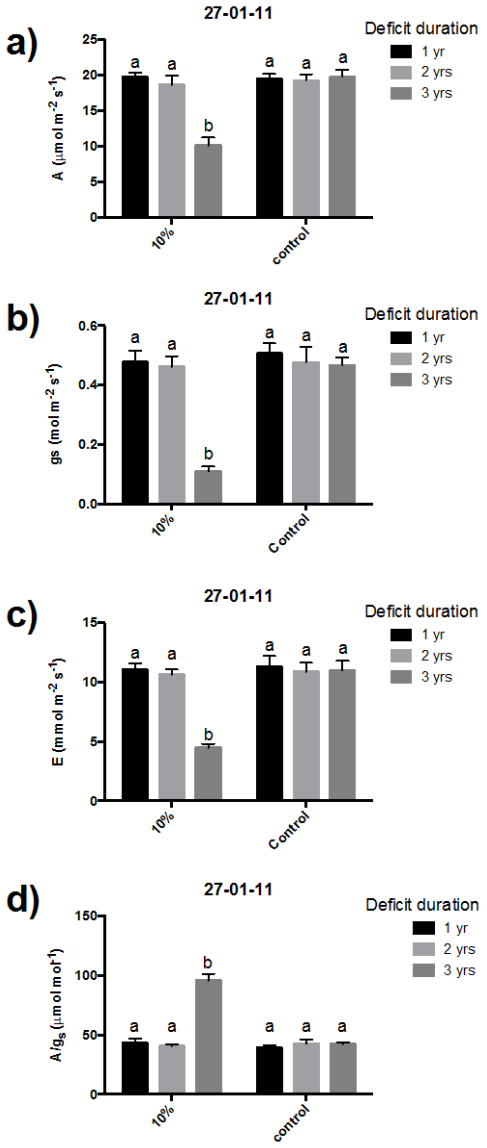

Figure 8 Gas exchange: a) Net assimilation (A), b) stomatal conductance (g_s), c) transpiration (E), and d) WUEi (A/g_s) comparing recoveries from one level of deficit irrigation (10%) for 1, or 2 years on another occasion during Jan 2011. In this case (cf Fig 7) complete recovery was evident i.e. only the 3 full years of deficit (including the current season, 2011) showed a significant effect (different letter indicates significant difference $P<0.05$, 2-way ANOVA with Holm-Sidak's multiple comparisons test). Error bars = mean +/- SEM.

In season 3 a complete survey was performed of the midday stem water potential across most of the treatments comparing 1, 2, and 3 years of stress (Figure 9). This was done on 6 Dec. 2010. For years 1 and 2 the vines had 2 and 1 year of recovery respectively. What is evident from Figure 9 is that for the 10% treatment the vines had not recovered stem water potential despite having about half a season of full irrigation (control levels). Interestingly for the 30% and 50% treatments there was no significant difference between three years or continuous stress and recoveries and these were not significantly different from controls. Thus water potentials also indicate that recovery is not complete for

the 10% deficit after two years of deficit and approximately one half a growth season in recovery.

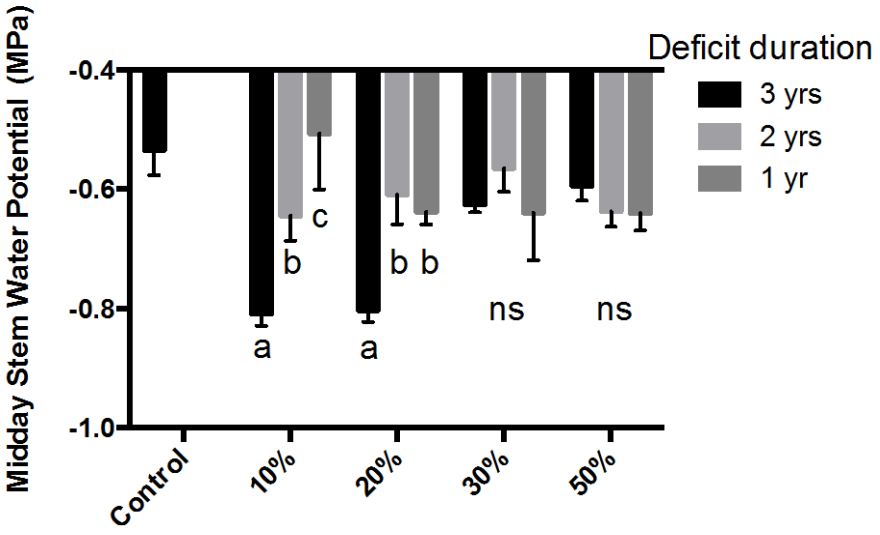

Figure 9 Stem water potential measured across most of the deficit treatments and allowing comparison of the degree of recovery (for 1 or 2 years) after deficit. Three years is continuous deficit including the current 2011-12 season. Only for the 10% and 20% was there a significant difference between years (different letters indicate significant difference, $P<0.05$, 2-way ANOVA with Holm-Sidak's multiple comparisons test). For 10% there was incomplete recovery of stem water potential after two years of deficit and full irrigation up to the time of measurement (6-12-11). 30%D was not measured on this occasion. Error bars = mean +/- SEM.

Season 4

For season 4 we could compare the long term deficit (3 years) with recovery to full irrigation in the current season. Figure 10a,b,c,d shows gas exchange parameters (A, g_s, E, A/g_s) measured on two consecutive days early in the season (16 and 17 Nov. 2011). Here comparison is made between four years of continuous deficit and three years of deficit with a short part of the season in recovery. As for previous seasons, assimilation was the least sensitive parameter, while g_s particularly, and E declined with all reduced irrigation treatments. Stomatal conductance generally did not show full recovery after three years at 10% with part of a season of recovery (compare black bars in Fig 10b on the two separate days). There was also a tendency again for the 30% D treatment to show a greater degree of stress reflected as lower g_s compared to the 30% treatment, though this was not significant.

Leaf water potentials measured over the same two days as the gas exchange measures revealed a significant effect of VPD (Figure 11), since on this occasion during the measurements there was a large variation in VPD during the day. In all cases the regressions of leaf water potential versus VPD were highly significant. The 30% D treatment of 3 year + current season of recovery was the only one that did not show recovery, since the regression was significantly different to that of the control and to the continuous (4yr) of 30% D (Figure 11b). The 10% treatment showed incomplete recovery, but this was not

significantly different from the controls (Figure 11c). The slope of the relationship of leaf water potential versus VPD was not significantly different between 10% 4 years of deficit and recovery or control (Fig 11c), however there was a tendency with the deficit treatments for the slope to be steeper. This may be indicative of a lower hydraulic conductance through the vine (higher resistance) in response to the deficit treatments (and see below).

Later in the season another set of measurements was made on leaf water potential and when VPD was less variable (Figure 12). In this case complete recovery was evident for 30%, 30% D and 10 % treatments while the continuous deficit for four years showed significant decrease in water potential. In this case there was no significant difference between 30% and 30%D.

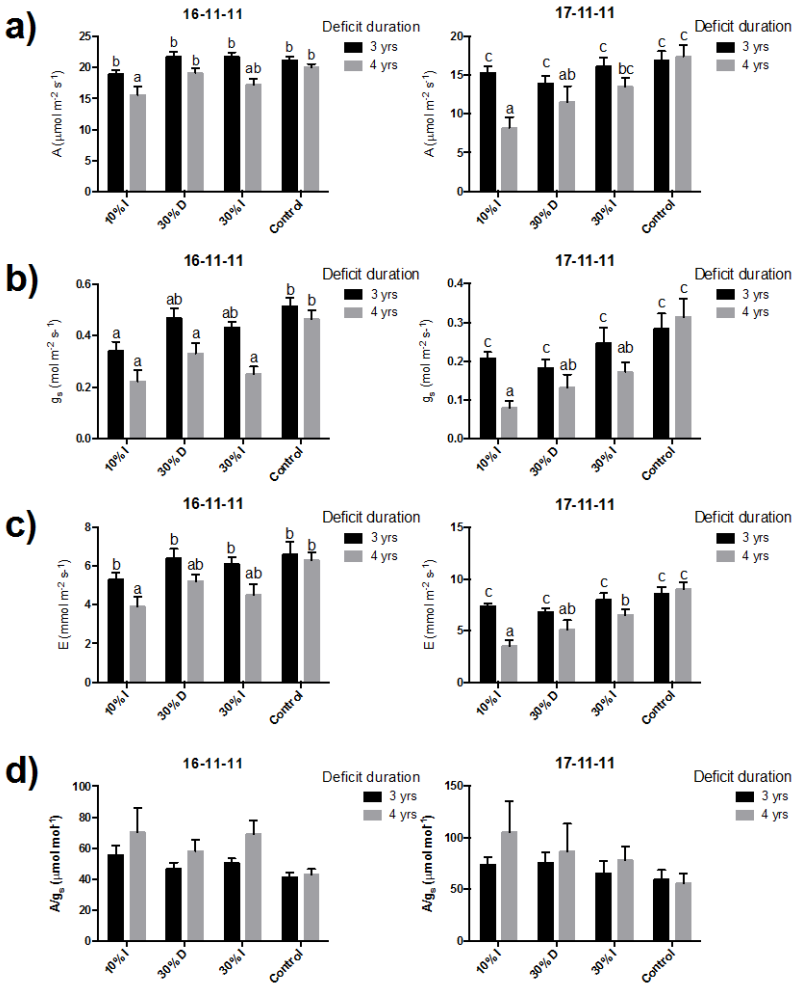

Figure 10 Gas exchange characteristics: a) Net assimilation (A), b) stomatal conductance (g_s), c) transpiration (E), and d) WUEi (A/g_s) for a selection of the treatments (10%, 30%, 30% D, Control) measured on two consecutive days in Season 4. Degree of recovery is evident by comparison of year 3 (yr 3) versus year 4 (yr 4) for each of the treatments. Significant differences are indicated by different letter combinations ($P<0.05$, 2-way ANOVA with Holm-Sidak's multiple comparisons test). Lack of recovery is only evident in g_s on the 16-11-11. Error bars = mean +/- SEM.

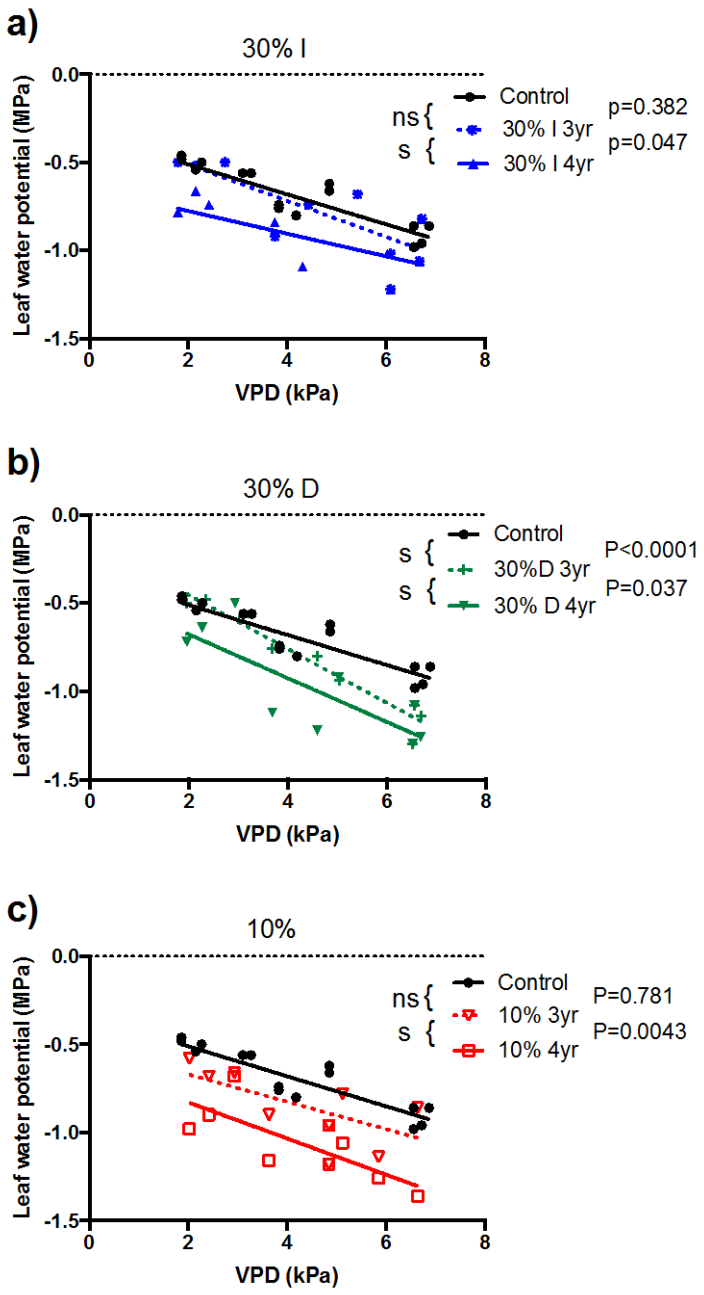

Figure 11 Leaf water potentials as a function of VPD measured on 16 and 17 Nov 2011. Also shown are the regression lines for each deficit treatment and comparing four continuous years of deficit treatment with three3 years of deficit and one year of recovery. The significance of the difference between the regression lines is indicated on the right of each figure. Note that the 3 yr regression line for the 30% D treatment is significantly different to the control indicating that this treatment did not show recovery. For the 10% and 30% the recoveries were not significantly different to the controls.

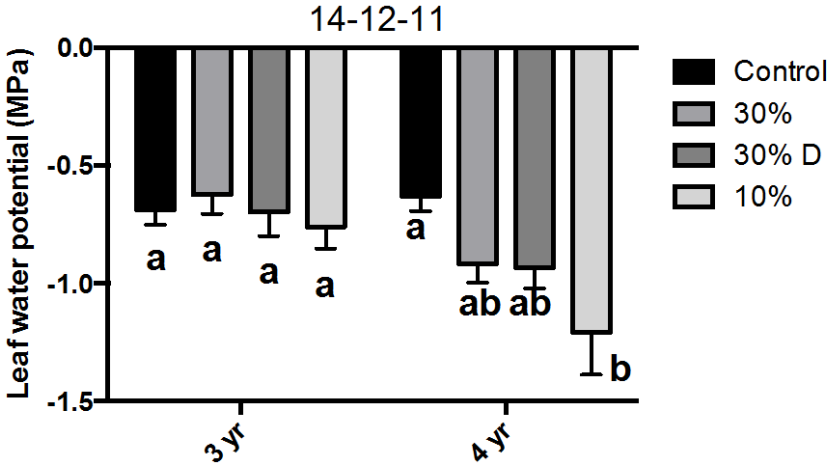

Figure 12 Leaf water potentials measured later in the fourth season within a narrow range of VPD. Different letter indicates significant difference within each year group (2-way ANOVA with Holm-Sidak's multiple comparisons test). Error bars = mean +/- SEM.

Combined data and effects across seasons

Vine conductance

Sap flow measurements were also undertaken on a selected number of vines comparing the 10% and 50% treatments that had continued deficit for three years and recovery for one year after two years of deficit. This was coordinated with a campaign of diurnal water potential measurements during one day to examine the dynamics of stress development during the day and how this correlates with sap flow. Figure 13 shows stem water potential (Figure 13a), sap flow over three days across the period of water potential measures (Figure 13b) and calculated vine conductance (Figure 13c). The 10% treatment results in poor recovery of stem water potential during the afternoon compared to recovery vines, control and 50%. Also there is clearly a significant depression of sap flow in the middle of the day in the 10% treatment (Figure 13b) and note also for the 10% recovery vines. The hydraulic conductance of the vines can be calculated from the difference in predawn water potential and stem water potential and the measured sap flow (i.e. sap flow/gradient). These conductances are not normalised to the size of the vines, thus a higher conductance can occur because a vine is larger. This shows that the deficit treatments tended to have higher conductances in the morning and reduced conductances in the afternoon compared to recovery and controls. This corresponds to a higher sap flow in the morning in the deficit treatments, but low sap flow in the afternoon. There has been previously reported a correlation between transpiration and root hydraulic conductivity under drought stress in vines that may explain this observation (Vandeleur et al. 2009). The lower conductance in the 10% treatments, including recovery, was a general feature also observed with a different method of determining conductance (see below).

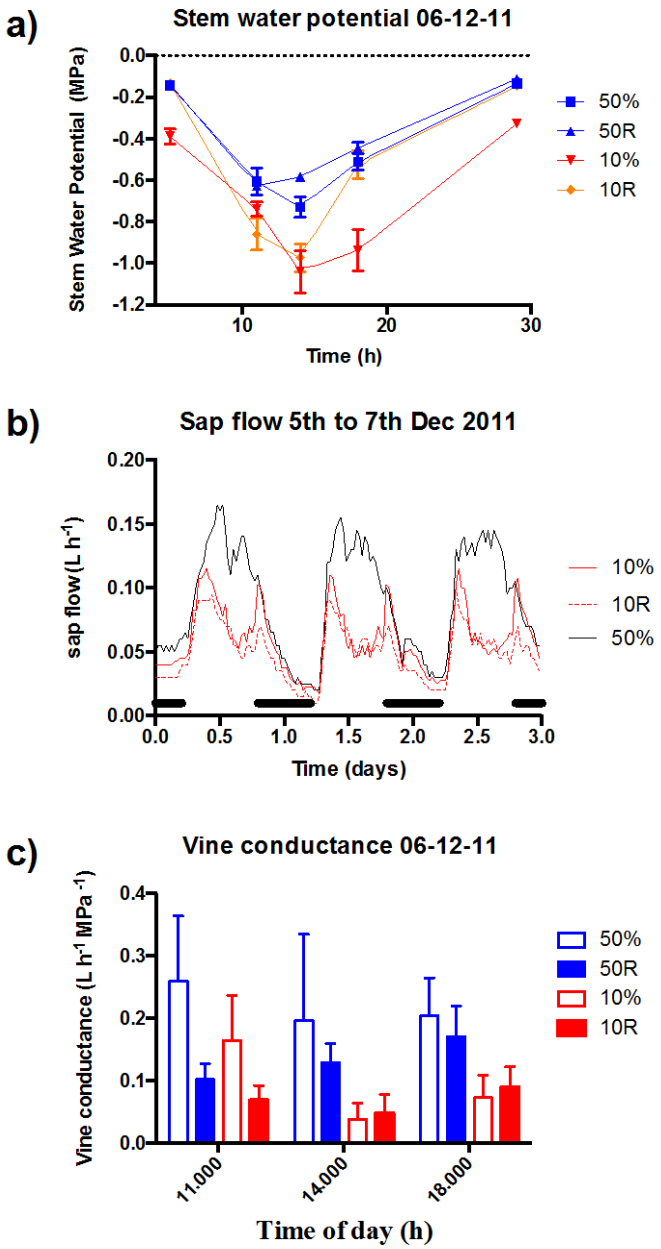

Figure 13 Vine hydraulic conductance (L h^{-1} MPa^{-1}) estimated through a day (6/12/2011) in season 4 from measurements of stem water potential and sap flow comparing 50% and 10% treatments after 3.5 years of continuous deficit and recovery for 0.5 year after three years of deficit (denoted R). a) Stem water potential measured from pre-dawn through the day and into the early morning of the following day. Note that the 10% recovery declines to a low value in the middle of the day but recovers to the 50% level in the afternoon. b) Sapflow measurements recorded over three consecutive days (part of a larger data set). Black bars denote night-time. Note the significant depression of sapflow after midday and partial recovery in the late afternoon in the 10% and 10%R. c) Calculated vine conductances. Although there were no significant differences, the 10% treatments showed reduced hydraulic conductances in the afternoon. Error bars = mean +/- SEM.

Whole plant hydraulic conductance can also be determined from the leaf measurements of transpiration and the gradient in water potential. Thus the difference in stem water potential (*SWP*) between pre-dawn (*PDWP*) (taken as the soil water potential) and midday can be considered as the driving force for water movement between the soil and the stem. The hydraulic conductance

between root and stem ($K_{root\text{-}stem}$) can then be calculated by dividing the transpiration rate measured at midday (E_{md}) by this gradient (Romero, et al. 2010,Tsuda and Tyree 2000):

$$K_{root\text{-}stem} = E_{md}/(SWP\text{-}PDWP).$$

Figure 14 shows $K_{root\text{-}stem}$ plotted against stem water potential (Fig 14a) and pre-dawn water potential (Fig 14b) for the Control, 50%, 50R 10% and 10%R in season 4 (2011-12). $K_{root\text{-}stem}$ declines significantly with decrease in SWP (Fig 14c), but is not correlated with PDWP (Fig 14b). This relationship has been observed previously for deficit irrigated field-grown Monastrell grapevines (Romero, et al. 2010). Chardonnay shows greater sensitivity to SWP and higher conductances than Monastrell (Monastrell: $K_{root\text{-}stem}$ = 0.23 + 0.14 x SWP; Chardonnay on Ramsey: $K_{root\text{-}stem}$ = 0.46 + 0.44 x SWP (g m^{-2} s^{-1} MPa^{-1}). This reduction in $K_{root\text{-}stem}$ is very similar to the reduction in root hydraulic conductivity observed in potted Chardonnay vines under water stress that was linked to increased suberisation and lignification of the roots (Vandeleur, et al. 2009). There was a reduction in $K_{root\text{-}stem}$ in the deficit treatments below 50% (Fig 15a,b). After three years of deficit and one year of recovery the 10% treatment did not show recovery in $K_{root\text{-}stem}$ (Fig 15 c). It is likely that this lack of recovery in $K_{root\text{-}stem}$ is related to the requirement for new root growth and may reflect the long root longevity observed for these vines in this environment (see Chapter 6.5).

a)

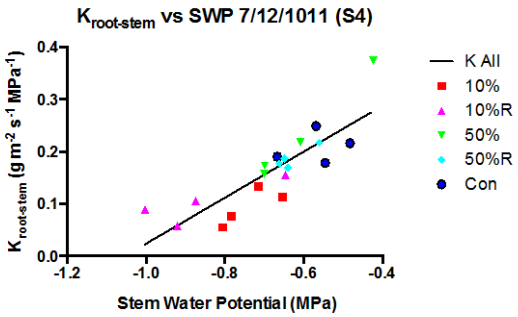

b)

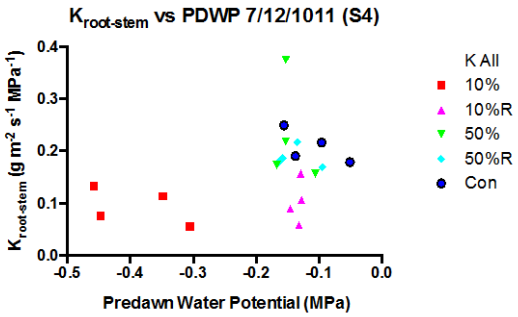

c)

	K All
Best-fit values	
Slope	0.4397 ± 0.06548
Y-intercept when X=0.0	0.4637 ± 0.04546
X-intercept when Y=0.0	-1.055
1/slope	2.274
95% Confidence Intervals	
Slope	0.3021 to 0.5772
Y-intercept when X=0.0	0.3682 to 0.5592
X-intercept when Y=0.0	-1.233 to -0.9575
Goodness of Fit	
R square	0.7147
Sy.x	0.04084
Is slope significantly non-zero?	
F	45.09
DFn, DFd	1.000, 18.00
P value	< 0.0001
Deviation from zero?	Significant

Figure 14 Vine hydraulic conductance ($K_{root\text{-}stem}$) normalised on a leaf area basis as a function of water potential for Chardonnay (on Ramsay) vines in season 4 under various deficit treatments and 1 year of recovery (indicated by R). $K_{root\text{-}stem}$ was significantly correlated to midday SWP (a,c) but not to PDWP (b).

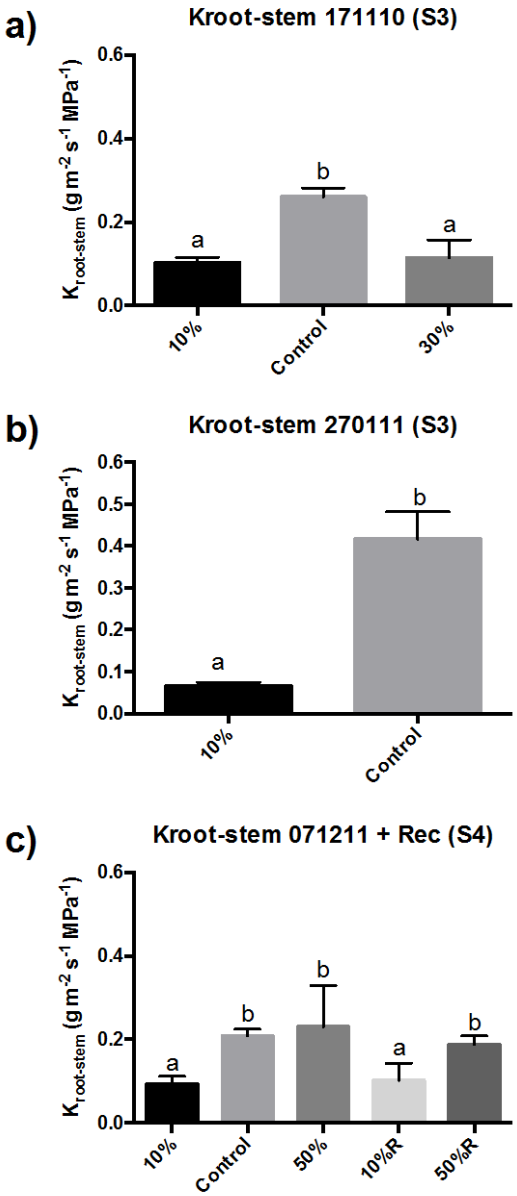

Figure 15 Summary of mean $K_{root\text{-}stem}$ measured on three different occasions for three seasons of deficit (a,b) or four years of deficit and three years of deficit and recovery (c). Shown are the mean (SEM), with different letter indicating significant difference ($P<0.05$, one way ANOVA, Fishers LSD).

Assimilation versus stomatal conductance as a threshold indicator of optimum irrigation deficit

Thresholds in water potential and gas exchange parameters may indicate the optimum level of deficit irrigation to achieve good water use efficiency, reasonable yields and good quality grapes for winemaking (Flexas, et al. 2010,Romero, et al. 2010). In the Romero et al. study maximum TSS for Monastrell grapes was achieved during ripening under regulated deficit irrigation (15% or 30% ETc) when average net assimilation rates were over 10-12 µmol m^{-2} s^{-1}. This corresponded to g_s values of between 0.1 and 0.15 mol m^{-2} s^{-1}. Maximum extractable polyphenols and total anthocyanins were obtained with midday post-veraison SWP of between -1.2 and -1.3 MPa. Although the

Romero et al. study used regulated deficit and ours used continuous deficit, it is instructive to compare the thresholds listed above with the equivalent values observed in our study.

Figure 16 shows A as a function of g_s for season 4 (2011-12) for Control, 10%, 30%, 30%D (continuous and recovery after one year) illustrating the typical saturation in A with high g_s. It is clear that a substantial reduction in g_s could occur from the very high values observed (0.6 mol m^{-2} s^{-1}) without much reduction in net assimilation. The thresholds suggested from Romero et al (2010) are also indicated. The data are well fit by a single exponential, which is very similar to the fit found by Romero et al, (2010) and others (Flexas, et al. 2010,Williams 2012). Our data are also compared with that of (Williams 2012) (Fig 16c) showing that assimilation on average for Chardonnay is higher than that for Thompson Seedless for any given g_s. It is also instructive to compare the recovery vines with the continuous deficit (Fig 16b). Note that the recovery vines sit on the same curve (details in Fig 16d), thus there has been no change in the relationship between A and g_s as a result of 3 years of continuous deficit in this case.

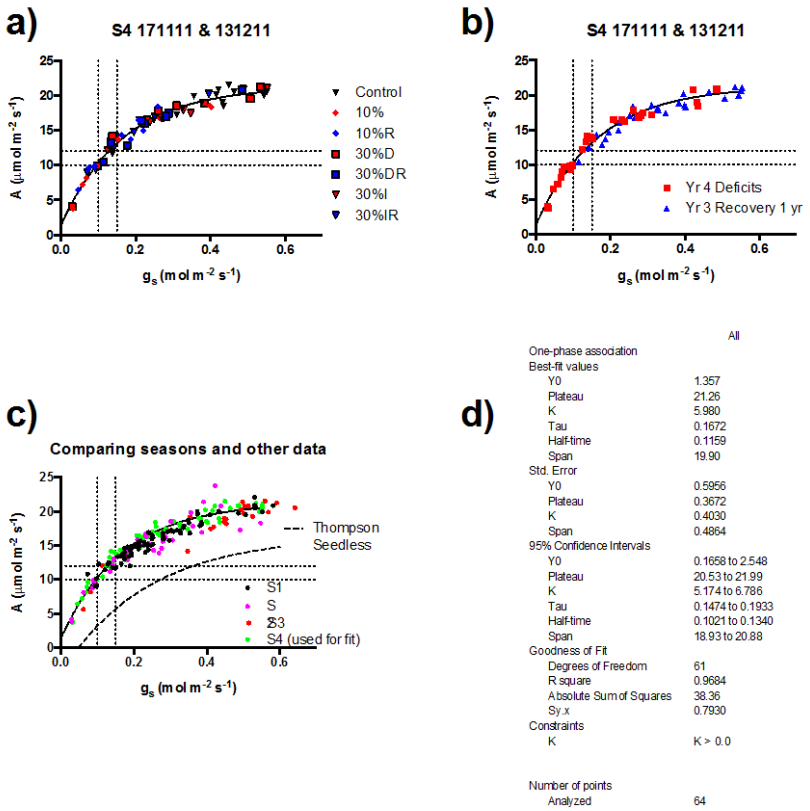

Fig ure 16 Assimilation (A) versus stomatal conductance (g_s). For season 4 (2011-12) Control, 10%, 30%, 30%D (continuous and recovery after one year) (a), and comparing recovery and three years continuous deficit (b), and all seasons and all deficits (c). Also shown in (c) is the fit to the data for Thompson Seedless from Williams (2012). The fit parameters to a single exponential association is shown in (d) used for all the fits shown. The range in thresholds for g_s and A suggested to be optimal by Romero et al. (2010) are indicated as dotted vertical and horizontal lines (respectively) in each graph.

If we now take all the data from across all seasons, these also fit on exactly the same relationship between A and g_s (Fig 16c). This indicates that deficit irrigation is not altering the intrinsic relationship between assimilation and stomatal conductance and probably indicates that carboxylation rates were saturated for all treatments. This would indicate that the vines were not nitrogen limited as a result of the treatments. However it also would suggest that the relationship between internal mesophyll conductance and stomatal conductance was not altered as a result of the stress level or long durations of these stresses. The mesophyll conductance of grapevine leaves can be as large, or larger than the stomatal conductance and it shows a linear correlation with net assimilation across several varieties (Tomas, et al. 2014).

Returning to the thresholds discussed by Romero et al (2010), it is instructive to examine which irrigation treatments gave these levels of A, g_s and water potential. Figure 17 shows the frequency distribution of g_s for each deficit treatment and recovery. The left hand column of distributions shows each continuous deficit compared to control, while the right hand column shows the respective recoveries. In this case all numbers of years of continuous deficits have been lumped together since it makes no difference if we compare 1, 2, 3, or 4 years of deficit since these give exactly the same responses. The irrigation treatment that corresponded to the optimum range of g_s corresponded to the 20% treatment and also probably the 30% D treatment (i.e. mode of the distribution was in the range of 100 to 150 mmol m^{-2} s^{-1}). This would also correspond to the optimum range in assimilation of between 10-12 μmol m^{-2} s^{-1}. When examining Figure 17 it is also instructive to note that the 10% recoveries did not return to the control levels of g_s (top right graph). This contrasts to all the other deficit treatments.

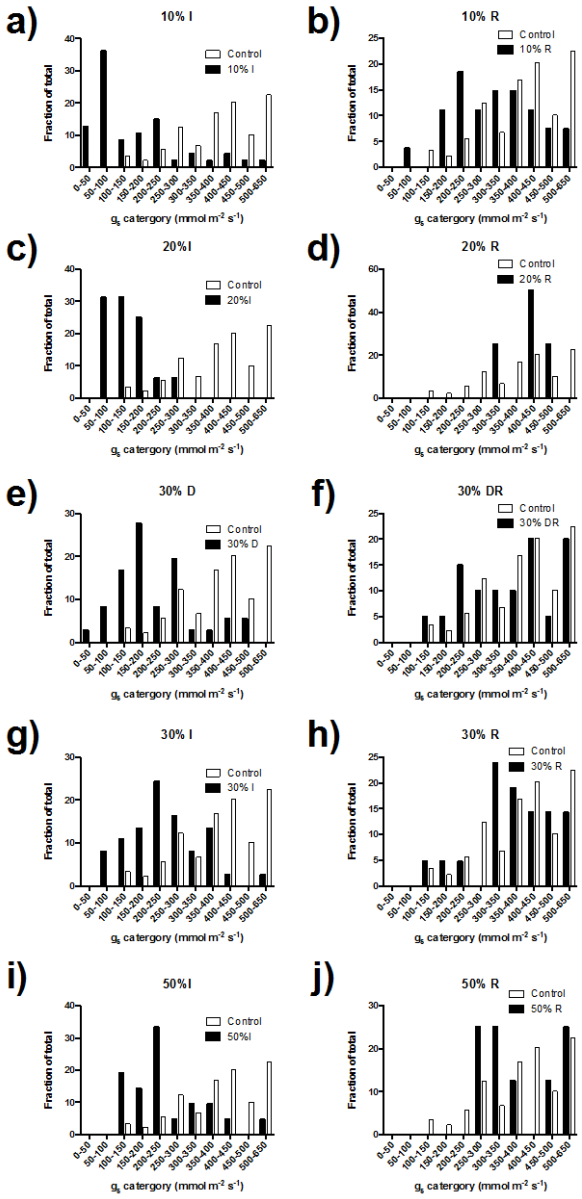

Fig 17. Frequency distributions of stomatal conductance (g_s) across all seasons for each irrigation treatment and comparison with recovery. a) 10%, c) 20%, e) 30D%, g) 30%, i) 50%, and respective recoveries b), d), f), h), j). Corresponding controls are compared in each case, which are different for each treatment.

Figure 18 shows a summary of leaf gas exchange data and LWP across all four seasons comparing continuous deficit and recoveries. The 10% treatment gave the highest WUEi, but according to Romero et al. (2010) the g_s and A would be below the optimum. It should be noted that several studies have now questioned the utility of WUEi to indicate whole vine water use efficiency (Medrano, et al. 2015,Poni, et al. 2014). This will be discussed in more detail in relation to the productivity and yield of vines. The 20% treatment, which achieves the Romero threshold in g_s and A provides an intermediate WUEi between the 10% and control treatments, but this may not be reflected in water productivity.

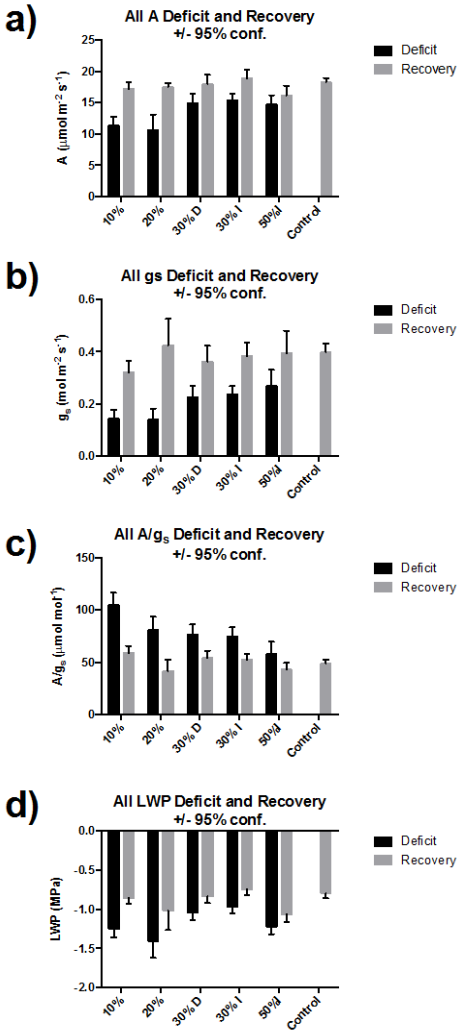

Figure 18 Summary of all season data combined for: a) Net assimilation (A), b) stomatal conductance (g_s), c) WUEi (A/g_s) and midday leaf water potential across the treatments and comparing recoveries (one year). Error bars are 95% confidence limits.

Finally Figure 19 demonstrates the relationships with midday leaf water potential between A, g_s and WUEi for all data across all seasons and compared with similar field compiled data from the literature for other grapevine varieties under water deficit treatments. As expected, both A and g_s decline with decreasing leaf water potential (increasing water stress). The relationship with A is very similar to other published regressions for Monastrell (Romero, et al. 2010) and Thompson Seedless (Williams 2012), while that with g_s is rather different with Chardonnay falling approximately between the responses of these two varieties. In this case the slope of the relationship of g_s with leaf water potential may indicate the degree of isohydry/anisohydry between the varieties; i.e. the steeper the slope the potentially more isohydric the variety (Martorell, et al. 2015), in which case Chardonnay on Ramsey would be intermediate between the two varieties shown. However a note of caution is required here because the long-term associations shown for our data may not reflect short-term daily regulation of stomatal conductance. The relationship of WUEi with leaf water

potential is consistent with many studies previously reported and is compared with that of Monastrell (Romero, et al. 2010) in the figure. However, this leaf based measure may not indicate an increase in whole vine water productivity under deficit irrigation (Medrano, et al. 2015).

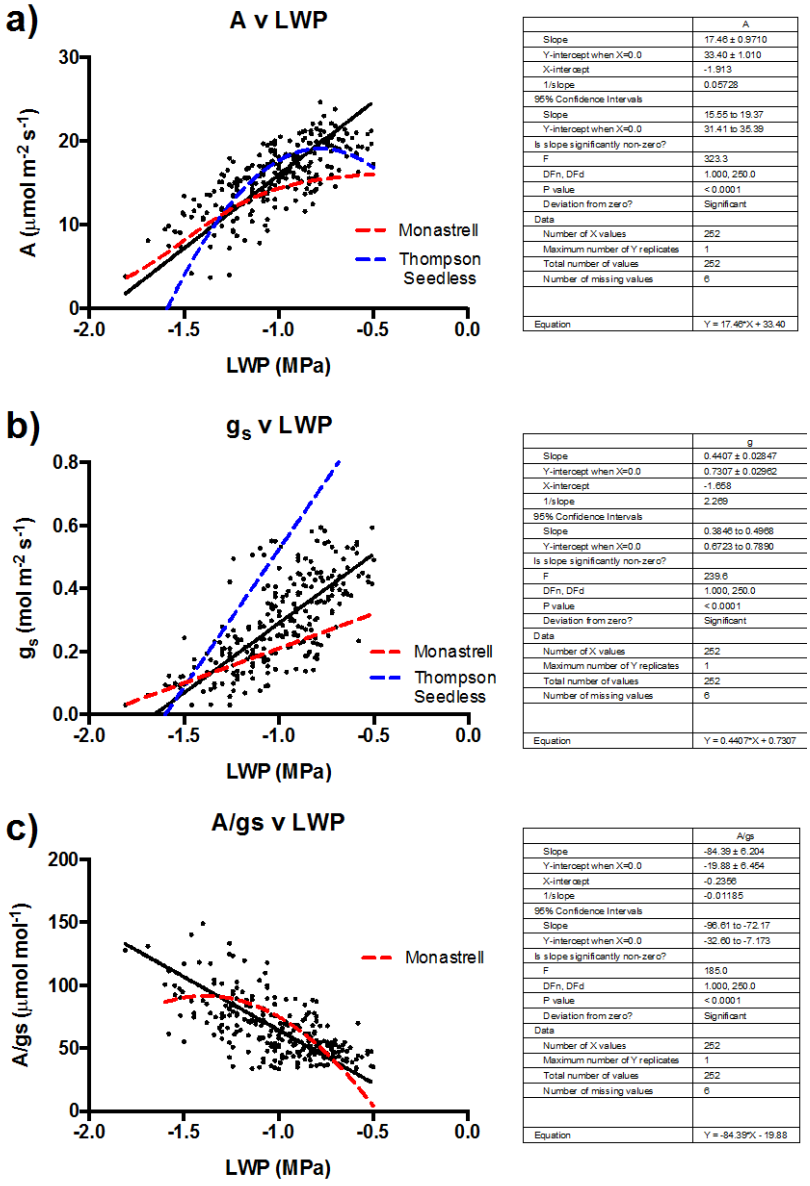

	A
Slope	17.46 ± 0.9710
Y-intercept when X=0.0	33.40 ± 1.010
X-intercept	-1.913
1/slope	0.05728
95% Confidence Intervals	
Slope	15.55 to 19.37
Y-intercept when X=0.0	31.41 to 35.39
Is slope significantly non-zero?	
F	323.3
DFn, DFd	1.000, 250.0
P value	< 0.0001
Deviation from zero?	Significant
Data	
Number of X values	252
Maximum number of Y replicates	1
Total number of values	252
Number of missing values	6
Equation	Y = 17.46*X + 33.40

	g
Slope	0.4407 ± 0.02847
Y-intercept when X=0.0	0.7307 ± 0.02982
X-intercept	-1.658
1/slope	2.269
95% Confidence Intervals	
Slope	0.3846 to 0.4968
Y-intercept when X=0.0	0.6723 to 0.7890
Is slope significantly non-zero?	
F	239.6
DFn, DFd	1.000, 250.0
P value	< 0.0001
Deviation from zero?	Significant
Data	
Number of X values	252
Maximum number of Y replicates	1
Total number of values	252
Number of missing values	6
Equation	Y = 0.4407*X + 0.7307

	A/gs
Slope	-84.39 ± 6.204
Y-intercept when X=0.0	-19.88 ± 6.464
X-intercept	-0.2356
1/slope	-0.01185
95% Confidence Intervals	
Slope	-96.61 to -72.17
Y-intercept when X=0.0	-32.60 to -7.173
Is slope significantly non-zero?	
F	185.0
DFn, DFd	1.000, 250.0
P value	< 0.0001
Deviation from zero?	Significant
Data	
Number of X values	252
Maximum number of Y replicates	1
Total number of values	252
Number of missing values	6
Equation	Y = -84.39*X - 19.88

Figure 19 Relationship of leaf gas exchange properties with midday leaf water potential for all treatments and across all seasons. a) Net assimilation (A), b) stomatal conductance (g_s), c) WUEi (A/g_s) as a function of leaf water potential. Associated linear regression equations and significance are given in the associated tables. For comparison data from the literature are compared where equations were provided from field trial studies under water deficit (Monastrell (Romero, et al. 2010), Thompson Seedless (Williams 2012)).

Conclusion

The irrigation reductions had the desired effects on both the water relations and leaf gas exchange, though the 50% treatment generally did not show a strong effect if any. Over the course of the four seasons we generally found that the 10% and 30% D treatment tended to cause the greatest degree of physiological stress, and when recovery was not attained in the first season of full irrigation after continuous stress, it was more likely to be observed in these two treatments earlier in the season and after longer periods of deficit irrigation, i.e more than one season of deficit. It is possible that this is caused by decrease root hydraulic conductance or carry-over of high ABA levels in the vines (Tombesi, et al. 2015). The gas exchange parameters were more likely to show an effect of lack of recovery and here the stomatal conductance was generally the most sensitive parameter both to reduced water potential and in terms of recovery after full irrigation. Stomatal conductance can show greater sensitivity to water stress than assimilation (Williams 2012) at less extreme deficits because of mesophyll limitations (non stomatal) on assimilation (Pou, et al. 2012,Tomas, et al. 2014).

With respect to the levels of deficit and their absolute effects on vine physiology, it is interesting to note that often the 50% and occasionally the 30% treatments showed only small reductions in leaf water potential or leaf gas exchange. This would indicate that this level of reduction in irrigation would have only minimal effects on vine physiology, yet the reductions in amount of water applied are substantial. Such deficits to 50% of full ETc have been previously noted to have only minor effects (Chaves, et al. 2007). Nevertheless, yield and other biomass measurements and carbohydrate content may reveal a different sensitivity (see Chapter 6.2 and 6.4) since these integrate gas exchange for the whole vine and over the whole season.

Overall there was surprisingly little carry-over of continuous stress on the leaf gas exchange and water relations of the vines in recovery. Only in the first half of the recovery season after a long-term deficit was there incomplete recovery observed when this occurred, but usually by the end of the first season of recovery the water relations and gas exchange at the leaf level had returned to that of controls. There are no comparable studies that we are aware of that have investigated leaf water relations and gas exchange during recovery over seasons after long-term deficits. Short-term recovery experiments on potted vines are more common e.g. (Pou, et al. 2012). Though a long term recovery experiment has been conducted for saline irrigated vines (Stevens and Partington 2013) gas exchange data are not available. Another study investigated long-term deficits on Chardonnay productivity, but there are no data on leaf physiology (Williams 2014) or recoveries from deficit.

Of all the deficit treatments the 20%I appeared to give the optimum g_s and A suggested by Romero et al. (2010), but leaf water potentials were often more negative than observed in the other treatments, suggesting that the 30% treatments may be a safer option as a target based on leaf physiology, but this will be further explored in consideration of yield and vine productivity.

References

Chaves, M.M., T.P. Santos, C.R. Souza, M.F. Ortuno, M.L. Rodrigues, C.M. Lopes, J.P. Maroco, and J.S. Pereira (2007) Deficit irrigation in grapevine improves water-use efficiency while controlling vigour and production quality. Annals of Applied Biology 150, 237-252. doi: 10.1111/j.1744-7348.2006.00123.x.

Cifre, J., J. Bota, J.M. Escalona, H. Medrano, and J. Flexas (2005) Physiological tools for irrigation scheduling in grapevine (Vitis vinifera L.): An open gate to improve water-use efficiency? Agriculture, Ecosystems & Environment 106, 159-170.

Flexas, J., J. Galmes, A. Galle, J. Gulias, A. Pou, M. Ribas-Carbo, M. Tomas, and H. Medrano (2010) Improving water use efficiency in grapevines: potential physiological targets for biotechnological improvement. Australian Journal of Grape and Wine Research 16, 106-121. doi: 10.1111/j.1755-0238.2009.00057.x.

Martorell, S., A. Diaz-Espejo, M. Tomas, A. Pou, H. El Aou-Ouad, J.M. Escalona, J. Vadell, M. Ribas-Carbo, J. Flexas, and H. Medrano (2015) Differences in water-use-efficiency between two Vitis vinifera cultivars (Grenache and Tempranillo) explained by the combined response of stomata to hydraulic and chemical signals during water stress. Agricultural Water Management 156, 1-9. doi: 10.1016/j.agwat.2015.03.011.

Medrano, H., M. Tomas, S. Martorell, J. Flexas, E. Hernandez, J. Rossello, A. Pou, J.M. Escalona, and J. Bota (2015) From leaf to whole-plant water use efficiency (WUE) in complex canopies: Limitations of leaf WUE as a selection target. Crop Journal 3, 220-228. doi: 10.1016/j.cj.2015.04.002.

Naor, A., Y. Gal, and B. Bravdo (1997) Crop load affects assimilation rate, stomatal conductance, stem water potential and water relations of field-grown Sauvignon blanc grapevines. J. Exp. Bot. 48, 1675-1680. doi: 10.1093/jxb/48.9.1675.

Poni, S., M. Galbignani, E. Magnanini, F. Bernizzoni, A. Vercesi, M. Gatti, and M.C. Merli (2014) The isohydric cv. Montepulciano (Vitis vinifera L.) does not improve its whole-plant water use efficiency when subjected to pre-veraison water stress. Scientia Horticulturae 179, 103-111. doi: 10.1016/j.scienta.2014.09.021.

Pou, A., H. Medrano, M. Tomas, S. Martorell, M. Ribas-Carbo, and J. Flexas (2012) Anisohydric behaviour in grapevines results in better performance under moderate water stress and recovery than isohydric behaviour. Plant and Soil 359, 335-349. doi: 10.1007/s11104-012-1206-7.

Romero, P., J. Ignacio Fernandez-Fernandez, and A. Martinez-Cutillas (2010) Physiological Thresholds for Efficient Regulated Deficit-Irrigation Management in Winegrapes Grown under Semiarid Conditions. American Journal of Enology and Viticulture 61, 300-312.

Sibille, I., H. Ojeda, J. Prieto, S. Maldonado, J.-N. Lacapere, and A. Carbonneau (2007) Relation between the values of three pressure chamber modalities (midday leaf, midday stem and predawn water potential) of 4 grapevine cultivars in drought situation of the southern of France. Applications for the irrigation control. In Proceedings of XVth Conference GESCO. Porec, Croatia. p. 685-695.

Stevens, R.M. and D.L. Partington (2013) Grapevine recovery from saline irrigation was incomplete after four seasons of non-saline irrigation. Agricultural Water Management 122, 39-45. doi: 10.1016/j.agwat.2013.02.003.

Stevens, R.M., J.M. Pech, M.R. Gibberd, R.R. Walker, J.A. Jones, J. Taylor, and P.R. Nicholas (2008) Effect of reduced irrigation on growth, yield, ripening rates and water relations of Chardonnay vines grafted to five rootstocks. Australian Journal of Grape and Wine Research 14, 177-190. doi: 10.1111/j.1755-0238.2008.00018.x.

Tomas, M., H. Medrano, E. Brugnoli, J.M. Escalona, S. Martorell, A. Pou, M. Ribas-Carbo, and J. Flexas (2014) Variability of mesophyll conductance in grapevine cultivars under water stress conditions in relation to leaf anatomy and water use efficiency. Australian Journal of Grape and Wine Research 20, 272-280. doi: 10.1111/ajgw.12069.

Tombesi, S., A. Nardini, T. Frioni, M. Soccolini, C. Zadra, D. Farinelli, S. Poni, and A. Palliotti (2015) Stomatal closure is induced by hydraulic signals and maintained by ABA in drought-stressed grapevine. Scientific Reports 5, 12. doi: 10.1038/srep12449.

Tregoat, O., Van Leeuwen C., Choné X., and G.J. P. (2002) Etude du régime hydrique et de la nutrition azotée de la vigne per des indicateurs physiologiques. Influence sur le comportement de la vigne et la maturation du raisin (Vitis vinifera L. cv. Merlot, 2000, Bordeaux). Journal International des Sciences de la Vigne et du Vin 36, 133-142.

Tsuda, M. and M.T. Tyree (2000) Plant hydraulic conductance measured by the high pressure flow meter in crop plants. Journal of Experimental Botany 51, 823-828. doi: 10.1093/jexbot/51.345.823.

Vandeleur, R.K., G. Mayo, M.C. Shelden, M. Gilliham, B.N. Kaiser, and S.D. Tyerman (2009) The Role of Plasma Membrane Intrinsic Protein Aquaporins in Water Transport through Roots: Diurnal and Drought Stress Responses Reveal Different Strategies between Isohydric and Anisohydric Cultivars of Grapevine. Plant Physiology 149, 445-460. doi: 10.1104/pp.108.128645.

Williams, L.E. (2012) Effects of applied water amounts at various fractions of evapotranspiration (ETc) on leaf gas exchange of Thompson Seedless grapevines. Australian Journal of Grape and Wine Research 18, 100-108. doi: 10.1111/j.1755-0238.2011.00176.x.

Williams, L.E. (2014) Effect of Applied Water Amounts at Various Fractions of Evapotranspiration on Productivity and Water Footprint of Chardonnay Grapevines. American Journal of Enology and Viticulture 65, 215-221. doi: 10.5344/ajev.2014.12105.

Williams, L.E. and F.J. Araujo (2002) Correlations among predawn leaf, midday leaf, and midday stem water potential and their correlations with other measures of soil and plant water status in Vitis vinifera. Journal of the American Society for Horticultural Science 127, 448-454.

Williams, L.E. and T.J. Trout (2005) Relationships among vine- and soil-based measures of water status in a Thompson Seedless vineyard in response to high-frequency drip irrigation. American Journal of Enology and Viticulture 56, 357-366.

6.2 Effect of SDI and recovery on vine productivity, water productivity and vine balance.

Introduction

Deficit irrigation is a term used to describe the application of water that is supplied at levels below full crop evapotranspiration (ET_c) throughout the growing season or in specific phenological stages (Chaves, et al. 2010). Here our treatments consisted of sustained deficit irrigation (SDI) throughout the growing season. As outlined in Table1 (Chapter 5 Methods) the reduced treatments applied in this study were below ETc and were sustained through the entire growing season. Regulated deficit irrigation, where the deficit is applied at a specific period during development has the potential to reduce yields, although this depends on when the deficit is applied (McCarthy 1997). The loss in yield has been attributed to fewer berries per cluster, fewer clusters per vine and decreased berry weight (Matthews and Anderson 1989). There are two peer-reviewed studies that have examined long term sustained deficit irrigation and their effects on general vine productivity, vine balance and berry composition. In one study Merlot vines were subjected to 70% and 35% of the standard irrigation over eight growing seasons and they observed large effects on yield, pruning weight and berry parameters (only reported for the last three seasons) which can be compared with the work reported here (Shellie 2014). Likewise (Lopez, et al. 2007) examined an extreme option of no irrigation or full irrigation on several Spanish varieties over four years. In many respects this study was interesting for comparison because the ET were similar to those in our study and similar seasonal rainfalls were recorded. Vine productivity, vine balance and berry characteristics were recorded (Lopez, et al. 2007) and make interesting comparison with those of our study. In both of these studies recoveries were not examined, making our study quite unique given the practical value of knowing the time for recovery and the influence of the deficit on this recovery.

Methods

At harvest in each season, the fruit from three vines in each replicate was picked by hand on two separate days within a seven-day period. The total number of bunches removed per vine was counted and the total fruit weight of each vine was weighed with a flat bed, digital field scale (Mettler Toledo, Australia). The 100-berry sample was generated by sampling bunches on both sides of the vine and picking berries from the left, right, top, bottom, back and front of the bunch. The samples were transported from the field to the laboratory in a chilled insulated container. We derived the number of berries per bunch from the measures of yield, bunch number and berry weight.

Pruning wood weights were measured in the winters. The wood was removed from the canopy using hand secateurs.

Dry and fresh weight of leaves was determined on one occasion. For dry weight leaves were dried to constant weight at 80°C and leaf water fraction was taken as the difference divided by the fresh weight.

Leaf area index (LAI) was measured with a Li-Cor LAI-2000 Plant Canopy Analyser according to the manufacturer's instructions. Further details can be found in Chapter 6.9.

Results and Discussion

Yield components as a function of time and after variable periods of water stress and recovery.

In this section the data will be presented for each irrigation treatment in the order of increasing irrigation (i.e. from 10%, 20% etc). In each case three Figures are presented providing: 1) Yield per vine, 2) Mean bunch weight, 3) Mean bunch number and, 4) The preceding parameters as a fraction of the control. Each of the yield components figures will be provided for: a) one year of deficit and four years of recovery, b) two years of deficit and three years of recovery, c) three years of deficit and two years of recovery and, d) four years of deficit and one year of recovery. The data are also presented as a fraction of control for each yield component in a manner that allows comparison of the time required for recovery between irrigation treatments. As will be indicated in the following sections the yield in 2010 was generally depressed due to unfavourable climatic conditions during flowering across the region. It should also be noted that for each combination of deficit period and recovery the control vines and treatment vines are a different set of vines, though there are vines in common, therefore there are different means and errors for the same year. Similarly, due to the splitting of a treatment in the final year (2013) there are no previous year data.

10% treatment

Figure 1 shows the yield per vine as a function of year of treatment between seasons 2008-09 and 2012-13, being the full five seasons that the trial was carried out. Figure 1a shows the effect of one year of deficit followed by four years of recovery, Figure 1b shows two years of deficit and three years of recovery, Figure 1c shows three years of deficit and two years of recovery, Figure 1d shows four years of deficit and one year of recovery. Significant differences between treatment and controls are indicated (2-way ANOVA with Holm Sidak's multiple comparison test). Clearly the 10% treatment causes a substantial reduction in yield, however in only one combination of deficit period and recovery was there a significant reduction in the yield relative to controls during the following recovery year. This occurred after two years of deficit with the following year showing a significant reduction despite receiving one year of full irrigation (Figure 1b). Surprisingly three years and four years of deficit at 10% did not show a carryover in yield reduction in the following year of recovery (Figure 1c,d). This may indicate that the 2009-10 season was exceptional in that a combination of factors led to the carry-over in yield reduction caused by the deficit.

Figure 2 shows the corresponding data for bunch weight where again it can be seen that the 10% treatment resulted in a significant reduction relative to controls. In this case however there was carry-over of reduced bunch weight in the recovery period only for the 2008-09 (1 year) of treatment (Figure 2a). This was not seen for the two years of deficit (Figure 2b) contrasting with the total yield data. Again surprisingly there was no carry-over in bunch weight reduction in the years of recovery even after three and four years of continual deficit irrigation (Figure 2c,d).

Figure 3 shows the corresponding data for bunch number across the treatment periods and recoveries. In this case there was no significant effect of treatment time or recovery.

Figure 4 shows the data for yield per vine, bunch weight and bunch number as a fraction of the control where the different treatment periods and recoveries can be compared on the same graph. The 95% confidence intervals are shown and where these overlap with the horizontal line corresponding to the respective controls this would indicate non-significant difference to the control. This representation of the data agrees with the previous set, but demonstrates that the 10% irrigation treatment results in about a 50% reduction in yield that is attributed completely to the reduction in bunch weight, and not to bunch number. There was a trend for the yield to further decline in the second consecutive year of deficit, but this was not evident after three years of deficit.

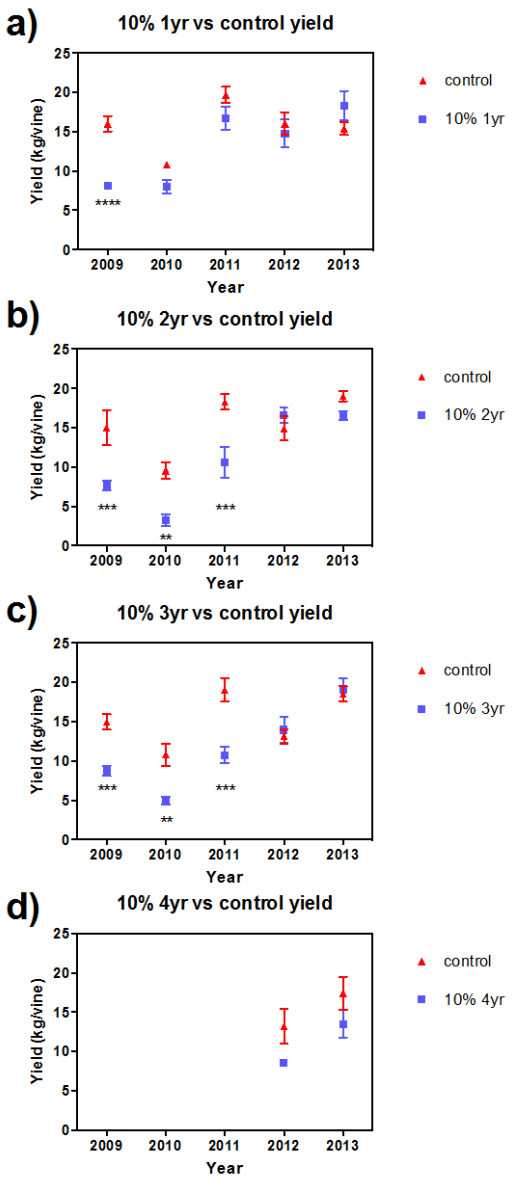

Figure 1 Yield for each season for the 10% irrigation treatment applied for one season (2008-09) then four seasons of recovery (a), two seasons (08-09, 09-10) then three seasons of recovery (b), three seasons (2008-09, 2009-10, 2010-11) then two years of recovery (c) or four seasons (2008-09, 2009-10, 2010-11, 2011-12) and one year of recovery (d) each compared to the respective controls (red triangle symbols). Mean +/- SEM is shown and level of significant difference within a year is indicated (*<0.05 **<0.01 *** <0.001 ****<0.0001, 2-way ANOVA with Holm Sidak's multiple comparison).

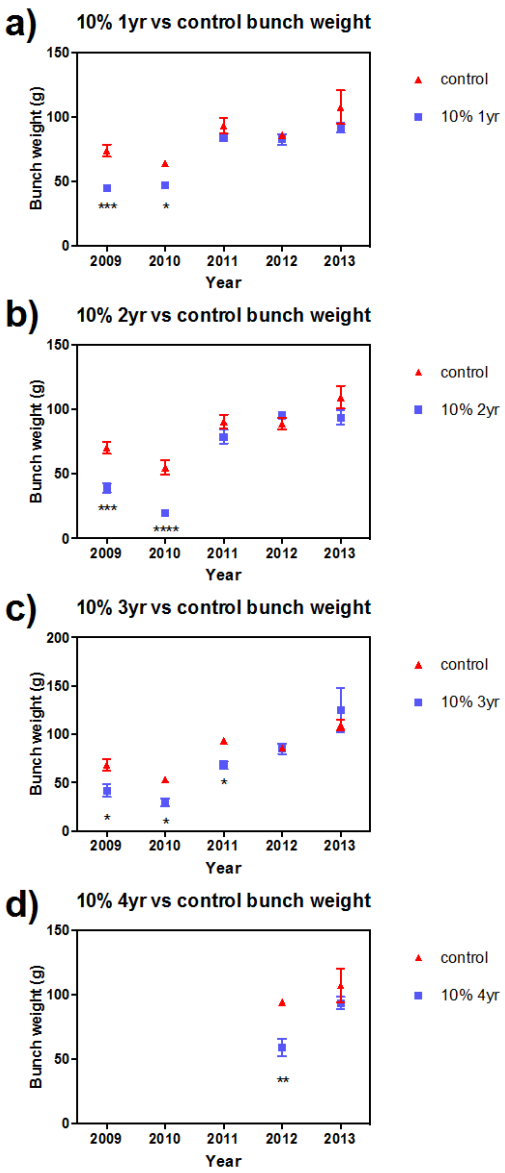

Figure 2 Bunch weight for each season for the 10% irrigation treatment applied for one season (08-09) then four seasons of recovery (a), two seasons (2008-09, 2009-10) then three seasons of recovery (b), three seasons (2008-09, 2009-10, 2010-11) then two years of recovery (c) or four seasons (2008-09, 2009-10, 2010-11, 2011-12) and one year of recovery (d) each compared to the respective controls (red triangle symbols). Mean +/- SEM is shown and level of significant difference within a year is indicated (*<0.05 **<0.01 *** <0.001 ****<0.0001, 2-way ANOVA with Holm Sidak's multiple comparison).

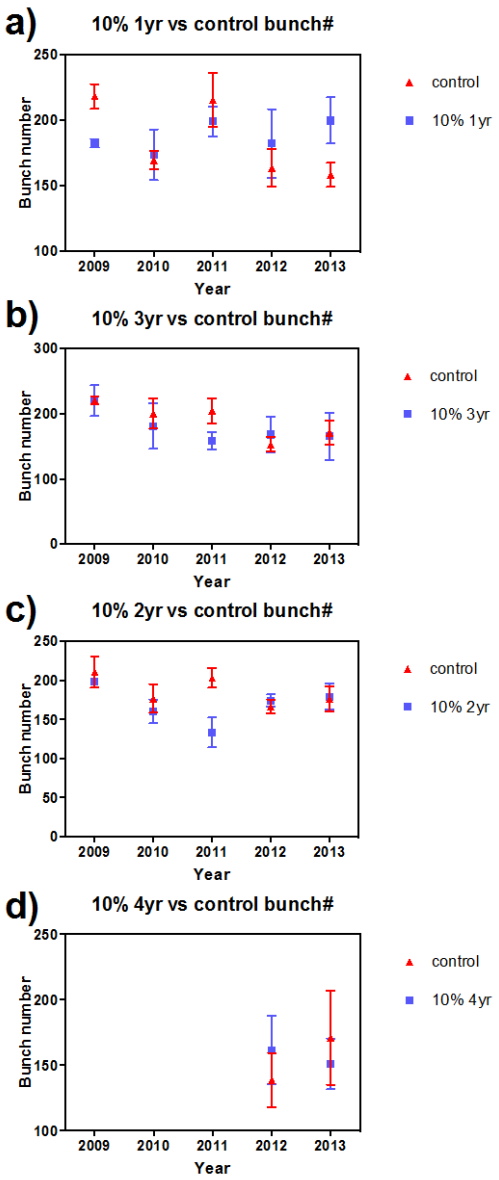

Figure 3 Bunch number for each season for the 10% irrigation treatment applied for one season (08-09) then four seasons of recovery (a), two seasons (2008-09, 2009-10) then three seasons of recovery (b), three seasons (2008-09, 2009-10, 2010-11) then two years of recovery (c) or four seasons (2008-09, 2009-10, 2010-11, 2011-12) and one year of recovery (d) each compared to the respective controls (red triangle symbols). Mean +/- SEM is shown and level of significant difference within a year is indicated (*<0.05 **<0.01 *** <0.001 ****<0.0001, 2-way ANOVA with Holm Sidak's multiple comparison).

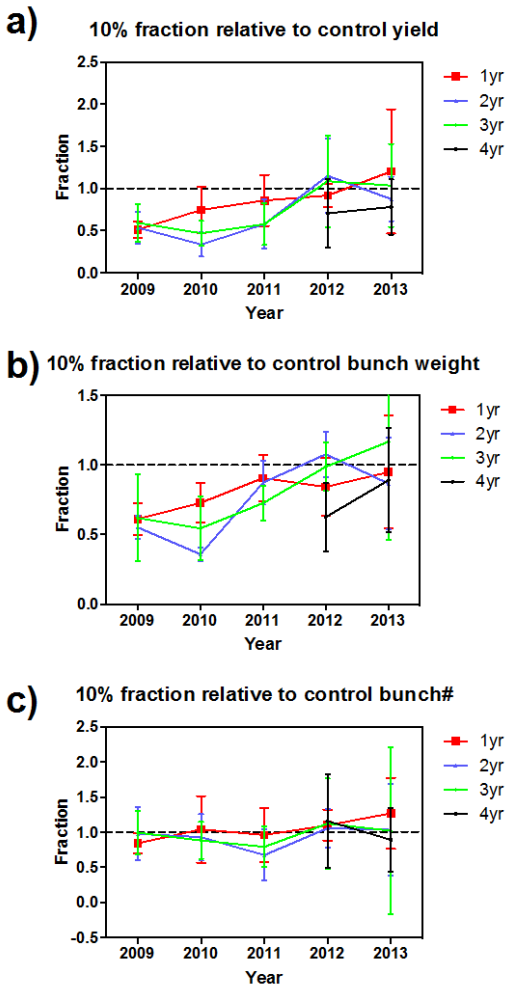

Figure 4 Relative yield (a), bunch weight (b) and number of bunches (c) expressed as a fraction of the respective control in each year plotted as a function of time for the 10% treatment. Mean +/- 95% confidence interval is shown. The number of years indicates the continuous numbers of seasons with reduced irrigation

20% treatment

The same series of Figures (Figs 5,6,7,8) are shown as per the 10% treatment and these largely reflect the same trends observed for the 10% treatment except that the yield reductions are smaller and generally above 50%, though after two years of consecutive deficit there was a reduction in yield to about 50% of the controls. Again this was not evident after three consecutive years, perhaps indicating a specific effect of the 2009-10 season combined with the deficit. There was also a trend for bunch number to decline in year 2 of deficit relative to controls, though this was not significant.

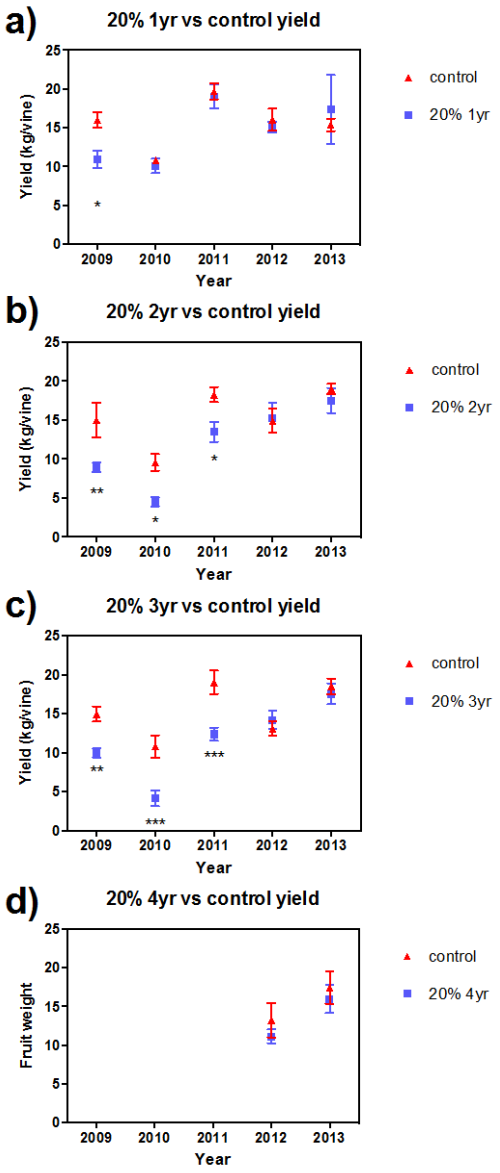

Figure 5 Yield for each season for the 20% irrigation treatment applied for one season (2008-09) then four seasons of recovery (a), two seasons (2008-09, 2009-10) then three seasons of recovery (b), three seasons (2008-09, 2009-10, 2010-11) then two years of recovery (c) or four seasons (2008-09, 2009-10, 2010-11, 2011-12) and one year of recovery (d) each compared to the respective controls (red triangle symbols). Mean +/- SEM is shown and level of significant difference within a year is indicated (*<0.05 **<0.01 *** <0.001 ****<0.0001, 2-way ANOVA with Holm Sidak's multiple comparison).

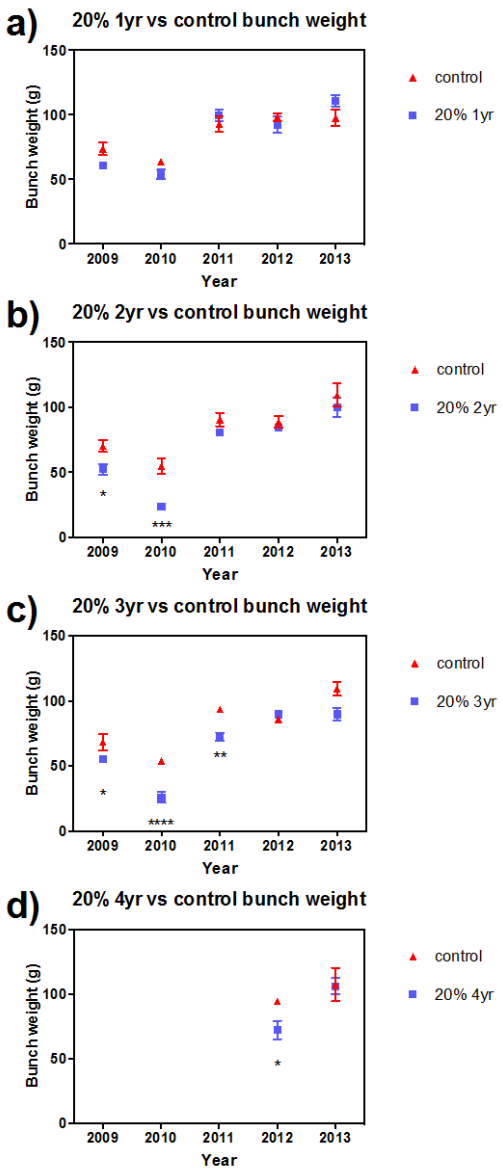

Figure 6 Bunch weight for each season for the 20% irrigation treatment applied for one season (08-09) then four seasons of recovery (a), two seasons (2008-09, 2009-10) then three seasons of recovery (b), three seasons (2008-09, 2009-10, 2010-11) then two years of recovery (c) or four seasons (2008-09, 2009-10, 2010-11, 2011-12) and one year of recovery (d) each compared to the respective controls (red triangle symbols). Mean +/- SEM is shown and level of significant difference within a year is indicated (*<0.05 **<0.01 *** <0.001 ****<0.0001, 2-way ANOVA with Holm Sidak's multiple comparison).

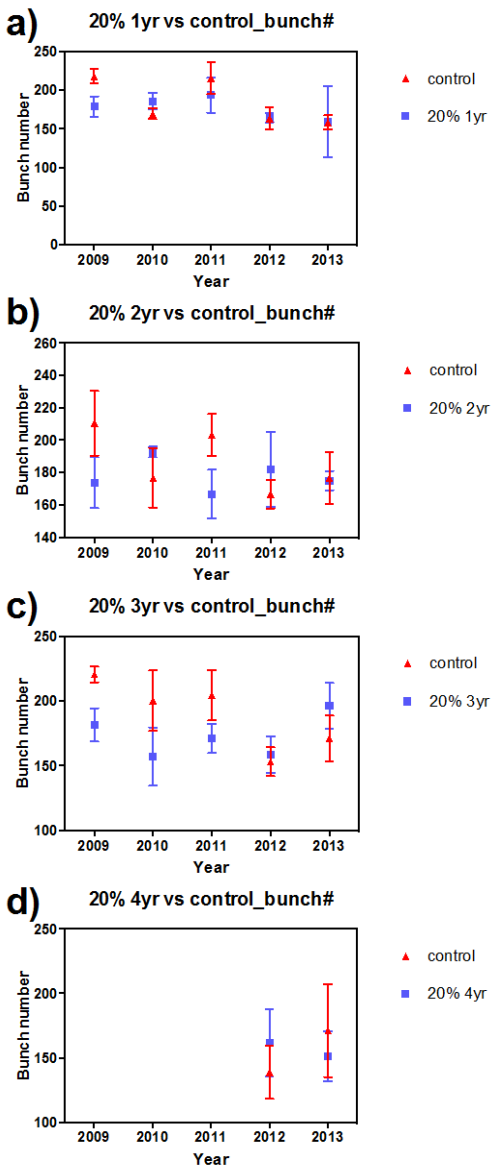

Figure 7 Bunch number for each season for the 20% irrigation treatment applied for one season (2008-09) then four seasons of recovery (a), two seasons (2008-09, 2009-10) then three seasons of recovery (b), three seasons (2008-09, 2009-10, 2010-11) then two years of recovery (c) or four seasons (2008-09, 2009-10, 2010-11, 2011-12) and one year of recovery (d) each compared to the respective controls (red triangle symbols). Mean +/- SEM is shown and level of significant difference within a year is indicated (*<0.05 **<0.01 *** <0.001 ****<0.0001, 2-way ANOVA with Holm Sidak's multiple comparison).

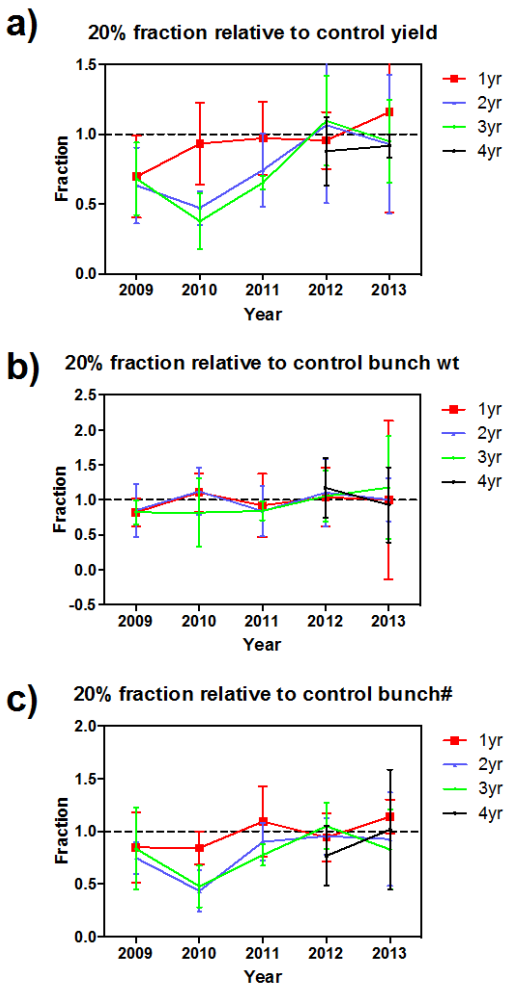

Figure 8 Relative yield (a), bunch weight (b) and number of bunches (c) expressed as a fraction of the respective control in each year plotted as a function of time for the 20% treatment. Mean +/- 95% confidence interval is shown. The number of years indicates the continuous numbers of seasons with reduced irrigation.

30% treatment

Figures (Figs 9,10,11,12) are shown as per the 10% and 20% treatments and these largely reflect the same trends observed except that the yield reductions are smaller (Figure 9, 12). Significant reductions were still observed in yield during the deficit years but there was no carry over into the recovery period except for the odd result of a significant increase in yield in the fourth year of recovery after one year of deficit (Figure 9a). In this case the yield increase was due to an increase in bunch number (Figure 11a), but generally bunch weight appeared to be the major contributor to the reduced yield as opposed to bunch number.

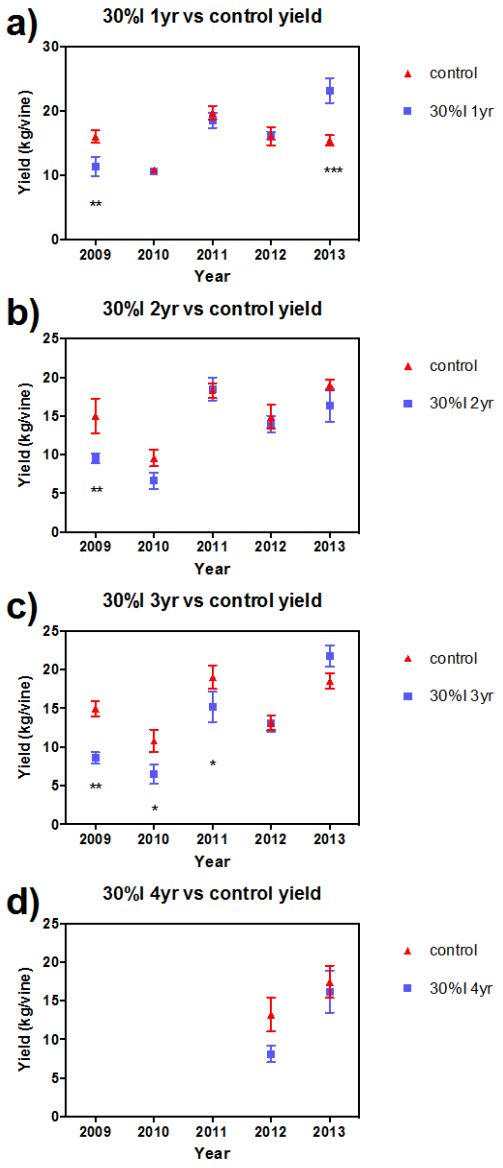

Figure 9 Yield for each season for the 30% irrigation treatment applied for one season (2008-09) then four seasons of recovery (a), two seasons (2008-09, 2009-10) then three seasons of recovery (b), three seasons (2008-09, 2009-10, 2010-11) then two years of recovery (c) or four seasons (2008-09, 2009-10, 2010-11, 2011-12) and one year of recovery (d) each compared to the respective controls (red triangle symbols). Mean +/- SEM is shown and level of significant difference within a year is indicated (*<0.05 **<0.01 *** <0.001 ****<0.0001, 2-way ANOVA with Holm Sidak's multiple comparison).

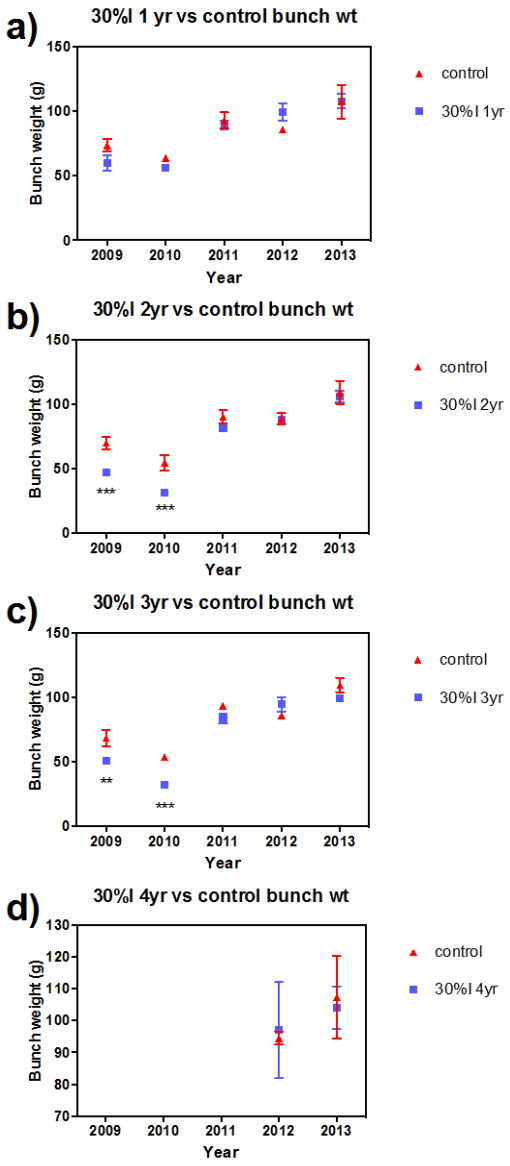

Figure 10 Bunch weight for each season for the 30% irrigation treatment applied for one season (08-09) then four seasons of recovery (a), two seasons (2008-09, 2009-10) then three seasons of recovery (b), three seasons (2008-09, 2009-10, 2010-11) then two years of recovery (c) or four seasons (2008-09, 2009-10, 2010-11, 2011-12) and one year of recovery (d) each compared to the respective controls (red triangle symbols). Mean +/- SEM is shown and level of significant difference within a year is indicated (*<0.05 **<0.01 *** <0.001 ****<0.0001, 2-way ANOVA with Holm Sidak's multiple comparison).

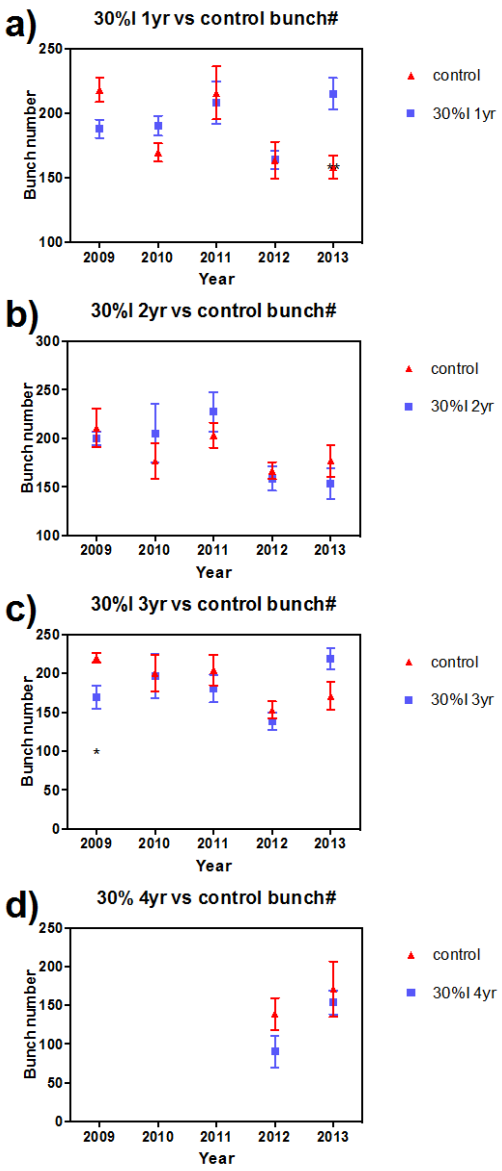

Figure 11 Bunch number for each season for the 30% irrigation treatment applied for one season (08-09) then four seasons of recovery (a), two seasons (2008-09, 2009-10) then three seasons of recovery (b), three seasons (2008-09, 2009-10, 2010-11) then two years of recovery (c) or four seasons (2008-09, 2009-10, 2010-11, 2011-12) and one year of recovery (d) each compared to the respective controls (red triangle symbols). Mean +/- SEM is shown and level of significant difference within a year is indicated (*<0.05 **<0.01 *** <0.001 ****<0.0001, 2-way ANOVA with Holm Sidak's multiple comparison).

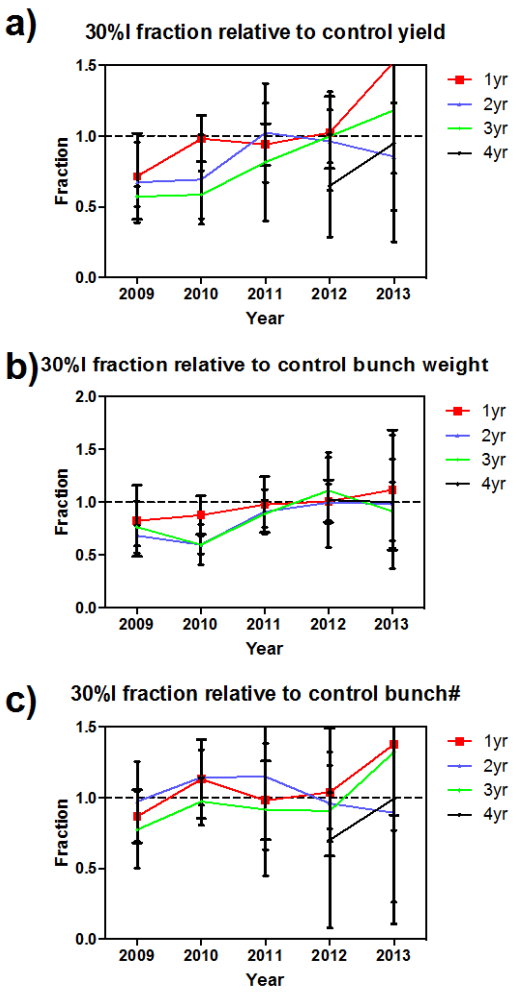

Figure 12 Relative yield (a), bunch weight (b) and number of bunches (c) expressed as a fraction of the respective control in each year plotted as a function of time for the 30% treatment. Mean +/- 95% confidence interval is shown. The number of years indicates the continuous numbers of seasons with reduced irrigation.

30% D treatment

As a reminder, the 30%D treatment consists of irrigations that are at the same frequency and time as the controls, but with reduced depth of irrigation. This contrasts with the 30% treatment given above that is reduced due to reduced frequency of irrigations. Figures (Figs 13,14,15,16) are shown as per previous treatments. Significant reductions are observed in yield during the deficit years (Figure 13), though not significant for 4 years of deficit (Figure 13d) and there was some carry-over of yield reduction and bunch weight into the recovery period for yield in the two year deficit (Figure 13b) and bunch weight for the three year deficit (Figure 14c). This contrasts to the 30% treatment suggesting that 30%D is generally more stressful. Again bunch weight appeared to be the major contributor to the reduced yield as opposed to bunch number (Figs 15, 16).

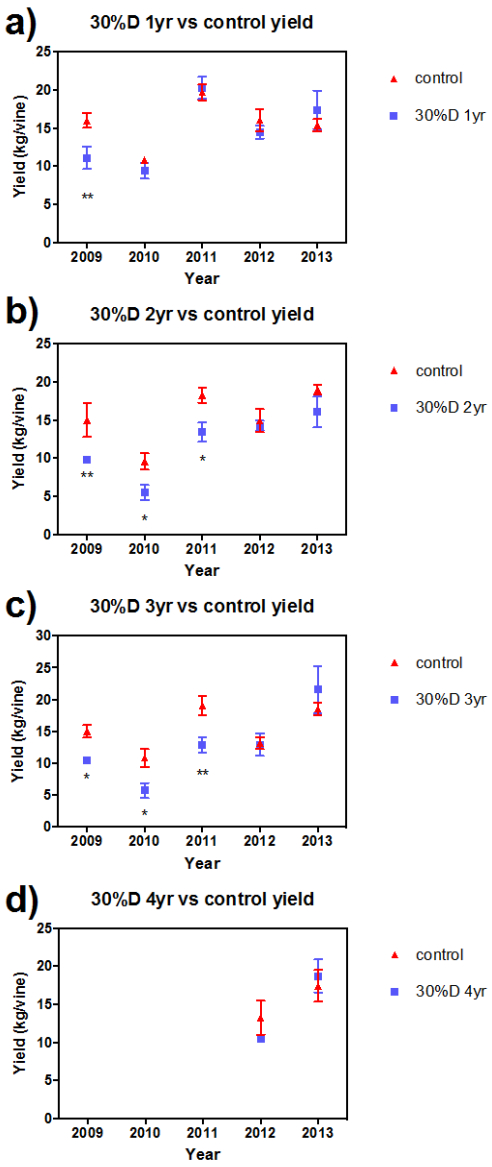

Figure 13 Yield for each season for the 30%D (reduced depth) irrigation treatment applied for one season (08-09) then four seasons of recovery (a), two seasons (2008-09, 2009-10) then three seasons of recovery (b), three seasons (2008-09, 2009-10, 2010-11) then two years of recovery (c) or four seasons (2008-09, 2009-10, 2010-11, 2011-12) and one year of recovery (d) each compared to the respective controls (red triangle symbols). Mean +/- SEM is shown and level of significant difference within a year is indicated (*<0.05 **<0.01 *** <0.001 ****<0.0001, 2-way ANOVA with Holm Sidak's multiple comparison).

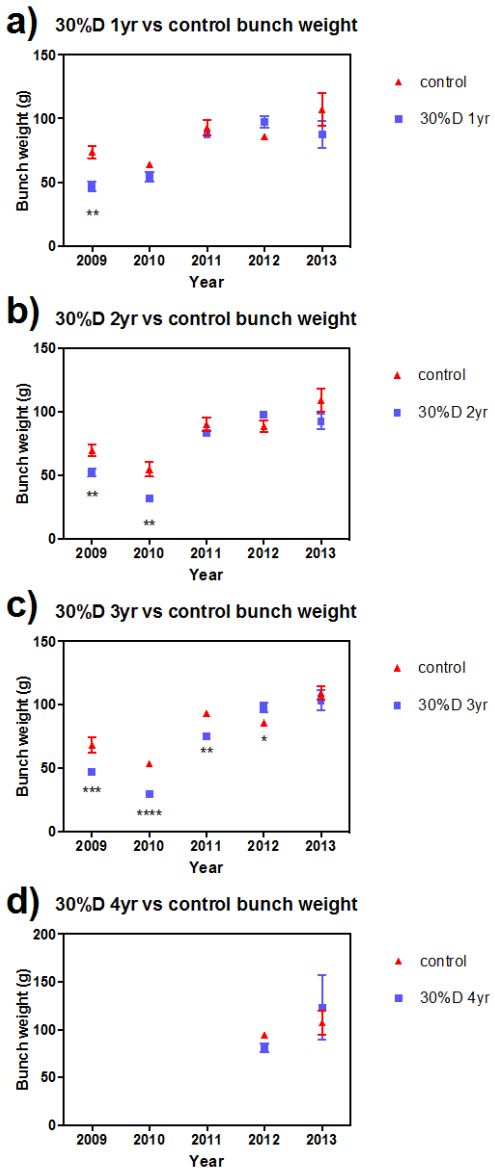

Figure 14 Bunch weight for each season for the 30%D (reduced depth) irrigation treatment applied for one season (08-09) then four seasons of recovery (a), two seasons (2008-09, 2009-10) then three seasons of recovery (b), three seasons (08-09, 09-10, 10-11) then two years of recovery (c) or four seasons (2008-09, 2009-10, 2010-11, 2011-12) and one year of recovery (d) each compared to the respective controls (red triangle symbols). Mean +/- SEM is shown and level of significant difference within a year is indicated (*<0.05 **<0.01 *** <0.001 ****<0.0001, 2-way ANOVA with Holm Sidak's multiple comparison).

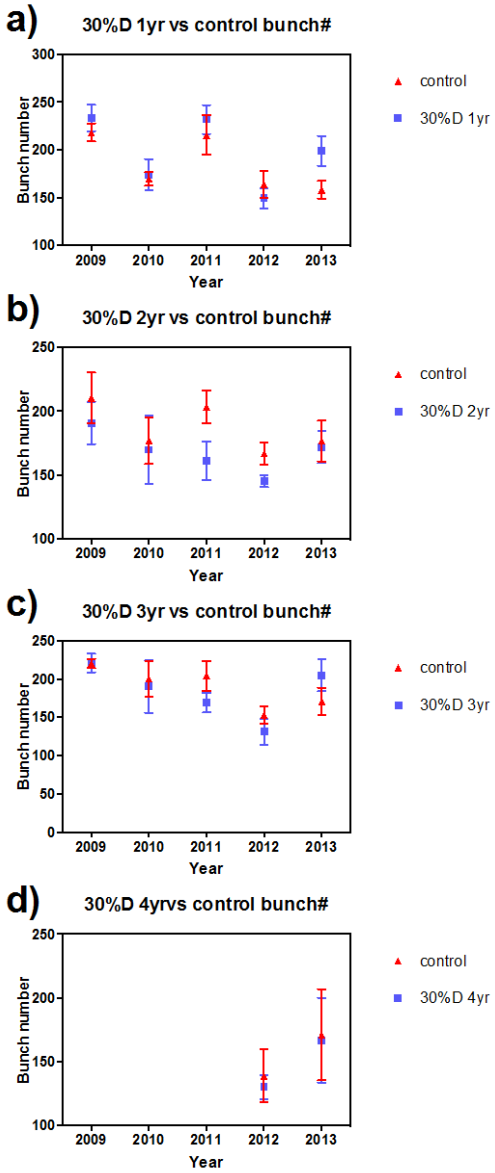

Figure 15 Bunch number for each season for the 30%D (reduced depth) irrigation treatment applied for one season (08-09) then four seasons of recovery (a), two seasons (2008-09, 2009-10) then three seasons of recovery (b), three seasons (2008-09, 2009-10, 2010-11) then two years of recovery (c) or four seasons (2008-09, 2009-10, 2010-11, 2011-12) and one year of recovery (d) each compared to the respective controls (red triangle symbols). Mean +/- SEM is shown and level of significant difference within a year is indicated (*<0.05 **<0.01 *** <0.001 ****<0.0001, 2-way ANOVA with Holm Sidak's multiple comparison).

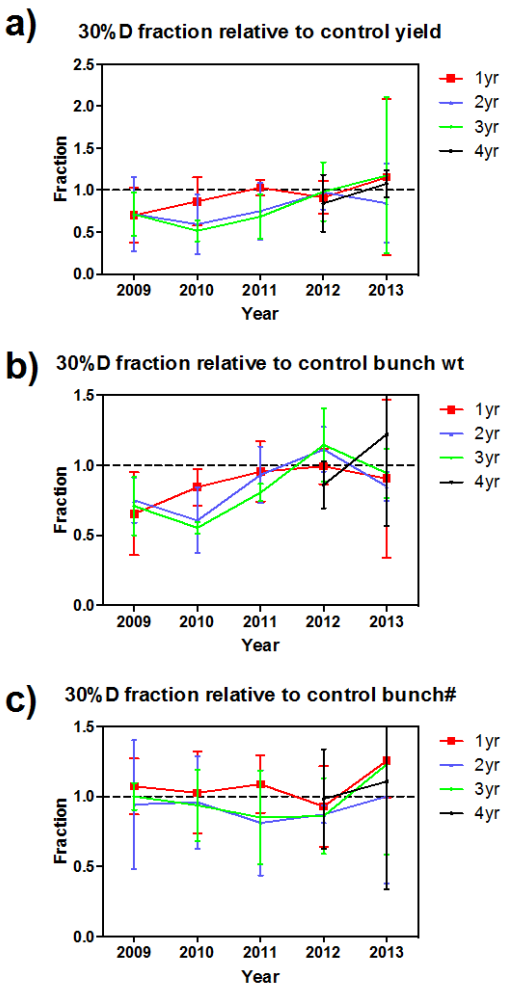

Figure 16 Relative yield (a), bunch weight (b) and number of bunches (c) expressed as a fraction of the respective control in each year plotted as a function of time for the 30%D (reduced depth) treatment. Mean +/- 95% confidence interval is shown. The number of years indicates the continuous numbers of seasons with reduced irrigation.

50% treatment

Figures (Figs 17,18,19,20) are shown as per previous treatments. Reductions are observed in yield during the deficit years (Figure 17), but not consistently across all years reflecting the less stressful effect of the 50% reduction. There was no carryover of yield reduction or bunch weight in the recovery periods except for the odd reduction in bunch weight in the second year of recovery after three years of deficit (Figure 18c). Again bunch weight appeared to be the major contributor to the reduced yield as opposed to bunch number (Figs 19, 20).

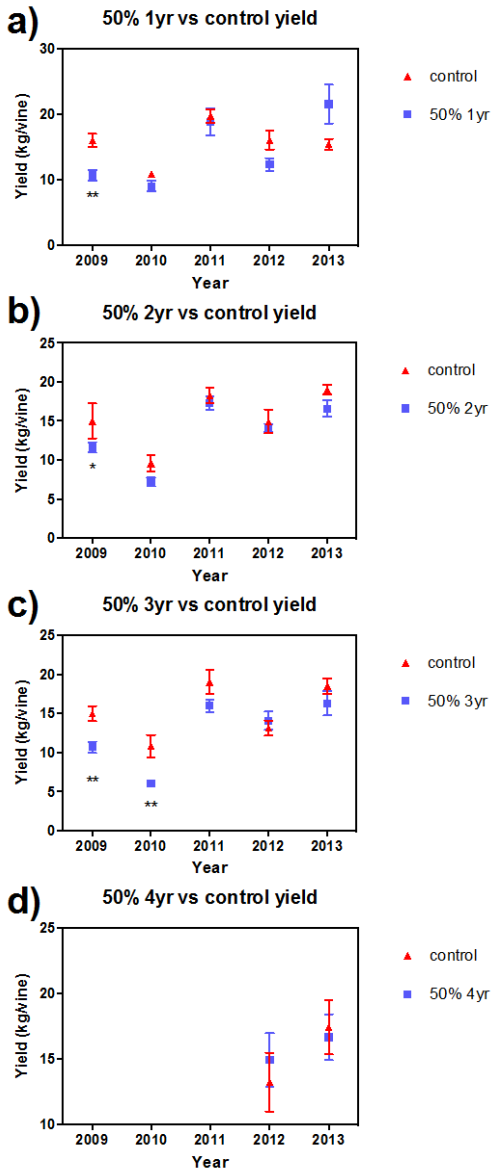

Figure 17 Yield for each season for the 50% irrigation treatment applied for one season (2008-09) then four seasons of recovery (a), two seasons (2008-09, 2009-10) then three seasons of recovery (b), three seasons (2008-09, 2009-10, 2010-11) then two years of recovery (c) or four seasons (2008-09, 2009-10, 2010-11, 2011-12) and one year of recovery (d) each compared to the respective controls (red triangle symbols). Mean +/- SEM is shown and level of significant difference within a year is indicated (*<0.05 **<0.01 *** <0.001 ****<0.0001, 2-way ANOVA with Holm Sidak's multiple comparison).

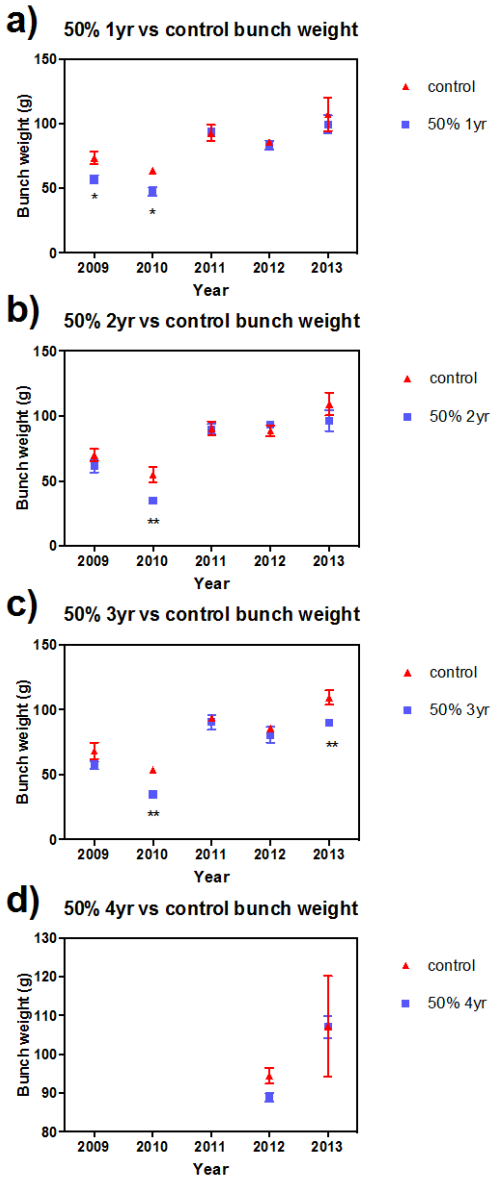

Figure 18 Bunch weight for each season for the 50% irrigation treatment applied for one season (2008-09) then four seasons of recovery (a), two seasons (2008-09, 2009-10) then three seasons of recovery (b), three seasons (2008-09, 2009-10, 2010-11) then two years of recovery (c) or four seasons (2008-09, 2009-10, 2010-11, 2011-12) and one year of recovery (d) each compared to the respective controls (red triangle symbols). Mean +/- SEM is shown and level of significant difference within a year is indicated (*<0.05 **<0.01 *** <0.001 ****<0.0001, 2-way ANOVA with Holm Sidak's multiple comparison).

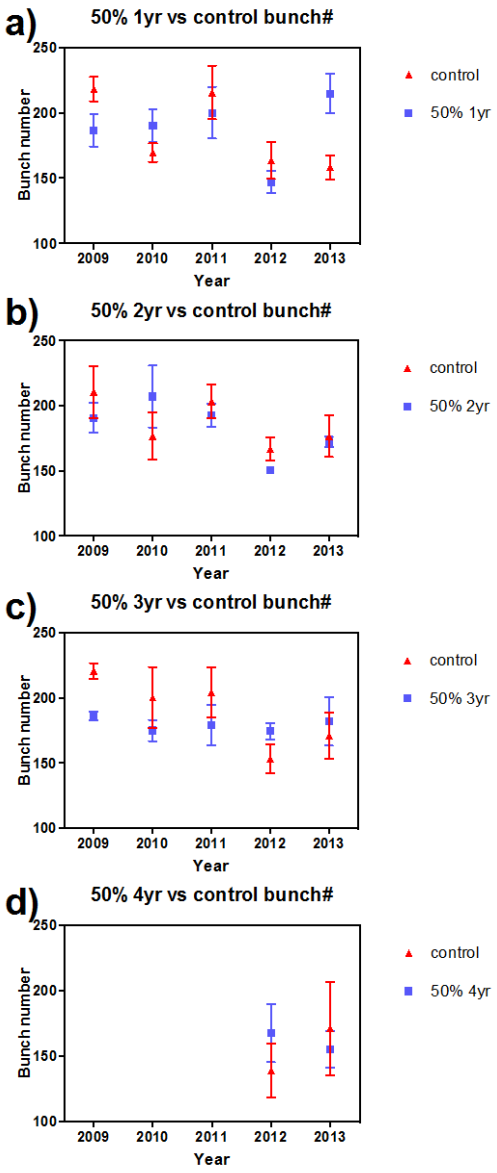

Figure 19 Bunch number for each season for the 50% irrigation treatment applied for one season (08-09) then four seasons of recovery (a), two seasons (2008-09, 2009-10) then three seasons of recovery (b), three seasons (2008-09, 2009-10, 2010-11) then two years of recovery (c) or four seasons (2008-09, 2009-10, 2010-11, 2011-12) and one year of recovery (d) each compared to the respective controls (red triangle symbols). Mean +/- SEM is shown and level of significant difference within a year is indicated (*<0.05 **<0.01 *** <0.001 ****<0.0001, 2-way ANOVA with Holm Sidak's multiple comparison).

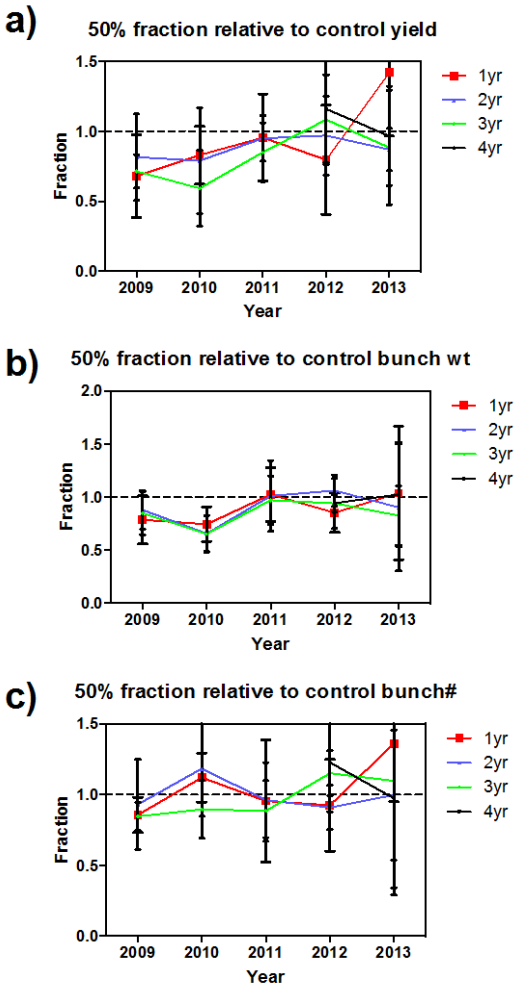

Figure 20 Relative yield (a), bunch weight (b) and number of bunches (c) expressed as a fraction of the respective control in each year plotted as a function of time for the 50% treatment. Mean +/- 95% confidence interval is shown. The number of years indicates the continuous numbers of seasons with reduced irrigation.

Conclusions

It is clear from the data for yield components that the length of time that the deficit occurs is an irrelevant factor in terms of the time for recovery, since there was no difference in the time for recovery of yield components between one year of deficit or four years of deficit. This is a surprising result and has important ramifications for predicting the impacts of reduced irrigation options under water restrictions. In each case it was more common that recovery of yield occurred completely during the first year of full irrigation, even for the more extreme 10% treatment, though there was a (non-significant) trend for the yield to be reduced in the first year of recovery in the 10% treatment. This trend will be further examined in relation to the impacts on general vine productivity. The effects of the deficit treatments on yield seemed to be entirely due to bunch weight rather than bunch number. In part the bunch number is dependent on the number of buds left at pruning, which was similar in each year. Therefore the lack of effect of deficit on bunch number may indicate that there was no effect on bud fruitfulness. This result is similar to that observed for Merlot over a three year deficit regime where 35% and 70% of standard irrigation had no

significant effect on bunches per vine except for the 35% treatment in the first season, but bunch weight was the main contributor to reduced yield (Lopez, et al. 2007). The data from Chaves et al (2010) for Moscatel and Castela˜o are similar to those we observed in that it was mainly bunch weight that contributed to yield reduction under 50% deficit irrigation. This is in contrast to (Matthews and Anderson 1989), though in their data it was clear that cluster weight was the main factor and cluster number per vine had a relative small effect.

Berry weight and berries per bunch as a function of time and after variable periods of water stress and recovery.

As per the previous section the data will be presented for each irrigation treatment in the order of increasing irrigation (i.e. from 10%, 20% etc). In each case two Figures are presented providing: 1) Mean berry weight and, 2) Mean berries per bunch. Each of the figures will be provided for: a) one year of deficit and two years of recovery, b) two years of deficit and one year of recovery, c) three years of deficit. The collection of these data was not extended into the fourth and fifth years due to the general trends observed that indicated that no further new information would be obtained and in view of the conclusions drawn from the sections above. The data are provided here for completeness.

10% treatment

Figure 21 shows mean berry weight versus year of treatment between 2009 and 2011. Figure 21a shows the effect of one year of deficit followed by two years of recovery, Figure 21b shows two years of deficit and one year of recovery, Figure 21c shows three years of deficit. Significant differences between treatment and controls are indicated (2-way ANOVA with Holm Sidak's multiple comparison test). Mean berry weight is reduced by almost 50% by the 10% treatment and this occurred for both one year and two years of deficit (Figure 21a, b), but surprisingly not in the third year after three years of deficit (Figure 21c). There was no indication of carry-over of reduction in berry weight in the recovery year after both one year and two years of deficit.

Figure 22 shows the corresponding data for berries per bunch where the 10% treatment resulted in a reduction relative to controls, though this was only significant for year 1 of the two and three year deficits (Figure 22b,c). For the two year deficit treatment there was carry-over of reduced berries per bunch in the recovery year (Figure 22b). This was not seen for the two years of deficit (Figure 2b) contrasting with the total yield data. Again surprisingly there was no carry-over in bunch weight reduction in the years of recovery even after three and four years of continual deficit irrigation (Figure 2c,d).

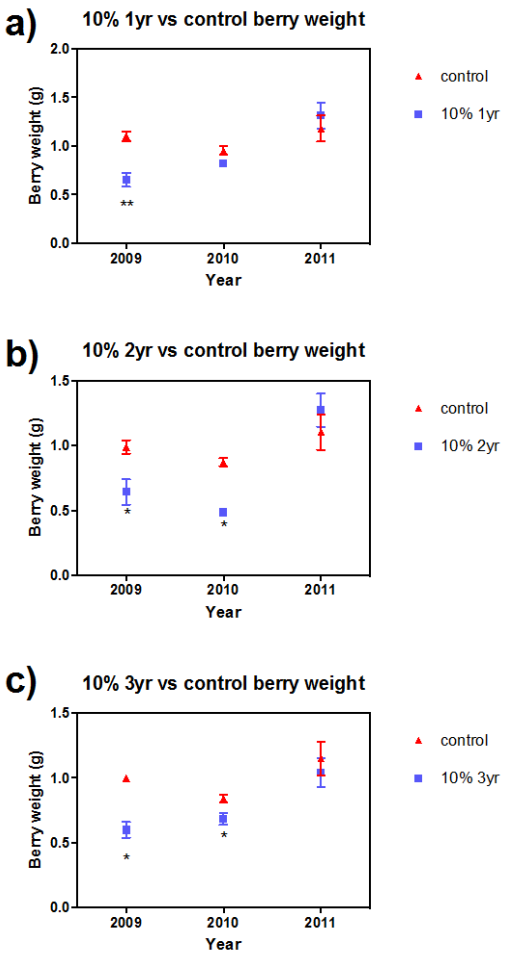

Figure 21 Berry weight for the 10% irrigation treatment applied for one season (2008-09) then two seasons of recovery (a), two seasons (2008-09, 2009-10) then one season of recovery (b), three seasons (2008-09, 2009-10, 2010-11) (c) each compared to the respective controls (red triangle symbols) plotted over time. Mean +/- SEM is shown and level of significant difference within a year is indicated (*<0.05 **<0.01 *** <0.001 ****<0.0001, 2-way ANOVA with Holm Sidak's multiple comparison).

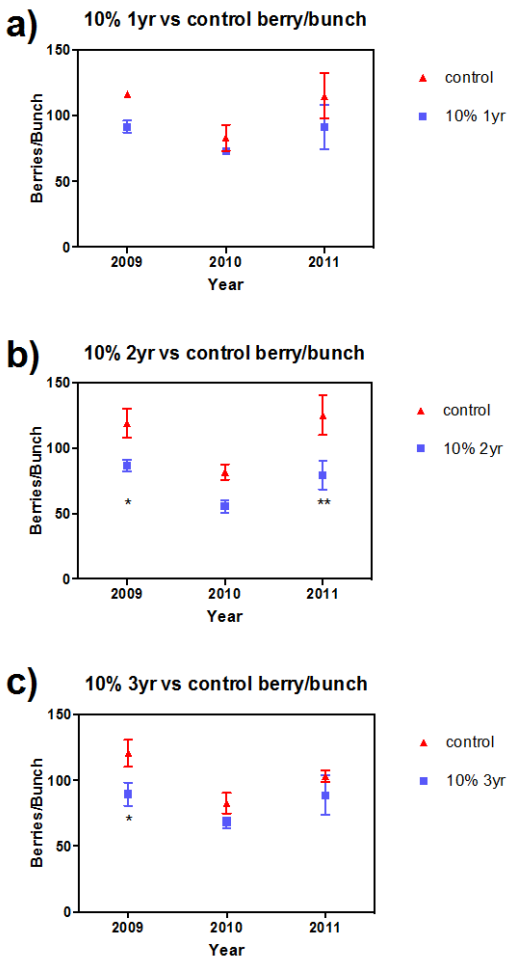

Figure 22 Berries per bunch for the 10% irrigation treatment applied for one season (2008-09) then two seasons of recovery (a), two seasons (2008-09, 2009-10) then one season of recovery (b), three seasons (2008-09, 2009-10, 2010-11) (c) each compared to the respective controls (red triangle symbols) plotted over time. Mean +/- SEM is shown and level of significant difference within a year is indicated (*<0.05 **<0.01 *** <0.001 ****<0.0001, 2-way ANOVA with Holm Sidak's multiple comparison).

20% treatment

Figure 23 and Figure 24 show the corresponding data for the 30% treatment for mean berry weight and berries per bunch. The effects are similar to those observed for the 10% treatment though the reduction in berry weight due to the deficit is less. Berries per bunch is reduced during the deficit period but the only significantly reduction occurred in the first year of recovery after two years of deficit.

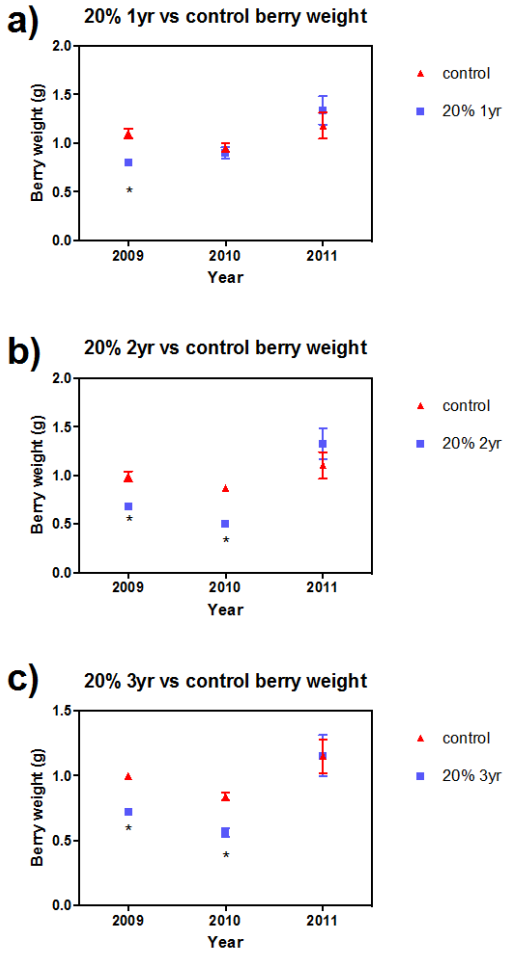

Figure 23 Berry weight for the 20% irrigation treatment applied for one season (2008-09) then two seasons of recovery (a), two seasons (2008-09, 2009-10) then one season of recovery (b), three seasons (2008-09, 2009-10, 2010-11) (c) each compared to the respective controls (red triangle symbols) plotted over time. Mean +/- SEM is shown and level of significant difference within a year is indicated (*<0.05 **<0.01 *** <0.001 ****<0.0001, 2-way ANOVA with Holm Sidak's multiple comparison).

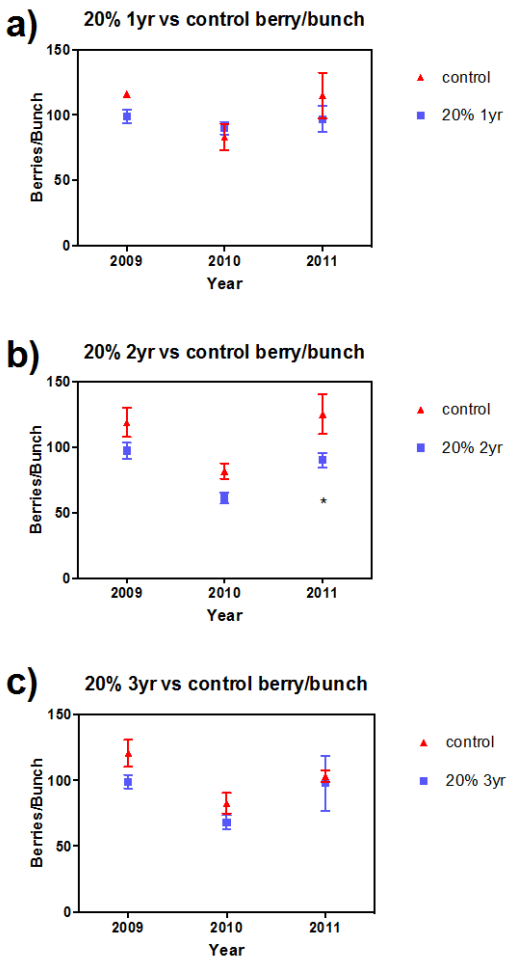

Figure 24 Berries per bunch for the 20% irrigation treatment applied for one season (2008-09) then two seasons of recovery (a), two seasons (2008-09, 2009-10) then one season of recovery (b), three seasons (2008-09, 2009-10, 2010-11) (c) each compared to the respective controls (red triangle symbols) plotted over time. Mean +/- SEM is shown and level of significant difference within a year is indicated (*<0.05 **<0.01 *** <0.001 ****<0.0001, 2-way ANOVA with Holm Sidak's multiple comparison).

30% treatment

Figure 25 and Figure 26 show the corresponding data for the 30% treatment for mean berry weight and berries per bunch. The effects are similar to those observed for the previous treatments though the reduction in berry weight due to the deficit is less. Berries per bunch is reduced during the deficit period but the only significantly in the second year of the three year deficit and a significant reduction occurred in the first year of recovery after two years of deficit as observed in the 20% treatment.

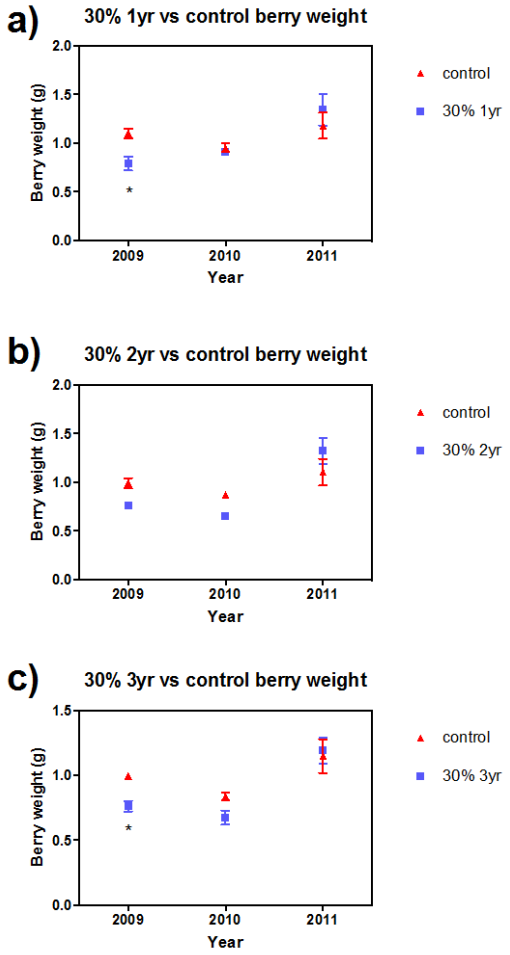

Figure 25 Berry weight for the 30% irrigation treatment applied for one season (2008-09) then two seasons of recovery (a), two seasons (2008-09, 2009-10) then one season of recovery (b), three seasons (2008-09, 2009-10, 2010-11) (c) each compared to the respective controls (red triangle symbols) plotted over time. Mean +/- SEM is shown and level of significant difference within a year is indicated (*<0.05 **<0.01 *** <0.001 ****<0.0001, 2-way ANOVA with Holm Sidak's multiple comparison).

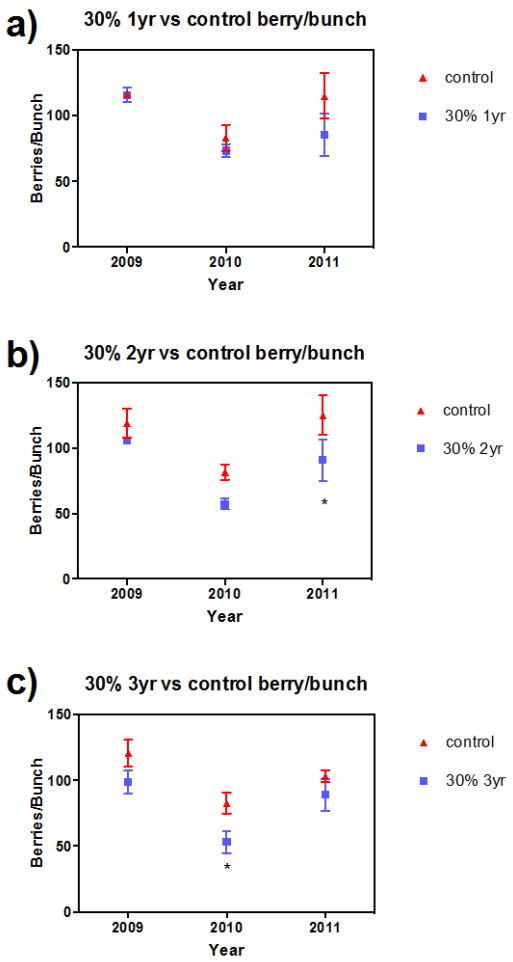

Figure 26 Berries per bunch for the 30% irrigation treatment applied for one season (2008-09) then two seasons of recovery (a), two seasons (2008-09, 2009-10) then one season of recovery (b), three seasons (2008-09, 2009-10, 2010-11) (c) each compared to the respective controls (red triangle symbols) plotted over time. Mean +/- SEM is shown and level of significant difference within a year is indicated (*<0.05 **<0.01 *** <0.001 ****<0.0001, 2-way ANOVA with Holm Sidak's multiple comparison).

30%D treatment

Figure 27 and Figure 28 show the corresponding data for the 30D% treatment for mean berry weight and berries per bunch respectively. The effects are similar to those observed for the 30% treatment though the reduction in berry weight due to the deficit is generally larger and more often significant than that of the 30%. However, berries per bunch is not generally reduced during the deficit period but a significant reduction occurred in the first year of recovery after two years of deficit (Figure 28b) as observed in the 10%, 20% and 30% treatments.

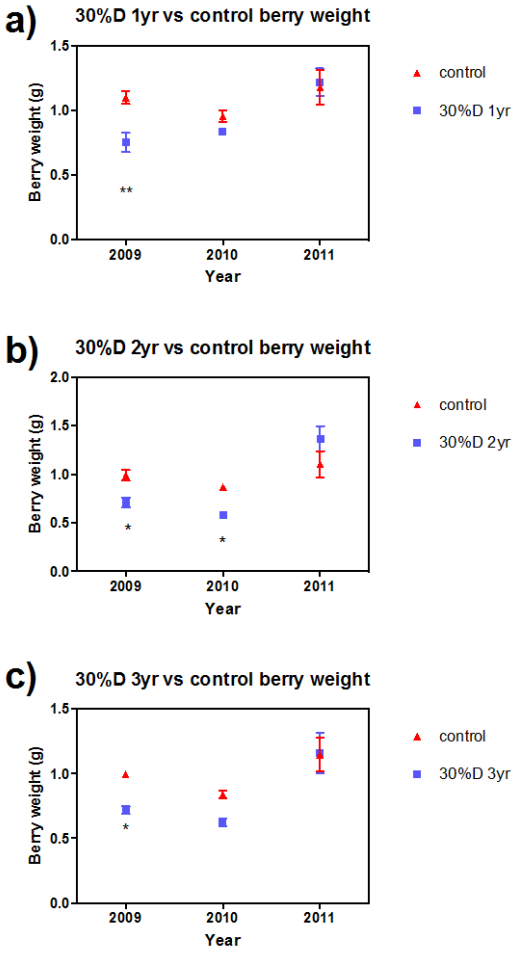

Figure 27 Berry weight for the 30%D irrigation treatment applied for one season (2008-09) then two seasons of recovery (a), two seasons (2008-09, 2009-10) then one season of recovery (b), three seasons (2008-09, 2009-10, 2010-11) (c) each compared to the respective controls (red triangle symbols) plotted over time. Mean +/- SEM is shown and level of significant difference within a year is indicated (*<0.05 **<0.01 *** <0.001 ****<0.0001, 2-way ANOVA with Holm Sidak's multiple comparison).

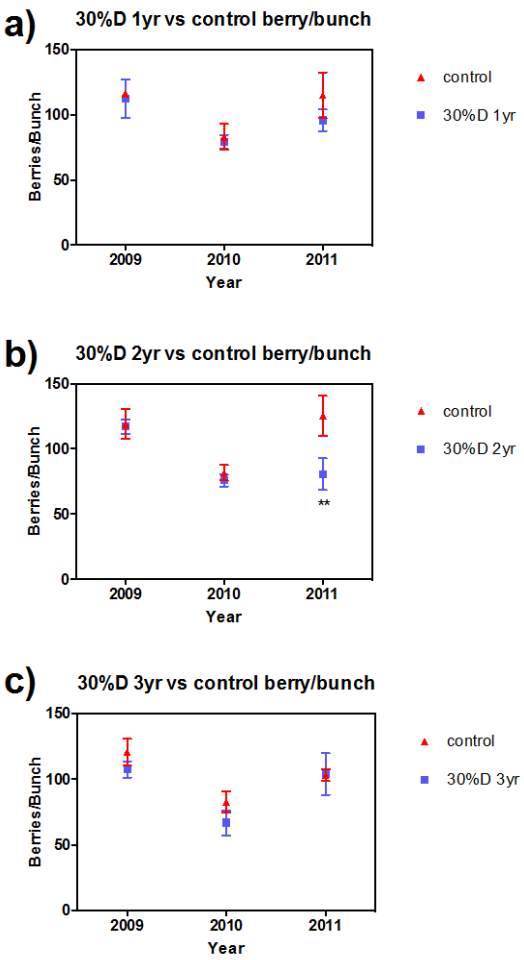

Figure 28 Berries per bunch for the 30%D irrigation treatment applied for one season (2008-09) then two seasons of recovery (a), two seasons (2008-09, 2009-10) then one season of recovery (b), three seasons (2008-09, 2009-10, 2010-11) (c) each compared to the respective controls (red triangle symbols) plotted over time. Mean +/- SEM is shown and level of significant difference within a year is indicated (*<0.05 **<0.01 *** <0.001 ****<0.0001, 2-way ANOVA with Holm Sidak's multiple comparison).

50% treatment

Figure 29 and Figure 30 show the corresponding data for the 50% treatment for mean berry weight and berries per bunch respectively. There was no significant effect of this treatment on either mean berry weight or berries per bunch, though berry weight appeared to be reduced during the deficit periods (Figure 29).

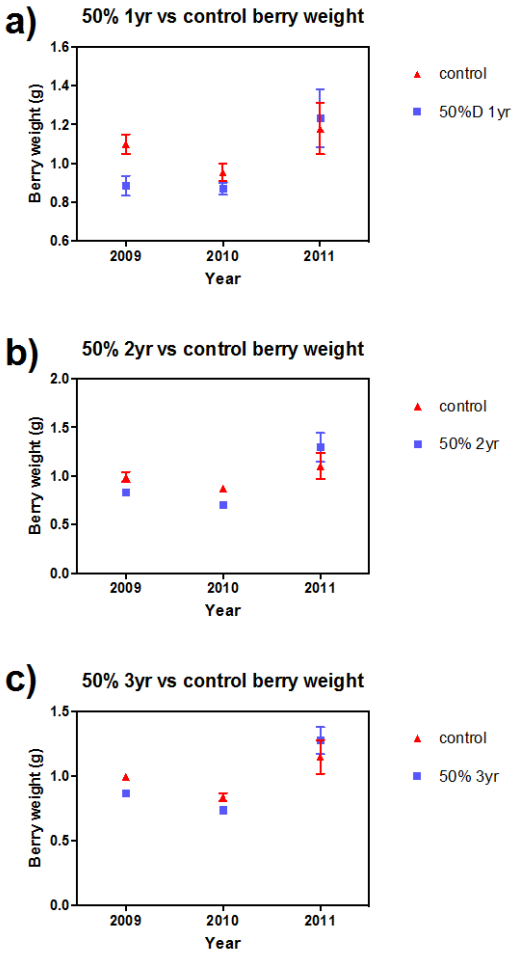

Figure 29 Berry weight for the 50% irrigation treatment applied for one season (2008-09) then two seasons of recovery (a), two seasons (2008-09, 2009-10) then one season of recovery (b), three seasons (2008-09, 2009-10, 2010-11) (c) each compared to the respective controls (red triangle symbols) plotted over time. Mean +/- SEM is shown and level of significant difference within a year is indicated (*<0.05 **<0.01 *** <0.001 ****<0.0001, 2-way ANOVA with Holm Sidak's multiple comparison).

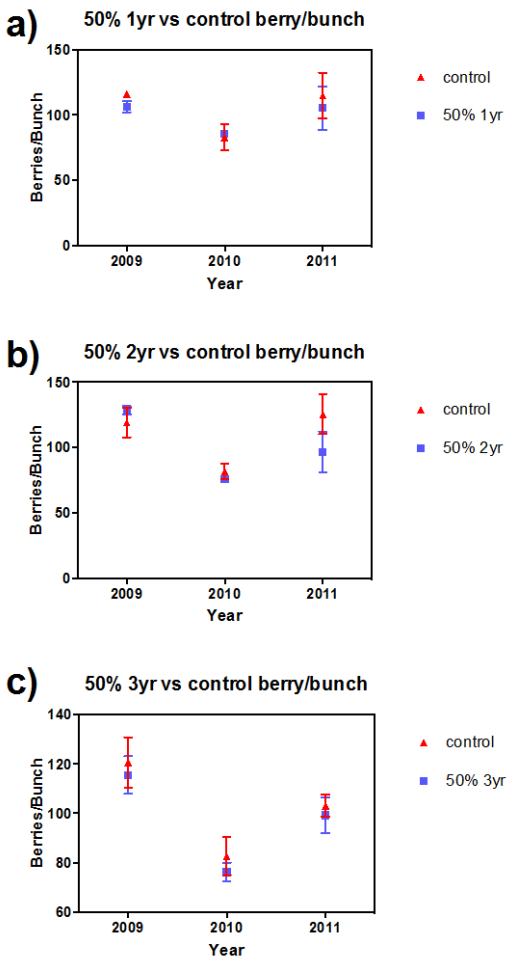

Figure 30 Berries per bunch for the 50% irrigation treatment applied for one season (2008-09) then two seasons of recovery (a), two seasons (2008-09, 2009-10) then one season of recovery (b), three seasons (2008-09, 2009-10, 2010-11) (c) each compared to the respective controls (red triangle symbols) plotted over time. Mean +/- SEM is shown and level of significant difference within a year is indicated (*<0.05 **<0.01 *** <0.001 ****<0.0001, 2-way ANOVA with Holm Sidak's multiple comparison).

Contribution of yield components to reduced yield under deficit

The reduction in bunch weights, which was the main component of the yield reduction due to the deficits (Figs 1 to 20, Figure 31), can be attributed to both reduced berry weight and reduced number of berries per bunch (Figure 32). This is similar to the conclusions drawn from the data of (Matthews and Anderson 1989) where Cabernet Franc on Ganzin A X R1 rootstock was examined under full deficit over three years at about the same treatment as our 20% based on the measured water potentials. However they also found that number of bunches per vine was correlated positively with yield in contrast to our results. Figure 31 provides the correlations between yield and bunch weight (Figure 31a) and bunch number (Figure 31b) for the 10% deficit and recovery treatments over all years and clearly illustrates the dominant effect of bunch weight on yield. Similar results are obtained for the other treatments (not shown). Bunch weight is determined by both berry weight and number of berries per bunch as is illustrated for the 10% deficit and recoveries in

Figure 32. Interestingly (Shellie 2014) did not observe a significant effect of long term deficits on berries per bunch for Merlot, suggesting a varietal difference between Merlot and Chardonnay in this respect. Their study however did observe a strong reduction in berry weight with increasing deficit as we have observed. An interesting observation from the data in Figures 31 and 32 is that the effect of deficit irrigation on the yield components appears to be similar to the year-to-year and plot-to-plot differences in the controls and recovery vines. This is indicated by the data being well fit by the same linear regression lines.

a)

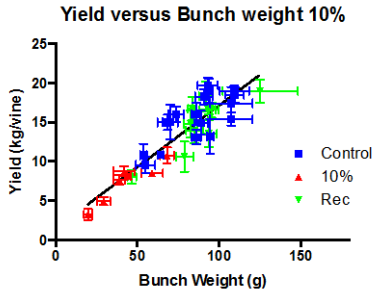

	Yield All
Best-fit values	
Slope	0.1573 ± 0.01349
Y-intercept when X=0.0	1.435 ± 1.094
X-intercept when Y=0.0	-9.123
1/slope	6.357
95% Confidence Intervals	
Slope	0.1298 to 0.1848
Y-intercept when X=0.0	-0.7952 to 3.665
X-intercept when Y=0.0	-28.03 to 4.335
Goodness of Fit	
R square	0.8094
Sy.x	1.943
Is slope significantly non-zero?	
F	135.9
DFn, DFd	1.000, 32.00
P value	< 0.0001
Deviation from zero?	Significant
Data	
Number of X values	34
Maximum number of Y replicates	1
Total number of values	34
Number of missing values	0
Equation	Y = 0.1573*X + 1.435

b)

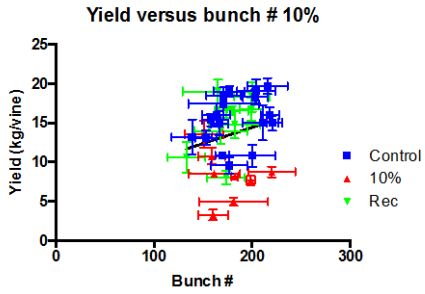

	Yield All
Best-fit values	
Slope	0.04097 ± 0.03257
Y-intercept when X=0.0	6.232 ± 5.895
X-intercept when Y=0.0	-152.1
1/slope	24.41
95% Confidence Intervals	
Slope	-0.02540 to 0.1073
Y-intercept when X=0.0	-5.780 to 18.24
X-intercept when Y=0.0	-infinity to 54.23
Goodness of Fit	
R square	0.04712
Sy.x	4.345
Is slope significantly non-zero?	
F	1.583
DFn, DFd	1.000, 32.00
P value	0.2175
Deviation from zero?	Not Significant

Figure 31 Contribution to yield of bunch weight (a) and number of bunches (b) shown for all 10%, 10% recoveries and controls. (a) Yield as a function of bunch weight where the details of the fitted regression line are shown in the adjacent table. (b) Yield as a function of bunch number where the details of the regression (not significant) are shown in the adjacent table. Means are shown +/- SEM.

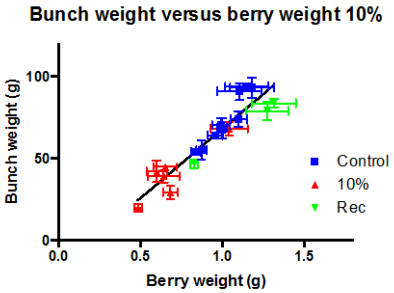

	Bunch Wt All
Best-fit values	
Slope	84.57 ± 8.143
Y-intercept when X=0.0	-16.58 ± 7.792
X-intercept when Y=0.0	0.1961
1/slope	0.01182
95% Confidence Intervals	
Slope	67.31 to 101.8
Y-intercept when X=0.0	-33.10 to -0.06648
X-intercept when Y=0.0	0.0009799 to 0.3277
Goodness of Fit	
R square	0.8708
Sy.x	8.160
Is slope significantly non-zero?	
F	107.9
DFn, DFd	1.000, 16.00
P value	< 0.0001
Deviation from zero?	Significant
Data	
Number of X values	18
Maximum number of Y replicates	1
Total number of values	18
Number of missing values	0
Equation	Y = 84.57*X - 16.58

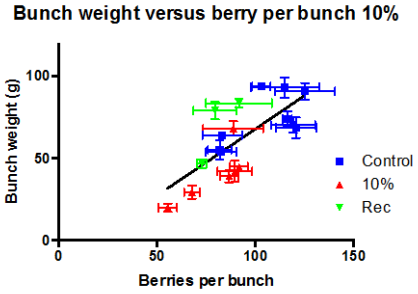

	Bunch Wt All
Best-fit values	
Slope	0.8123 ± 0.1905
Y-intercept when X=0.0	-13.56 ± 18.06
X-intercept when Y=0.0	16.69
1/slope	1.231
95% Confidence Intervals	
Slope	0.4084 to 1.216
Y-intercept when X=0.0	-51.84 to 24.73
X-intercept when Y=0.0	-59.79 to 43.16
Goodness of Fit	
R square	0.5319
Sy.x	15.54
Is slope significantly non-zero?	
F	18.18
DFn, DFd	1.000, 16.00
P value	0.0006
Deviation from zero?	Significant
Data	
Number of X values	18
Maximum number of Y replicates	1
Total number of values	18
Number of missing values	0
Equation	Y = 0.8123*X - 13.56

Figure 32 Contribution to bunch weight of mean berry weight (a) and berries per bunch (b) shown for al 10%, 10% recoveries and controls. (a) Bunch weight as a function of mean berry weight where the details of the fitted regression line are shown in the adjacent table. (b) Bunch weight as a function of berries per bunch where the details of the regression are shown in the adjacent table. Means are shown +/- SEM.

Vine biomass and pruning weights as a function of time and after variable periods of water stress and recovery.

Vine biomass parameters

During the second year of the trial an intensive field campaign was undertaken to examine above ground biomass in detail for a selection of the deficit treatments and recoveries after one year. Figure 33 provides a summary of the data collected, which included; average cane length (Figure 33a) and base width (Figure 33b), leaf and stem fresh weight per shoot (Figure 33c,d), fruit fresh weight (Figure 33e) and total fresh weight per shoot (Figure 33f), leaf water fraction (Figure 33g) and bunch number per shoot (Figure 33h). For each parameter except for leaf water fraction and bunch number there was a significant reduction observed for the 10% deficit treatment. Despite significant effects on yield (see above) for the 30% and 30%D treatments, there was no

significant effect of these treatments on shoot parameters, though fruit fresh weight was reduced consistent with the yield observations. Examination of the relationship between fruit weight per shoot and leaf weight per shoot for selected deficit treatments indicated that they were linearly related (Figure 34a). Interestingly the slopes of the relationships were not significantly different, but the intercepts (i.e. weight of fruit per shoot at zero leaf weight) were significantly different (Figure 34b). The deficit treatments all intersected near the origin while the recovery and controls had a positive offset. This may indicate a limitation at low leaf weight per shoot on obtaining carbohydrate reserves from other parts of the vine for berry growth under water deficit.

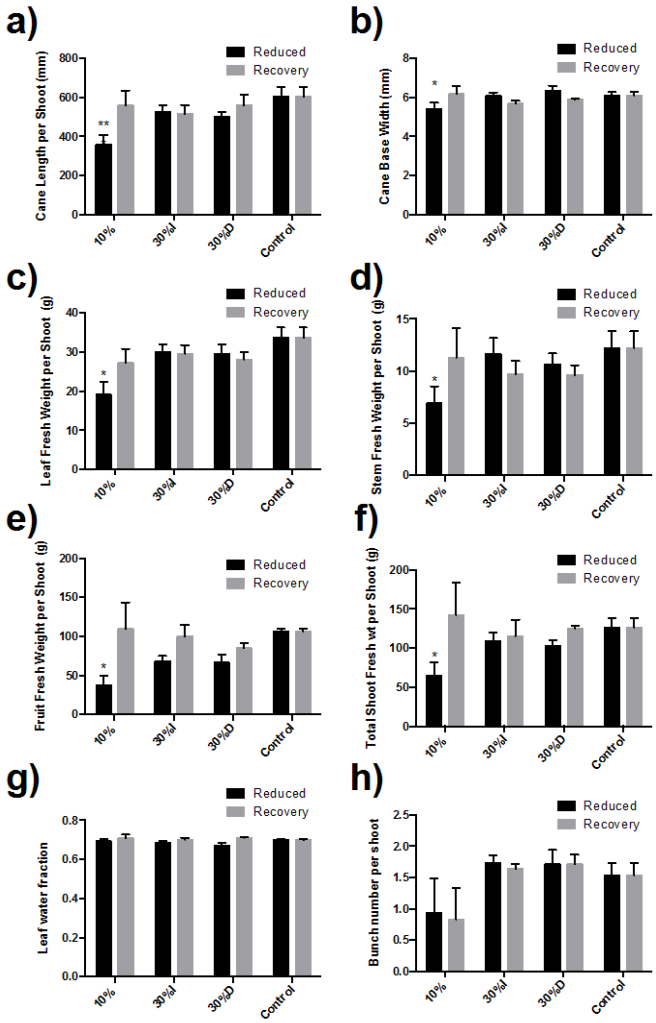

Figure 33 Above ground biomass components for a selection of the treatments measured in seasons 2009-10 (10%, 30%, 30%D and controls) and respective recoveries after one year. (a) Cane length per shoot, (b) Cane base width, (c) Leaf fresh weight per shoot, (d) Stem fresh weight per shoot, (e) Fruit fresh weight per shoot, (f) Total shoot fresh weight per shoot, (g) Leaf water fraction, (h) Bunch number per shoot. Mean +/- SEM are shown and level of significant difference to control indicated (2-way ANOVA with Fishers LSD).

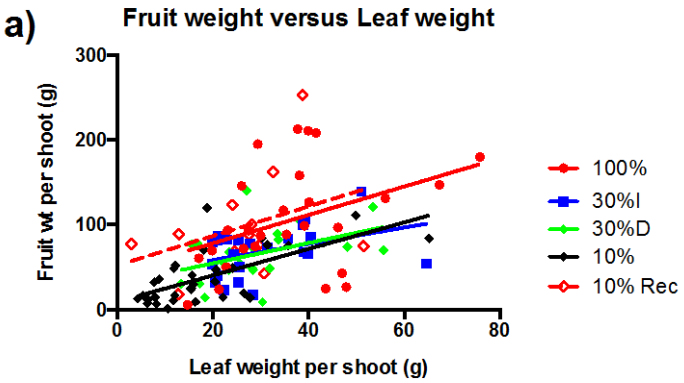

b)

Are the slopes equal?
F = 0.2168. DFn=4 DFd=106
P=0.9286

If the overall slopes were identical, there is a 93% chance of randomly choosing data points with slopes this different. You can conclude that the differences between the slopes are not significant.

Since the slopes are not significantly different, it is possible to calculate one slope for all the data. The pooled slope equals 1.46428

Are the elevations or intercepts equal?
F = 5.43724. DFn=4 DFd=110
P=0.0005

If the overall elevations were identical, there is a 0.05% chance of randomly choosing data points with elevations this different. You can conclude that the differences between the elevations are extremely significant.

Figure 34 Relationship between fruit fresh weight and leaf fresh weight for each of the selected treatments shown in Figure 33. The regressions shown in (a) were tested for differences between the treatments. Each point is for a single vine. (b) The slopes were not significantly different, but the intercepts were significantly larger for the control and recovery vines.

Pruning weights

Pruning weights were obtained for all treatments and recoveries over the five years of the trial. These are summarised in Figure 35. In this Figure the red bars are the deficit treatments for 1,2,3 or 4 years, and these can be compared with the recoveries (adjacent bars) for each of the deficit treatments. It is evident that pruning weights are strongly affected by the higher deficits (i.e. 10% 20% and 30%D). This can be more easily observed in Figure 36, which shows the pruning weights normalised to the respective controls. This also shows the difference

between the 30% and the more stressful 30%D treatments. Figure 37 (a,b,c,d) presents the data in a slightly different way for clarity where absolute pruning weights are given after year 1 (a), year 2 (b), year 3 (c) and year 5 (d) of the trial. Again it is clear that the 30%D has a greater negative impact on pruning weights than 30% (Figure 37b,c).

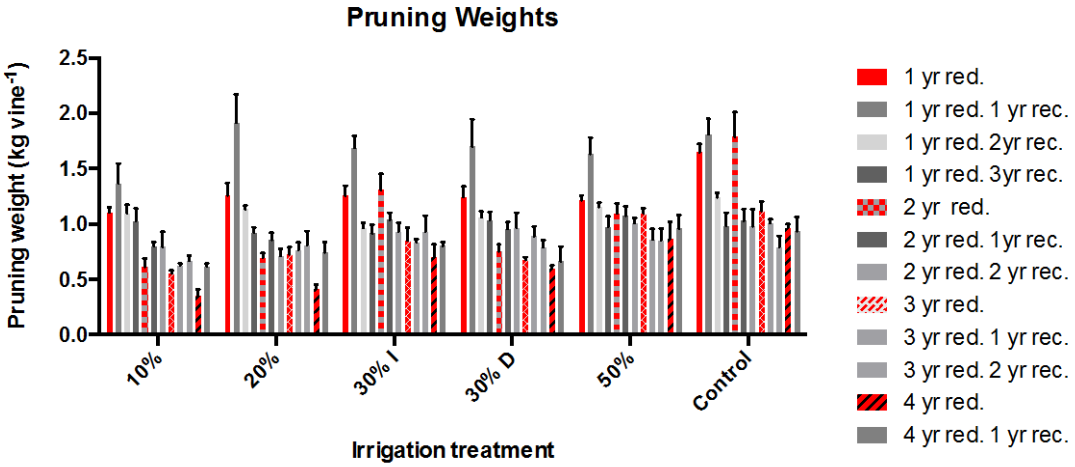

Figure 35 Summary of pruning weights for each irrigation treatment and for different durations of continuous deficit and recoveries. Red bars for each treatment are for vines under deficit for one, two, three or four years. The corresponding recoveries are shown adjacent to the respective deficit. Mean +/- SEM are shown.

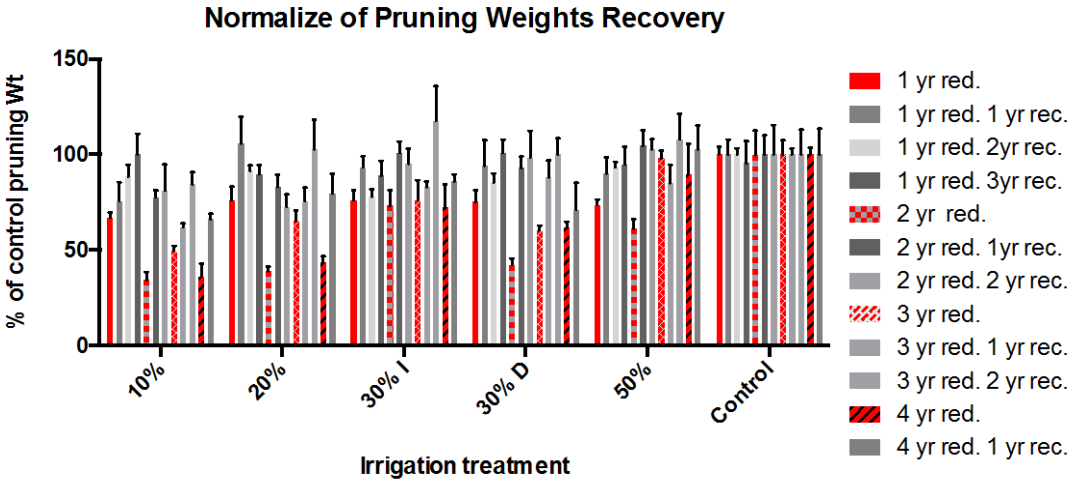

Figure 36 Summary of relative pruning weights (percent) for each irrigation treatment and for different durations of continuous deficit and recoveries. Red bars for each treatment are for vines under deficit for one, two, three or four years. The normalisation was based on the mean of the corresponding controls. This allows for an SEM to be obtained for the controls which will have a mean of 100%. The corresponding recoveries are shown adjacent to the respective deficit. Mean +/- SEM are shown.

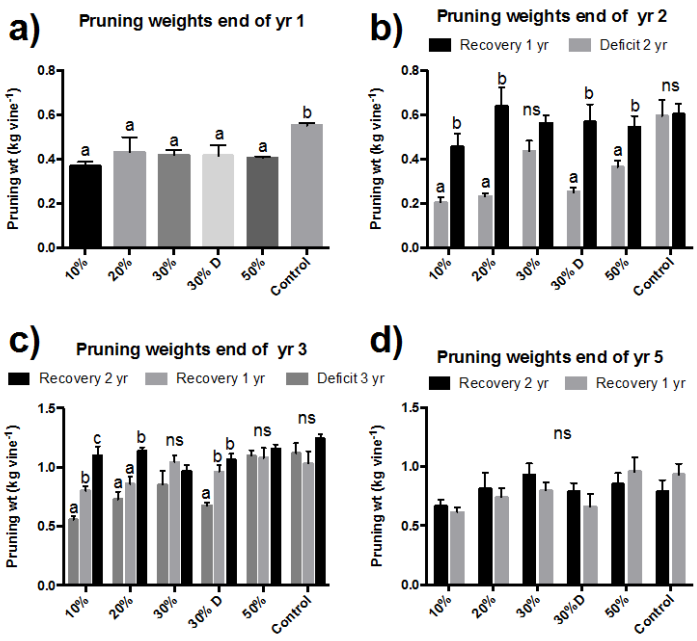

Figure 37 Pruning weights at the end of each year of the trial for each of the treatments. (a) End of season one (2008-09) and therefore no recovery vines. (b) End of season two (2009-10) where vines had two years of deficit and one year of recovery. (c) End of season three (2010-11) where vines had three years of deficit, two years of recovery or one year of recovery. (d) End of season four (2011-12) where vines are shown with one or two years of recovery after three or two years of deficit respectively. Different letter indicates significant difference between deficit treatments (a), or deficit and recovery (b,c), or between recoveries (d). (one- or 2-way ANOVA with Holm Sidak's multiple comparison).

Closer examination of recoveries after deficit and links between pruning weight, leaf area index and yield.

Here we examine normalised yields and pruning weights (relative to control in each year) and compare continuous deficit with recovery after one year of deficit. Since we have three to four seasons of recovery after one year of deficit, it allows close scrutiny of the time that may be required for vines to adjust back to full productivity under normal irrigation following a season of deficit.

10% treatment

Figure 38a shows the normalised yield as a function of years (seasons) for the continuous deficit (red symbols), and recovery (blue symbols) after the first year of 10% deficit, i.e. deficit in only year 1 (2008-09 season). It is evident that only in the third season of recovery did yield come back to being equivalent to that of the controls. It should be noted that according to the ANOVA described above for Figure 1 there was no significant effect of the deficit during the recovery compared with the controls. However it can be clearly seen from the trend in Figure 38a that there is a continued increase in yield back toward the controls that takes some three seasons. A regression analysis on this trend shows that it is highly significant, as indicated by the adjacent regression analysis in Figure 38a. For comparison the normalised pruning weights are shown plotted in the

same way as the yields (Figure 38b). A regression through the recovery data also indicates that only by the third season after the deficit did the pruning weight recover to that of the control. Comparing the continuous deficit yields and pruning trends it can be seen that there is a greater effect on pruning weight than on yield and that there is a trend for increasing yield over time during the continuous deficit. This will be seen to be common with the other continuous deficits treatments. This is of course all relative to the respective controls in the given year, and assumes that other climatic and biotic influences independent of the deficit treatments that will affect yield and pruning weight from year to year do not differentially affect the treatments compared to the controls. However, it should be noted that there was substantially different rainfall in the growing season between treatment years and this may have an impact. This will be discussed further below.

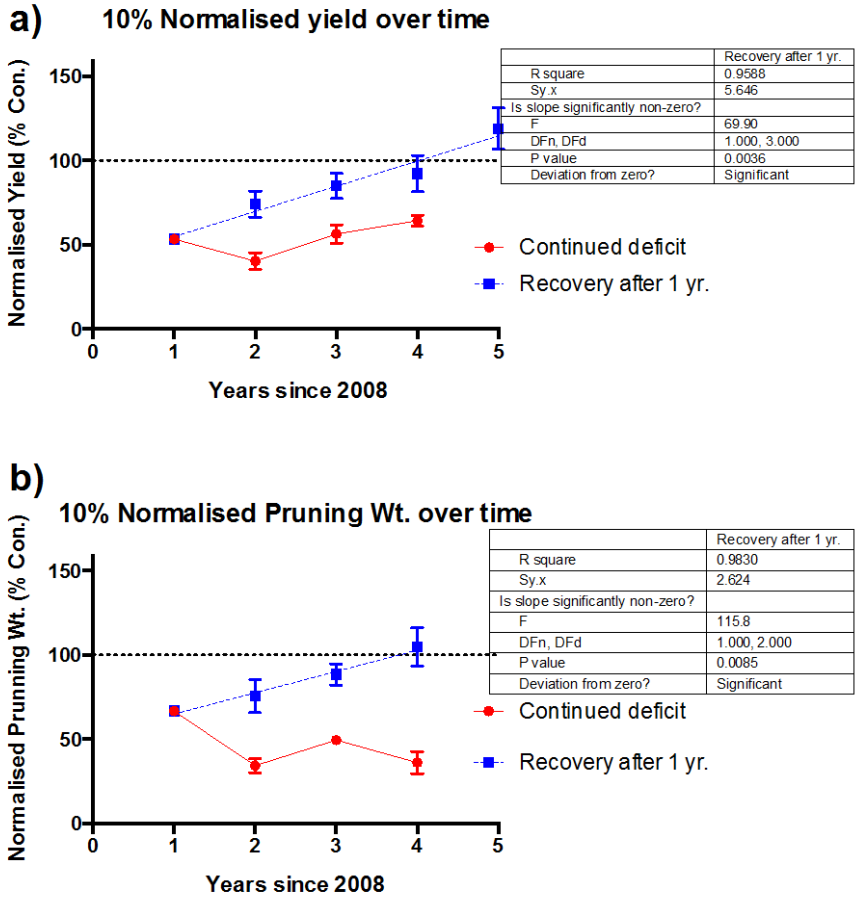

Figure 38 Normalised yields (a) and pruning weights (b) for successive (continued) 10% treatment (red circles) or recovery (blue squares) after one year of 10% deficit (season 2008-09) plotted against time. Normalisation occurred against the respective control in each year, and is indicated as the horizontal dotted line. The detail for the significant linear regressions through the recovery trajectory is shown adjacent to each Figure

20% treatment

In contrast to the 10% treatment the recovery after one year of deficit appeared to be significantly more rapid having reached the control yield in the first season of recovery (Figure 39a). The regression against time shown for the relative yield is only just significant, while that for the recovery of relative pruning weight is not significant (not shown in Figure 39b). As for the 10% treatment there is trend for the relative yield under continues deficit to increase back towards the controls (Figure 39a). This trend is not evident in the relative pruning weights, consistent with the 10% deficit treatment (Figure 39b).

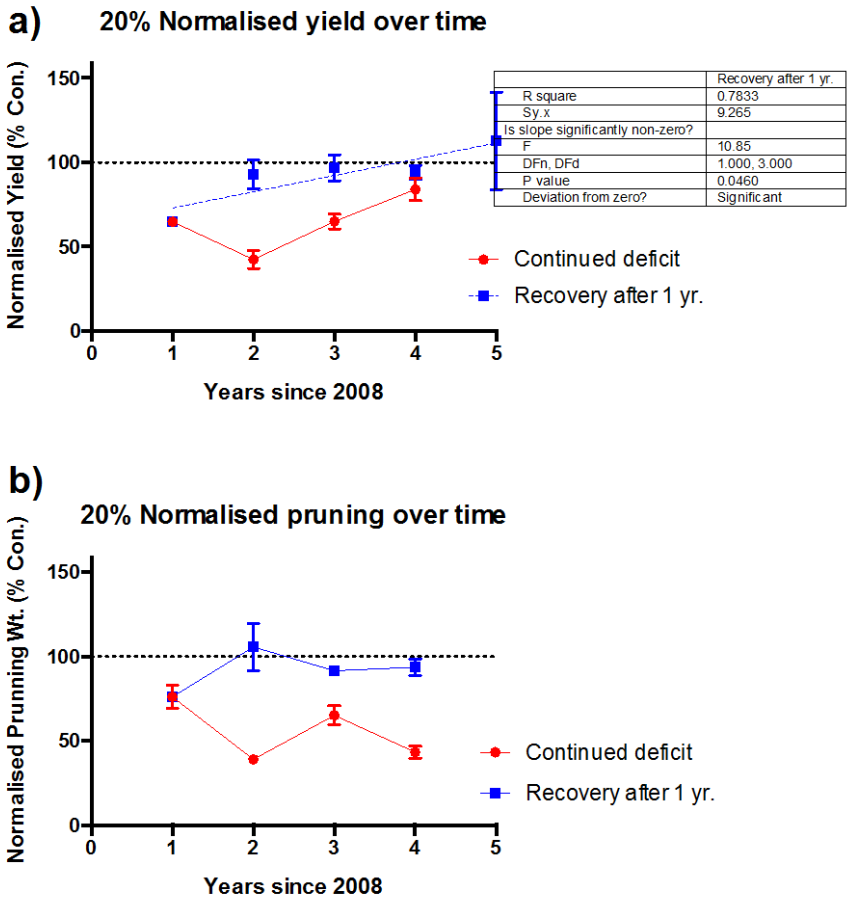

Figure 39 Normalised yields (a) and pruning weights (b) for successive (continued) 20% treatment (red circles) or recovery (blue squares) after one year of 20% deficit (season 2008-09) plotted against time. Normalisation occurred against the respective control in each year, and is indicated as the horizontal dotted line. The detail for the significant linear regression through the recovery trajectory for yield is shown adjacent to the Figure

30% treatment

The 30% deficit showed somewhat contrasting behaviour to the 10% and 20% in that the decrease in yield was larger than that of pruning weight (Figure 40). The recovery was also rapid (within one season) for both yield and pruning weight with no significant trend once the control levels were reached. There was also no recovery trend in the yield under continuous deficit that was evident in the 10% and 20% deficits. The peak in yield in year 5 for the recoveries is difficult to explain, but all treatments showed this response to different degrees so it may be a real effect, perhaps an over compensation.

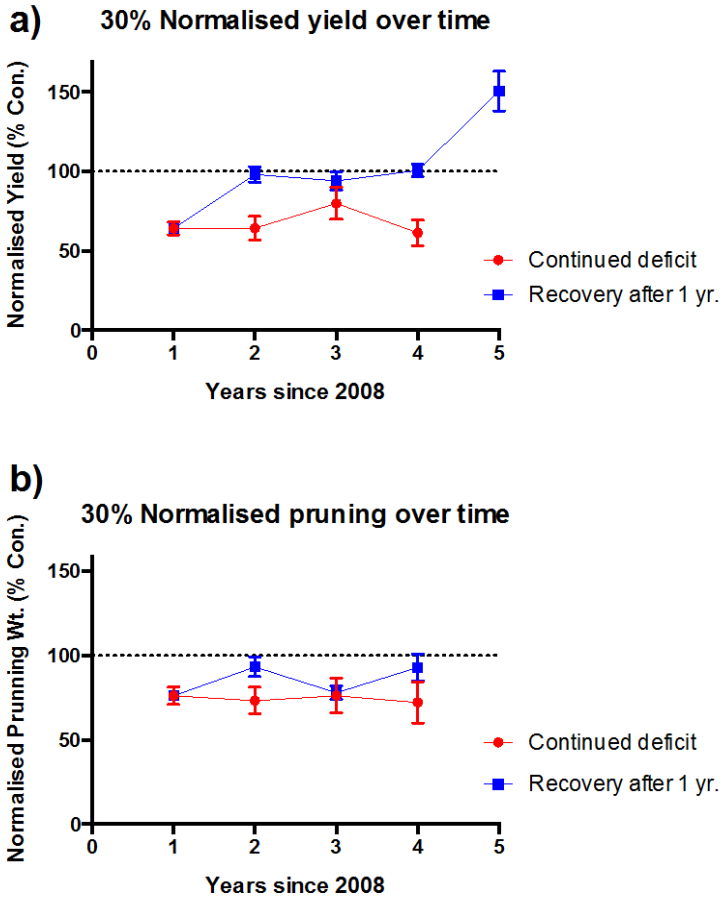

Figure 40 Normalised yields (a) and pruning weights (b) for successive (continued) 30% treatment (red circles) or recovery (blue squares) after one year of 30% deficit (season 2008-09) plotted against time. Normalisation occurred against the respective control in each year, and is indicated as the horizontal dotted line.

30% D treatment

The 30%D treatment (Figure 41) showed similar responses in relative yields and pruning weights to that of the 10% and 20% deficits but clearly contrasts to the minimal responses observed in the 30% treatment. This is consistent with the other comparisons in physiology and yield described above. The yield recovery shows a slower trend to the control levels but the linear regression is not significant (not shown). There is once again a consistent trend of yield compensation under continuous deficit in years 2, 3 and 4, which is not as evident in the relative pruning weights.

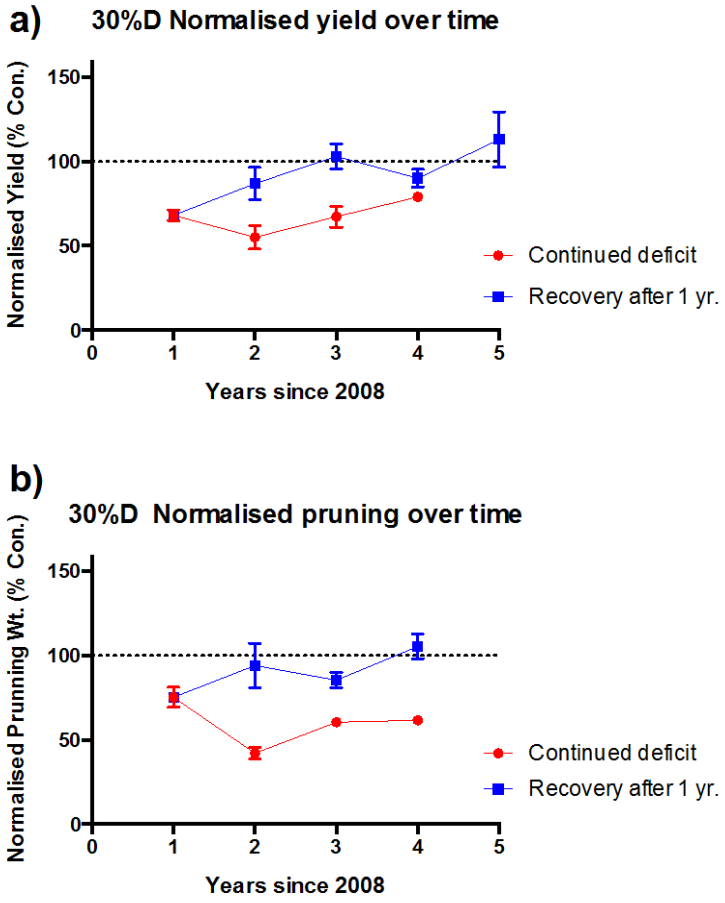

Figure 41 Normalised yields (a) and pruning weights (b) for successive (continued) 30%D treatment (red circles) or recovery (blue squares) after one year of 30%D deficit (season 2008-09) plotted against time. Normalisation occurred against the respective control in each year, and is indicated as the horizontal dotted line.

50% treatment

The 50% deficit shows some common features with the other treatments in that there is a trend for the relative yields to compensate towards that of the controls (Figure 42a). There are also the same trends in the recovery phase with an overshoot in year 5 as seen in the 30% treatment. Relative pruning weights also appeared to have recovered to control levels during the continued deficit by year 3 (Figure 42b).

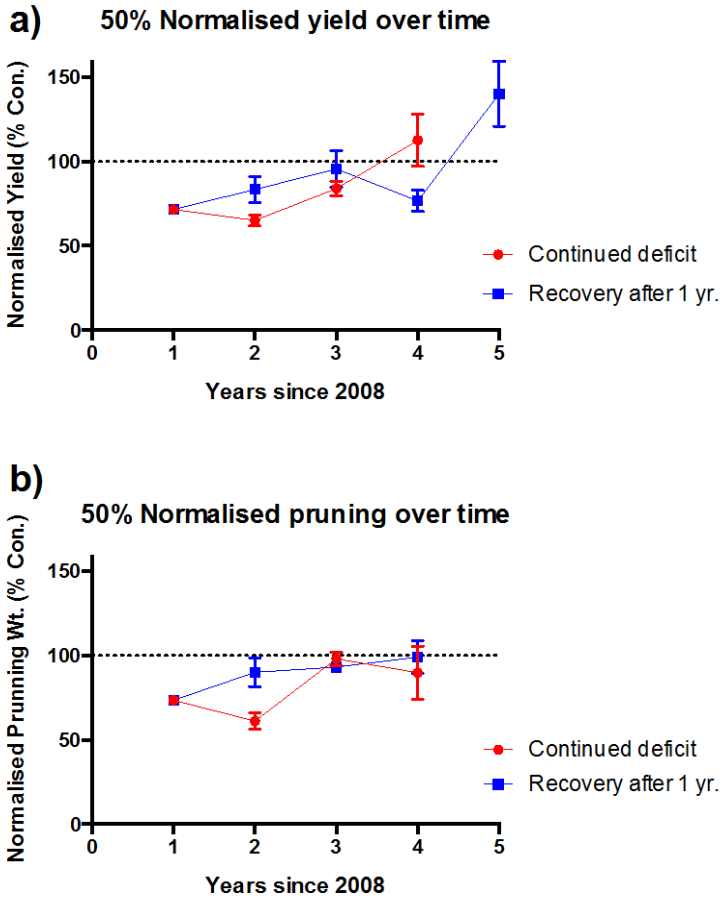

Figure 42 Normalised yields (a) and pruning weights (b) for successive (continued) 50% treatment (red circles) or recovery (blue squares) after one year of 50% deficit (season 2008-09) plotted against time. Normalisation occurred against the respective control in each year, and is indicated as the horizontal dotted line.

Leaf area index

Leaf area index (LAI) was also measured and Figure 43 shows measurements made in February 2012 and plotted against the duration of recovery. Zero in this case corresponds to four years of continuous deficit. It is clear that for every treatment except the 50% deficit there was a delay in recovery of full LAI. The data were best fit by a quadratic equation and all treatment except 50% and 100% were not significantly different. Full recovery did not occur until at least the second season of full irrigation (i.e. 100%).

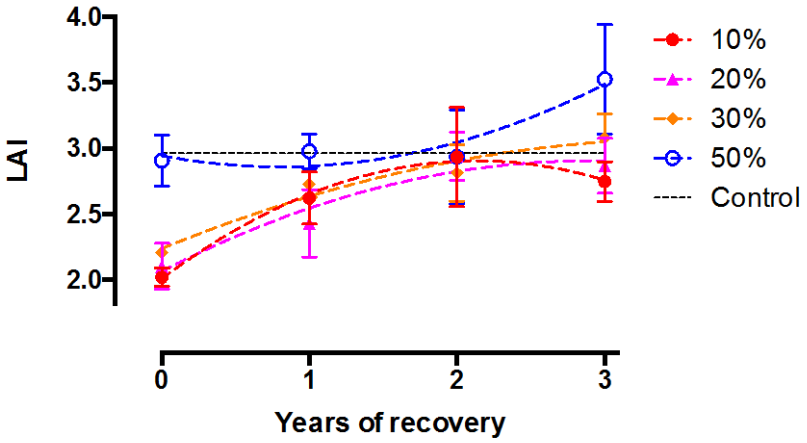

	10%	20%	30%	50%	Global (shared)
P value					0.0493
Conclusion (alpha = 0.05)					Reject null hypothesis
Preferred model					Different curve for each data set
F (DFn, DFd)					2.160 (9,36)
Different curve for each data set					
Best-fit values					
B0	2.009	2.065	2.239	2.944	
B1	0.8402	0.5798	0.4590	-0.2083	
B2	-0.1969	-0.1000	-0.06283	0.1298	
Std. Error					
B0	0.2106	0.1995	0.1456	0.2783	
B1	0.3383	0.3205	0.2338	0.4469	
B2	0.1081	0.1024	0.07470	0.1428	
95% Confidence Intervals					
B0	1.533 to 2.486	1.614 to 2.517	1.909 to 2.568	2.314 to 3.573	
B1	0.07492 to 1.605	-0.1451 to 1.305	-0.07000 to 0.9880	-1.219 to 0.8027	
B2	-0.4413 to 0.04756	-0.3316 to 0.1316	-0.2318 to 0.1062	-0.1932 to 0.4528	
Goodness of Fit					
Degrees of Freedom	9	9	9	9	
R square	0.5259	0.5334	0.6552	0.2396	
Absolute Sum of Squares	1.261	1.132	0.6027	2.201	
Sy.x	0.3743	0.3546	0.2588	0.4946	
One curve for all data sets					
Best-fit values					
B0	2.314	2.314	2.314	2.314	2.314
B1	0.4177	0.4177	0.4177	0.4177	0.4177
B2	-0.05749	-0.05749	-0.05749	-0.05749	-0.05749
Std. Error					
B0	0.1187	0.1187	0.1187	0.1187	0.1187
B1	0.1905	0.1905	0.1905	0.1905	0.1905
B2	0.06087	0.06087	0.06087	0.06087	0.06087
95% Confidence Intervals					
B0	2.075 to 2.553	2.075 to 2.553	2.075 to 2.553	2.075 to 2.553	2.075 to 2.553
B1	0.03387 to 0.8014	0.03387 to 0.8014	0.03387 to 0.8014	0.03387 to 0.8014	0.03387 to 0.8014
B2	-0.1801 to 0.06511	-0.1801 to 0.06511	-0.1801 to 0.06511	-0.1801 to 0.06511	-0.1801 to 0.06511
Goodness of Fit					
Degrees of Freedom					45
R square	0.3240	0.3988	0.6423	-0.4235	0.3200
Absolute Sum of Squares	1.798	1.458	0.6252	4.121	8.003
Sy.x					0.4217
Constraints					
B0	B0 is shared	B0 is shared	B0 is shared	B0 is shared	
B1	B1 is shared	B1 is shared	B1 is shared	B1 is shared	
B2	B2 is shared	B2 is shared	B2 is shared	B2 is shared	
Number of points					
Analyzed	12	12	12	12	

Figure 43 Leaf area index (LAI) measured on one day in February 2012 for selected treatments where the data are plotted against number of years of recovery for each deficit. Zero years of recovery indicates four continuous years of deficit, one year is three years of deficit and one year of recovery, etc. Mean and SEM of three replicates is shown. The data has been fitted to a quadratic equation and regressions compared between the treatments. There is no significant

difference between the fits for 10%, 20% and 30% that differ significantly from the control and the 50% treatment.

Summary of effects of one year of deficit and recovery.

As a summary of the data described above:

- There is a trend for the continuous deficit treatment to compensate yield towards that of the control. This compensation is not as evident in the pruning weights for the low irrigation rates but may occur for the 30% and 50% deficits.
- As a conservative estimate for complete recovery after one year of deficit this would be in the third season of full irrigation, but can occur earlier for less extreme reductions in irrigation.
- Leaf area index did not fully agree with pruning weight in that LAI did not show any difference in recovery kinetics between the 10%, 20%, 30% and 30%D, however for the 10% both LAI and pruning weight recoveries were in agreement.
- After recovery there may be an over compensation effect with higher yields in the fourth season of recovery.
- It should be noted that the 2008-09 season had a low effective rainfall during the growth season compared to the following three seasons in which recovery after one year of deficit was examined. Therefore, we have examined a scenario above where the deficit year was more extreme and the recovery years less extreme in terms of total water applied.

Association between yield components and water applied

Here we examine the association between the different yield components and total effect rain received during the growing season plus irrigation. Figure 44 shows yield as a function of irrigation plus effect rain for all sub-treatments across four seasons where data was available. This data reveal some remarkable features of how yield responds to total water applied.

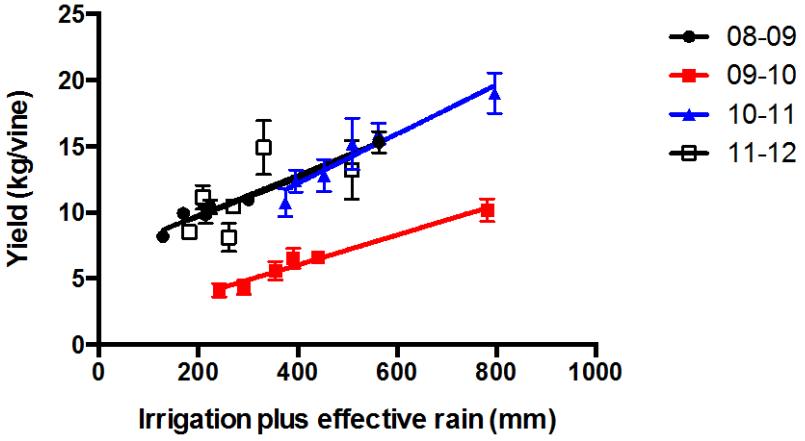

	2009	2010	2011	2012
Best-fit values				
Slope	0.01521 ± 0.001560	0.01133 ± 0.001468	0.01868 ± 0.003545	0.01448 ± 0.006013
Y-intercept when X=0.0	6.722 ± 0.4719	1.496 ± 0.6644	4.720 ± 1.895	6.800 ± 1.880
X-intercept when Y=0.0	-442.0	-132.0	-252.6	-469.7
1/slope	65.75	88.24	53.52	69.07
95% Confidence Intervals				
Slope	0.01209 to 0.01832	0.008375 to 0.01429	0.01133 to 0.02604	0.002008 to 0.02695
Y-intercept when X=0.0	5.780 to 7.665	0.1574 to 2.834	0.7893 to 8.651	2.900 to 10.70
X-intercept when Y=0.0	-627.4 to -318.6	-333.1 to -11.19	-756.2 to -30.60	-5217 to -109.9
Goodness of Fit				
R square	0.5760	0.5644	0.5580	0.2086
Sy.x	1.890	1.784	2.445	3.165
Is slope significantly non-zero?				
F	95.09	59.60	27.78	5.798
DFn, DFd	1.000, 70.00	1.000, 46.00	1.000, 22.00	1.000, 22.00
P value	< 0.0001	< 0.0001	< 0.0001	0.0249
Deviation from zero?	Significant	Significant	Significant	Significant
Data				
Number of X values	6	6	6	6
Maximum number of Y replicates	12	8	4	4
Total number of values	72	48	24	24
Number of missing values	216	240	264	264
Equation	Y = 0.01521*X + 6.722	Y = 0.01133*X + 1.496	Y = 0.01868*X + 4.720	Y = 0.01448*X + 6.800

Are the slopes equal?
F = 1.64908. DFn=3 DFd=160
P=0.1802

If the overall slopes were identical, there is a 18% chance of randomly choosing data points with slopes this different. You can conclude that the differences between the slopes are not significant.

Since the slopes are not significantly different, it is possible to calculate one slope for all the data. The pooled slope equals 0.0140539

Are the elevations or intercepts equal?
F = 101.051. DFn=3 DFd=163
P<0.0001

If the overall elevations were identical, there is a less than 0.01% chance of randomly choosing data points with elevations this different. You can conclude that the differences between the elevations are extremely significant.

Figure 44 Yield as a function of irrigation plus effective rain (Table 1, Methods Chapter 5) for all sub-treatments across four seasons. The season data (indicated with different symbols) includes deficit, recoveries and control treated vines. For the deficit treatments these can have up to four consecutive seasons of deficit (2011-12). Regression lines are through the combined data for the season with the regression details shown in the table below the graph. The slopes are not significantly different and the regressions for seasons 2008-09, 2010-11 and 2011-12 are not significantly different. Mean +/- SEM is shown.

For three out of four seasons (2008-09, 2010-11, 2011-12) the regressions lines are not significantly different and across all years the slope of the regression lines are not significantly different, providing a common slope of 0.014 kg vine^{-1} mm^{-1}. This translates to 21.1 kg ha^{-1} mm^{-1} or 2,108 kg ha^{-1} ML^{-1} gained in yield per hectare for every mm or ML total water applied respectively. Note that this is the incremental water productivity and not the absolute water productivity since the regression lines do not intercept at the origin. So for example, for

2008-09, 2010-11 and 2011-12 seasons the absolute water productivity at 200 mm of total water applied is 7.2 tonne ML^{-1} ha^{-1}.

Figure 45 shows the absolute water productivities calculated from the regression lines shown in Figure 44 where seasons 2008-09, 2010-11 and 2011-12 are combined and compared with season 09-10, which is somewhat of an outlier due to unfavourable flowering conditions. The lines are exponential decay functions that illustrate the effect in terms of a diminishing of returns function. Note that the rate constants for the exponential decay in absolute water productivity are the same for the two sets of seasons, but the final plateaus and initial starting points differ. From these functions one could deduce a target of yield relative to the water productivity, which is a decision based on the cost of water and the desired yield (quality).

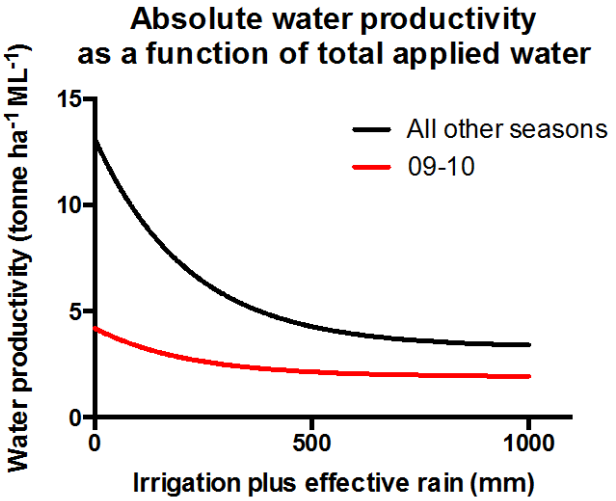

	All other seasons	09-10
Best-fit values		
Y0	13.12	4.193
Plateau	3.308	1.915
K	0.004622	0.004622
Half Life	150.0	150.0
Tau	216.3	216.3
Span	9.810	2.278

Figure 45 Water productivity obtained from the regression equations in Figure 44 plotted against irrigation plus effective rain. Note the actual data ranges from 150 mm to 800 mm while the regression lines shown are extrapolated to 0 and 1000 mm. The curves are exponential decay functions that perfectly fit the data in Figure 44 and the details are given in the table below the Figure

Another point to be made from the data in Figure 44 is that for seasons 2008-09, 2010-11 and 2011-12 the data all line up together on the same linear function despite the fact that in each season there are blocks of vines that have been treated for different periods under the deficits. For example in season 2011-12 the vines had endured the deficits for three prior years, yet they fit on the same function of yield versus water applied as the vines that had only one year of

deficit. Similarly all the 100% vines in each season line up on the same function. This would suggest that the main determining factor for yield is the total water applied in any season, irrespective of the number of prior seasons where water applied was above or below the average. Note this is slightly at odds with the observation of some yield compensation over time under continuous deficit observed above for the 10%, and 20% treatments. But these effects are relatively small compared to the overall effect of total water applied.

Yield components of bunch weight and berry weight are also given as a function of irrigation plus effect rain in Figures 46 and 47 respectively for completeness where these data were obtained. Note that bunch weight shows the same similarities to that of yield (Figure 44), but berry weight is somewhat different particularly for the data in season 2010-11 where there was no significant effect of effective rain plus irrigation on berry weight, and indicating that in this season berries per bunch must have contributed to the association of yield with effective rain plus irrigation.

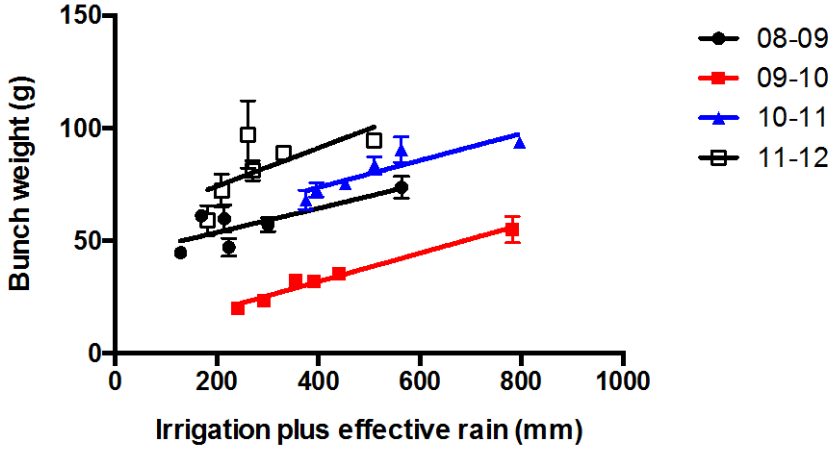

	2009	2010	2011	2012
Best-fit values				
Slope	0.05364 ± 0.01340	0.06317 ± 0.006911	0.05996 ± 0.01157	0.08510 ± 0.03233
Y-intercept when X=0.0	42.92 ± 4.055	6.556 ± 3.128	49.63 ± 6.184	57.11 ± 10.11
X-intercept when Y=0.0	-800.1	-103.8	-827.8	-671.1
1/slope	18.64	15.83	16.68	11.75
95% Confidence Intervals				
Slope	0.02585 to 0.08144	0.04883 to 0.07750	0.03597 to 0.08395	0.01804 to 0.1522
Y-intercept when X=0.0	34.51 to 51.33	0.06893 to 13.04	36.81 to 62.46	36.14 to 78.08
X-intercept when Y=0.0	-1952 to -431.0	-263.2 to -0.9025	-1727 to -440.9	-4262 to -241.2
Goodness of Fit				
R square	0.4214	0.7915	0.5498	0.2395
Sy.x	9.377	5.938	7.978	17.02
Is slope significantly non-zero?				
F	16.02	83.54	26.87	6.927
DFn, DFd	1.000, 22.00	1.000, 22.00	1.000, 22.00	1.000, 22.00
P value	0.0006	< 0.0001	< 0.0001	0.0152
Deviation from zero?	Significant	Significant	Significant	Significant
Data				
Number of X values	6	6	6	6
Maximum number of Y replicates	4	4	4	4
Total number of values	24	24	24	24
Number of missing values	72	72	72	72
Equation	Y = 0.05364*X + 42.92	Y = 0.06317*X + 6.556	Y = 0.05996*X + 49.63	Y = 0.08510*X + 57.11

Are the slopes equal?
F = 1.74369. DFn=2 DFd=66
P=0.1828

If the overall slopes were identical, there is a 18% chance of randomly choosing data points with slopes this different. You can conclude that the differences between the slopes are not significant.

Since the slopes are not significantly different, it is possible to calculate one slope for all the data. The pooled slope equals 0.0143943

Are the elevations or intercepts equal?
F = 83.0882. DFn=2 DFd=68
P<0.0001

If the overall elevations were identical, there is a less than 0.01% chance of randomly choosing data points with elevations this different. You can conclude that the differences between the elevations are extremely significant.

Figure 46 Bunch weight as a function of irrigation plus effective rain for all sub-treatments across four seasons. The season data (indicated with different symbols) includes deficit, recoveries and control treated vines. For the deficit treatments these can have up to four consecutive seasons of deficit (2011-12). Linear regression lines are through the combined data for the season with the regression details shown in the table below the graph. The slopes are not significantly different but the intercepts are significantly different between season 2009-10 and the other seasons. Mean +/- SEM is shown.

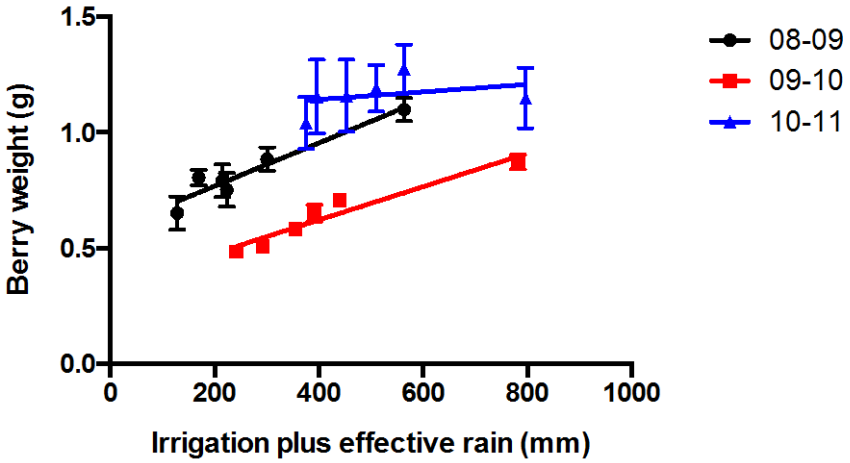

	2009	2010	2011
Best-fit values			
Slope	0.0009317 ± 0.0001653	0.0007205 ± 7.016e-005	0.0001636 ± 0.0003539
Y-intercept when X=0.0	0.5817 ± 0.05003	0.3333 ± 0.03175	1.076 ± 0.1892
X-intercept when Y=0.0	-624.3	-462.6	-6579
1/slope	1073	1388	6111
95% Confidence Intervals			
Slope	0.0005888 to 0.001275	0.0005750 to 0.0008661	-0.0005704 to 0.0008977
Y-intercept when X=0.0	0.4779 to 0.6855	0.2674 to 0.3991	0.6841 to 1.469
X-intercept when Y=0.0	-1147 to -380.4	-688.7 to -311.3	-infinity to -771.2
Goodness of Fit			
R square	0.5907	0.8274	0.009622
Sy.x	0.1157	0.06028	0.2441
Is slope significantly non-zero?			
F	31.75	105.5	0.2137
DFn, DFd	1.000, 22.00	1.000, 22.00	1.000, 22.00
P value	< 0.0001	< 0.0001	0.6484
Deviation from zero?	Significant	Significant	Not Significant
Data			
Number of X values	6	6	6
Maximum number of Y replicates	4	4	4
Total number of values	24	24	24
Number of missing values	72	72	72
Equation	Y = 0.0009317*X + 0.5817	Y = 0.0007205*X + 0.3333	Y = 0.0001636*X + 1.076

Are the slopes equal?
F = 1.74369. DFn=2 DFd=66
P=0.1828

If the overall slopes were identical, there is a 18% chance of randomly choosing data points with slopes this different. You can conclude that the differences between the slopes are not significant.

Since the slopes are not significantly different, it is possible to calculate one slope for all the data. The pooled slope equals 0.0143943

Are the elevations or intercepts equal?
F = 83.0882. DFn=2 DFd=68
P<0.0001

If the overall elevations were identical, there is a less than 0.01% chance of randomly choosing data points with elevations this different. You can conclude that the differences between the elevations are extremely significant.

Figure 47 Berry weight as a function of irrigation plus effective rain for all sub-treatments across three seasons. The season data (indicated with different symbols) includes deficit, recoveries and control treated vines. For the deficit treatments these can have up to three consecutive seasons of deficit (2010-11). Linear regression lines are through the combined data for the season with the regression details shown in the table below the graph. The slope for season 2010-11 is not significantly different from zero. Mean +/- SEM is shown.

Comparison with other data for yield and water productivity

(Sadras 2009) compared water productivities for different types of deficit irrigation over a range of grapevine varieties and other crops (in g/L). Converting our data to that of (Sadras 2009) for comparison shows that for all seasons other than 2009-10 water productivities of between 3.6 and 7.2 g/L were obtained. This is at the lower end of the range for those compiled by (Sadras 2009), though many other varieties and conditions cluster in the range from about 2 to 10 g/L. The (Sadras 2009) compilation is also in terms of irrigation water applied rather than irrigation plus effective rain so our values would be increased somewhat if irrigation applied was only considered. Our values are also comparable to those of (Trigo-Cordoba, et al. 2015) for cv. 'Godello' and 'Treixadura' over three seasons under deficit (rain fed only) and irrigation in NW Spain. Perhaps the most comparable study was that of (Stevens, et al. 2008) where yield and irrigation water use index (IWUI) were compared for Chardonnay on various rootstocks for irrigation rates of 5 ML/ha and 8ML/ha. Yield per vine on Ramsey (the root stock used in our study) was 32.2 kg/vine, with an IWUI of 5.9 t/(ha·ML). In our case the maximum yield when irrigation plus effective rain approached 800 mm (=8 ML/ha), was about 19 kg/vine, and therefore significantly less than those reported by (Stevens, et al. 2008). Another study on Chardonnay on two rootstocks by (Williams 2014) gave water use efficiencies of between 2.6 and 18.5 (tonne/ML) for applied water rates of between 482 mm and 86 mm. At near 200 mm applied water, values ranging from 5.6 to 10.9 tonne/ML were obtained by (Williams 2014) over several years, which are not that dissimilar to the 7.2 tonne/ha that we obtained. Our water productivity (calculated as the index of yield/ha divided by irrigation plus effective rain) was between 3.6 and 7.2 t/(ha.ML) for 8 ML/ha and 2 ML/ha respectively.

Vine balance and water applied.

Vine balance can be conveniently parameterised as yield-to-pruning-weight ratio (Y/P) with values in the range 5 to 10 considered as optimal (Dry 2013). Figure 48 shows yield as a function of pruning weight for each of the seasons and across each of the deficit and controls in each season. The regressions are for each season. In each case the lines' intercepts are not significantly different to the origin and therefore the regression lines have been forced to pass through the origin. In each case the slope of the lines is equal to the yield-to-pruning-weight ratio, which is given for each season in the Table in Figure 48. First of all it is evident that deficit irrigation has not markedly changed the ratio as based on the linear fits where the lines pass through the origin. However, two outliers are evident for the 10% and 20% deficits in season 11-12. Second, the yield-to-pruning-weight ratio changes substantially in each season in order of increasing ratio as 5.7 (2009-10), 8.4 (2008-09), 16.1 (2011-12), 16.7 (2010-11). This indicates that the yield-to-pruning-weight ratio is more dependent upon season to season differences rather than irrigation and effective rain (compare with Table 1 Chapter 5). This is similar to conclusion arrive at by (Intrigliolo and Castel 2008) where they found a significant year to year effect (over six years) on yield-to-pruning-weight ratio, rather than any effect of irrigation versus non-

irrigation on Tempranillo in Requena, Spain. However, (Lopez, et al. 2007) found that yield-to-pruning-weight ratio was reduced on average from 6.7 to 8.2 across varieties under non-irrigation versus irrigation over four seasons for five Spanish varieties. On the other hand yield-to-pruning-weight ratios increased in each of three seasons for Merlot when irrigation was reduced from about 400 mm to 200 mm (Shellie 2014). (Shellie 2014) also observed a linear relation between yield and pruning weight but the regressions (not characterised) would appear to not pass through the origin in some years.

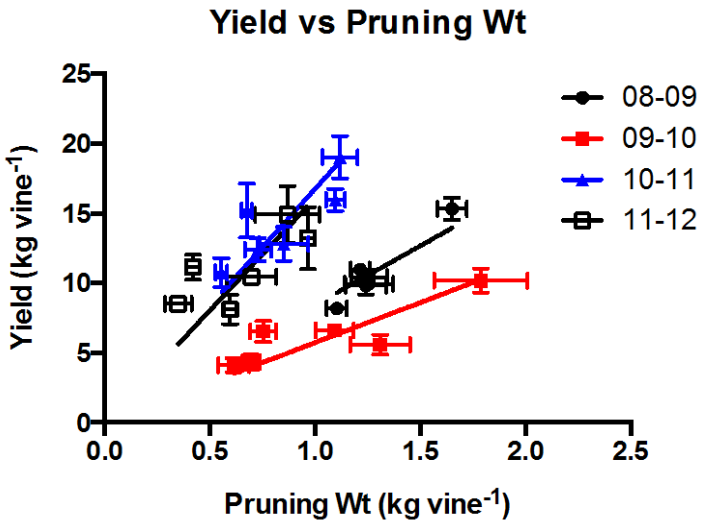

	2009	2010	2011	2012
Best-fit values				
Slope	8.444 ± 0.3020	5.734 ± 0.4929	16.75 ± 1.061	16.08 ± 1.612
Y-intercept when X=0.0	0.0	0.0	0.0	0.0
X-intercept when Y=0.0	0.0	0.0	0.0	0.0
1/slope	0.1184	0.1744	0.05969	0.06221
95% Confidence Intervals				
Slope	7.668 to 9.221	4.467 to 7.001	14.02 to 19.48	11.93 to 20.22
Goodness of Fit				
Sy.x	0.9609	1.353	2.245	2.712
Is slope significantly non-zero?				
t	27.96	11.63	15.79	9.971
DF	5.000	5.000	5.000	5.000
P value	< 0.0001	< 0.0001	< 0.0001	0.0002
Deviation from zero?	Significant	Significant	Significant	Significant
Data				
Number of X values	6	6	6	6
Maximum number of Y replicates	1	1	1	1
Total number of values	6	6	6	6
Number of missing values	18	18	18	18
Equation	Y = 8.444*X - 0.0	Y = 5.734*X - 0.0	Y = 16.75*X - 0.0	Y = 16.08*X - 0.0

Figure 48 Vine balance as indicated by plotting yield against pruning weights across the four seasons. The season data (indicated with different symbols) includes deficit, recoveries and control treated vines. For the deficit treatments these can have up to four consecutive seasons of deficit (2011-12). Linear regression lines are forced through the origin and the slope gives the overall average yield-to-pruning-weight ratio (Ravaz Index). The regression details shown in the table below the graph. Mean +/- SEM is shown.

From Figures 38 (10% irrigation) and 39 (20% irrigation) presented earlier it could be seen that there was a trend for recovery in yield with continuous deficit,

while pruning weight did not show any recovery. This suggests that for these more extreme treatments there was a tendency for the yield-to-pruning-weight ratio to increase with continuous deficit. This is examined in more detail in Figure 49 where the ratios are presented as a function of the number of years of continuous deficit and the number of years of recovery after one year of deficit. It can be seen that for the 10% and 20% treatments there is a trend for the yield-to-pruning-weight ratio to increase with time under deficit and more so than the season-to-season trend observed for the controls. This results in a significantly higher ratio for the 10% and 20% deficit treatments by the fourth season of deficit (season 11-12, Figure 49a,b). The ratios achieved are very high (25 to 30), i.e. extremely over-cropped, and well beyond the range suggested for optimum quality (5 to 10 (Dry 2013). This trend was also evident in the 30%D treatment but was not significant. It should also be noted that the recovery vines after one year of deficit (right hand side of the figures) were not significantly different to the respective controls for all deficits. The trend of increasing yield-to-pruning-weight ratio under the more extreme deficit treatments concurs with the observation of (Shellie 2014) for Merlot vines under continuous seasonal deficit.

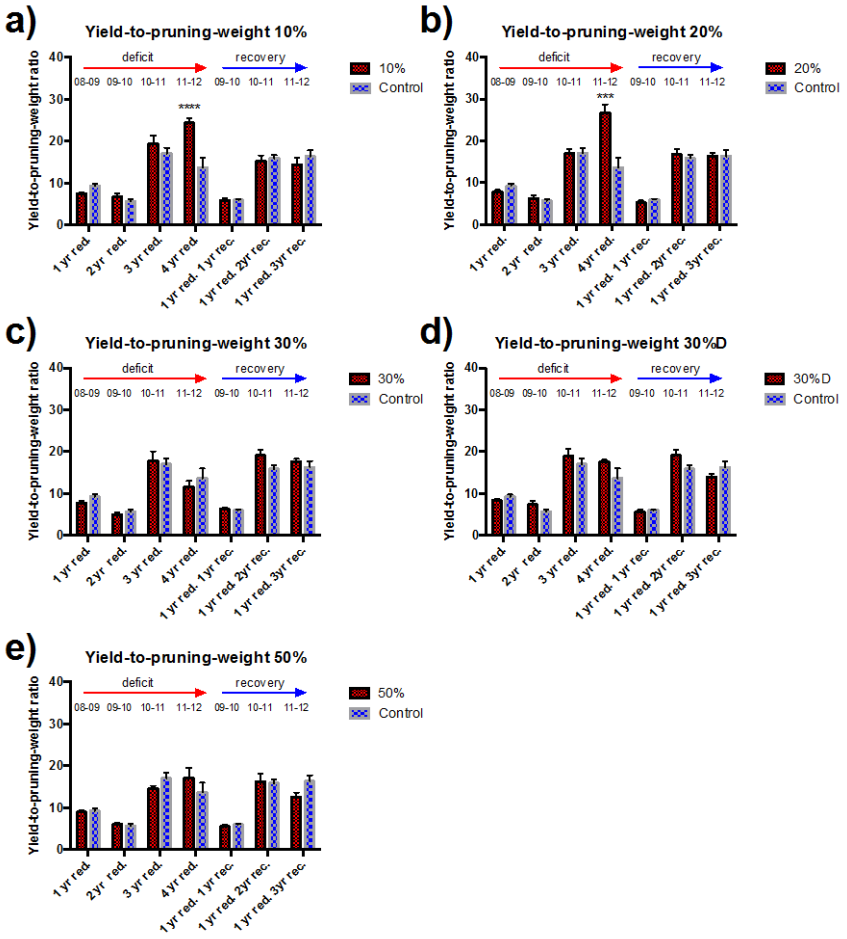

Figure 49 Yield-to-pruning-weight ratios for continuous deficit irrigation over four seasons and for recovery after one season of deficit over three seasons. Each season is compared with the respective control to illustrate season-to-season variation in the ratio (see Figure 48). The respective season is indicated above the data pair. (a) 10%, (b) 20%, (c) 30%, (d) 30%D, (e) 50%. Significant difference to controls is indicated by asterisk (2-way ANOVA with Holm-Sidak multiple comparison test). Mean +/- SEM are shown.

References

Chaves, M.M., O. Zarrouk, R. Francisco, J.M. Costa, T. Santos, A.P. Regalado, M.L. Rodrigues, and C.M. Lopes (2010) Grapevine under deficit irrigation: hints from physiological and molecular data. Annals of Botany 105, 661-676. doi: 10.1093/aob/mcq030.

Dry, P. (2013) Can the production of flow alcohol wines start in the vineyard? Wine and Viticulture Journal 28, 40-43.

Intrigliolo, D.S. and J.R. Castel (2008) Effects of irrigation on the performance of grapevine cv. Tempranillo in Requena, Spain. American Journal of Enology and Viticulture 59, 30-38.

Lopez, M.-I., M.-T. Sanchez, A. Diaz, P. Ramirez, and J. Morales (2007) Influence of a deficit irrigation regime during ripening on berry composition in grapevines (Vitis vinifera L.) grown in semi-arid areas. International Journal of Food Sciences and Nutrition 58, 491-507. doi: 10.1080/09637480701311801.

Lopez, M.I., M.T. Sanchez, A. Diaz, P. Ramirez, and J. Morales (2007) Influence of a deficit irrigation regime during ripening on berry composition in grapevines (Vitis vinifera L.) grown in semi-arid areas. International Journal of Food Sciences and Nutrition 58, 491-507. doi: 10.1080/09637480701311801.

Matthews, M.A. and M.M. Anderson (1989) Reproductive development in grape (Vitis-vinifera l) - responses to seasonal water deficits. American Journal of Enology and Viticulture 40, 52-59.

Mccarthy, M.G. (1997) The effect of transient water deficit on berry development of cv. Shiraz (Vitis vinifera L.). Australian Journal of Grape and Wine Research 3, 102-108.

Sadras, V.O. (2009) Does partial root-zone drying improve irrigation water productivity in the field? A meta-analysis. Irrigation Science 27, 183-190. doi: 10.1007/s00271-008-0141-0.

Shellie, K.C. (2014) Water Productivity, Yield, and Berry Composition in Sustained versus Regulated Deficit Irrigation of Merlot Grapevines. American Journal of Enology and Viticulture 65, 197-205. doi: 10.5344/ajev.2014.13112.

Stevens, R.M., J.M. Pech, M.R. Gibberd, R.R. Walker, J.A. Jones, J. Taylor, and P.R. Nicholas (2008) Effect of reduced irrigation on growth, yield, ripening rates and water relations of Chardonnay vines grafted to five rootstocks. Australian Journal of Grape and Wine Research 14, 177-190. doi: 10.1111/j.1755-0238.2008.00018.x.

Trigo-Cordoba, E., Y. Bouzas-Cid, I. Orriols-Fernandez, and J.M. Miras-Avalos (2015) Effects of deficit irrigation on the performance of grapevine (Vitis vinifera L.) cv. 'Godello' and 'Treixadura' in Ribeiro, NW Spain. Agricultural Water Management 161, 20-30. doi: 10.1016/j.agwat.2015.07.011.

Williams, L.E. (2014) Effect of Applied Water Amounts at Various Fractions of Evapotranspiration on Productivity and Water Footprint of Chardonnay Grapevines. American Journal of Enology and Viticulture 65, 215-221. doi: 10.5344/ajev.2014.12105.

6.3 Effect of SDI and recovery on berry composition and ripening

Introduction

Final harvest berry composition and the evolution of composition during ripening are expected to be sensitive to reduced irrigation since the water balance of the berry and the vine is linked to the rate of sugar accumulation (Greenspan, et al. 1996), berry transpiration (Rebucci, et al. 1997), and berry cell death (Bonada, et al. 2013). Although the sugar available for berry ripening would be expected to be dependent on the photosynthetic capacity of the vine and carbohydrate storage which are both effected by water deficit (Schultz and Matthews 1988,Tarara, et al. 2011), variation in maximum concentration of soluble solids in berries was unrelated to source size, source activity, sink size, and source : sink ratio (Sadras, et al. 2008). However, the rate of change in concentration of berry soluble solids was positively correlated to stomatal conductance (Sadras, et al. 2008), which is very sensitive to water stress. There are variable results in the literature depending on the degree of water stress, season-to-season interaction related to climatic variation, and differences between warm and cool climates. For example (Keller, et al. 2008) found no interaction between crop load and deficit irrigation on berry composition while others have found significant effects of deficit irrigation (Shellie 2014). The berry compositional changes due to deficits have also not been examined in terms of recovery after long-term continuous water deficit. The impact of reduced irrigation and then the time for recovery on basic berry composition in a warm, low humidity environment such as the Riverland is important for predicting impacts on wine quality when water is limiting and to determine the time for full recovery after water restrictions.

Methods

After weighing, the 100-berry sample was crushed and the extracted juice centrifuged to clarify. Clarified juice was separated from the pellet to determine total soluble solids (TSS) measured by a refractometer (corrected to 20°C). pH and titratable acidity (TA) was measured by a Metrohm auto endpoint titrator set to an endpoint pH of 8.2.

Results and Discussion

Berry ripening kinetics as affected by continuous water deficits

Three seasons of deficit treatments were examined with respect to the evolution of berry composition and ripening. Berry weight, total soluble solids (TSS as ^{o}Brix), sugars per berry, juice pH and titratable acidity (TA) were measured over the course of ripening for each of the deficit treatments. Using a two-way analysis of variance the significance of time, treatment and interaction was examined. These ANOVA tables are reported with each figure below and for each of the three seasons constituting, one year, two years and three years of continuous deficit respectively.

Season 2008-09: One year of deficit

The evolution of berry weight, TSS, sugar per berry, pH and TA are shown respectively in Figures 1,2,3,4,5. The evolution of berry weight (Figure 1) in this season (one of the driest) was in contrast to those shown below since berry weight had already reached its maximum relatively early and the deficit treatments all showed a decline in berry weight. Even the control showed a reduction in the last sample. In this case there was a significant effect of deficit treatment and time, but also a significant interaction, probably indicating the greater berry weight loss in the deficit treatments. Such weight loss is relatively rare for Chardonnay (Tilbrook and Tyerman 2008,Tilbrook and Tyerman 2009). Total soluble solids increased steadily and similarly across treatments (Figure 2). There was a significant difference with time and treatment but no significant interaction. This is interesting considering the greater weight loss in the more extreme deficits. The kinetics of the accumulation of sugars per berry showed the greatest difference between treatments (Figure 3), with a significant interaction between time and treatment. These results indicate a slower accumulation of sugar per berry for the more extreme deficits resulting in a much reduced sugar content per berry for the extreme deficits. Juice pH increased steadily for all treatments with higher pH achieved in the greater deficits (Figure 4), however, there was no significant interaction between time and treatment. Juice TA declined as would be expected during ripening, and despite different start values the final ripened levels of TA were very similar across treatments. Again there was no interaction between time and treatment (Figure 5).

a)

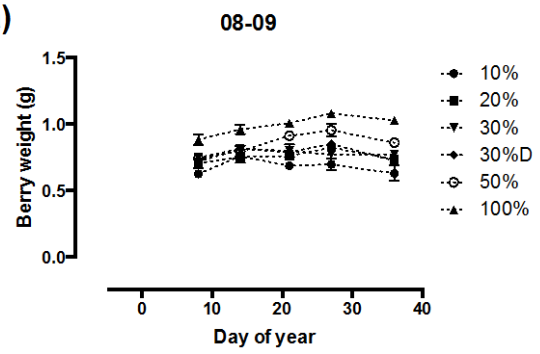

b)

Two-way ANOVA	Ordinary				
Alpha	0.05				
Source of Variation	% of total variation	P value	P value summary	Significant?	
Interaction	7.654	0.0294	*	Yes	
DOY	11.57	< 0.0001	****	Yes	
Irrigation	61.89	< 0.0001	****	Yes	
ANOVA table	SS	DF	MS	F (DFn, DFd)	P value
Interaction	0.1402	20	0.007008	F (20, 90) = 1.824	P = 0.0294
DOY	0.2119	4	0.05298	F (4, 90) = 13.79	P < 0.0001
Irrigation	1.133	5	0.2266	F (5, 90) = 58.98	P < 0.0001
Residual	0.3458	90	0.003843		
Number of missing values	0				

Figure 1 Evolution of berry weight, season 2008-09. a) Berry weight as a function of the day of the year (DOY) for each irrigation treatment. Mean +/- SEM are shown. b) Two-way ANOVA indicating significant effects of irrigation and DOY, and a significant interaction indicating that the evolution of berry weight differed between the treatments.

a)

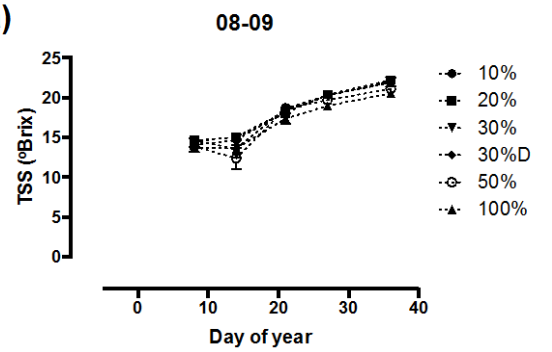

b)

Two-way ANOVA	Ordinary				
Alpha	0.05				
Source of Variation	% of total variation	P value	P value summary	Significant?	
Interaction	1.514	0.6779	ns	No	
DOY	88.23	< 0.0001	****	Yes	
Irrigation	1.990	0.0014	**	Yes	
ANOVA table	SS	DF	MS	F (DFn, DFd)	P value
Interaction	18.96	20	0.9480	F (20, 90) = 0.8248	P = 0.6779
DOY	1105	4	276.1	F (4, 90) = 240.3	P < 0.0001
Irrigation	24.91	5	4.982	F (5, 90) = 4.335	P = 0.0014
Residual	103.4	90	1.149		
Number of missing values	0				

Figure 2 Evolution of concentration of total soluble solids (TSS), season 2008-09. a) TSS as a function of the day of the year (DOY) for each irrigation treatment. Mean +/- SEM are shown. b) Two way ANOVA indicating significant effects of irrigation and DOY, but no significant interaction, indicating that the evolution of TSS did not differ between the treatments.

a)

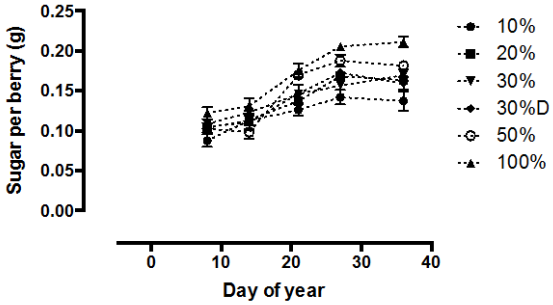

b)

Two-way ANOVA	Ordinary				
Alpha	0.05				
Source of Variation	% of total variation	P value	P value summary	Significant?	
Interaction	6.669	0.0029	**	Yes	
DOY	63.81	< 0.0001	****	Yes	
Irrigation	16.90	< 0.0001	****	Yes	
ANOVA table	SS	DF	MS	F (DFn, DFd)	P value
Interaction	0.009764	20	0.0004882	F (20, 90) = 2.380	P = 0.0029
DOY	0.09343	4	0.02336	F (4, 90) = 113.8	P < 0.0001
Irrigation	0.02475	5	0.004950	F (5, 90) = 24.13	P < 0.0001
Residual	0.01846	90	0.0002052		
Number of missing values	0				

Figure 3 Evolution of sugar per berry, season 2008-09. a) Sugar per berry as a function of the day of the year (DOY) for each irrigation treatment. Mean +/- SEM are shown. b) Two way ANOVA indicating significant effects of irrigation and DOY, and a significant interaction indicating that the evolution of sugar per berry differed between the treatments.

a)

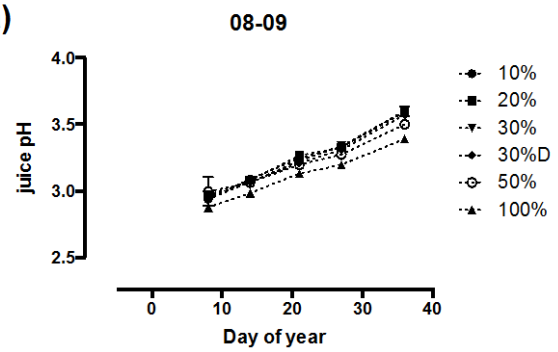

b)

Two-way ANOVA	Ordinary				
Alpha	0.05				
Source of Variation	% of total variation	P value	P value summary	Significant?	
Interaction	1.073	0.5213	ns	No	
DOY	89.61	< 0.0001	***	Yes	
Irrigation	4.262	< 0.0001	***	Yes	
ANOVA table	SS	DF	MS	F (DFn, DFd)	P value
Interaction	0.06058	20	0.003029	F (20, 90) = 0.9659	P = 0.5213
DOY	5.060	4	1.265	F (4, 90) = 399.1	P < 0.0001
Irrigation	0.2406	5	0.04813	F (5, 90) = 15.19	P < 0.0001
Residual	0.2852	90	0.003169		
Number of missing values	0				

Figure 4 Evolution of berry juice pH, season 2008-09. a) pH as a function of the day of the year (DOY) for each irrigation treatment. Mean +/- SEM are shown. b) Two-way ANOVA indicating significant effects of irrigation and DOY, but no significant interaction, indicating that the evolution of pH did not differ between the treatments.

a)

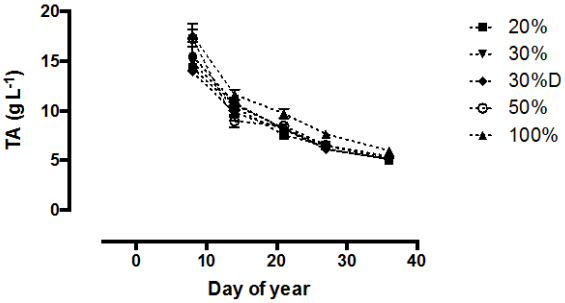

b)

Two-way ANOVA	Ordinary				
Alpha	0.05				
Source of Variation	% of total variation	P value	P value summary	Significant?	
Interaction	2.097	0.1036	ns	No	
DOY	88.91	< 0.0001	***	Yes	
Irrigation	2.669	< 0.0001	***	Yes	
ANOVA table	SS	DF	MS	F (DFn, DFd)	P value
Interaction	36.73	20	1.836	F (20, 90) = 1.493	P = 0.1036
DOY	1557	4	389.3	F (4, 90) = 316.4	P < 0.0001
Irrigation	46.73	5	9.346	F (5, 90) = 7.597	P < 0.0001
Residual	110.7	90	1.230		
Number of missing values	0				

Figure 5 Evolution of berry juice titratable acidity (TA), season 2008-09. a) TA as a function of the day of the year (DOY) for each irrigation treatment. Mean +/- SEM are shown. b) Two-way ANOVA indicating significant effects of irrigation and DOY, but no significant interaction, indicating that the evolution of TA did not differ between the treatments.

Season 2009-10: Two years of deficit

Evolution of berry weight, TSS, sugar per berry, pH and TA are shown as above in Figures 6,7,8,9,10. Berry weights were low in 2009-10 for the control and treatments but a larger increment in weight can be observed during ripening. In this season there was no indication of berry weight loss and there was no significant interaction between time and treatment (Figure 6). Total soluble solids showed a consistent increase between all treatments with no obvious plateau except at the very last sample time (Figure 7). Again there were significant differences between treatments but no interaction between time and treatment. Sugars per berry again showed a divergence in the rate of accumulation with a significant interaction between time and treatment indicating that sugars accumulated more slowly with deficits on a per berry basis (Figure 8). Juice pH and TA were only recorded on three occasions in this season, but showed the same general trends observed for only one continuous year of deficit. There were no interactions between time and treatment (Figure 9,10).

a)

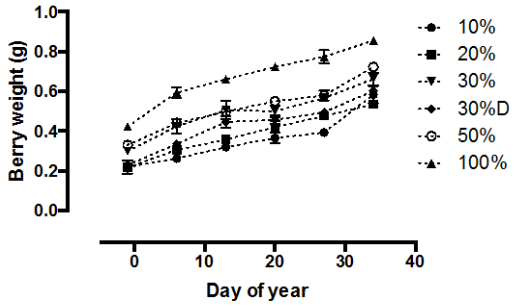

b)

Two-way RM ANOVA	Matching: Stacked				
Alpha	0.05				
Source of Variation	% of total variation	P value	P value summary	Significant?	
Interaction	1.661	0.0512	ns	No	
DOY	47.05	< 0.0001	****	Yes	
Irrigation	37.23	< 0.0001	****	Yes	
Subjects (matching)	5.081	< 0.0001	****	Yes	
ANOVA table	SS	DF	MS	F (DFn, DFd)	P value
Interaction	0.1396	25	0.005586	F (25, 210) = 1.554	P = 0.0512
DOY	3.956	5	0.7912	F (5, 210) = 220.1	P < 0.0001
Irrigation	3.130	5	0.6260	F (5, 42) = 61.54	P < 0.0001
Subjects (matching)	0.4272	42	0.01017	F (42, 210) = 2.830	P < 0.0001
Residual	0.7549	210	0.003595		

Figure 6 Evolution of berry weight, season 2009-10. a) Berry weight as a function of the day of the year (DOY) for each irrigation treatment. Mean +/- SEM are shown. b) Two-way ANOVA indicating significant effects of irrigation and DOY, but no significant interaction, indicating that the evolution of berry weight did not differ between the treatments.

a)

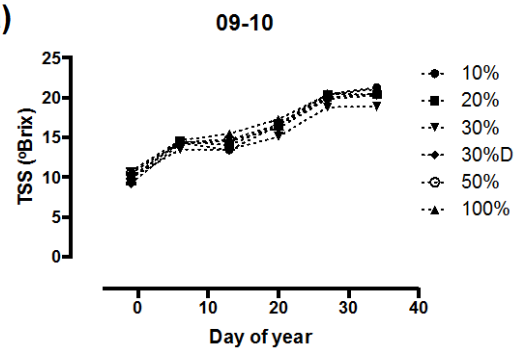

b)

Two-way ANOVA	Ordinary				
Alpha	0.05				
Source of Variation	% of total variation	P value	P value summary	Significant?	
Interaction	0.9255	0.1982	ns	No	
DOY	89.65	< 0.0001	****	Yes	
Irrigation	1.751	< 0.0001	****	Yes	
ANOVA table	SS	DF	MS	F (DFn, DFd)	P value
Interaction	37.74	25	1.509	F (25, 251) = 1.248	P = 0.1962
DOY	3655	5	731.0	F (5, 251) = 604.3	P < 0.0001
Irrigation	71.38	5	14.28	F (5, 251) = 11.80	P < 0.0001
Residual	303.6	251	1.210		
Number of missing values	1				

Figure 7 Evolution of concentration of total soluble solids (TSS), season 2009-10. a) TSS as a function of the day of the year (DOY) for each irrigation treatment. Mean +/- SEM are shown. b) Two-way ANOVA indicating significant effects of irrigation and DOY, but no significant interaction, indicating that the evolution of TSS did not differ between the treatments.

a)

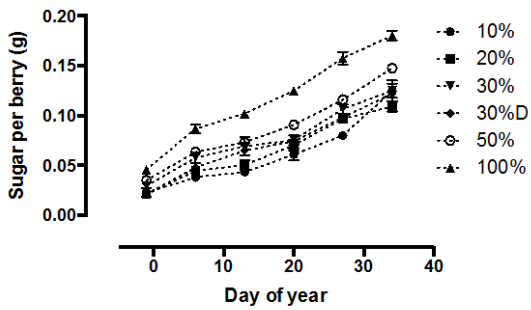

b)

Two-way ANOVA	Ordinary				
Alpha	0.05				
Source of Variation	% of total variation	P value	P value summary	Significant?	
Interaction	2.359	0.0001	***	Yes	
DOY	68.82	< 0.0001	****	Yes	
Irrigation	19.39	< 0.0001	****	Yes	
ANOVA table	SS	DF	MS	F (DFn, DFd)	P value
Interaction	0.01168	25	0.0004671	F (25, 251) = 2.561	P = 0.0001
DOY	0.3407	5	0.06813	F (5, 251) = 373.6	P < 0.0001
Irrigation	0.09597	5	0.01919	F (5, 251) = 105.2	P < 0.0001
Residual	0.04578	251	0.0001824		
Number of missing values	1				

Figure 8 Evolution of sugar per berry, season 2009-10. a) Sugar per berry as a function of the day of the year (DOY) for each irrigation treatment. Mean +/- SEM are shown. b) Two-way ANOVA indicating significant effects of irrigation and DOY, and a significant interaction indicating that the evolution of sugar per berry differed between the treatments.

a)

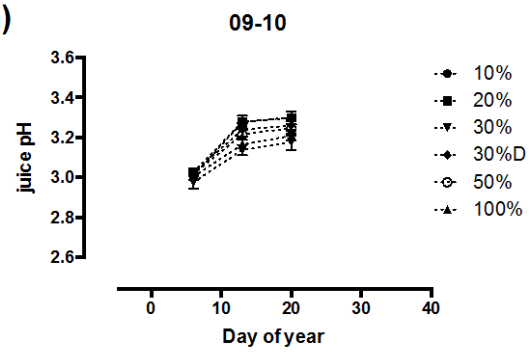

b)

Two-way ANOVA	Ordinary				
Alpha	0.05				
Source of Variation	% of total variation	P value	P value summary	Significant?	
Interaction	1.733	0.6376	ns	No	
DOY	62.99	< 0.0001	****	Yes	
Irrigation	7.669	< 0.0001	****	Yes	
ANOVA table	SS	DF	MS	F (DFn, DFd)	P value
Interaction	0.04507	10	0.004507	F (10, 126) = 0.7908	P = 0.6376
DOY	1.638	2	0.8191	F (2, 126) = 143.7	P < 0.0001
Irrigation	0.1995	5	0.03989	F (5, 126) = 7.000	P < 0.0001
Residual	0.7180	126	0.005699		
Number of missing values	0				

Figure 9 Evolution of berry juice pH, season 2009-10. a) pH as a function of the day of the year (DOY) for each irrigation treatment. Mean +/- SEM are shown. b) Two-way ANOVA indicating significant effects of irrigation and DOY, but no significant interaction, indicating that the evolution of pH did not differ between the treatments.

a)

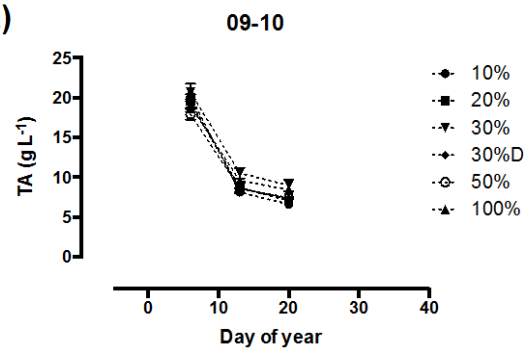

b)

Two-way ANOVA	Ordinary				
Alpha	0.05				
Source of Variation	% of total variation	P value	P value summary	Significant?	
Interaction	0.7601	0.3626	ns	No	
DOY	89.31	< 0.0001	****	Yes	
Irrigation	1.473	0.0011	**	Yes	
ANOVA table	SS	DF	MS	F (DFn, DFd)	P value
Interaction	33.88	10	3.388	F (10, 125) = 1.120	P = 0.3626
DOY	3980	2	1990	F (2, 125) = 657.9	P < 0.0001
Irrigation	65.63	5	13.13	F (5, 125) = 4.339	P = 0.0011
Residual	378.1	125	3.025		
Number of missing values	1				

Figure 10 Evolution of berry juice titratable acidity (TA), season 2009-10. a) TA as a function of the day of the year (DOY) for each irrigation treatment. Mean +/- SEM are shown. b) Two-way ANOVA indicating significant effects of irrigation and DOY, but no significant interaction, indicating that the evolution of TA did not differ between the treatments.

Season 2010-11: Three years of deficit

Evolution of berry weight, TSS, sugar per berry, pH and TA are shown as above in Figures 11,12,13,14,15. Berry weights were higher in 2010-11 for the control and treatments and a large increment in weight can be observed during ripening. Again there was no indication of berry weight loss and there was no significant interaction between time and treatment (Figure 11). Total soluble solids showed a consistent increase between all treatments with no obvious plateau except at the very last sample time (Figure 12). As for 08-09 and 09-10 there were significant differences between treatments but no interaction between time and treatment. In contrast to the first two seasons sugars per berry did not show a divergence in the rate of accumulation and there was no significant difference between treatments and no significant interaction between time and treatment (Figure 13). Juice pH and TA showed the same general trends observed for the previous two seasons and there were no interactions between time and treatment (Figure 14,15).

a)

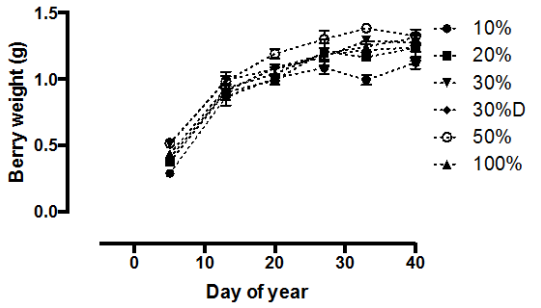

b)

Two-way ANOVA	Ordinary				
Alpha	0.05				
Source of Variation	% of total variation	P value	P value summary	Significant?	
Interaction	2.728	0.9406	ns	No	
Row Factor	71.77	< 0.0001	****	Yes	
Irrigation	6.947	< 0.0001	****	Yes	
ANOVA table	SS	DF	MS	F (DFn, DFd)	P value
Interaction	0.1709	25	0.006835	F (25, 89) = 0.5769	P = 0.9406
Row Factor	4.496	5	0.8989	F (5, 89) = 75.87	P < 0.0001
Irrigation	0.4351	5	0.08702	F (5, 89) = 7.345	P < 0.0001
Residual	1.054	89	0.01185		
Number of missing values	19				

Figure 11 Evolution of berry weight, season 2010-11. a) Berry weight as a function of the day of the year (DOY) for each irrigation treatment. Mean +/- SEM are shown. b) Two-way ANOVA indicating significant effects of irrigation and DOY, but no significant interaction, indicating that the evolution of berry weight did not differ between the treatments.

a)

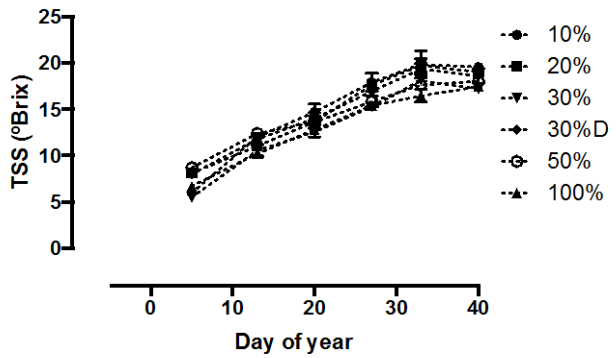

b)

Two-way ANOVA	Ordinary				
Alpha	0.05				
Source of Variation	% of total variation	P value	P value summary	Significant?	
Interaction	2.061	0.7994	ns	No	
Time	82.73	< 0.0001	****	Yes	
Irrigation	3.463	< 0.0001	****	Yes	
ANOVA table	SS	DF	MS	F (DFn, DFd)	P value
Interaction	33.27	25	1.331	F (25, 89) = 0.7424	P = 0.7994
Time	1335	5	267.1	F (5, 89) = 149.0	P < 0.0001
Irrigation	55.91	5	11.18	F (5, 89) = 6.237	P < 0.0001
Residual	159.6	89	1.793		
Number of missing values	19				

Figure 12 Evolution of concentration of total soluble solids (TSS), season 2010-11. a) TSS as a function of the day of the year (DOY) for each irrigation treatment. Mean +/- SEM are shown. b) Two-way ANOVA indicating significant effects of irrigation and DOY, but no significant interaction, indicating that the evolution of TSS did not differ between the treatments.

a)

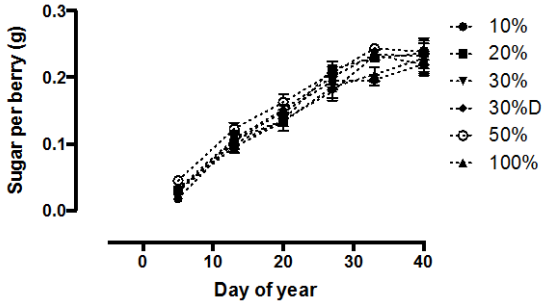

b)

Two-way ANOVA	Ordinary				
Alpha	0.05				
Source of Variation	% of total variation	P value	P value summary	Significant?	
Interaction	1.566	0.9859	ns	No	
Time	84.34	< 0.0001	****	Yes	
Irrigation	1.393	0.0816	ns	No	
ANOVA table	SS	DF	MS	F (DFn, DFd)	P value
Interaction	0.007331	25	0.0002932	F (25, 89) = 0.4567	P = 0.9859
Time	0.3951	5	0.07903	F (5, 89) = 123.1	P < 0.0001
Irrigation	0.006525	5	0.001305	F (5, 89) = 2.033	P = 0.0816
Residual	0.05714	89	0.0006420		
Number of missing values	19				

Figure 13 Evolution of sugar per berry, season 2010-11. a) Sugar per berry as a function of the day of the year (DOY) for each irrigation treatment. Mean +/- SEM are shown. b) Two-way ANOVA indicating no significant effects of irrigation, and no significant interaction between DOY and irrigation indicating that the evolution of sugar per berry did not differ between the treatments.

a)

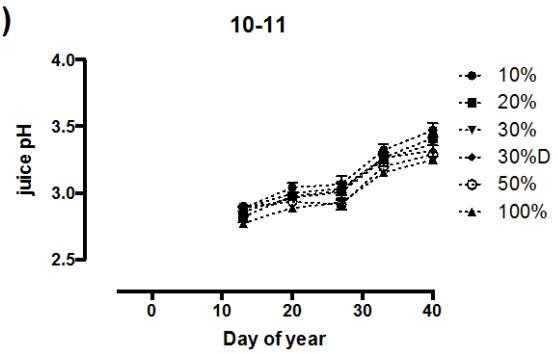

b)

Two-way ANOVA	Ordinary				
Alpha	0.05				
Source of Variation	% of total variation	P value	P value summary	Significant?	
Interaction	1.657	0.7997	ns	No	
Time	81.55	< 0.0001	****	Yes	
Irrigation	5.859	< 0.0001	****	Yes	
ANOVA table	SS	DF	MS	F (DFn, DFd)	P value
Interaction	0.08185	20	0.004092	F (20, 88) = 0.7161	P = 0.7997
Time	4.029	4	1.007	F (4, 88) = 176.3	P < 0.0001
Irrigation	0.2895	5	0.05790	F (5, 88) = 10.13	P < 0.0001
Residual	0.5029	88	0.005714		
Number of missing values	2				

Figure 14 Evolution of berry juice pH, season 2010-11. a) pH as a function of the day of the year (DOY) for each irrigation treatment. Mean +/- SEM are shown. b) Two-way ANOVA indicating significant effects of irrigation and DOY, but no significant interaction, indicating that the evolution of pH did not differ between the treatments.

a)

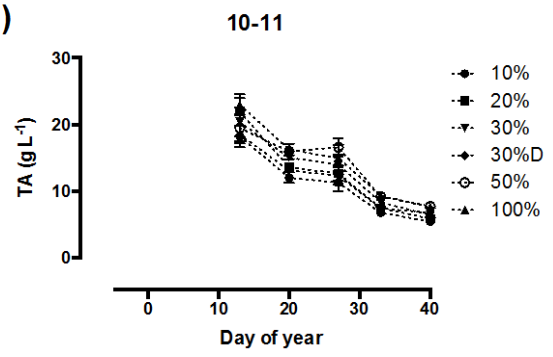

b)

Two-way ANOVA	Ordinary				
Alpha	0.05				
Source of Variation	% of total variation	P value	P value summary	Significant?	
Interaction	1.927	0.8687	ns	No	
Time	79.56	< 0.0001	****	Yes	
Irrigation	4.833	< 0.0001	****	Yes	
ANOVA table	SS	DF	MS	F (DFn, DFd)	P value
Interaction	67.21	20	3.360	F (20, 87) = 0.6430	P = 0.8687
Time	2775	4	693.7	F (4, 87) = 132.7	P < 0.0001
Irrigation	168.6	5	33.71	F (5, 87) = 6.451	P < 0.0001
Residual	454.6	87	5.226		
Number of missing values	3				

Figure 15 Evolution of berry juice titratable acidity (TA), season 2010-11. a) TA as a function of the day of the year (DOY) for each irrigation treatment. Mean +/- SEM are shown. b) Two-way ANOVA indicating significant effects of irrigation and DOY, but no significant interaction, indicating that the evolution of TA did not differ between the treatments.

Final harvest berry composition and the effect of deficit and recovery

10% treatment

Figure 16 shows TSS and sugar per berry over three seasons in which these were measured, 2008-09 to 2010-11 for the 10% irrigation treatment, and for various periods of continuous deficit and recovery. There were no significant differences in TSS for one year of deficit and two years of recovery (Figure 16a), but higher TSS was obtained when vines were subjected to two years of deficit plus one year of recovery (Figure 16c) and three years of deficit (Figure 16e). The 2009-10 season in each case did not show a difference in TSS, but in this season the yield was substantially reduced compared to other seasons. Generally sugar per berry was reduced significantly by one, two or three years of deficits (Figure 16b,d,f), though the vines subjected to three continuous years of 10% irrigation showed less response in the second and third year (Figure 16f). In terms of recoveries, there appeared to be no consistent carry-over from the deficit year(s) to the recovery season(s) except for the two year deficit where significant differences in both TSS and sugars per berry were observed in the recovery season (Figure 16c,d)

Figure 17 shows juice pH and titratable acidity (TA) in the same format as for Figure 16 over the three seasons. More consistent differences were observed for pH than for TSS with one, two and three seasons of continuous deficit showing significantly increased pH (Figure 17a,c,e respectively). TA was reduced by the 10% irrigation treatment, but less consistently between the three combinations of deficit and recovery. Only in year two (2010-11) of the two year and three year continuous deficit was there a significant reduction in TA (Figure 17d,f), and as mentioned earlier this season was an outlier in terms of much reduced total yield across all treatments.

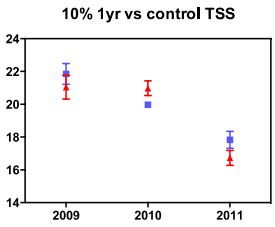

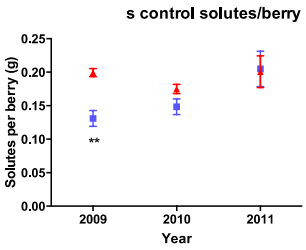

Figure 16 Concentration of total soluble solids (TSS) (a,c,e) and sugars per berry (b,d,f) for the 10% irrigation treatment applied for one season (2008-09) then two seasons of recovery (a,b), two seasons (2008-09, 2009-10) then one season of recovery (c,d), three seasons (2008-09, 2009-10, 2010-11) (e,f) each compared to the respective controls (red triangle symbols) plotted over time. Mean +/- SEM is shown and level of significant difference within a year is indicated (*<0.05 **<0.01 *** <0.001 ****<0.0001, 2-way ANOVA with Holm Sidak's multiple comparison).

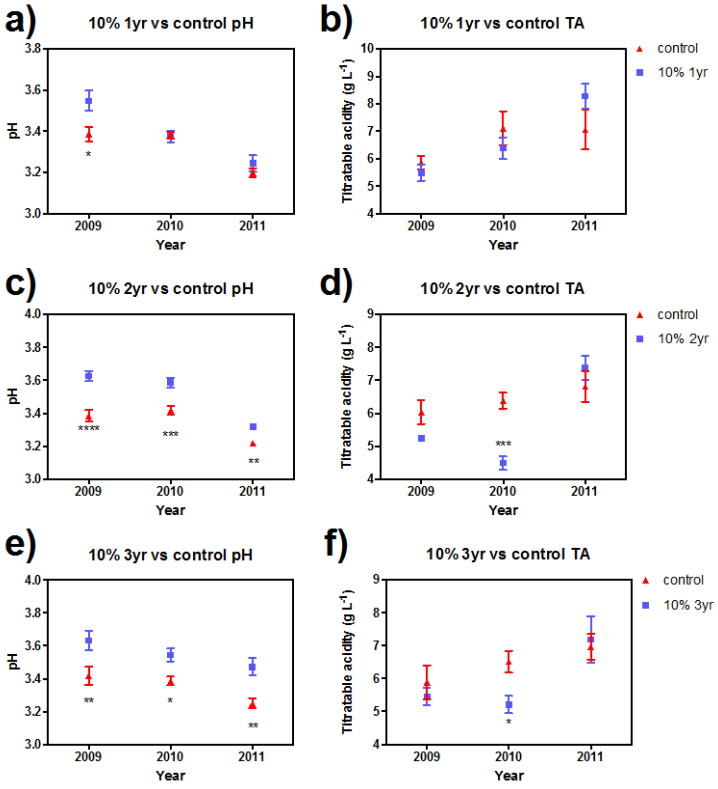

Figure 17 Berry juice pH (a,c,e) and titratable acidity (b,d,f) for the 10% irrigation treatment applied for one season (2008-09) then two seasons of recovery (a,b), two seasons (2008-09, 2009-10) then one season of recovery (c,d), three seasons (2008-09, 2009-10, 2010-11) (e,f) each compared to the respective controls (red triangle symbols) plotted over time. Mean +/- SEM is shown and level of significant difference within a year is indicated (*<0.05 **<0.01 *** <0.001 ****<0.0001, 2-way ANOVA with Holm Sidak's multiple comparison).

20% treatment

Figure 18 shows TSS and sugar per berry for the 20% treatment over three seasons in the same format as presented above for the 10% treatment. There were no significant differences in TSS for one year of deficit and three years of deficit (Figure 18a,e), though the trend was for higher TSS except in season 2009-10. The two-year deficit and one year recovery showed significant differences and a possible lack of full recovery in the 2010-11 season (Figure 18c). As per the 10% treatment sugar per berry was reduced significantly in some combinations of continuous deficit (Figure 18b,d,f), though the vines subjected to three continuous years of 20% irrigation showed less response in the second and third year (Figure 18f) as was also observed for the 10% treatment. There appeared to be no consistent carry over from the deficit year(s) to the recovery season(s) except for the two -year deficit where significant differences in both TSS and sugars per berry were observed in the recovery season (Figure 16c,d). There was an overshoot in sugar per berry in the recovery season (Figure 18d), a trend that was also observed for the 10% treatment.

Figure 19 shows juice pH and titratable acidity (TA) in the same format as above over the three seasons. Again more consistent differences were observed for pH than for TSS with one, two and three seasons of continuous deficit showing significantly increased pH (Figure 19a,c,e respectively). TA was reduced by the 20% treatment but with less consistency between duration as also observed for 10%. The second season (2010-11) of the two year and three year continuous deficit showed a significant reduction in TA (Figure 19d,f). There was a significant increase in pH of vines that had one year of recovery after two years of continuous deficit (Figure 19c).

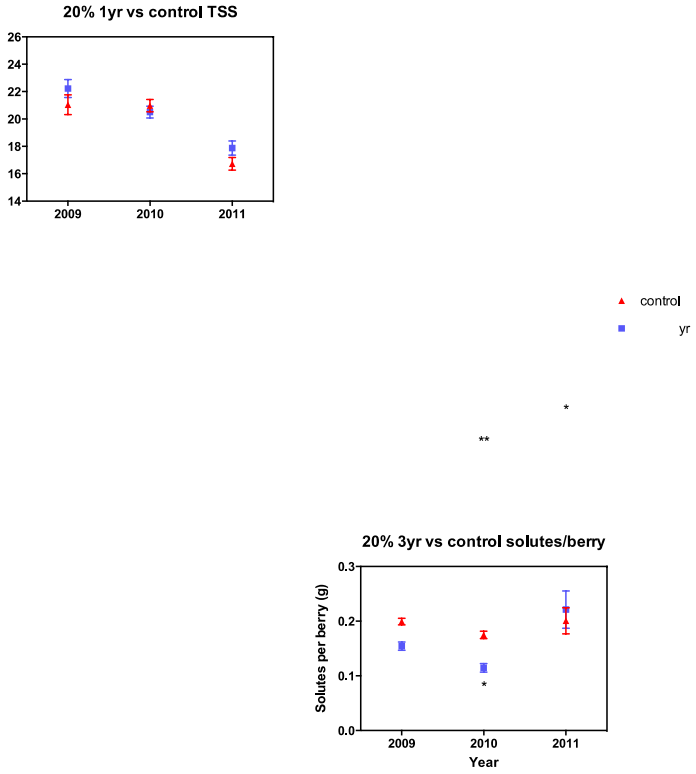

Figure 18 Concentration of total soluble solids (TSS) (a,c,e) and sugars per berry (b,d,f) for the 20% irrigation treatment applied for one season (2008-09) then two seasons of recovery (a,b), two seasons (08-09, 09-10) then one season of recovery (c,d), three seasons (2008-09, 2009-10, 2010-11) (e,f) each compared to the respective controls (red triangle symbols) plotted over time. Mean +/- SEM is shown and level of significant difference within a year is indicated (*<0.05 **<0.01 *** <0.001 ****<0.0001, 2-way ANOVA with Holm Sidak's multiple comparison).

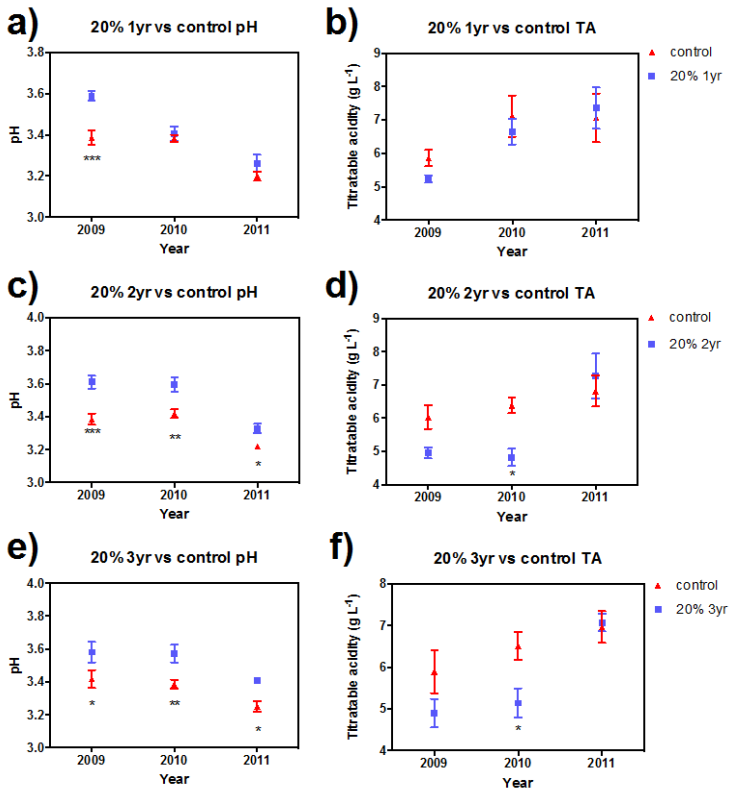

Figure 19 Berry juice pH (a,c,e) and titratable acidity (b,d,f) for the 20% irrigation treatment applied for one season (2008-09) then two seasons of recovery (a,b), two seasons (2008-09, 2009-10) then one season of recovery (c,d), three seasons (2008-09, 2009-10, 2010-11) (e,f) each compared to the respective controls (red triangle symbols) plotted over time. Mean +/- SEM is shown and level of significant difference within a year is indicated (*<0.05 **<0.01 *** <0.001 ****<0.0001, 2-way ANOVA with Holm Sidak's multiple comparison).

30% treatment

Figure 20 shows TSS and sugar per berry for the 30% treatment over three seasons in the same format as presented above. The first season (2008-09) of the continuous deficits showed an increase in TSS, though only significant in the three-year continuous deficit set (Figure 20e). Season 2009-10 showed a significant decrease in TSS under deficit for the two year and three year continuous set (Figure 20c,e). There was no apparent carry-over effect into the recovery years for each of the treatment durations. As for the 10% and 20% treatments sugar per berry was reduced significantly in some combinations of continuous deficit (Figure 20b,d,f), though the vines subjected to three continuous years of 30% irrigation showed less response in the third year (Figure 18f) as was also observed for the 20% treatment. There was an overshoot in sugar per berry in the recovery season after two years of deficit (Figure 20d), a trend that was also observed for the 10% and 20% treatment.

Figure 21 shows juice pH and titratable acidity (TA) in the same format as above. Higher pH was observed only in the first season (2008-09), also the driest, of the continuous deficit treatments (Figure 21a,c,e). TA was reduced by the 30% treatment but with less consistency between duration as also observed for 10%. There was no clear carry-over effect into the recovery years for any of the combinations.

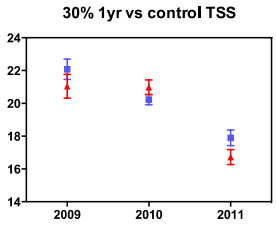

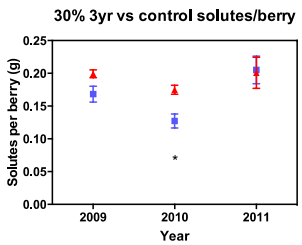

Figure 20 Concentration of total soluble solids (TSS) (a,c,e) and sugars per berry (b,d,f) for the 30% irrigation treatment applied for one season (2008-09) then two seasons of recovery (a,b), two seasons (2008-09, 2009-10) then one season of recovery (c,d), three seasons (2008-09, 2009-10, 2010-11) (e,f) each compared to the respective controls (red triangle symbols) plotted over time. Mean +/- SEM is shown and level of significant difference within a year is indicated (*<0.05 **<0.01 *** <0.001 ****<0.0001, 2-way ANOVA with Holm Sidak's multiple comparison).

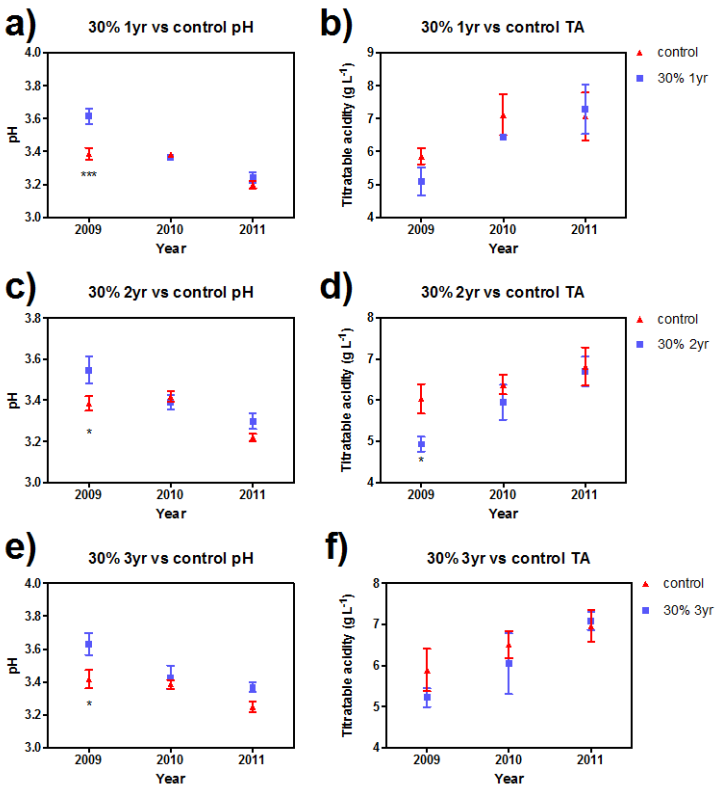

Figure 21 Berry juice pH (a,c,e) and titratable acidity (b,d,f) for the 30% irrigation treatment applied for one season (2008-09) then two seasons of recovery (a,b), two seasons (2008-09, 2009-10) then one season of recovery (c,d), three seasons (2008-09, 2009-10, 2010-11) (e,f) each compared to the respective controls (red triangle symbols) plotted over time. Mean +/- SEM is shown and level of significant difference within a year is indicated (*<0.05 **<0.01 *** <0.001 ****<0.0001, 2-way ANOVA with Holm Sidak's multiple comparison).

30%D treatment

Figure 22 shows TSS and sugar per berry for the 30%D (reduced depth) treatment over three seasons in the same format as presented above. There were significant differences in TSS for the two year deficit and one year recovery (Figure 22c). As for other treatments sugar per berry was reduced under continuous deficit (Figure 22b,d,f), though the vines subjected to three continuous years of 30%D irrigation showed less no response in the third year (Figure 22f) as was also observed for the other deficit treatments. There appeared to be no consistent carry over from the deficit season(s) to the recovery season(s) except for the two-year deficit where significant differences in both TSS and sugars per berry were observed in the recovery season (Figure 22c,d). There was an overshoot in sugar per berry in the recovery season (Figure 22d), a trend that was also observed for the other treatments.

Figure 23 shows juice pH and titratable acidity (TA) in the same format as above. Consistent differences were observed for pH with one and two seasons of continuous deficit showing significantly increased pH (Figure 23a,c

respectively). This was not consistent with the third year of continuous deficit (Figure 23e. The second season (2010-11) of the two year and three year continuous deficit showed a significant reduction in TA (Figure 23d,f). There was a significant increase in juice pH from vines that had one year of recovery after two years of continuous deficit (Figure 23c), similar to that observed for the other deficit treatments.

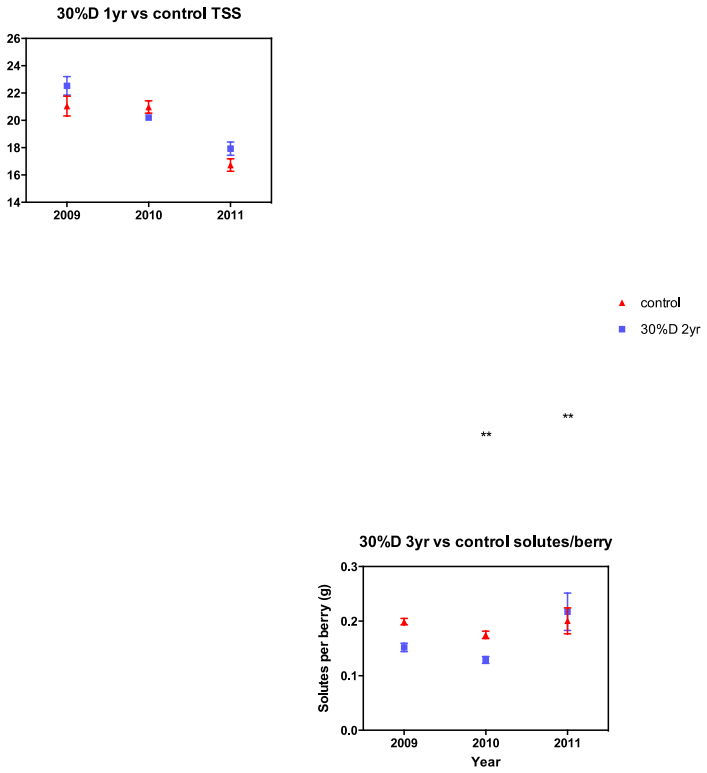

Figure 22 Concentration of total soluble solids (TSS) (a,c,e) and sugars per berry (b,d,f) for the 30%D (reduced depth) irrigation treatment applied for one season (2008-09) then two seasons of recovery (a,b), two seasons (2008-09, 2009-10) then one season of recovery (c,d), three seasons (2008-09, 2009-10, 2010-11) (e,f) each compared to the respective controls (red triangle symbols) plotted over time. Mean +/- SEM is shown and level of significant difference within a year is indicated (*<0.05 **<0.01 *** <0.001 ****<0.0001, 2-way ANOVA with Holm Sidak's multiple comparison).

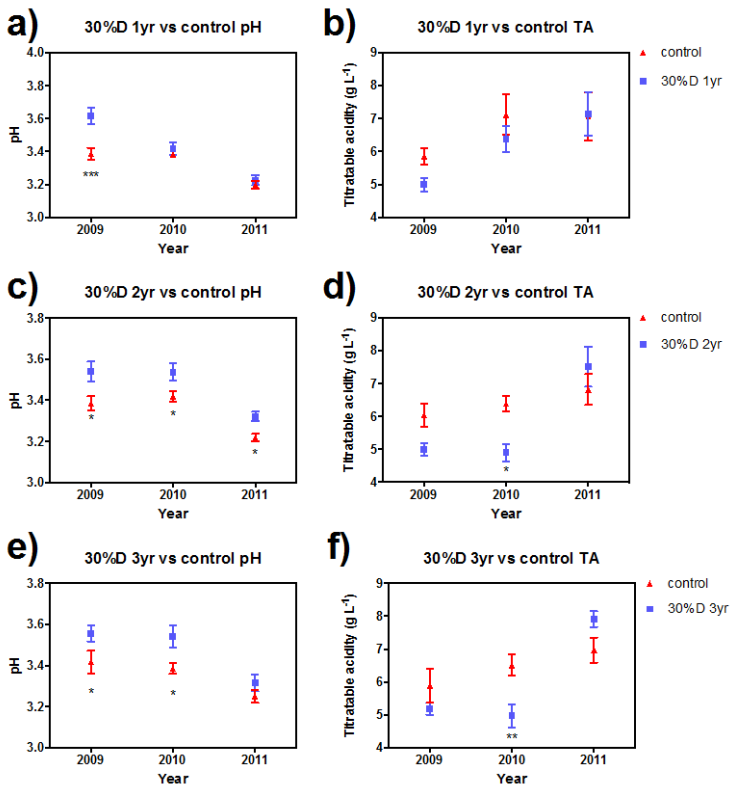

Figure 23 Berry juice pH (a,c,e) and titratable acidity (b,d,f) for the 30%D (reduced depth) irrigation treatment applied for one season (2008-09) then two seasons of recovery (a,b), two seasons (2008-09, 2009-10) then one season of recovery (c,d), three seasons (2008-09, 2009-10, 2010-11) (e,f) each compared to the respective controls (red triangle symbols) plotted over time. Mean +/- SEM is shown and level of significant difference within a year is indicated (*<0.05 **<0.01 *** <0.001 ****<0.0001, 2-way ANOVA with Holm Sidak's multiple comparison).

50% treatment

Figure 24 (TSS, solutes per berry) and Figure 25 (pH, TA) are shown in the same formats as above. Only small or no treatment effects were observed with the 50% deficit treatment, but the trends were in the same direction as for more extreme deficits with sometimes increases in TSS and decreases in solutes per berry. There were no carry-over effects into the recovery seasons. Similar effects were observed for pH and TA with an increase in pH with deficit and decrease in TA (Figure 25).

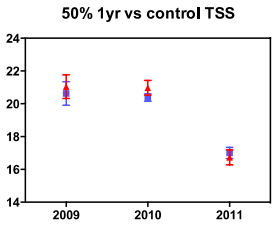

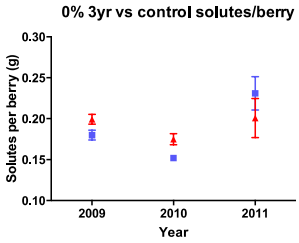

Figure 24 Concentration of total soluble solids (TSS) (a,c,e) and sugars per berry (b,d,f) for the 50% irrigation treatment applied for one season (2008-09) then two seasons of recovery (a,b), two seasons (2008-09, 2009-10) then one season of recovery (c,d), three seasons (2008-09, 2009-10, 2010-11) (e,f) each compared to the respective controls (red triangle symbols) plotted over time. Mean +/- SEM is shown and level of significant difference within a year is indicated (*<0.05 **<0.01 *** <0.001 ****<0.0001, 2-way ANOVA with Holm Sidak's multiple comparison).

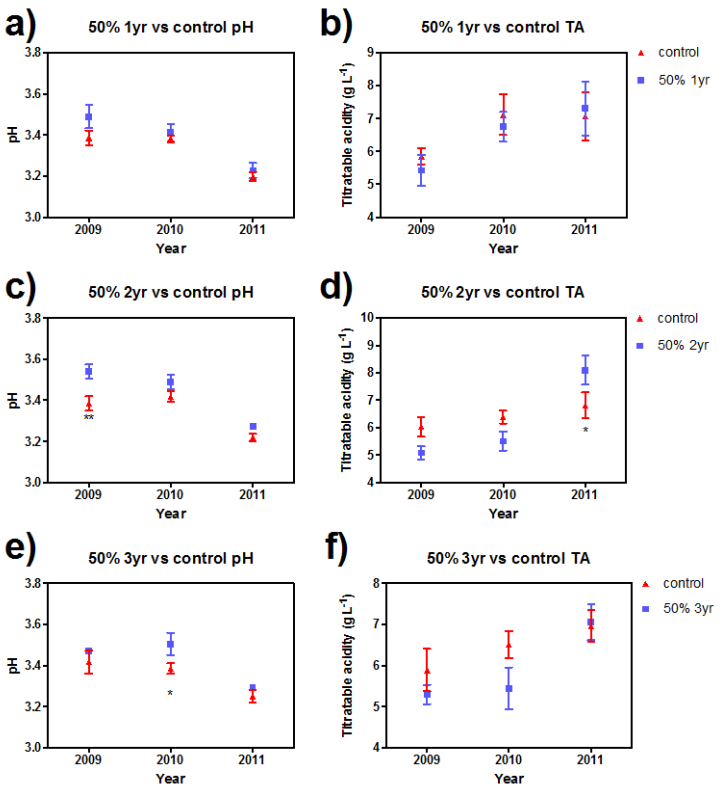

Figure 25 Berry juice pH (a,c,e) and titratable acidity (b,d,f) for the 50% irrigation treatment applied for one season (2008-09) then two seasons of recovery (a,b), two seasons (2008-09, 2009-10) then one season of recovery (c,d), three seasons (2008-09, 2009-10, 2010-11) (e,f) each compared to the respective controls (red triangle symbols) plotted over time. Mean +/- SEM is shown and level of significant difference within a year is indicated (*<0.05 **<0.01 *** <0.001 ****<0.0001, 2-way ANOVA with Holm Sidak's multiple comparison).

Association between berry components and irrigation plus effective rain.

Figure 26 shows TSS plotted as a function of irrigation plus effective rain over each of three growing seasons. Within each season there is only a small and generally insignificant effect of total incident water on TSS of juice at harvest (Figure 26b), however the effect of the different rainfall amounts from season to season can be seen as a general increase in TSS with reduced rainfall in the order of (reducing rainfall) 2010-11 < 2009-10 < 2008-09. In fact if the controls are removed there is a highly significant negative correlation between increasing irrigation plus effective rain and decreasing TSS. Given that within a season there was no effect of total incident water, the correlation between TSS and incident water across all seasons may be related to a common environmental factor with rainfall, for example mean January temperature or total growing degree days. Although 2010-11 was the coolest (GDD = 1849 ^{o}C day) and wettest season, which matches to the lower TSS, it is difficult to reconcile the difference between season 2008-09 (GDD = 2129 ^{o}C day) and 2009-10 (GDD = 2331 ^{o}C day), though the latter also had a much reduced yield due to unfavourable conditions at flowering.

Sugar per berry is plotted against irrigation and effective rain in Figure 27a showing strong and positive correlations in 2008-09 and 2009-10 but not in 2010-11 (Figure 27b). These correlations are very similar to those for berry weight as a function of irrigation plus effective rain across the three seasons (see Figure 47 in 6.2). As a speculation the 2008-09 and 2010-11 data could indicate a saturation of berry size and sugar content at the high end of rainfall plus irrigation.

Juice pH at harvest consistently increased with reduced irrigation plus effective rain across each of the three seasons (Figure 28a). The slopes of the fitted linear regressions were highly significant and not significantly different between the three seasons (Figure 28b). The pooled slope is 0.0367 pH unit decline per 100 mm of irrigation plus effective rain.

Titratable acidity did not show a consistent correlation with irrigation plus effective rain except in season 2009-10 where there was a decline in TA with decreasing irrigation plus effective rain (Figure 29a,b). This trend was observed in 2008-09 but was not significant.

a)

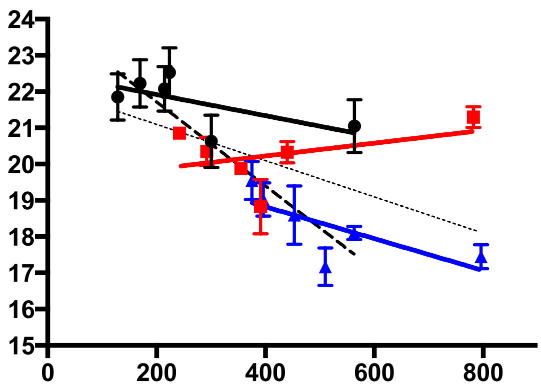

b)

					01158*X + 24.03

Figure 26 Concentration of total soluble solids (TSS) as a function of irrigation plus effective rain for all sub-treatments across three seasons. The season data (indicated with different symbols) includes deficit and control treated vines. For the deficit treatments these can have up to three consecutive seasons of deficit (2010-11). Regression lines are through the combined data for each season with the regression details shown in the table below the graph (b). A linear regression through all the data for the combined three seasons (All, dotted line) was significant,

as was the regression through the combined data minus controls (All-controls, dashed line). Means +/- SEM are shown.

a)

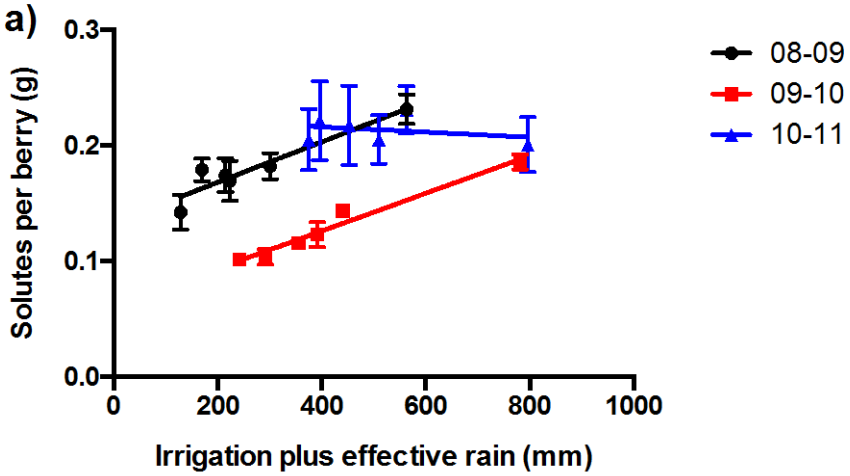

b)

	2009	2010	2011
Best-fit values			
Slope	0.0001747 ± 3.785e-005	0.0001626 ± 1.508e-005	-2.236e-005 ± 7.322e-005
Y-intercept when X=0.0	0.1330 ± 0.01145	0.06089 ± 0.006826	0.2248 ± 0.03914
X-intercept when Y=0.0	-761.4	-374.5	10055
1/slope	5723	6150	-44721
95% Confidence Intervals			
Slope	9.622e-005 to 0.0002532	0.0001313 to 0.0001939	-0.0001742 to 0.0001295
Y-intercept when X=0.0	0.1093 to 0.1568	0.04673 to 0.07505	0.1437 to 0.3060
X-intercept when Y=0.0	-1605 to -438.2	-566.7 to -243.0	1733 to +infinity
Goodness of Fit			
R square	0.4920	0.8409	0.004221
Sy.x	0.02648	0.01296	0.05050
Is slope significantly non-zero?			
F	21.31	116.2	0.09326
DFn, DFd	1.000, 22.00	1.000, 22.00	1.000, 22.00
P value	0.0001	< 0.0001	0.7629
Deviation from zero?	Significant	Significant	Not Significant
Data			
Number of X values	6	6	6
Maximum number of Y replicates	4	4	4
Total number of values	24	24	24
Number of missing values	48	48	48
Equation	Y = 0.0001747*X + 0.1330	Y = 0.0001626*X + 0.06089	Y = -2.236e-005*X + 0.2248

Are the slopes equal?
F = 1.74369. DFn=2 DFd=66
P=0.1828

If the overall slopes were identical, there is a 18% chance of randomly choosing data points with slopes this different. You can conclude that the differences between the slopes are not significant.

Since the slopes are not significantly different, it is possible to calculate one slope for all the data. The pooled slope equals 0.0143943

Are the elevations or intercepts equal?
F = 83.0882. DFn=2 DFd=68
P<0.0001

If the overall elevations were identical, there is a less than 0.01% chance of randomly choosing data points with elevations this different. You can conclude that the differences between the elevations are extremely significant.

Figure 27 Sugars per berry as a function of irrigation plus effective rain for all sub-treatments across three seasons. The season data (indicated with different symbols) includes deficit and control treated vines. For the deficit treatments these can have up to three consecutive seasons of deficit (2010-11). Regression lines are through the combined data for each season with the regression details shown in the table below the graph (b). Season 2010-11 was not significant. Means +/- SEM are shown.

a)

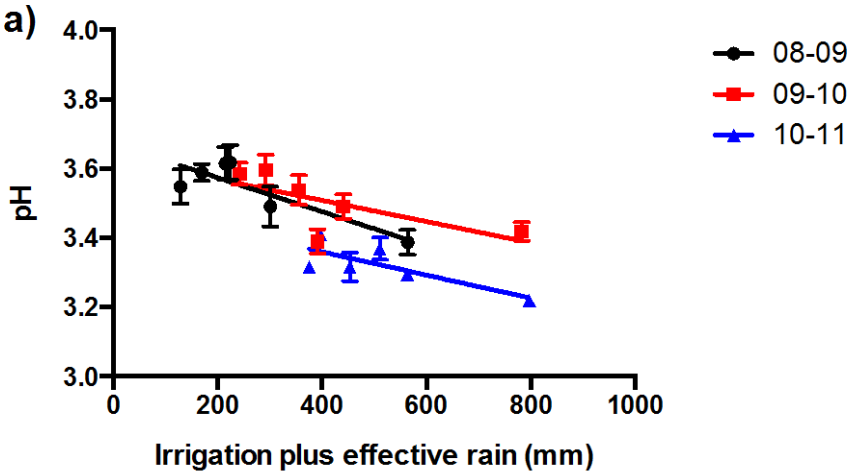

b)

	2009	2010	2011
Best-fit values			
Slope	-0.0004919 ± 0.0001330	-0.0003052 ± 0.0001037	-0.0003340 ± 8.476e-005
Y-intercept when X=0.0	3.672 ± 0.04024	3.630 ± 0.04693	3.493 ± 0.04531
X-intercept when Y=0.0	7466	11896	10458
1/slope	-2033	-3277	-2994
95% Confidence Intervals			
Slope	-0.0007676 to -0.0002161	-0.0005202 to -9.010e-005	-0.0005098 to -0.0001582
Y-intercept when X=0.0	3.589 to 3.756	3.533 to 3.728	3.399 to 3.587
X-intercept when Y=0.0	4879 to 16655	7150 to 39296	7029 to 21505
Goodness of Fit			
R square	0.3835	0.2825	0.4138
Sy.x	0.09303	0.08909	0.05845
Is slope significantly non-zero?			
F	13.68	8.661	15.53
DFn, DFd	1.000, 22.00	1.000, 22.00	1.000, 22.00
P value	0.0013	0.0075	0.0007
Deviation from zero?	Significant	Significant	Significant
Data			
Number of X values	6	6	6
Maximum number of Y replicates	4	4	4
Total number of values	24	24	24
Number of missing values	48	48	48
Equation	Y = -0.0004919*X + 3.672	Y = -0.0003052*X + 3.630	Y = -0.0003340*X + 3.493

Are the slopes equal?
F = 0.822517. DFn=2 DFd=66
P=0.4438

If the overall slopes were identical, there is a 44% chance of randomly choosing data points with slopes this different. You can conclude that the differences between the slopes are not significant.

Since the slopes are not significantly different, it is possible to calculate one slope for all the data.
The pooled slope equals -0.000366871

Are the elevations or intercepts equal?
F = 19.2183. DFn=2 DFd=68
P<0.0001

If the overall elevations were identical, there is a less than 0.01% chance of randomly choosing data points with elevations this different. You can conclude that the differences between the elevations are extremely significant.

Figure 28 Berry juice pH as a function of irrigation plus effective rain for all sub-treatments across three seasons. The season data (indicated with different symbols) includes deficit and control treated vines. For the deficit treatments these can have up to three consecutive seasons of deficit (2010-11). Regression lines are through the combined data for each season with the regression details shown in the table below the graph (b). The slopes are not significantly different giving a combined slope for all seasons of -0.000366871 pH/mm. Means +/- SEM are shown.

a)

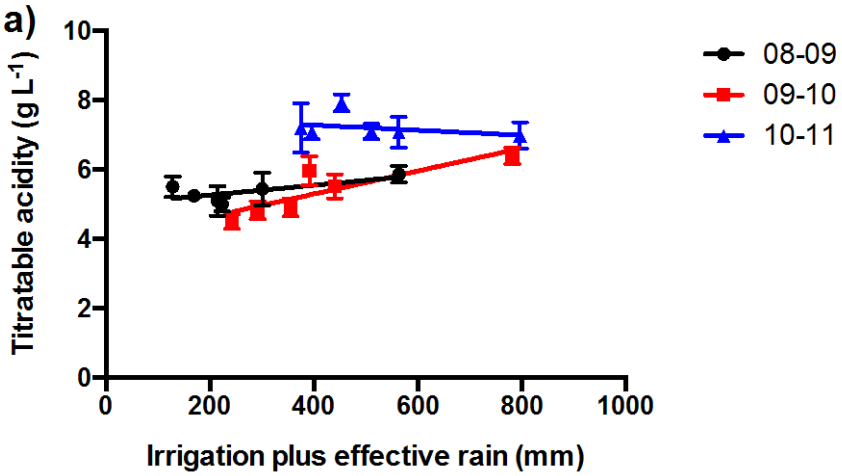

b)

	2009	2010	2011
Best-fit values			
Slope	0.001420 ± 0.0008742	0.003305 ± 0.0007478	-0.0007329 ± 0.001158
Y-intercept when X=0.0	4.970 ± 0.2645	3.965 ± 0.3384	7.564 ± 0.6231
X-intercept when Y=0.0	-3500	-1200	10320
1/slope	704.3	302.6	-1364
95% Confidence Intervals			
Slope	-0.0003932 to 0.003233	0.001754 to 0.004856	-0.003143 to 0.001677
Y-intercept when X=0.0	4.422 to 5.519	3.263 to 4.667	6.268 to 8.860
X-intercept when Y=0.0	-infinity to -1384	-2633 to -678.7	2801 to +infinity
Goodness of Fit			
R square	0.1071	0.4703	0.01870
Sy.x	0.6116	0.6425	0.7955
Is slope significantly non-zero?			
F	2.638	19.53	0.4003
DFn, DFd	1.000, 22.00	1.000, 22.00	1.000, 21.00
P value	0.1186	0.0002	0.5338
Deviation from zero?	Not Significant	Significant	Not Significant
Data			
Number of X values	6	6	6
Maximum number of Y replicates	4	4	4
Total number of values	24	24	23
Number of missing values	48	48	49
Equation	Y = 0.001420*X + 4.970	Y = 0.003305*X + 3.965	Y = -0.0007329*X + 7.564

Figure 29 Titratable acidity (TA) as a function of irrigation plus effective rain for all sub-treatments across three seasons. The season data (indicated with different symbols) includes deficit and control treated vines. For the deficit treatments these can have up to three consecutive seasons of deficit (2010-11). Regression lines are through the combined data for each season with the regression details shown in the table below the graph (b). Season 2009-10 was the only season showing a significant decline in TA with reduced irrigation plus effective rain. Means +/- SEM are shown.

Conclusion

Evolution of berry composition

Generally there was no effect of deficit treatment on the rate of evolution of berry weight, TSS, pH or TA despite there being significant differences between treatments in initial and final levels of these parameters. For the first two seasons comprising one and two years of continuous deficit, there were significant interactions between time and treatment for sugar accumulation on a per berry basis indicating that sugar accumulation per berry was decreased under increased deficit. However, this difference was not reflected in the TSS or berry weight kinetics. The three years of continuous deficit did not show this characteristic and may be reflecting the compensation effect that was observed in yield after three years of continuous deficit. (Matthews and Anderson 1989) also did not see any differences in the rates of berry expansion (they measured

berry diameter) over a range of deficit treatment despite large differences in midday water potential.

In terms of TSS increase (Stevens, et al. 2008) also found that rates of ripening of Chardonnay on Ramsey were not affected by water deficit. The ripening kinetics of Tempranillo grapes subjected to irrigation and no irrigation was studied over a three year period by (Esteban, et al. 1999). They observed a large reduction in the rate of glucose accumulation on a per berry basis in non-irrigated vines, which is very similar to the observation we have made for sugar per berry for the first two seasons. A similar result was obtained for the rate of sugar accumulation in Grenache berries, which was lowered with reduced irrigation and reduced leaf to fruit ratio (Etchebarne, et al. 2010). Given that the leaf area index is lower and yield is also lower under the deficit treatments, the reduced rate of accumulation of sugar on a per berry basis can be attributed to lower total net photosynthesis under the deficit treatments we imposed. The fact that final total soluble solids accumulated appeared to be less affected in our study indicates interesting control factors that balance water influx to the berry with sugar influx. Sugar transporters are proposed to compensate for decreased assimilation rate of leaves to compensate to some degree of reduced sugar transport to berries under water stress (Pastenes, et al. 2014). It is interesting to note that the positive correlation observed by (Sadras, et al. 2008) between stomatal conductance and rate of accumulation of TSS was not evident in our study given that low stomatal conductances occurred at the low irrigation rates and there was no clear differences in the rates of accumulation of TSS.

The general features of the effect of deficit and recovery on berry composition can be summarised as follows:

- Only for the more extreme deficit treatments were there consistent increases in TSS across seasons. However there was clearly a seasonal interaction most probably related to the rainfall received and the yield in the particular season.
- Solutes per berry were reduced by deficit in proportion to the degree of deficit and generally gave more significant responses than TSS.
- Juice pH increased proportionally with deficit treatment and was the most sensitive of the berry composition parameters measured.
- Titratable acidity decreased with deficit.
- Recovery in berry composition after one year of deficit was complete, but there was a carry-over into the recovery season after two years of continuous deficit. This was more obvious at low irrigation rates and with juice pH.
- There was a trend for overshoot in solutes per berry in subsequent recovery years after a deficit year that was more obvious for the lower irrigation rates.

Comparing these observations with those of other studies, TSS shows variable responses to reduced irrigation under various timing of the deficits. For Merlot subjected to sustained and regulated deficit irrigation over eight growing seasons, juice soluble solids concentration increased for the more reduced rates

of irrigation under both types of deficits (Shellie 2014) consistent with our observations. On the other hand Tempranillo subjected to greater water deficit (rain fed) compared to 70% ETc had lower TSS across three seasons (Intrigliolo, et al. 2012). Another study on Tempranillo showed variable responses in sugar concentration (glucose and fructose) over three seasons comparing non-irrigated and irrigated vines, but in all cases the sugar content per berry was strongly reduced under zero irrigation (Esteban, et al. 1999). Chardonnay on various rootstock subjected to a 35% reduced irrigation over four seasons only showed slight but non-significant increases in TSS and pH, but did show significantly reduced TA (Stevens, et al. 2008) consistent with our results. More extreme deficits applied to Chardonnay resulted in significant increases in TSS in some years over an eight year study (Williams 2014). There is a trend in our data for this effect. Both sugar concentration and sugars per berry decreased under rapid and extreme water stress for Chardonnay (Bahar, et al. 2011). There are also variable results reported in the literature in terms of the effect of reduced irrigation on pH across varieties. For Tempranillo under several deficit irrigation strategies over five seasons the only detrimental effect on wine composition was an increase in pH (Intrigliolo and Castel 2008). Juice pH of Tempranillo also increased under water deficit for two out of three seasons (Esteban, et al. 1999). This contrasts to the lack of any effect on pH of juice from Monastrell grapes subjected to 15% ET_c from fruit set to harvest over two years (Romero, et al. 2010). For Merlot subjected to sustained and regulated deficit irrigation over eight growing seasons juice pH increased, and TA decreased under both types of deficits (Shellie 2014) consistent with our observations. Juice pH increased under rapid and extreme water stress for Chardonnay (Bahar, et al. 2011). In a cool climate and comparing un-irrigated and fully irrigated vines of Chardonnay there was a significantly higher pH (though small) in un-irrigated vines in three out of four seasons (Reynolds, et al. 2007) also consistent with our results.

Overall, juice pH and sugars per berry would appear to be the most sensitive berry compositional characters that in some cases revealed a carry-over effect from previous years of deficit irrigation into the recovery seasons. However, it is surprising that successive seasons of reduced irrigation would give the same characteristics of the effects of total water applied on pH, indicating that if carry-over occurred from previous deficits this did not change significantly the response in pH to total water received by the vines.

References

Bahar, E., A. Carbonneau, and I. Korkutal (2011) The effect of extreme water stress on leaf drying limits and possibilities of recovering in three grapevine (Vitis vinifera L.) cultivars. African Journal of Agricultural Research 6, 1151-1160.

Bonada, M., V. Sadras, M. Moran, and S. Fuentes (2013) Elevated temperature and water stress accelerate mesocarp cell death and shrivelling, and decouple sensory traits in Shiraz berries. Irrigation Science 31, 1317-1331. doi: 10.1007/s00271-013-0407-z.

Esteban, M.A., M.J. Villanueva, and J.R. Lissarrague (1999) Effect of irrigation on changes in berry composition of Tempranillo during maturation. Sugars, organic acids, and mineral elements. American Journal of Enology and Viticulture 50, 418-434.

Etchebarne, F., H. Ojeda, and J.J. Hunter (2010) Leaf:Fruit Ratio and Vine Water Status Effects on Grenache Noir (Vitis vinifera L.) Berry Composition: Water, Sugar, Organic Acids and Cations. South African Journal of Enology and Viticulture 31, 106-115.

Greenspan, M.D., H.R. Schultz, and M.A. Matthews (1996) Field evaluation of water transport in grape berries during water deficits. Physiologia Plantarum 97, 55-62. doi: 10.1034/j.1399-3054.1996.970109.x.

Intrigliolo, D.S. and J.R. Castel (2008) Effects of irrigation on the performance of grapevine cv. Tempranillo in Requena, Spain. American Journal of Enology and Viticulture 59, 30-38.

Intrigliolo, D.S., D. Perez, D. Risco, A. Yeves, and J.R. Castel (2012) Yield components and grape composition responses to seasonal water deficits in Tempranillo grapevines. Irrigation Science 30, 339-349. doi: 10.1007/s00271-012-0354-0.

Keller, M., R.P. Smithyman, and L.J. Mills (2008) Interactive effects of deficit irrigation and crop load on Cabernet Sauvignon in an arid climate. American Journal of Enology and Viticulture 59, 221-234.

Matthews, M.A. and M.M. Anderson (1989) Reproductive development in grape (Vitis-vinifera l) - responses to seasonal water deficits. American Journal of Enology and Viticulture 40, 52-59.

Pastenes, C., L. Villalobos, N. Rios, F. Reyes, R. Turgeon, and N. Franck (2014) Carbon partitioning to berries in water stressed grapevines: The role of active transport in leaves and fruits. Environmental and Experimental Botany 107, 154-166. doi: 10.1016/j.envexpbot.2014.06.009.

Rebucci, B., S. Poni, C. Intrieri, E. Magnanini, and A.N. Lakso (1997) Effects of manipulated grape berry transpiration on post-veraison sugar accumulation. Australian Journal of Grape and Wine Research 3, 57-65. doi: 10.1111/j.1755-0238.1997.tb00116.x.

Reynolds, A.G., W.D. Lowrey, L. Tomek, J. Hakimi, and C. De Savigny (2007) Influence of irrigation on vine performance, fruit composition, and wine quality of Chardonnay in a cool, humid climate. American Journal of Enology and Viticulture 58, 217-228.

Romero, P., J. Ignacio Fernandez-Fernandez, and A. Martinez-Cutillas (2010) Physiological Thresholds for Efficient Regulated Deficit-Irrigation Management in Winegrapes Grown under Semiarid Conditions. American Journal of Enology and Viticulture 61, 300-312.

Sadras, V.O., M. Collins, and C.J. Soar (2008) Modelling variety-dependent dynamics of soluble solids and water in berries of Vitis vinifera. Australian Journal of Grape and Wine Research 14, 250-259. doi: 10.1111/j.1755-0238.2008.00025.x.

Schultz, H.R. and M.A. Matthews (1988) VEGETATIVE GROWTH DISTRIBUTION DURING WATER DEFICITS IN VITIS-VINIFERA L. Australian Journal of Plant Physiology 15, 641-656.

Shellie, K.C. (2014) Water Productivity, Yield, and Berry Composition in Sustained versus Regulated Deficit Irrigation of Merlot Grapevines. American Journal of Enology and Viticulture 65, 197-205. doi: 10.5344/ajev.2014.13112.

Stevens, R.M., J.M. Pech, M.R. Gibberd, R.R. Walker, J.A. Jones, J. Taylor, and P.R. Nicholas (2008) Effect of reduced irrigation on growth, yield, ripening rates and water relations of Chardonnay vines grafted to five rootstocks. Australian Journal of Grape and Wine Research 14, 177-190. doi: 10.1111/j.1755-0238.2008.00018.x.

Tarara, J.M., J.E.P. Pena, M. Keller, R.P. Schreiner, and R.P. Smithyman (2011) Net carbon exchange in grapevine canopies responds rapidly to timing and extent of regulated deficit irrigation. Functional Plant Biology 38, 386-400. doi: 10.1071/fp10221.

Tilbrook, J. and S.D. Tyerman (2008) Cell death in grape berries: varietal differences linked to xylem pressure and berry weight loss. Functional Plant Biology 35, 173-184. doi: 10.1071/fp07278.

Tilbrook, J. and S.D. Tyerman (2009) Hydraulic connection of grape berries to the vine: varietal differences in water conductance into and out of berries, and potential for backflow. Functional Plant Biology 36, 541-550. doi: 10.1071/fp09019.

Williams, L.E. (2014) Effect of Applied Water Amounts at Various Fractions of Evapotranspiration on Productivity and Water Footprint of Chardonnay Grapevines. American Journal of Enology and Viticulture 65, 215-221. doi: 10.5344/ajev.2014.12105.

6.4 Effect of SDI and recovery on carbohydrate dynamics

Introduction

Grapevines use stored carbon reserves to sustain early spring growth (Huglin and Schneider 1998,Scholefield, et al. 1978). According to (Yang, et al. 1980) the mobilisation reaches a maximum at the 8 to 10 leaf stage. After that, photosynthesis of newly formed leaves will support new growth, and carbohydrate produced by lower leaves is exported back to perennial organs. There are many studies on non-structural carbohydrate (NSC) content in grapevines, which examine seasonal dynamics, source-sink relations, mobilisation for early season growth, control of fruitfulness, and reserves status (Holzapfel, et al. 2010). Previous studies have indicated that altering NSC production during the growing season can influence vine growth and yield in the following season (Holzapfel and Smith 2012, Holzapfel, et al. 2006, Koblet, et al. 1994) but cultural practices had a limited effect on NSC dynamics (Holzapfel and Smith 2012). Differences in the seasonal maxima of NSC in roots and trunk have been attributed to water deficits (Smith and Holzapfel 2009). However, deficit irrigation treatments had no significant effect on NSC concentrations in the wood of Shiraz vines over four consecutive seasons (Holzapfel and Smith 2012). (Dayer, et al. 2013) evaluated the long term effect of severe water stress (25% and 38% ETo) and high crop load on NSC of trunk wood in Malbec vines. They found that both severe water stress and high crop load reduced trunk starch concentration, but NSC was not affected.

One study has examined the impact of altered NSC reserves in Chardonnay in a cool climate where defoliation was used to reduce NSC and to examine subsequent season reproduction and productivity (Bennett, et al. 2005). They concluded that reduced NSC reserves have a negative impact on flowering and productivity. Here we examine the impact of long term reductions in irrigation and then recovery on the seasonal dynamics of NSC in trunks and leaves for Chardonnay vines on Ramsey rootstock and examine the interactions with yield components and berry sugar accumulation.

Methods

Trunk samples: Wood samples were taken from the trunks at key phenological stages starting from harvest 2009 (11 February 2009). In order to minimise a possible effect of the distance from the shoots/roots on the NSC concentration in the trunk, samples were taken from different zones of the trunk (top, middle and bottom) making sure that replicates were equally sampled from each zone. The same plant was not sampled more than twice. The samples were removed from the trunk using a 5 mm diameter drill bit, inserted all the way through the trunk with the insertion being perpendicular to the trunk. The drilled material was collected in a paper bag and immediately frozen in liquid nitrogen, stored in dry ice in the field and then at -80 °C until freeze dried.

Leaf samples: Leaves were selected at the fifth position from the shoot tip, in order to have leaf samples at similar developmental stage at the time of

sampling. After sampling, the leaves were placed in a paper bag and snap-frozen in liquid nitrogen. Samples were stored in dry ice for transport and then stored at -80 °C until chemical analysis.

Root samples: roots were obtained fresh from soil cores and immediately frozen in liquid nitrogen in the field, stored in dry ice in the field and then at -80 °C until freeze dried.

Chemical analysis: The samples were freeze-dried using a Telstar LyoQuest freeze-drier (AVT Services Pty Ltd., Seven Hills, NSW, Australia) and then ground using a Labtech Essa LM1-P mill (Labtech Essa Pty Ltd., Bassendea, WA, Australia). The freeze-dried and ground samples were analysed for starch and sugar concentration according to (Edwards, et al. 2011). The procedure for the analysis of soluble carbohydrate and starch consisted of a series of extractions of the ground material in deionised water, where the supernatant was kept and dried for soluble carbohydrate analysis while the pellet was dried and used for starch determination. The concentration of sugars (expressed in mg/g of fructose equivalents) and starch were analysed using a commercial enzyme assays (Megazyme International, Bray, Ireland). For the soluble carbohydrate measure the supernatant was resuspended in water and 1 mL of the anthrone reagent was added (0.2% anthrone in 70% concentrated sulphuric acid). For the determination of insoluble starch the pellet was resuspended with 150 µL of thermostable α-amylase solution with a sodium acetate buffer and GOPOD reagent. The samples were transferred in 300 µL aliquots to a microplate well and absorbance was read at 600 nm with a Labtech FLUOstar Optima microplate reader (BMG Labtech, Mornignton, VIC).

Results and Discussion

Seasonal trunk NSC

The seasonal changes of total NSC concentration in trunks and its components of starch and soluble sugars for the selected continuous irrigation treatments are presented in Figure 1. NSC concentration (Figure 1c) was at a maximum at dormancy and rapidly declined from budburst until flowering, probably due to reserves being used to support spring growth. It was evident that changes in sugar concentration accounted for much of the season variation (compare Figure 1a and 1b) with sugar concentration doubling between budburst and dormancy. Reduced irrigation treatments did result in reduced trunk NSC concentrations shortly after harvest in both the 2008-09 and 2009-10 seasons (Figure 2). At the time of lowest NSC concentrations in the trunk (budburst), water stressed vines had lower NSC concentration but this was not significantly different from the control (Figure 3).

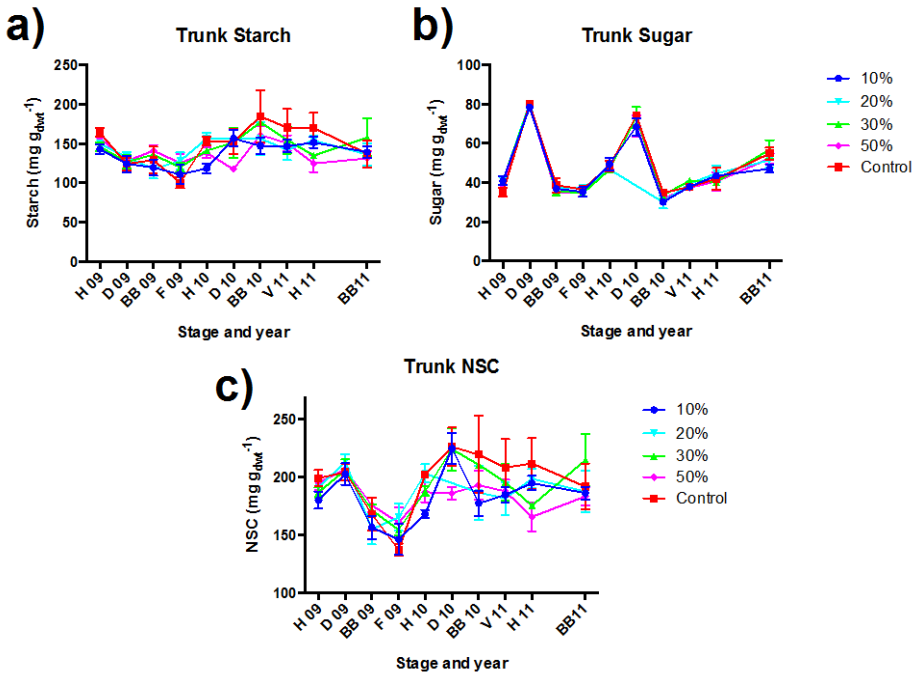

Figure 1 Trunk starch (a), sugars (b) and total non-structural carbohydrate (NSC) (c) as a function of key phenological stages plotted approximately in proportion to the time and for each irrigation treatment as indicated by different symbols and colours. Note some stages were not measured in some seasons. H=harvest, D=dormancy, BB=budburst, F=flowering, V=veraison. Means +/- SEM are shown.

a)

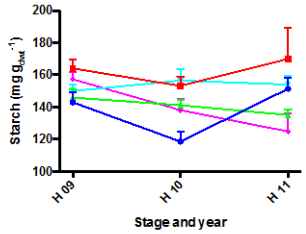

b)

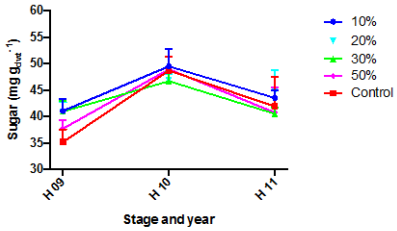

c)

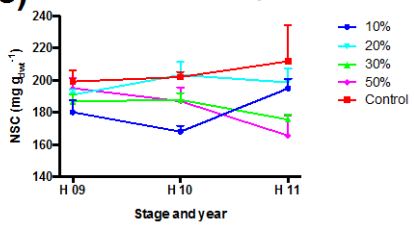

d)

Table Analyzed	Trunk Starch Harvest Only			
Two-way ANOVA	Ordinary			
Alpha	0.05			
Source of Variation	% of total variation	P value	P value summary	Significant?
Interaction	20.87	0.0652	ns	No
Season	11.15	0.0391	*	Yes
Irrigation	28.12	0.0025	**	Yes

e)

Table Analyzed	Trunk Sugar Harvest Only			
Two-way ANOVA	Ordinary			
Alpha	0.05			
Source of Variation	% of total variation	P value	P value summary	Significant?
Interaction	4.862	0.8336	ns	No
Season	45.81	0.0001	***	Yes
Irrigation	2.980	0.6459	ns	No

f)

Table Analyzed	Trunk NSC Harvet Only			
Two-way ANOVA	Ordinary			
Alpha	0.05			
Source of Variation	% of total variation	P value	P value summary	Significant?
Interaction	23.10	0.0924	ns	No
Season	0.9968	0.7683	ns	No
Treatment	25.91	0.0099	**	Yes

Figure 2 Trunk concentrations of carbohydrates at harvest across three seasons and for each irrigation treatment (starch a, sugar b, NSC c). Mean +-/ SEM. Two-way ANOVA revealed significant season-to-season differences in sugar and starch, but not NSC, and treatment differences in starch and NSC (d,e,f). There was no interaction between season and treatment.

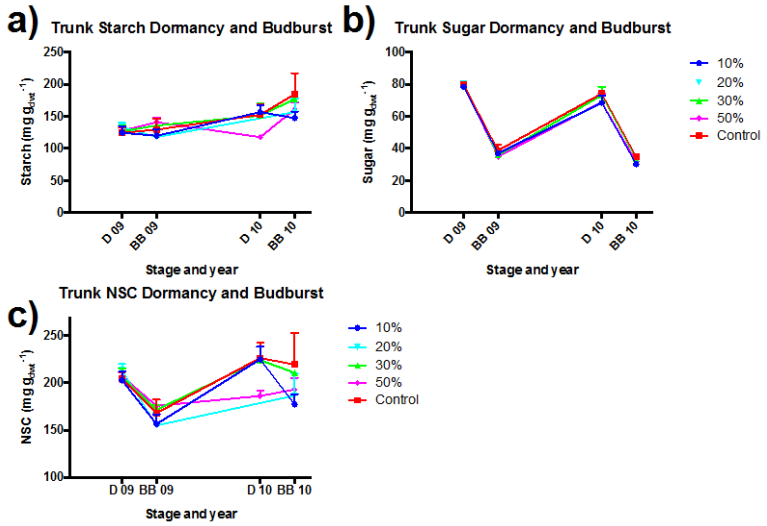

d)

Table Analyzed	Trunk Starch D BB			
Two-way ANOVA	Ordinary			
Alpha	0.05			
Source of Variation	% of total variation	P value	P value summary	Significant?
Interaction	13.22	0.3831	ns	No
Stage	35.58	0.0001	***	Yes
Irrigation	3.960	0.4066	ns	No

e)

Table Analyzed	Trunk Sugar D BB			
Two-way ANOVA	Ordinary			
Alpha	0.05			
Source of Variation	% of total variation	P value	P value summary	Significant?
Interaction	0.2174	0.9730	ns	No
Stage	96.38	< 0.0001	****	Yes
Irrigation	0.4435	0.1691	ns	No

f)

Table Analyzed	Trunk NSC D BB			
Two-way ANOVA	Ordinary			
Alpha	0.05			
Source of Variation	% of total variation	P value	P value summary	Significant?
Interaction	12.75	0.3655	ns	No
Stage	37.34	< 0.0001	****	Yes
Treatment	5.664	0.2282	ns	No

Figure 3 Trunk concentrations of carbohydrates at dormancy and budburst across two seasons and for each irrigation treatment (starch a, sugar b, NSC c). Mean +-/ SEM. Two-way ANOVA revealed very significant season-to-season differences in sugar starch, and NSC, but no treatment differences or interaction between treatment and stage (d,e,f).

Recovery of trunk NSC

Returning stressed vines to control levels of irrigation after one year or two years of low irrigation treatments resulted in carbohydrate reserves at harvest recovering almost to control levels after one season. Although the data were variable between treatments and seasons, a general pattern can be observed (Figure 4a,b,c). For the most extreme reduction in irrigation (10%) there appeared to be a longer lag for recovery for trunk starch at harvest (Figure 4d)

where complete recovery of starch concentration after one year of reduced irrigation occurred at the end of the second season. However there was no significant effect on both sugars and NSC (Figure 4e,f). One obvious feature of NSC seasonal dynamics was that at dormancy, concentration in trunk was similar for all the treatments, despite large differences in water supply that resulted in large effects on other physiological parameters.

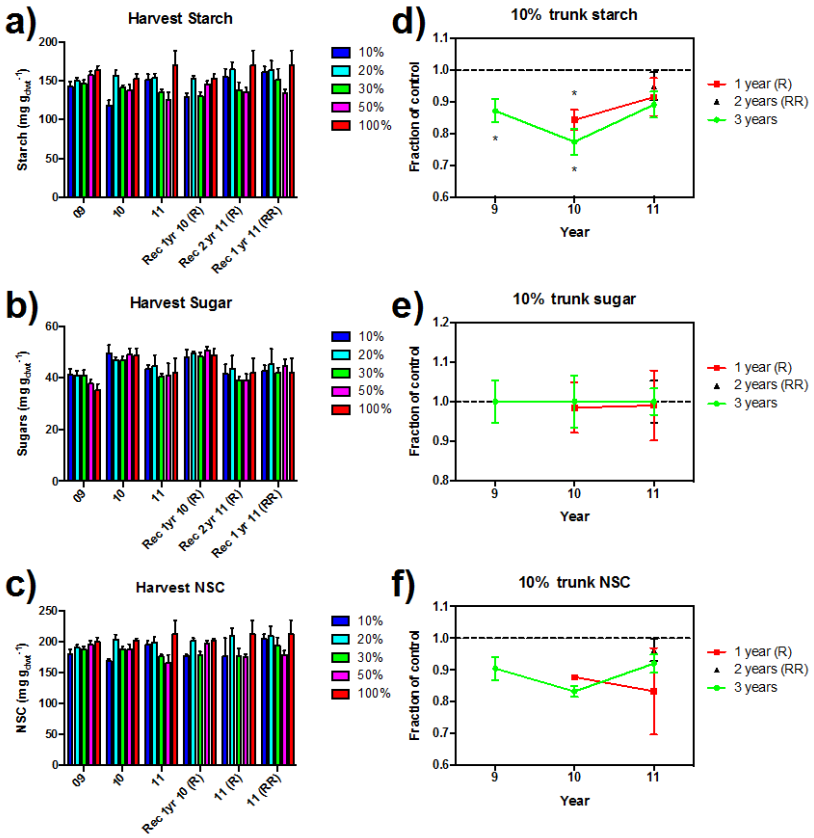

Figure 4 Recovery of trunk concentrations of carbohydrates at harvest across three seasons and for each irrigation treatment (starch a, sugar b, NSC c). Recovery seasons are shown for 2009-10 as one year of reduced irrigation (R) and one season of recovery; 2010-11 as one year of reduced irrigation (R) and two seasons of recovery; 2010-11 as two years of reduced irrigation (RR) and one season of recovery. Also shown is the concentrations relative to that of the controls in each season and for recovery (d,e,f). Only for starch concentration was there a significant carry over into the following recovery season as a lower concentration (d), however this non-recovery was not observed for two years of reduced irrigation and one year of recovery. Mean +-/ SEM are shown.

Total trunk capacity

The total capacity of perennial components of the vine to store carbohydrate also depends on the volume of the parts. To examine if the volume of the trunk was substantially altered by the reduced irrigation the diameter of the trunk was measured across treatments and recoveries just after harvest in 2012, i.e. four seasons of reduced irrigation. It was clear that the diameter was not uniform, i.e. the trunk was elliptical in cross section, and that there was a trend in some treatments for the North-South (NS) diameter to be smaller than the East-West (EW) (direction of the row) diameter. Figure 5a shows diameters in both directions and as a function of the continuous reductions in irrigation. For the 10% treatment the NS direction only showed a significant difference from the

control. For the EW direction there was no significant difference for the 10% treatment, but the 20% treatment was significantly smaller. Figure 5b shows the difference between EW and NS diameters across the treatments. Only the 10% and Control treatments showed differences that were significantly different from zero. Using the measured diameters it is possible to calculate the cross sectional area of the trunk, assuming that it is described by an ellipse (Figure 5c). In this case both the 10% and 20% treatments were significantly smaller than the controls. From the cross sectional area the trunk volume can be calculated from the height of the trunk, and a trunk "capacity" for carbohydrate storage can be obtained by multiplying the volume by the average NSC concentration. Without the wood density (i.e. g m^{-3}) it is not possible to convert this to the absolute quantity of NSC in the trunk, but the "capacity" that is obtained is expected to be proportional to the total quantity of NSC in the trunk for comparison between treatments. This would not hold if the wood densities were different between treatments, which is a possibility. Inspection of Figure 5d shows that the reduced irrigation treatments after four years results in a substantial reduction in total capacity, almost 50%, to store carbohydrate. Also shown are the recoveries after one year of full irrigation from three years of continuous reduction. It can be seen that the 10% is about half way recovered, but the 30% appears to be still much reduced. For both 50% continuous over four years and recovery from 50% there was no difference in capacity to that of the controls.

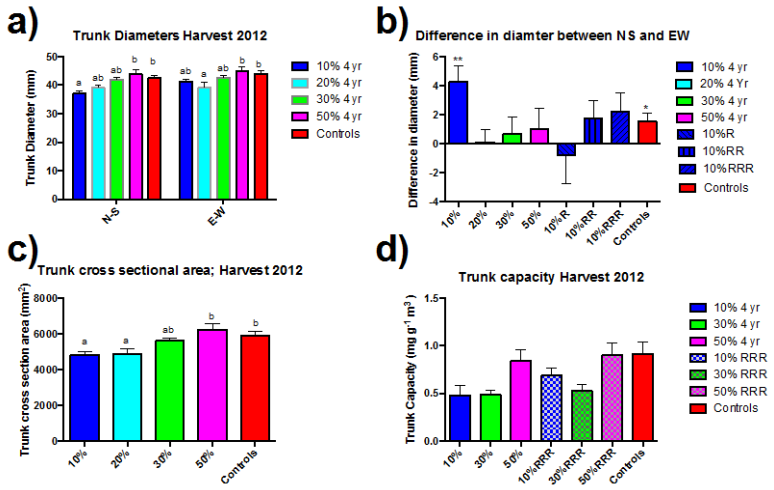

Figure 5 Trunk diameter and storage capacity measured at harvest in season 2011-12 showing the effect of irrigation treatment (over 4 years) and the asymmetry in diameter. (a) Two directions were recorded, East-West (E-W, parallel to row direction) and North-South (N-S, perpendicular to row direction). Different letter indicates significant difference ($P<0.05$) between treatments within a direction class (1-way ANOVA). (b) Difference in diameter between E-W and N-S across the treatments and recoveries for the 10% treatment (R = one year of deficit and three years of recovery, RR = two years of deficit and two years of recovery, RRR = three years of deficit and one year of recovery). Only 10% (four years) and Controls showed significant asymmetry in diameters. (c) Trunk cross sectional area using the formula for an ellipse. In this case both the 10% and 20% treatments become significantly different to controls. (d) Trunk storage capacity calculated as NSC concentration times trunk volume. This demonstrates a large difference between 10% and 30% on one hand and controls and 50% treatment on the other after four years of deficit irrigation. Mean +/- SEM are shown.

Seasonal leaf NSC

Changes in leaf starch, sugars and NSC are shown in Figure 6 for continuous reductions in irrigation (Figure 6 a,b,c) and for one or two years of recovery (Figure 6 d,e,f). It is evident that the dynamics of leaves are very different to those of the trunk. Leaves show greater changes in starch concentration with lower concentrations occurring at veraison and harvest (Figure 6 a,d). Leaf sugars on the other hand are quite constant in contrast to that of the trunk (Figure 6 b,e). There were no significant effects of irrigation treatment or interaction with phenological stage on leaf NSC or components. Likewise there was no indication of any recovery effect (Figure 6 d,e,f).

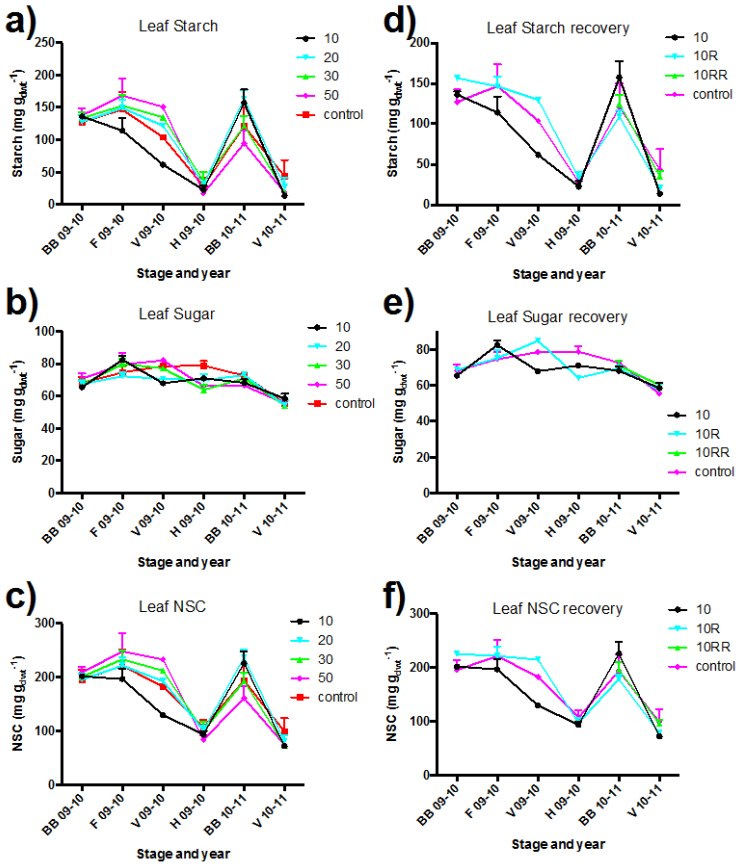

Figure 6 Leaf starch (a), sugars (b) and total non-structural carbohydrate (NSC) (c) as a function of key phenological stages for each irrigation treatment as indicated by different symbols and colours. Also shown are the recoveries compared to continuous deficit for the 10% treatment, for starch (d), sugar (e) and NSC (f) after one season of reduced (R) and two seasons of reduced (RR) irrigation. Two-way ANOVA showed that phenological stage was significant for starch, sugar and NSC, but there was no effect of treatment and no interaction. H=harvest, BB=budburst, F=flowering, V=veraison. Means +/- SEM are shown. Mean +/- SEM are shown.

Root NSC

A set of root coring campaigns was undertaken at budburst in 2009 to collect roots for each irrigation treatment. Unfortunately root collection from the 10% and 30% treatments were problematical and not enough samples were obtained for NSC analysis. However, roots were obtained from the 20%, 50% and Control

treatments at budburst after one season of deficit. Roots could be separated into large (greater than 2 mm diameter) and fine and analysed separately (Figure 7 a,b,c). Both large and fine roots had more than 50% of dry weight as NSC (Figure 7c), but fine roots had significantly higher NSC than large roots (Figure 7d). There was a trend for increasing concentration of NSC in fine roots with increasing irrigation in the previous season, largely accounted for by starch concentration, however this was not significant. Comparison between trunk NSC measured at near the same time (Figure 7e) demonstrated that roots certainly contain a larger proportion of NSC, as also found in some other investigations (Holzapfel and Smith 2012), but not always (Holzapfel, et al. 2010).

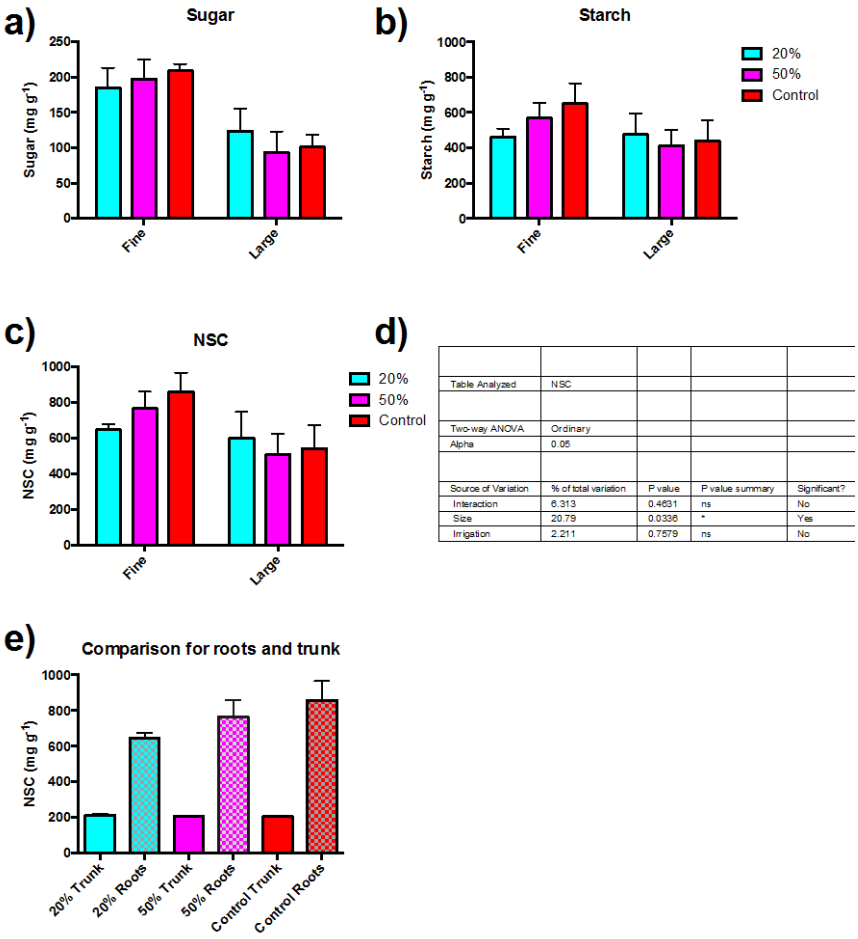

Figure 7 Root carbohydrate analysis (sugar a, starch b, NSC c) carried out at budburst in 2009-10 for a selection of irrigation treatments and comparison between root size classes (fine < 2 mm diameter). (d) Two-way ANOVA showed a significant difference in NSC concentration between large and fine roots but no difference between treatments or interaction between size and treatment. (e) Comparison in NSC concentrations between roots and trunk sampled at a similar stage in the same season. Mean +/- SEM are shown.

Effects of water applied

Examination of trunk carbohydrates at harvest as a function of irrigation and effective rain revealed positive correlations for starch and NSC in seasons 2008-09 and 2010-11 (Figure 8) but this was not consistent across the three seasons with season 2009-10 showing no correlations and also large variance in some of the treatments. Sugars showed no consistent trend with irrigation plus effective

rain (Figure 8b), although in the driest of the three seasons (2008-09) there was an inverse correlation with higher trunk sugars at the lowest water applied (Figure 8b). The correlation we observed for starch is consistent with the results of (Dayer, et al. 2013) for Malbec who found a negative correlation between trunk starch concentration and increasing water stress, though in their case the correlation was observed with trunk starch at dormancy rather than just after harvest. In our study we did not observe large differences between irrigation treatments and starch concentration in trunks at dormancy.

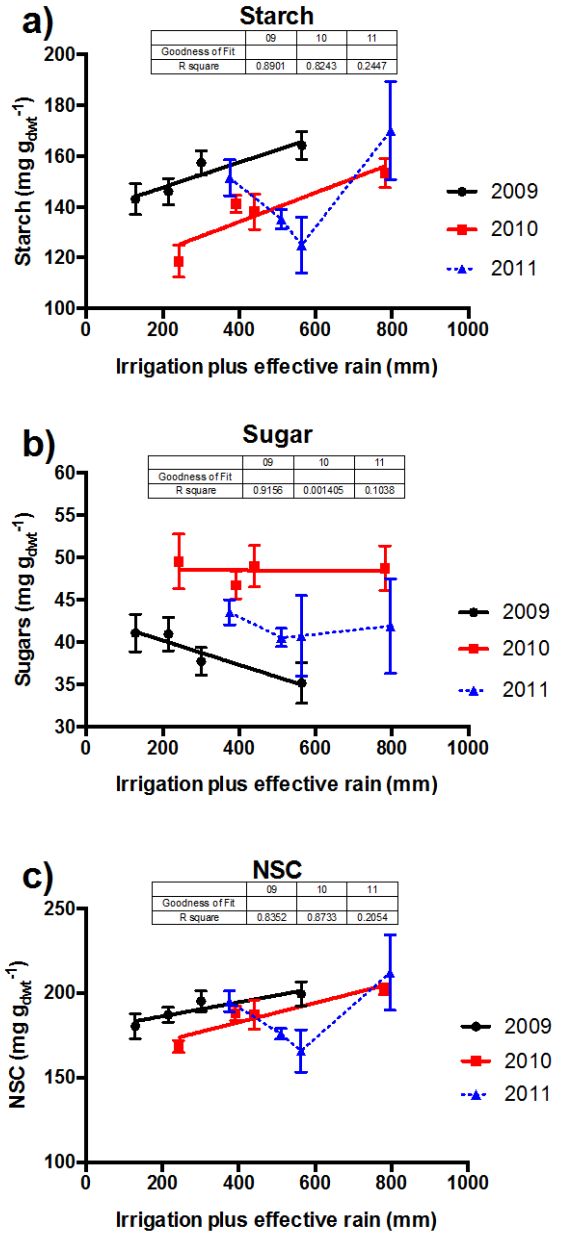

Figure 8 Correlations between trunk carbohydrate reserves (starch a, sugar b, NSC c) at harvest and irrigation plus effect rain received in the respective season. Also shown for each is the R^2 for each season.

Relationships with yield

Figure 9 shows regression analysis of trunk carbohydrates measured at harvest versus the yield (for the same harvest) for each of three seasons of reduced irrigation. Trunk starch concentration only positively correlated with yield in the 2008-09 seasons which was also the driest (Figure 9a,b), and there was no confluence between the three seasons. Trunk sugar concentrations at harvest however, showed a consistent negative correlation with yield that broadly correlated also between the three seasons (Figure 9c,d). A regression through all three seasons' data gave a significant correlation (Figure 9d) but this only accounted for about 37% of the variation between irrigation treatments and seasons. NSC reflected largely the same response as starch concentration (Figure 9e), but the combination of a positive correlation for starch and a negative correlation for sugar resulted in a less significant positive correlation for NSC in the 2008-09 season (Figure 9e,f).

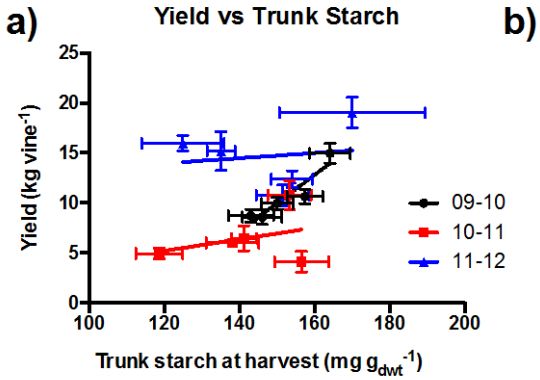

b)

Yield 09	Yield 10	Yield 11
0.2813 ± 0.06375	0.05771 ± 0.09359	0.02580 ± 0.1052
-32.20 ± 9.710	-1.693 ± 13.31	10.87 ± 15.57
114.5	29.35	-421.3
3.555	17.33	38.76
0.07843 to 0.4841	-0.2401 to 0.3555	-0.3090 to 0.3606
-63.10 to -1.302	-44.04 to 40.65	-38.66 to 60.40
16.54 to 130.8	-infinity to 128.0	-infinity to 109.3
0.8665	0.1125	0.01965
1.096	2.809	3.685
19.47	0.3802	0.06014
1.000, 3.000	1.000, 3.000	1.000, 3.000
0.0216	0.5811	0.8221
Significant	Not Significant	Not Significant
5	5	5
1	1	1
5	5	5
10	10	10
Y = 0.2813*X - 32.20	Y = 0.05771*X - 1.693	Y = 0.02580*X + 10.87

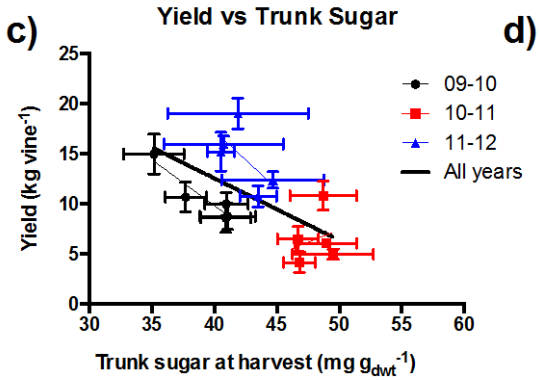

d)

Yield 09	Yield10	Yield 11	Allyears
-0.9197 ± 0.1981	0.4888 ± 1.128	-1.154 ± 0.7904	-0.6193 ± 0.2231
46.61 ± 7.774	-16.91 ± 54.31	63.46 ± 33.44	37.33 ± 9.681
50.69	34.81	54.98	50.27
-1.087	2.088	-0.8664	-1.615
-1.550 to -0.2893	-3.103 to 4.074	-3.669 to 1.361	-1.101 to -0.1374
21.88 to 71.35	-189.7 to 155.9	-42.94 to 169.9	16.42 to 58.24
45.83 to 75.93	-infinity to 46.96	46.03 to +infinity	52.41 to 120.6
0.8778	0.09825	0.4154	0.3721
1.049	2.888	2.846	3.564
21.55	0.1856	2.132	7.705
1.000, 3.000	1.000, 3.000	1.000, 3.000	1.000, 13.00
0.0188	0.6967	0.2404	0.0157
Significant	NotSignificant	Not Significant	Significant
5	5	5	15
1	1	1	1
5	5	5	15
10	10	10	0
Y = -0.9197*X + 46.61	Y = 0.4888*X - 16.91	Y = -1.154*X + 63.46	Y = -0.6193*X + 37.33

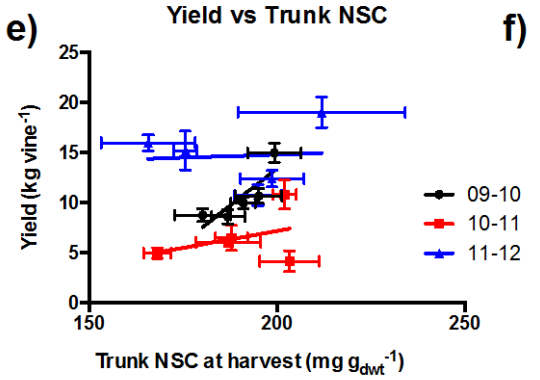

f)

Yield 09	Yield 10	Yield 11
0.2969 ± 0.1094	0.06770 ± 0.09685	0.01213 ± 0. 1001
-45.97 ± 20.85	-6.367 ± 18.41	12.37 ± 19.02
154.8	94.05	-10.20
3.366	14.77	82.47
-0.05111 to 0.6449	-0.2405 to 0.3759	-0.3083 to 0.3305
-112.3 to 20.37	-64.96 to 52.23	-48.16 to 72.90
-infinity to 174.8	-infinity to 176.8	-infinity to 148.1
0.7107	0.1401	0.004871
1.614	2.766	3.713
7.370	0.4886	0.01469
1.000, 3.000	1.000, 3.000	1.000, 3.000
0.0729	0.6349	0.9112
Not Significant	Not Significant	Not Significant
5	5	5
1	1	1
5	5	5
10	10	10
Y = 0.2969*X - 45.97	Y = 0.06770*X - 6.367	Y = 0.01213*X + 12.37

Figure 9 Correlations between trunk carbohydrates (starch a, sugar c, NSC e) at harvest and the yield of that harvest across three seasons. The corresponding linear regression analysis is shown in b, d, and e. There was a consistent negative correlation between trunk sugar concentration at harvest and yield across all seasons and one regression is also shown for the entire data set which was significant (d). Mean +/- SEM are shown.

Previous studies have shown that the carbohydrate reserves in the trunk at dormancy preceding the current season could be correlated to the yield based on the impact of defoliation post-harvest (Holzapfel, et al. 2006). We therefore examined the correlations between carbohydrate reserves at the beginning of the season and the yield in that season. Figure 10 shows the relationships between NSC at either budburst or dormancy and yield. There was a significant positive correlation between yield and NSC at budburst across three seasons accounting for 58% of the variation between irrigation and season (Figure 10d). Note season 2008-09 could not be included in this analysis since carbohydrates were not measured at the beginning of that season. There was no correlation between yield and NSC concentration in the trunk at dormancy (Figure 10 b).

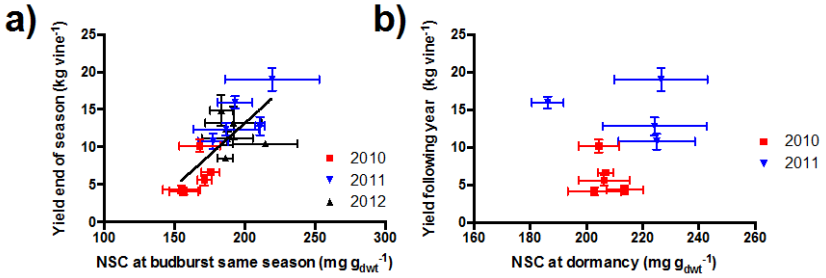

c)

	All BB
Best-fit values	
Slope	0.1701 ± 0.04045
Y-intercept when X=0.0	-20.85 ± 7.532
X-intercept when Y=0.0	122.6
1/slope	5.879
95% Confidence Intervals	
Slope	0.08271 to 0.2575
Y-intercept when X=0.0	-37.12 to -4.579
X-intercept when Y=0.0	54.95 to 145.3
Goodness of Fit	
R square	0.5763
Sy.x	2.915
Is slope significantly non-zero?	
F	17.68
DFn, DFd	1.000, 13.00
P value	0.0010
Deviation from zero?	Significant
Data	
Number of X values	15
Maximum number of Y replicates	1
Total number of values	15
Number of missing values	9
Equation	Y = 0.1701*X - 20.85

Figure 10 Correlation between yield and NSC at budburst (a) for the same season and for dormancy preceding the current season (b). (c) Linear regression analysis for (a, solid line)) showing significant correlation between yield and NSC at budburst across three seasons.

Conclusions

- The largest differences in trunk NSC occurred between dormancy and flowering, as observed in other studies (Holzapfel, et al. 2010).
- Root sugar and starch concentration were very high on a dry weight basis and was higher in fine roots compared to larger roots. The concentrations of NSC were 3 to 4-fold higher than that of the trunk. There was a trend for higher values at higher irrigation rates but this was not significant.
- Leaf carbohydrates fluctuated with phenological stage but were not affected by irrigation treatment at any stage.
- Harvest concentrations of carbohydrates in the trunk were affected by reduced irrigation. However, the differences in NSC concentration between treatments were low; the 10% irrigation treatment resulted in reductions of only 14.6% and 22.6% at harvest compared to the control in 2009 and 2010 respectively.
- At dormancy there were no significant differences between any treatments, suggesting that post-harvest leaf photosynthesis in stressed vines was adequate to replenish the NSC in trunks to control levels, despite lower LAI in deficit treatments and lower assimilation rates. In warm climates, where canopies can photosynthesise for several weeks after harvest, NSC may continue to accumulate in trunks as previously observed for Thompson Seedless (Williams 1996). It is surprising that despite large reductions in irrigation, the vines seemed to be able to restore levels of NSC in the trunks at dormancy to the same as the control vines.
- Trunk NSC concentration at harvest was correlated with irrigation plus effective rain in two out of three seasons.
- There was an effect on budburst trunk NSC concentrations, which correlated with the final harvest yield in that season. This correlation not only explained variation caused by irrigation reduction but also differences between seasons and in particular the large difference in yield between the 2009-10 season (low yield) and the other seasons. This correlation may be explained by the yield potential of the vines being dependent on NSC at a particular stage since it has been suggested that sugar availability at flowering may be a critical determinant of final yield (Lebon, et al. 2008).
- Concentrations of trunk sugar at harvest were negatively correlated with yield and was consistent across seasons including the low yield in season 2009-10 that was independent of the total amount of water received. This may suggest that when yield is high there is a greater demand for mobilisation of stored reserves resulting in a lower sugar concentration in the trunk.
- For the most extreme reduction in irrigation (10%) there appeared to be a longer lag for recovery for trunk starch at harvest, but complete recovery of starch concentration after one year of reduced irrigation occurred at the end of the second season.

- Trunk capacity to store NSC is also dependent on total wood volume and after four years of continuous deficit there were significant (50%) reductions in storage capacity for the 10%, 20% and 30% treatments, but not for the 50% treatment. Recovery in trunk capacity is slower than recovery in concentration of NSC since it requires a growth response to compensate for reduced growth over previous seasons of deficit.
- An interesting phenomenon was observed in the asymmetry of trunk diameter where the larger diameter aligned with the row direction in the more extreme (10%) treatment. This has not been described in the literature and we hypothesise that this is due to greater phloem accumulation on the side of the trunk correlating with root distribution. In the 10% treatment more roots would be confined along the row with virtually no roots found in the inter-row.

References

Bennett, J., P. Jarvis, G.L. Creasy, and M.C.T. Trought (2005) Influence of defoliation on overwintering carbohydrate reserves, return bloom, and yield of mature Chardonnay grapevines. American Journal of Enology and Viticulture 56, 386-393.

Dayer, S., J.A. Prieto, E. Galat, and J.P. Pena (2013) Carbohydrate reserve status of Malbec grapevines after several years of regulated deficit irrigation and crop load regulation. Australian Journal of Grape and Wine Research 19, 422-430. doi: 10.1111/ajgw.12044.

Edwards, E.J., A.F. Downie, and P.R. Clingeleffer (2011) A Simple Microplate Assay to Quantify Nonstructural Carbohydrates of Grapevine Tissues. American Journal of Enology and Viticulture 62, 133-137. doi: 10.5344/ajev.2010.10051.

Holzapfel, B.P. and J.P. Smith (2012) Developmental Stage and Climatic Factors Impact More on Carbohydrate Reserve Dynamics of Shiraz than Cultural Practice. American Journal of Enology and Viticulture 63, 333-342. doi: 10.5344/ajev.2012.11071.

Holzapfel, B.P., J.P. Smith, S.K. Field, and W.J. Hardie (2010) Dynamics of carbohydrate reserves in cultivated grapevines. Horticultural Reviews 37, 143-211.

Holzapfel, B.P., J.P. Smith, R.M. Mandel, and M. Keller (2006) Manipulating the postharvest period and its impact on vine productivity of Semillon grapevines. American Journal of Enology and Viticulture 57, 148-157.

Huglin, P. and C. Schneider (1998) Biology and ecology of the grapevine. (

Koblet, W., M.C. Candolfivasconcelos, W. Zweifel, and G.S. Howell (1994) Influence of leaf removal, rootstock, and training system on yield and fruit composition of pinot-noir grapevines. American Journal of Enology and Viticulture 45, 181-187.

Lebon, G., G. Wojnarowiez, B. Holzapfel, F. Fontaine, N. Vaillant-Gaveau, and C. Clément (2008) Sugars and flowering in the grapevine (Vitis vinifera L.). Journal of Experimental Botany 59, 2565-2578. doi: 10.1093/jxb/ern135.

Scholefield, P.B., T.F. Neales, and P. May (1978) Carbon balance of sultana vine (vitis-vinifera l) and effects of autumn defoliation by harvest-pruning. Australian Journal of Plant Physiology 5, 561-570.
Smith, J.P. and B.P. Holzapfel (2009) Cumulative Responses of Semillon Grapevines to Late Season Perturbation of Carbohydrate Reserve Status. American Journal of Enology and Viticulture 60, 461-470.
Williams, L.E. (1996) Grape. In: Photoassimilate Distribution in Plants and Crops: Source-Sink Relationships, Eds. A.A. Schaffer and E. Zamski (Marcel Dekker: New York) pp. 851–883
Yang, Y.S., Y. Hori, and R. Ogata (1980) Studies on re translocation of accumulated assimilates in grapevines vitis-labruscana cultivar delaware 2. re translocation of assimilates accumulated during the previous growing season. Tohoku Journal of Agricultural Research 31, 109-119.

6.5 Effects of SDI and recovery on root growth and distribution

Introduction

Any study of the allocation or use of carbon in plants must necessarily address below-ground components as all below-ground carbon in a grapevine is assimilated by the shoot. Estimates of standing below-ground biomass, such as those from soil cores, necessarily underestimate the total below-ground carbon allocation because they do not account for carbon used by root respiration, root exudates or root turnover (roots that grow and die between measurements). Mini-rhizotrons are probably the most commonly used method of assessing root turnover and the only currently available method that is suitable for use in commercially managed vineyards of mature vines. The few published studies of root turnover in grapevines using mini-rhizotrons have been in climates and soils that are not representative of the majority of Australian viticulture; Concord (*Vitis labrusca*) growing in New York state in the US (Comas, et al. 2005) and grafted Riesling, growing in the Rheingau in Germany (Lehnart, et al. 2008). Differences in soil water availability, such as those generated by the sustained deficit irrigation (SDI) regimes used in this project, have the potential to affect root fraction (Chaves, et al. 2002), root respiration (Burton, et al. 1998), root morphology (Kato and Okami 2011) and root turnover (Mainiero and Kazda 2006). Furthermore, the surface area of fine roots and their positioning in soils that receive water after a period of drought are likely to have an effect on the ability of a vine to rapidly recover from water stress.

Methods

Mini-rhizotrons
The mini-rhizotron tubes consisted of 3 mm thick clear acrylic, with a length of 915 mm and an OD of 34 mm (Acrilix Plastics PTY LTD, Welland, SA). Each was engraved with 55 numbered, consecutive windows, 22 mm wide x 16.5 mm high along one side. The tubes were installed at 70° from the horizontal, approximately 150 mm from the base of the chosen vine, with the distance from the dripline and along the dripline from the trunk being equal. Each tube was sealed with a 'Suba Seal' (Sigma-Aldrich, Castle Hill, NSW) and the end covered with a plastic cap.

The initial tranche of 36 mini-rhizotron installations used three tubes in each 'year 3' replicate for the control, 50% and 30% irrigation treatments and were installed in December 2009. In September 2011 each 'year 3' replicate was split into two sections, one reverted to standard irrigation and the second maintained at the current irrigation level. One to two existing tubes were in each of the new sections, where a sub-plot did not have a second tube a new tube was installed in September 2011.

The imaging system was an Olympus Iplex FX Industrial Videoscope, with a side-view AT80S-IU86 optical adaptor (80° field of view) and integrated LED light source. Test images were taken in early 2010, with regular imaging beginning at

budburst of the 2010-11 growing season. For logistical reasons, only every fourth window was imaged down a tube, resulting in either 12 or 13 images per tube at intervals representing 4 cm of soil depth. Images were analysed using the open-source 'RootFly' software (http://www.ces.clemson.edu/~stb/rootfly/), which allowed each individual root in an image to be numbered and measured for length and maximum diameter. Each root could then be followed throughout the rest of the project.

Soil coring
Soil coring to estimate root biomass was undertaken at budburst and post-veraison in the three seasons from 2010-11 to 2012-13. A jack-hammer with custom made attachment was used to hammer 50 mm diameter stainless steel soil corers to a depth of 0.75 m. Each sample was split into three depth classes, 0-25, 25-50 and 50-75 cm, sealed in a ziplock plastic bag and stored in a cool room at 3°C until the roots were extracted.

On 26/8/2010, 28/1/2011, 14/9/2011, 9/1/2012 and 31/1/2013 a single core was taken from each replicate at approximately 0.2 m from the dripline and 0.2 m from the chosen vine trunk. On 3/9/2012, a set of three cores was taken in a transect from dripline to midrow at 0.2, 0.75 and 1.5 m from the dripline. All roots were extracted from each core sub-section using sieving and washing. The roots were then measured for length and diameter using WinRhizo (Regent Instruments, Canada), before being oven dried at 60°C and weighed.

Results and Discussion

Root production under control irrigation and assessment of methodology used
Rhizotrons, or root windows, have been used to study root growth for over 100 years, but by providing a barrier they have an impact on the very root growth they are intended to study. Taking advantage of modern imaging systems, the mini-rhizotron came into use during the 1980s, the intention being that the mini-rhizotron should be as small as possible, providing no greater an impact on root growth than a natural obstruction in the soil such as a stone. However, this means that a given tube can provide access to only a very small volume of soil and, as with traditional rhizotrons, they still only access a two-dimensional surface within a soil volume. Consequently, whilst mini-rhizotrons remain the only practical method available for studying root dynamics and demography in a vineyard, there is a high degree of tube-to-tube variability in the number of roots intercepted, due to their size compared with the root density in vineyard soil. This necessitates as many tubes as possible to be used in an experimental set-up, but even with modern software, the image analysis is labour intensive, so any study utilising mini-rhizotrons represents a trade-off between labour and statistical power.

In addition to the mini-rhizotron system, this project utilised soil coring to examine the standing crop of roots, thereby enabling the relationship between measured root length and root biomass to be established as well as examining the coherence between the two methods at a given point in time.
(Anderson, et al. 2003) report fine root survivorship in the mini-rhizotron study on Concord, determining that only a few percent survive for more than one

growing season, with 75% survivorship typically being under 150 days. Our measurements began in 2010-11, almost a full year after tube installation in 2009, to allow for any effect of installing the tubes on root growth. If fine root lifetimes were typically less than a single season this period would be adequate to allow a 'steady-state' of root turnover to be assessed over the subsequent three seasons. However, the majority of roots observed lasted from their first appearance to the end of the experiment, making root lifespan indeterminable, but greatly in excess of 150 days.

For example, Figure 1 provides most of the images collected for a single window at a depth of 43 cm in a tube in the control treatment over the course of three full seasons; 2010-11 to 2012-13. In the first image taken two brown roots are already visible (marked with yellow arrows, Figure 1a), these are clearly still turgid and still live, presumably originating in the 2009-10 season following tube installation. Their appearance is unchanged at the start of the 2012-13 season (marked with yellow arrows, Figure 1c) and they are still present in the final image taken in that season.

In the second image, taken 19 days later, two new roots have appeared (marked with white arrows, Figure 1a). These roots remain white in the following image, but are pigmented in the image taken 44 days after their appearance. One of these roots also remains throughout all subsequent images, but the second starts to shrivel and die in the 2012-13 season (marked with red arrows, Figure 1c), giving a lifespan of over 700 days, but still being the shortest lived root of a known age in this window.

The visual classification of roots as white, pigmented (brown), black/shrivelled or disappeared, matched those of (Comas, et al. 2000), who observed that whilst the pigmented roots were still alive, their metabolic activity was 77% less than white roots. It is unlikely that the brown roots are involved in nutrient or water uptake, with their primary purpose probably being to transport water from elsewhere in the root system. The period prior to roots becoming pigmented was variable; for example most of the new roots visible in sample window used for Figure 1 during the 2011-12 season were already pigmented by the time they were observed, typically less than 21 days (Figure 1b). The only white roots in those images appeared on 6/2/2012 and became pigmented over the next two images (1/3/2012 and 26/3/2012).

The longevity of the fine roots observed using the mini-rhizotrons makes it unlikely that the root turnover measured using the system was in 'steady state' as a full cohort of roots from birth to death needs to be observed to be certain this is the case. As a result, a year on year increase in root length would be expected until the initial cohort of roots had died. Indeed, this was observed, with the root length in the control treatment increasing in each season (Figure 2a).

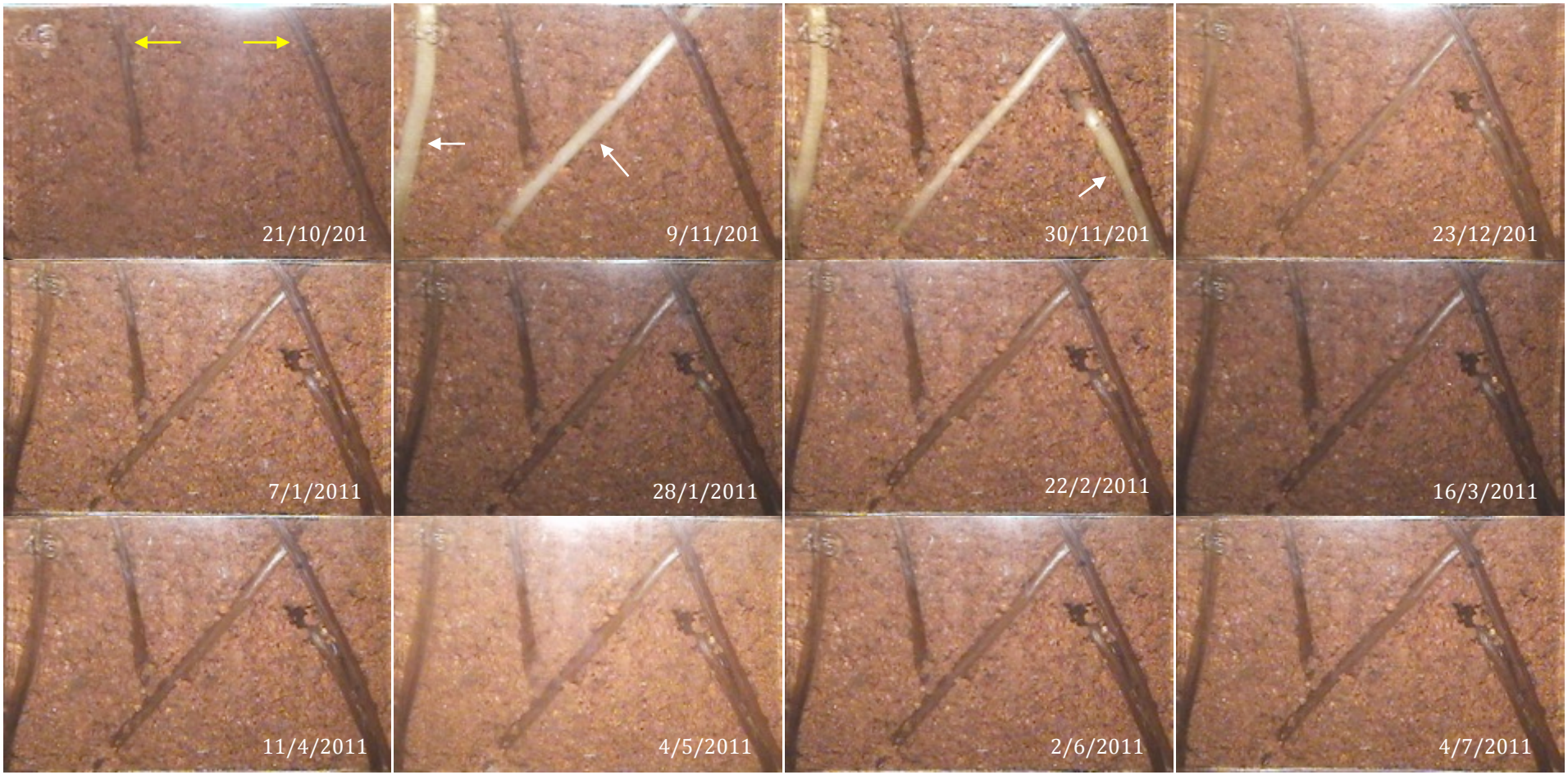

Figure 1a Images of a single mini-rhizotron window from a tube in the control irrigation treatment at a depth of approximately 43 cm. The images represent those taken during the 2010-11 season (10 months after installation). New roots are marked with white arrows in the image in which they first appear. The yellow arrows denote the existing roots at the time of the first image (see text).

Figure 1b Images of a same mini-rhizotron window as Figure 1a. The images represent those taken during the 2011-12 season (22 months after installation). New roots are marked with white arrows in the image in which they first appear.

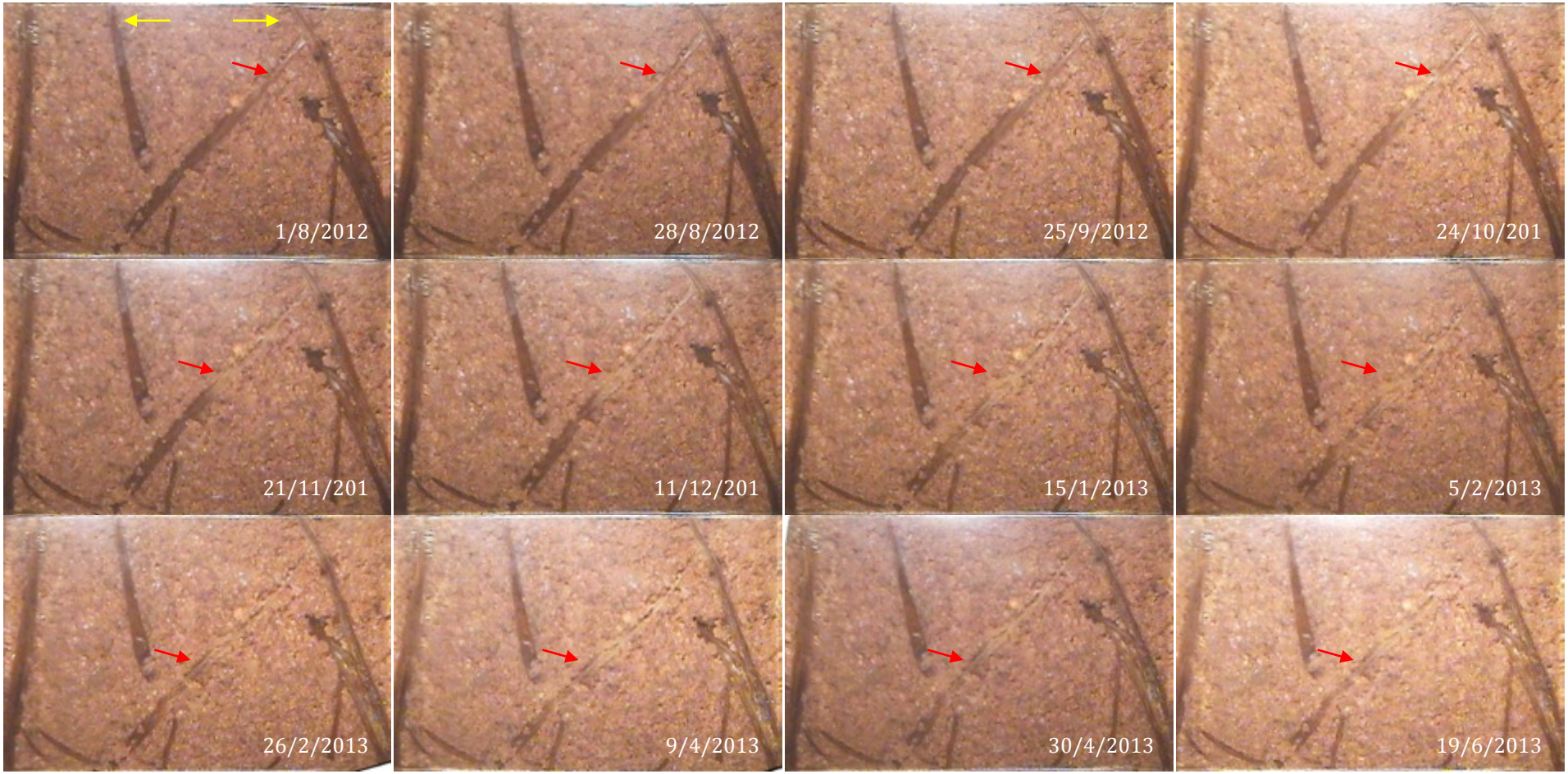

Figure 1c Images of a same mini-rhizotron window as Figs 1a & b. The images represent those taken during the 2012-13 season (34 months after installation). A progressively decaying root is marked with red arrow. The yellow arrows denote the existing roots at the time of the first image in 2010 (cf. Figure 1a).

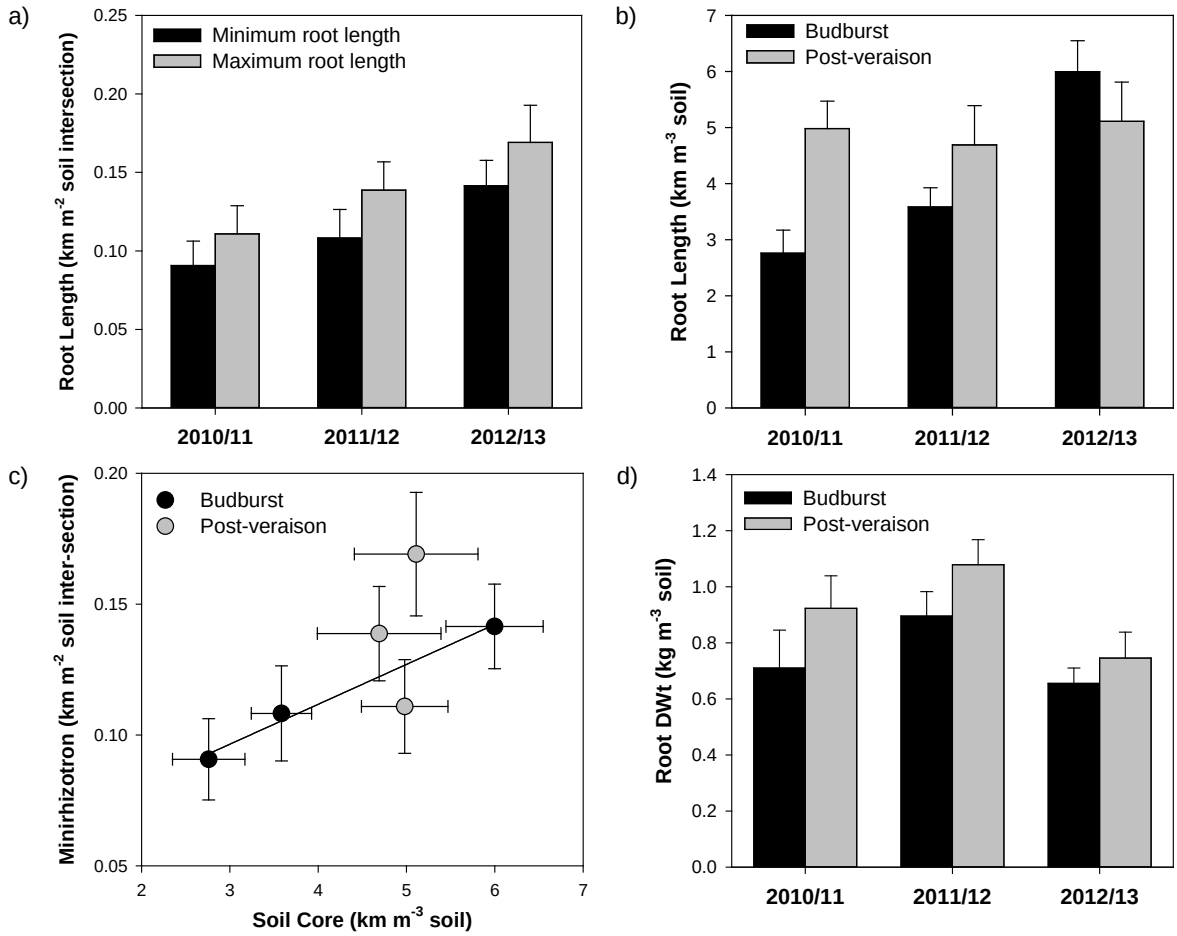

Figure 2 Root parameters of control irrigated vines measured over three seasons, 2010-11 to 2012-13, a) maximum and minimum root length per season from mini-rhizotron data, b) root length from soil core data, c) correlation between mini-rhizotron and soil core estimates of maximum root length at budburst (adj. $R^2 = 0.980$) and post-veraison (no significant relationship) and d) root dry weight from soil core data.

The vines used in the study were seven years old at the start of the 2010-11 season and assumed to be mature. Consequently it was likely that the actual fine root length in the controls was at, or close to, steady state (root births equal to root deaths). However, even if this was true there was the potential for differences in rainfall over the course of the experiment to have a season-to-season impact. Such effects should be visible in the data from the soil coring, even though this method had the potential to underestimate impacts on fine root turnover.

Root length at veraison in the soil cores did not significantly vary between seasons (Figure 2b), but the budburst data increased each season, resulting in a significant relationship between the root length data gathered from the mini-rhizotrons and that gathered from the soil coring at budburst, but not veraison (Figure 2c). This suggests that there was a very good coherence between root length results obtained using the mini-rhizotrons and those obtained using root coring, at least at budburst, and that the root system of these vines was still increasing in size during the project. However, caution is needed in making this conclusion as *n* was only 3, logic dictates that the mini-rhizotron data will increase year-on-year (see above) and the soil core root length result from budburst 2012 does not match the root dry weight result from the same sample (Figure 2d). This latter result could represent a large change in specific root length (root

length per unit dry weight) at this time, or could be a result of the limited replication in the trial (four) in combination with the likely high degree of heterogeneity of root distribution in the soil. With the exception of the soil core root length data in 2012-13 all of the collected data demonstrated an increase in the root system of the control irrigated vines during the growing season relative to the winter dormancy period (Figure 2a-c), as would be expected from past studies (Comas, et al. 2010,Eissenstat, et al. 2006). The relative increase in root dry weight (Figure 2c) was greatest in 2010-11 at 30%, but declined in subsequent seasons, being 20% in 2011-12 and 15% in 2012-13. The absolute root biomass was greatest in 2011-12, both at budburst and at veraison. The 2010-11 season was one of extremely high rainfall, which can potentially result in greater fine root growth (Comas, et al. 2010), and it appears that there was little root dieback in the following autumn/winter as the root biomass in January 2011 (veraison) was similar to that in the following August (budburst), explaining the greater root biomass in 2011-12 than 2010-11. Presumably the less extreme weather experienced in 2011-12 led to more typical root responses in autumn 2012 and the loss of fine root length prior to the 2012-13 season.

The mini-rhizotron system used in this study utilised tubes with a smaller diameter than are often used for woody perennials (e.g. the 2 inch diameter tubes normally supplied by Bartz Technology Corporation, Carpinteria, CA, USA), albeit still larger than can be used for grassland systems, to minimise artefacts such as roots growing down the length of the tube. This was successful, in that roots growing down the side of tubes were rarely observed, but resulted in a smaller surface area with which to assess root growth and turnover. In addition, root length density, estimated by coring, was much lower in this study than is observed in grasslands, approx. 3-4 km m^{-3} cf. 100-200 km m^{-3} in a temperate model pasture (Edwards *et al.* 2004) and spatial variability across the vineyard was also high (see below). Despite this, and the limited replication available due to size constraints on a layout that was already large, the mini-rhizotron results provided data with a level of detail not obtainable by any other practical means. On the other hand, the longevity of the fine roots in the vineyard studied limited the ways in which the additional tubes, installed in 2011 for the project extension, could be used, as the results could not be combined with tubes installed at an earlier date (see below).

Effect of degree and duration of sustained deficit irrigation on root production

The mini-rhizotrons were installed early in the 2009-10 season, but, below ground measurements of any sort did not begin until the start of the 2010-11 season. As a result of the time required for monitoring the mini-rhizotron tubes and analysing the resulting images only the control, 50% and 30% treatments were instrumented and only in the 'year three' section of the trial, i.e. the plots receiving their third season of deficit irrigation in 2010-11. At the end of 2010-11 the extension to the project required the 'year three' plots to be split into two, creating 'year four' deficit irrigation plots, whilst the remaining part reverted to standard irrigation (see methods, Chapter 5). Although, additional mini-rhizotron tubes were installed into the 'year three' and 'year four' plots prior to the start of the 2011-12 season the unexpected fine root longevity (see above) prevented the data from being incorporated with the tubes installed in 2009. This was due to root length and turnover results from different installations not being comparable until the roots visible through those tubes are in 'steady-state' and this cannot occur until the initial flush of roots after installation have died. Consequently, the number of tubes per plot was three in 2010-11 (i.e. twelve tubes per treatment), but only one or two in subsequent seasons. Similarly, tubes were installed into the 10% deficit irrigation treatment in 2011, but

could not be examined in conjunction with the other treatments and that data has not been included here.

Whilst the mini-rhizotron tubes offered the only practical means of examining root production throughout the season, the data is based on a two-dimensional plane and corresponding data in three dimensions is required to estimate biomass in a volume of soil, which can then be used to assess changes in whole vine carbon allocation. This information was provided by using soil coring; generally only in the irrigation wetting zone, where most fine root growth would be expected (Soar and Loveys 2007), but transects of three cores were made in August 2012, budburst, to allow the whole root system to be examined. Soil coring and extraction of the fine roots is still a labour intensive process and was restricted to the control, 50%, 30% and 10% treatments, the 30%RD and 20% treatments being excluded.

Root coring was also able to include some of the plots in recovery in each season, e.g. 'year one' in 2010-11 and 'year two' in 2011-12, whereas the long-term requirements of the mini-rhizotron technique meant that recovery after re-watering could only be examined in the 'year three' and 'year four' plots. The data presentation within this chapter has been provided using a consistent scheme to minimise the complexities of the trial; a single colour has been used for plots that have received a given number of complete seasons of deficit irrigation, e.g. red is used for vines that received a single season of deficit irrigation, purple for vines that received two complete seasons of deficit or were in their second season, blue for vines that received three complete seasons of deficit or were in their third season and so on. Due to the way the trial was set-up this also means that a single colour also represents the season the measurements were made e.g. purple for measurements in 2010-11, blue for 2011-12 and green for 2012-13.

Data from soil coring is presented as fine root dry weight, relevant to biomass allocation, and fine root surface area, relevant to root function. The latter has been normalised to the control treatment within a given sample date to allow minimise the season to season differences in root growth and allow irrigation treatment effects to be more clearly observed. Plots receiving more than one season of deficit irrigation were analysed across all seasons using repeated measures ANOVA and each univariate ANOVA was used to analyse results from each season individually. A p value below 0.05 was taken as a significant effect.

Soil coring at the end of winter (budburst) took place in three seasons and included treatments representing vines that had received two, three and four complete seasons of deficit irrigation. In each case the control irrigated vines had the highest fine root dry weight, numerically, but there was no statistically significant effect of deficit irrigation, either across all seasons (p = 0.130) or in any individual season (Figure 3a). In 2011-12 there was a marginally significant effect (p = 0.069) of deficit irrigation. Furthermore, there was also no effect of season, despite the large differences in weather conditions between seasons, including the record rainfall experienced in 2010-11 noted above.

The sampling that occurred within the growing season (at veraison or shortly after) included only two seasons where deficit irrigation was in place, representing the third and fourth seasons of deficit, as all treatments had reverted to control irrigation in the final season of field work. In each season, fine root dry weight was greater at veraison than at budburst in all irrigation treatments (Figure 3b cf. Figure 3a), but the analysis across both seasons again demonstrated no effect of season or treatment. There was clearly no difference in root dry weight during 2010-11, and in the deficit treatments root dry weight was much higher than in the subsequent season

(Figure 3b), possibly due to the deficit irrigation having only a limited impact on the total water available to the vines (effective rain = 287 mm in 2010-11 versus 144 mm in 2011-12, see Table 1 Chapter 5). However, in the 2011-12 season, fine root dry weight was much greater in the control vines than the deficit treatments and there was a significant impact of deficit irrigation at this time (p = 0.010).

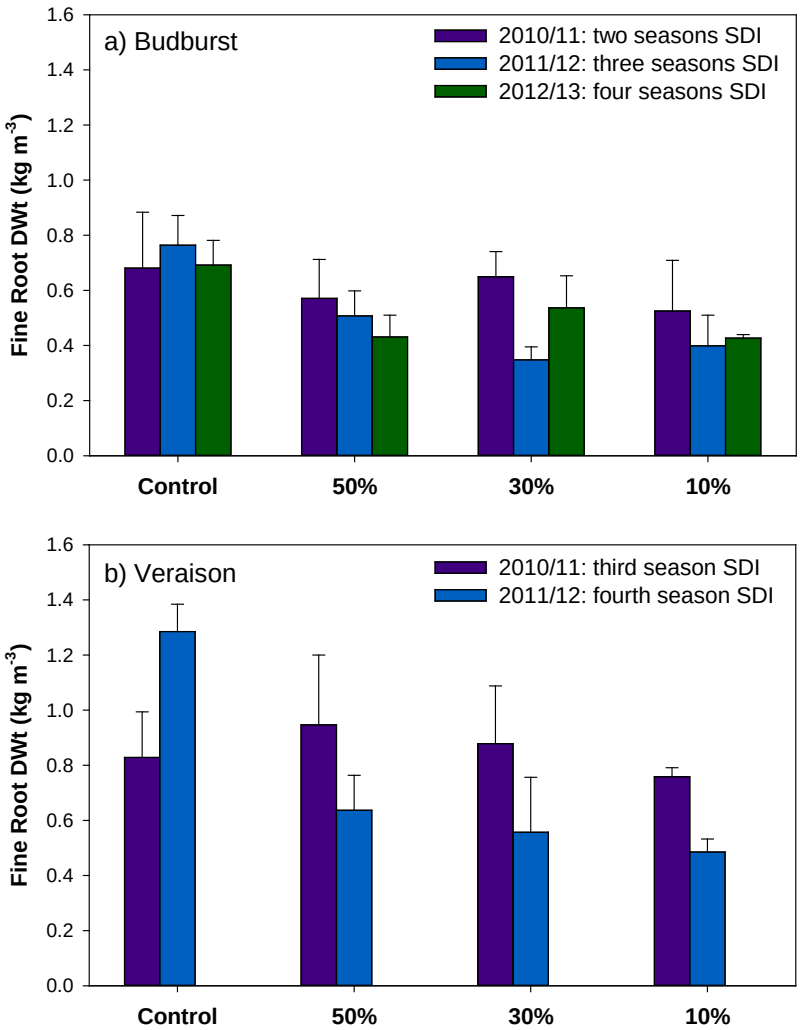

Figure 3 Fine root dry weight in the wetting zone of vines receiving control irrigation, 50% of control, 30% of control or 10% of control for two, three or four seasons, measured at a) budburst and b) veraison. No vines received deficit irrigation after anthesis in the 2012-13 season.

Fine root length and fine root surface area were significantly affected by season, both at budburst (p = 0.003) and during the growing season (p = 0.004), but deficit irrigation effects were only significant at budburst (p = 0.008). Within a given season, irrigation was only significant at budburst 2010-11 (p = 0.036), but there was no interaction between season and treatment in the repeated measures analysis. Irrigation effects were clearest when seasonality was removed by normalising fine root surface area to the control treatment within each season (Figure 4a). As the deficit increased, from 50% to 10% of control, fine root surface area decreased, with the vines receiving only 10% irrigation having approximately 60% of the root surface that the control vines had. There was no effect of increasing duration of deficit, from two to four seasons, on the impact of the deficit (Figure 4a). At veraison, there was no significant effect of deficit irrigation on fine root surface area in either season (Figure 4b).

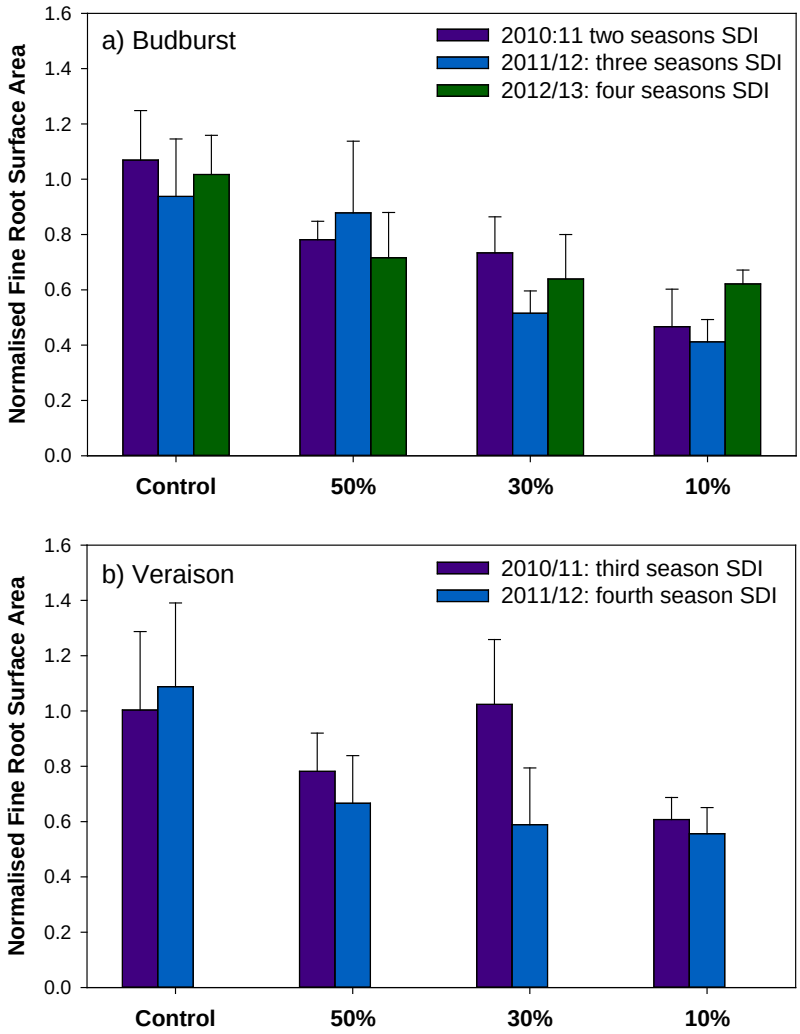

Figure 4 Fine root surface area, normalised to the control treatment for each season, in the wetting zone of vines receiving control irrigation, 50% of control, 30% of control or 10% of control for two, three or four seasons, measured at a) budburst and b) veraison. No vines received deficit irrigation after anthesis in the 2012-13 season.

The limited statistical significance of deficit irrigation effects on root biomass and surface area were probably due, in part, to a combination of spatial variability at the site and limited replication (n = 4) and the unusual 2010-11 season weather conditions are likely to have resulted in some recovery during that season, which could have impacted the following season via improved carbohydrate storage. However, the limited impact does demonstrate the resilience of the root system in deficit conditions and the ability of the vine to maintain carbon allocation to the root system in order to maintain a water supply to the shoot.

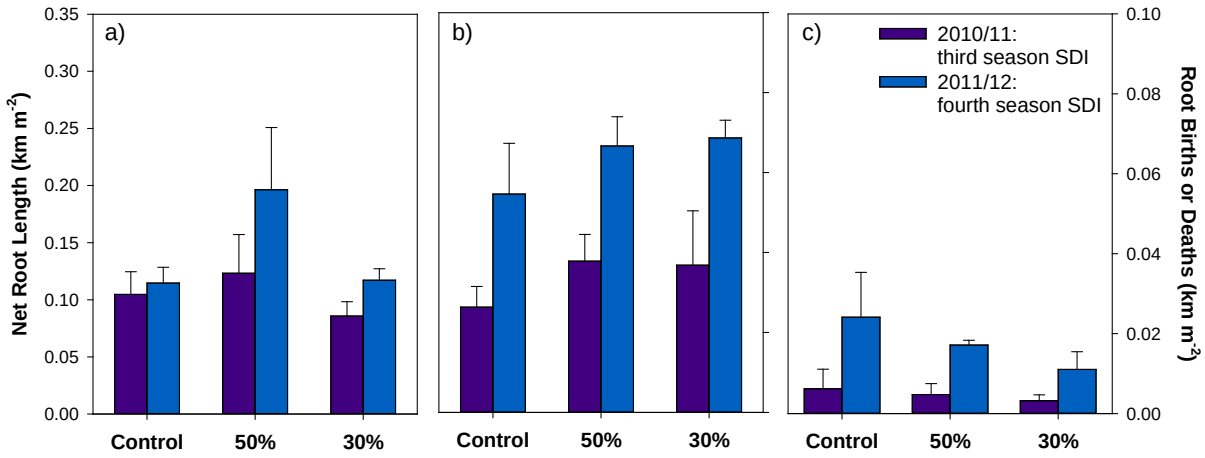

Figure 5 – directly measured parameters from mini-rhizotron images made in the wetting zone of vines during the third or fourth season of receiving control, 50% of control, or 30% of control irrigation; a) net root length, b) root births and c) root deaths per km^{-2} of soil intersection.

The most rigorous mini-rhizotron data (see above) were from the control plots (in all seasons) and from the 2010-11 season (all treatments). The analysis of the mini-rhizotron data included here was designed to be relevant to the soil coring data, but difference in the two techniques means that timing and measures to match completely.

Net root length was calculated from the maximum length of every observed root during a given season, subtracting root length lost and estimates the standing root crop at leaf fall. There was no impact of the two irrigation treatments examined on net root length (Figure 5a). The apparent increase in net root length in the 50% treatment during the 2011-12 season (p = 0.009) was an artefact of spatial variation at the site and the loss of tubes due to the splitting of the 'year three' plots in 2011. However, there was a significant effect of season on the production of new root length (Figure 5b; p = 0.001) and the loss of root length (Figure 5c; p = 0.045), with root production and root loss being much higher in 2011-12 than in 2010-11. There was no significant effect of deficit irrigation in either case.

The seasonal effect on root births and deaths could have been due to differences between the weather in those two seasons, e.g. the 2010-11 rainfall events, or a function of the non-steady state turnover at the tube surface (see above). An impact of weather on root births and deaths would be likely to have an effect on root turnover, whereas an increase in new root length as a result of increasing root density due to the installation of tubes would be less likely to have a large effect root turnover.

There is no set calculation for root turnover as it depends somewhat on the measurements made and the long-term development of the root system. The most common usage is new root per unit of existing root. This calculation is not ideal for the data presented here, as the continued development of roots around the mini-rhizotron tubes during the three years of measurement would result in a root turnover estimate greater than would be the case in a steady-state system. However, when this calculation is made, using *new root length / net root length* it is clear that there was no trend with irrigation treatment (Figure 6a). Further, there was no significant effect of season and at an average of 0.45 yr^{-1}, root turnover estimated in this way was indeed higher than would be expected for a system where root deaths were far less than root births.

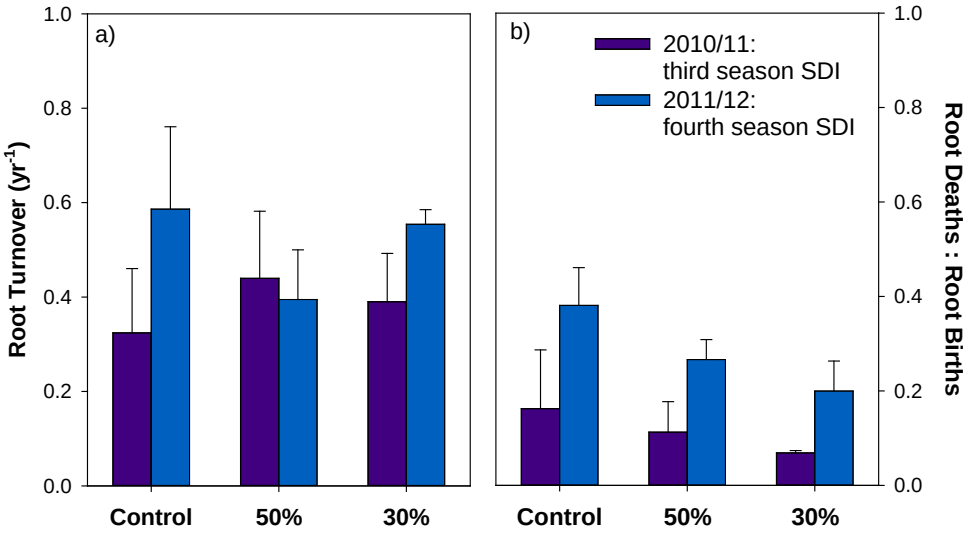

Figure 6 Parameters derived from mini-rhizotron images made in the wetting zone of vines during the third or fourth season of receiving control, 50% of control, or 30% of control irrigation; a) root turnover (root births/net root length) and b) the ratio of root deaths to root births.

A comparison of root births to deaths demonstrates that, even in the third season after installation of the tubes (2012-13), root deaths were only 40% of root births (Figure 6b; control). Although there was no significant effect of treatment on the birth:death ratio, there was a marginally significant seasonal effect (p = 0.076), suggesting that root growth and loss was trending towards an equilibrium. A mini-rhizotron study on Concord grapevines, found that only a few percent of fine roots survived for more than one growing season, with 75% survivorship typically being under 150 days (Anderson, et al. 2003). Our measurements began almost 12 months after tube installation to allow for the likely effect of the installation itself on root growth. If the lifespan of fine roots was generally less than a single season, this period would be adequate to allow a 'steady-state' of root turnover to occur. In contrast, our study found that the majority of roots observed lasted throughout the three seasons of observations, from their first appearance to the end of the experiment. As a result root lifespan was indeterminable for many roots, but clearly in excess of 150 days.

Effect of degree and duration of sustained deficit irrigation on root production after return to full irrigation

Root production after return to full irrigation was assessed in the same way as during the application of deficit irrigation, through coring and mini-rhizotron analysis. Soil cores from plots in recovery, those returned to control irrigation, were taken at the same time as those from plots under deficit in 2010-11 and 2011-12. In the 2012-13 season all plots were fully irrigated, but soil cores were taken at budburst and veraison as in previous seasons. As a result the plots that received on to three years of deficit irrigation were assessed by coring one season after being returned to control irrigation, at budburst, and during their second season after being returned to control irrigation, at veraison. Plots that received four years of deficit irrigation were only cored in their first season after being returned to control irrigation, at veraison. As mini-rhizotrons were only installed in the plots receiving three and four years of deficit, assessment via this method was only possible in those plots. Budburst 2013 was beyond the scope of the project, so no coring occurred, but the mini-rhizotrons were monitored for the entire 2012-13

season, so results from the full growing season after return to full irrigation were available through this technique.

Data have been presented in the same way as the previous section, with a single colour used to denote data from vines that have received a given number of complete seasons of deficit irrigation, including vines that received only a single season of deficit (coloured red). To minimise the possibility of confusion the vines that have had a full season of control irrigation, following deficit, are also denoted with hatching and the single set of vines that were studied for two full seasons of recovery ('year three') are denoted with cross-hatching.

Fine root dry weight at budburst was not significantly affected by deficit irrigation and, similarly, fine root dry weight at budburst in vines that had received full irrigation for one season after receiving deficit irrigation was not significantly affected by prior irrigation status when the whole data set was examined (Figure 7a). However, when individual seasons were examined separately, the root dry weight of vines that received two seasons of deficit irrigation prior to one of full irrigation was significantly reduced ($p = 0.041$). In contrast, vines that previously received three seasons of deficit were unaffected. As these measurements were made in different seasons (2011-12 and 2012-13 respectively) and deficit irrigation in the 2011-12 season had a marginal significant effect on root dry weight at budburst (see above), it is likely that these observed impacts of deficit and prior deficit were due to an interaction with the environmental conditions in that year. The measurements were made at budburst 2011 immediately following the extreme rainfall events of 2010-11. Both sets of vines, those in their third year of deficit and those in their first year of full irrigation following two seasons of deficit, had reduced irrigation in the 2008-09 and 2009-10 seasons. It is possible that the vines that had received two seasons of deficit prior to the 2010-11 season were not able to respond as effectively to the increased water availability provided by the extreme rainfall.

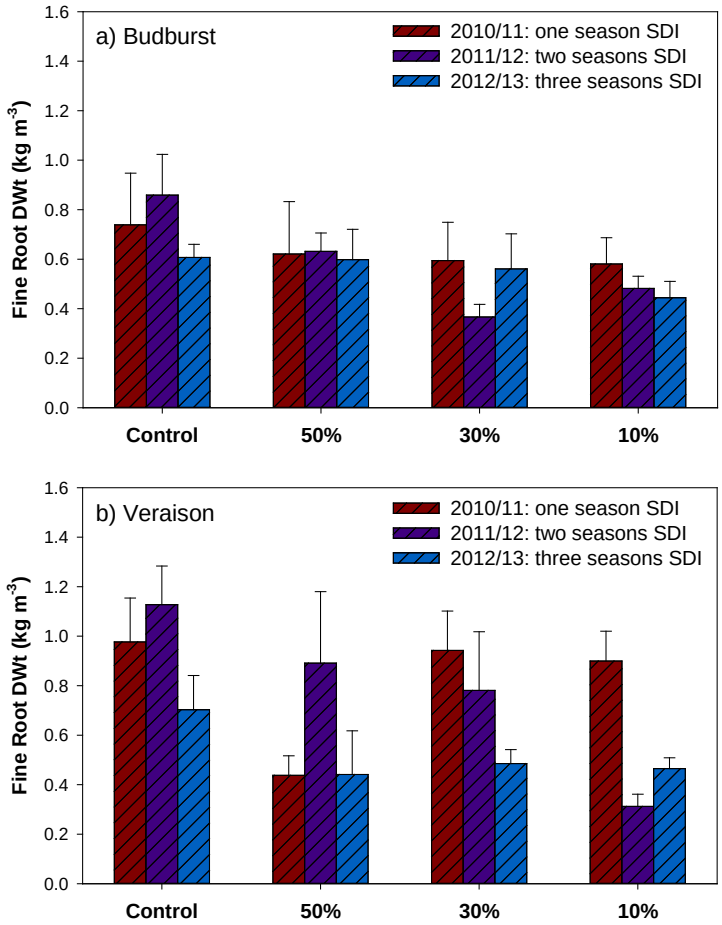

Figure 7 Fine root dry weight in the wetting zone of vines receiving control irrigation for at least one season after receiving control, 50% of control, 30% of control or 10% of control irrigation for one, two or three seasons, measured at a) budburst and b) veraison.

If this was occurring it might be expected that greater duration of deficit would lead to a greater disparity between vines previously deficit irrigated and vines previously receiving full irrigation, consequently, it would be expected that the vines receiving three or four seasons of deficit irrigation and then returned to full irrigation would exhibit this effect to a greater degree. This is not seen in Figure 7, but although the figure is showing vines with the same *status*, namely having received control irrigation for one season after receiving deficit irrigation, it does not show vines measured at the same *time*. Consequently, it is not possible to determine whether vines receiving more or less than two years of deficit irrigation would respond to extreme rainfall to a greater or lesser degree than shown here.

At the following veraison there was a significant effect of prior deficit irrigation across the whole data set (p = 0.025), but it was only marginally significant at best for any given season/duration of deficit (Figure 7b). The largest effect or prior deficit was on the vines that received two seasons of deficit, measured at veraison 2012. This was the same season that the vines still under deficit irrigation, in their fourth season, had the highest response to irrigation level, again suggesting a significant irrigation by season interaction.

The fine root surface area of the vines at budburst after a full season of recovery from deficit irrigation varied significantly between season/duration of prior deficit (p = 0.003; data not

shown), but not by the degree of deficit, even when normalised to account for seasonal variation (Figure 8a). There was also no significant effect apparent at the following veraison (Figure 8b).

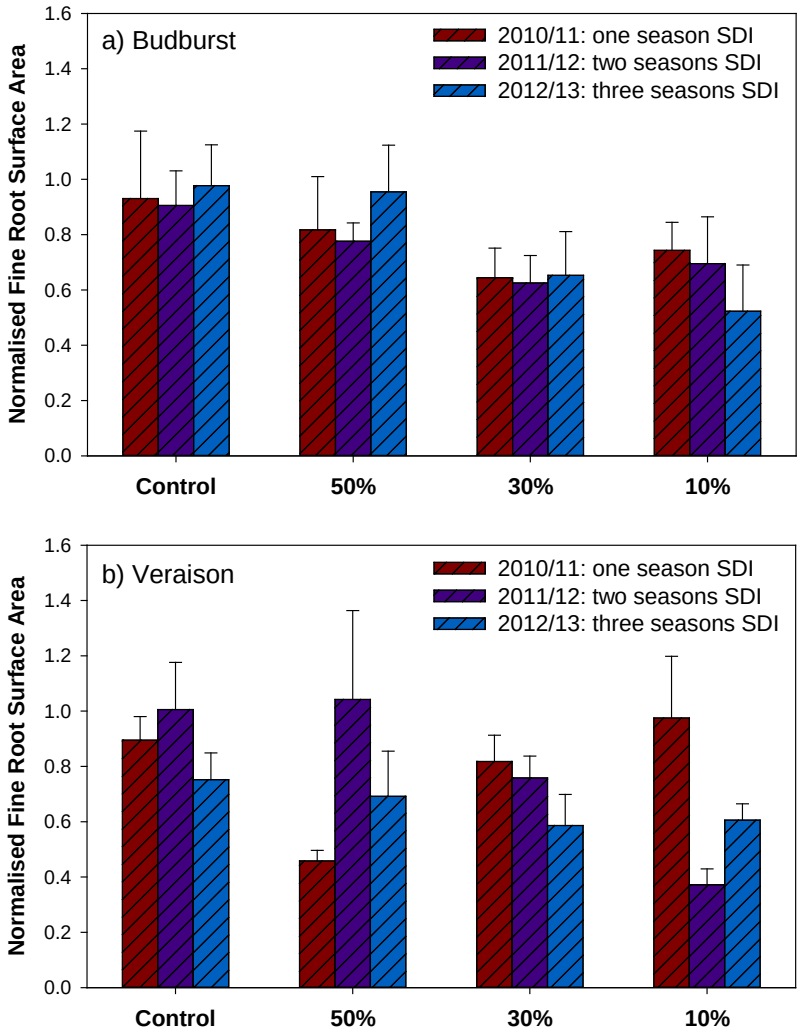

Figure 8 Fine root surface area, normalised to the control treatment for each season, in the wetting zone of vines receiving control irrigation for at least one season after receiving control, 50% of control, 30% of control or 10% of control irrigation for one, two or three seasons, measured at a) budburst and b) veraison.

The limited effects observed with the mini-rhizotrons during deficit irrigation were reflected in the data obtained from the vines undergoing recovery after return to control irrigation. There were no significant effects of prior irrigation on net root length (Figure 9a), root births (Figure 9c) or root deaths (Figure 9e) during the first season of control irrigation, nor during the second season (Figure 9b, d & f).

The data did demonstrate the continued increase of root length around the mini-rhizotron tubes, with the results from 2012-13 (Figure 9a & b) having a significantly greater net root length than 2011-12, which in turn had a greater net root length than 2010-11 (cf. Figure 5a). In all three seasons, whether vines were deficit or control irrigated, root births were much higher than root deaths, typically at least double. However, whereas root births were higher in 2011-12 than 2010-11 (Figure 5b), there was no further increase in root births in 2012-13. Despite this, there

was also no further increase in root deaths, without which the system could not reach equilibrium.

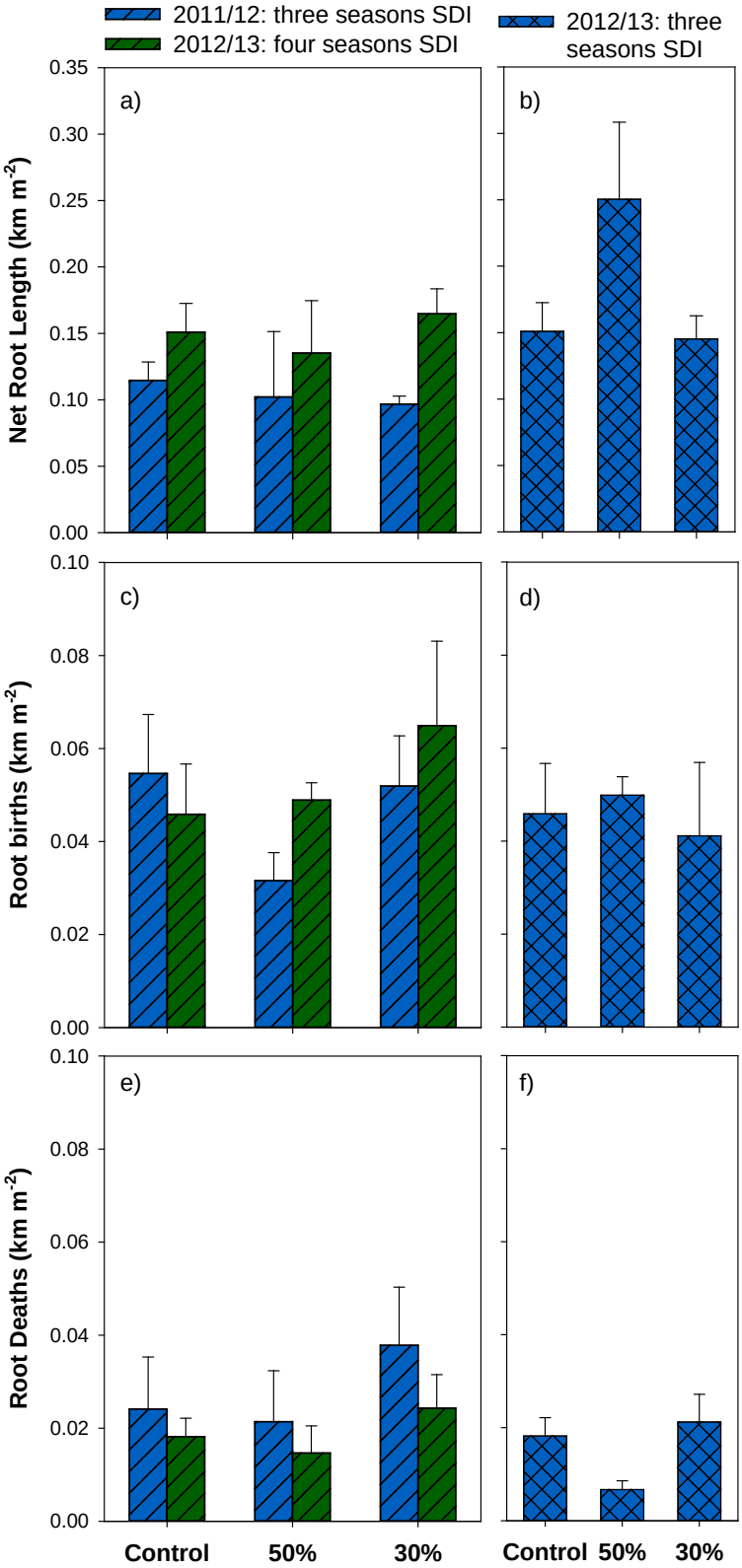

Figure 9 Directly measured parameters from mini-rhizotron images made in the wetting zone of vines receiving control irrigation for one season (a, c, e) or two seasons (b, d, f) after receiving control, 50% of control, or 30% of control irrigation; a & b) net root length, c & d) root births and e & f) root deaths per km^{-2} of soil intersection.

The 2011-12 season was the only season in which mini-rhizotron measurements were made in both deficit irrigated plots and plots returned to control irrigation after prior deficit. Although there was no significant difference in net root length, there was a significant difference in root births (p = 0.014). As no vine were under deficit irrigation in 2012-13 it isn't possible to be certain whether this was again an interaction with the environmental conditions within a given season, or a direct effect of the multiple seasons of deficit. However, the vines in recovery in 2011-12 after three years of deficit had root birth rates (numerically) the same as or less than controls, whereas the vines still under deficit had (numerically) greater rates. In contrast, the vines returned to control irrigation in 2012-13 after four years of deficit had root birth rates the same as or greater than controls, suggesting that again the interaction between prior irrigation state and current weather conditions may have been the driver of the observed difference.

Root turnover rates, defined as new root length per unit existing root length, of vines returned to control irrigation were not significantly affected by season or past irrigation regime (Figure 10a & b). Throughout the three seasons of work with the mini-rhizotrons, root turnover defined in this way was unaffected by either irrigation or inter-seasonal differences in weather. Using *root deaths / root births* as an alternative and analysing all the available data, deficit and recovery, there was a significant difference between 2010-11 and 2011-12 (p = 0.026) but no significant difference between 2011-12 and 2012-13 (Figs 6b and 10c & d). Again, it is difficult to ascertain whether this difference is to do with the developing root system around the tubes or an effect of the specific conditions in the difference growing seasons, but given the unexpected longevity of the fine roots, the former explanation is likely to be at least partially involved.

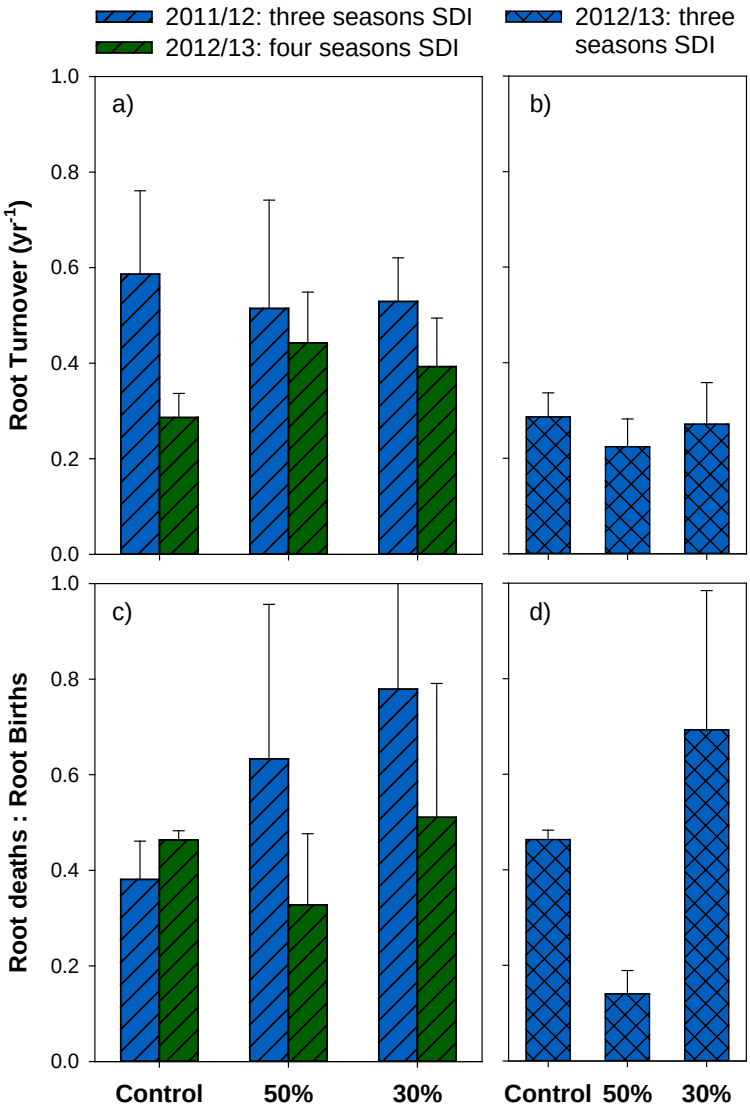

Figure 10 Parameters derived from mini-rhizotron images made in the wetting zone of vines receiving control irrigation for one season (a & c) or two seasons (b & df) after receiving control, 50% of control, or 30% of control irrigation; a & b) root turnover (root births/net root length) and c & d) the ratio of root deaths to root births.

Spatial distribution of roots and root production

Information on root distribution with depth was gained from both the soil coring and mini-rhizotron techniques, with the mini-rhizotron data tracking root growth at approximately 4 cm depth intervals to 0.5 m depth and the soil coring providing three depth groupings to 0.75 m depth. In addition, at budburst in 2012 additional coring was undertaken to generate a transect across the vine row. Although this was limited to three cores per transect, assuming that root distribution was similar either side of the vine row and along the vine row, it could reasonably be expected to be representative of the entire plot. (Edwards and Clingeleffer 2013) found no significant variation in root distribution along the row at a vineyard in a similar climate and soil type.

The data from the soil core transects allowed an estimate of whole vine root biomass, to 0.75 m depth, to be calculated. As a result, the proportion of the whole root system at a given depth or

distance from the dripline could be calculated, allowing the results to be expressed in this way as well as in absolute terms.

As noted above, for the dripline coring taken at budburst 2012-13, there was no significant effect of the four seasons of deficit irrigation on root dry weight, length or surface area, although a repeated measures ANOVA analysis including that data did indicate a significant effect of deficit irrigation. Not surprisingly, this resulted in a lack of significance when examining the distribution of roots from dripline to mid-row, whether considering root dry weight (Figure 11) or root length (Figure 12). Consequently, there was no impact of treatment on the proportion of the root system represented at each distance from the dripline. Averaged across the data set, the samples taken at 0.2 m from the dripline represented 32% of the soil surface area which contained 54% of the whole vine fine root mass and 65% of the whole vine root length, the samples taken at 0.75 m represented 43% of the soil surface, containing 31% of root mass and 25% of root length, whilst the samples taken at 1.5 m represented 25% of the soil surface area, but contained 12% of the root mass and 11% of the root length.

Across the site as a whole then, whilst the majority of fine roots were within the wetting zone of the irrigation system there was a significant investment in roots outside of the wetting zone. This may be a consequence of the drought tolerance and/or root spreading characteristic of Ramsey rootstock (Kidman, et al. 2014,Nagarajah 1987).

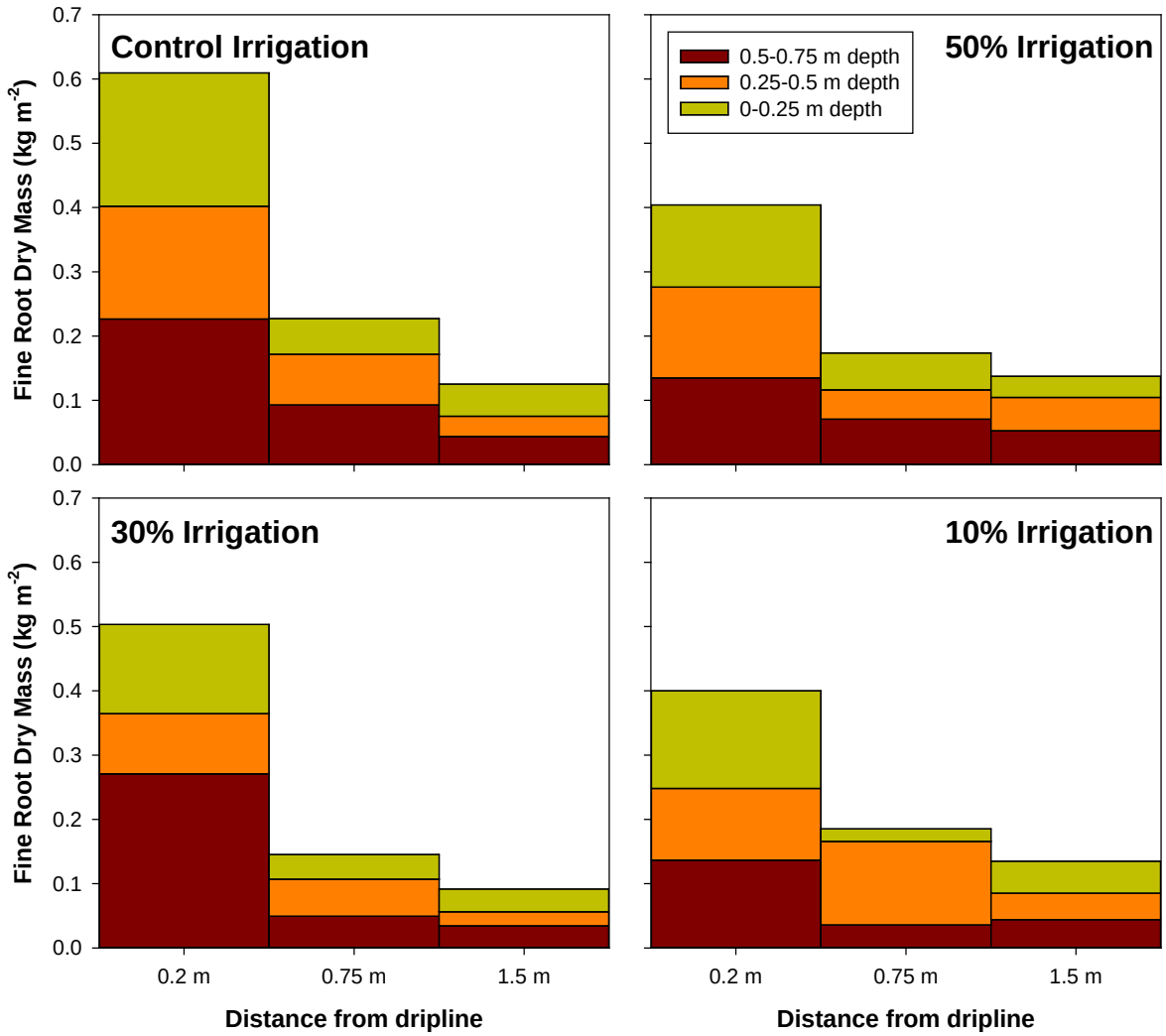

Figure 11 Fine root dry weight at budburst, expressed as kg per unit ground area, along a transect from the dripline to mid-row of vines that received control, 50% of control, 30% of control or 10% of control irrigation for four seasons immediately prior to sampling.

There was also no consistent effect of irrigation treatment on root distribution down to 0.75 m observed in the data obtained from the soil core transects (Figs. 11 & 12). Furthermore, the depth distribution was not significantly affected by distance from dripline. Drip irrigation of winegrapes in sandy soils is typically aimed at producing a wetting zone extending to about 0.6 m depth. Consequently investment in active fine roots to this depth is not surprising.

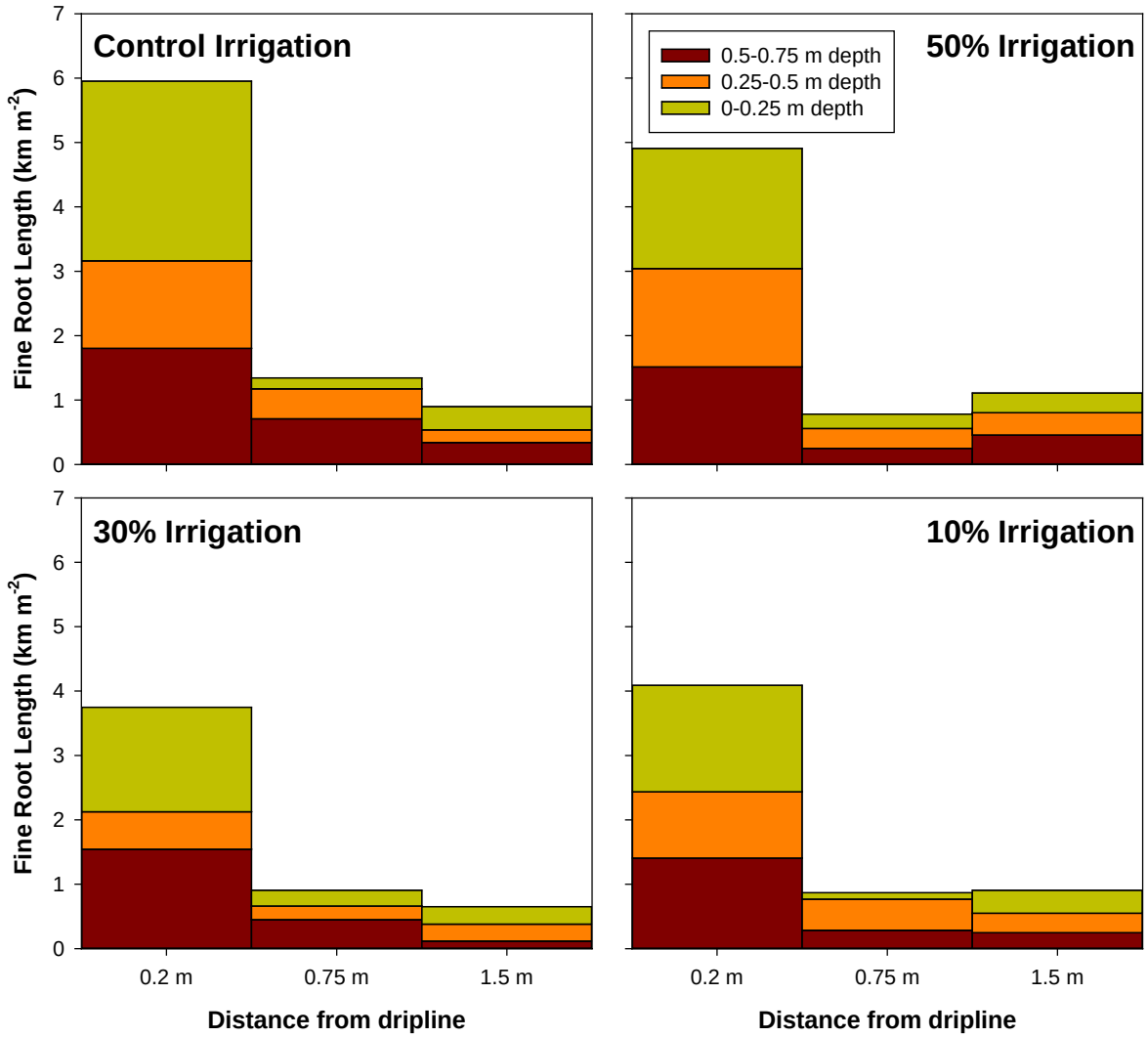

Figure 12 Fine root length at budburst, expressed as km per unit ground area, along a transect from the dripline to mid-row of vines that received control, 50% of control, 30% of control or 10% of control irrigation for four seasons immediately prior to sampling.

The difference in the proportion of root mass and root length at different positions from the dripline suggests a difference in the ratio of root length to root mass, known as specific root length. A difference in specific root length indicates a structural change, causing a change in density or, more commonly, a change in root diameter. The soil core transect data exhibited significant differences in both, with a higher specific root length and smaller average root diameter in the samples taken adjacent to the dripline (Table 1).

Thicker fine roots are sometimes a common response to drier soil conditions (Bauerle, et al. 2008) and would be expected away from the wetting zone. Surprisingly, the samples furthest from the wetting zone, those at 1.5 m from the dripline, had the smallest average root diameter of all and a higher specific root length than those taken 0.75 m from the dripline. This is in agreement with the observations of (Mapfumo, et al. 1994) where water stress was observed to have a greater effect on diameter than on length compared to well watered roots.

Table 1 Specific root length and average root diameter measured at budburst along a transect from dripline to mid-row. All irrigation treatments were combined.

	0.2 m from dripline		0.75 m from dripline		1.5 m from dripline	
	Mean	**SE**	**Mean**	**SE**	**Mean**	**SE**
Specific Root Length (m g^{-1})						
0-25 cm	11.7	2.1	4.6	0.6	7.3	0.8
25-50 cm	8.2	0.7	5.1	0.7	8.4	1.9
50-75 cm	8.1	0.5	6.8	0.7	8.2	0.9
Average root diameter (mm)						
0-25 cm	0.52	0.04	0.58	0.05	0.47	0.04
25-50 cm	0.60	0.01	0.59	0.05	0.48	0.03
50-75 cm	0.59	0.02	0.59	0.04	0.45	0.04

The specific root length data from the soil core transect also suggested a depth effect. As there was no significant impact of irrigation treatment on allocation of roots to different depths the entire data set was combined to examine root biomass, root length and specific root length at different depths, for the data collected at budburst and veraison over the three seasons studied. There was a small difference in fine root dry weight allocation with depth, the least allocation being in the 25-50 cm category, but the highest in the 50-75 cm category (Figure 13a). In contrast, the largest allocation of root length was to the upper layer, 0-25 cm, but there was a greater root length at 50-75 cm than 25-50 cm (Figure 13b). Not only was the root allocation to the 50-75 cm depth greater than the 25-50 cm depth, but there was also an increased allocation to that depth at veraison compared with at budburst.

As with the results from the soil core transect, the difference in allocation between fine root dry weight and fine root length suggested an effect on specific root length. Indeed this was seen with the greatest specific root length being in the upper layers of soil (Figure 13c), providing the greatest absorbing area for the least biomass investment in the region where irrigation was actually applied.

The mini-rhizotron results allowed for root depth effects to be looked at on a finer scale, albeit only in the wetting zone. The mini-rhizotrons were installed at an angle that bisected the wetting zone, passing from the soil surface, 0.15 m away from the vine on one side of the dripline, to 0.5 m deep, 0.15 m on the other side of the vine, with the tube directly under the vine trunk at about 0.25 m depth. As such the mini-rhizotron data should be highly representative of roots in the wetting zone, whereas the soil coring could only access the edge of that zone.

As with the soil core data, there was no impact of irrigation treatment on the allocation of root length to different depths, even in vines undergoing their fourth season of deficit (Figure 14a). Average diameter of the roots in the mini-rhizotrons also matched the coring data, with the average over 0-25 cm being 0.57 mm and from 25-50 cm the average was 0.60 mm, very similar to the data in Table 1. However, net root length in the individual mini-rhizotron windows increased with depth, from the surface to 50 cm deep. This contrasted with the soil core data,

where the top 25 cm had greater root length than 25-50 cm deep section. In Figure 14b the top 25 cm of soil contained a third more root length than the 25-50 cm section, compared with the 25-50 cm section having more than double the root length of the 0-25 cm section in the mini-rhizotron windows. For example, the net root length of the control tubes in 2012-13 was 656 mm in the top 25 cm, but 1820 mm over 25-50 cm.

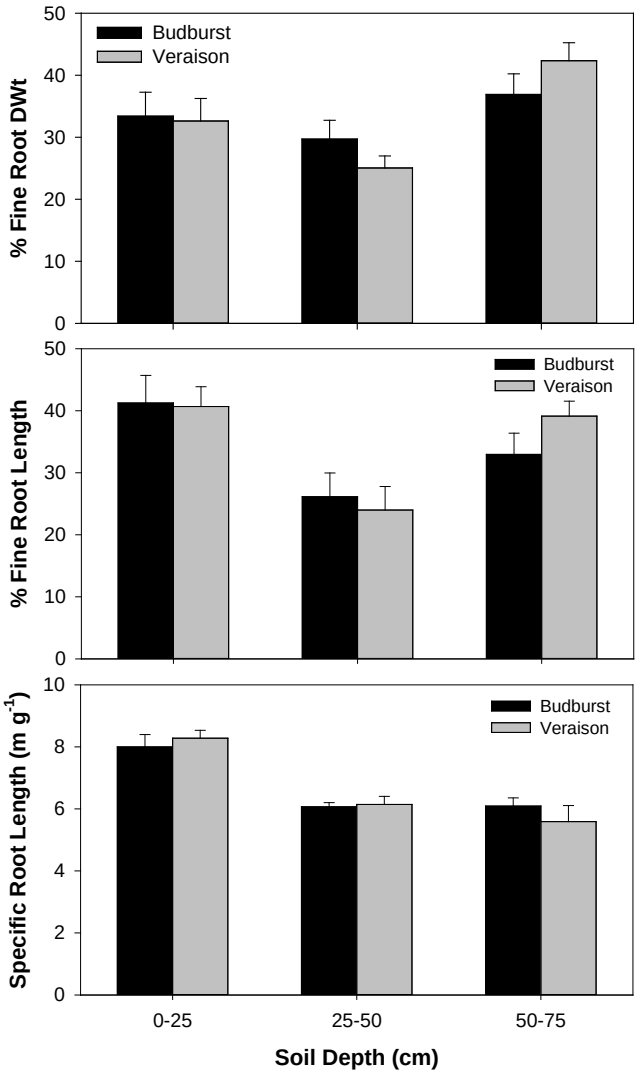

Figure 13 % fine root dry weight (a), % fine root length (b) and specific root length, averaged across three seasons and all irrigation treatments in three depth categories, taken at budburst or veraison in each season.

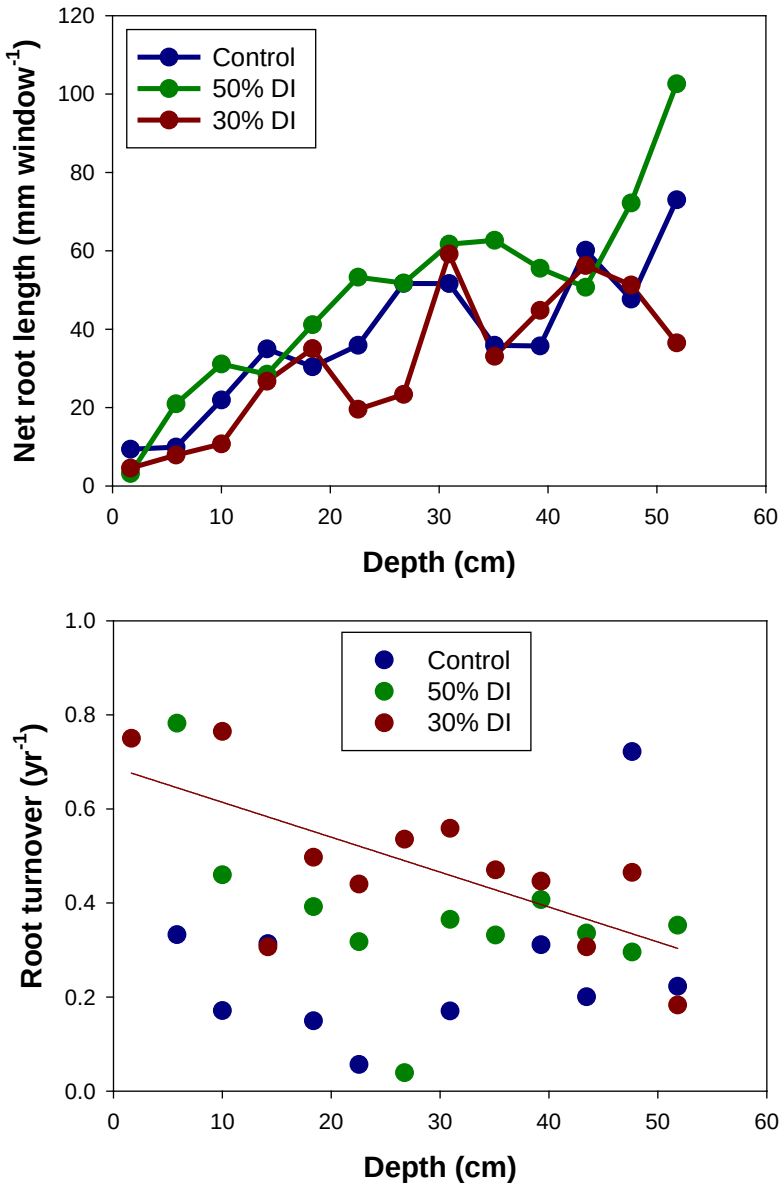

Figure 14 Net root length (a) and root turnover (b) calculated from mini-rhizotron imaging during the fourth season of irrigation treatments, 2012-13, and plotted against window depth.

There is no obvious explanation for the disparity in root length distribution with depth between the two techniques used, but the necessarily different positioning could be involved, or the lack of 'steady-state' root turnover around the tubes. New root length and root lost, at different depths were largely a function of the net root length present. When the individual irrigation treatments were examined separately, there was only a marginal relationship between turnover and depth in the 30% deficit treatment, with R^2 of 0.2 (Figure 14b).

Conclusions

Despite up to four seasons of deficit irrigation as low as 10% of control irrigation, only very limited effects were seen on the vine root systems. As the deficit increased, from 50% to 10% of control, fine root surface area decreased, with the vines receiving only 10% irrigation having

approximately 60% of the root surface that the control vines had. There was no effect of increasing duration of deficit, from two to four seasons, on the impact of the deficit. The mini-rhizotrons, positioned directly in the dripper wetting zone, saw no effects of deficit irrigation and soil coring at 0.2 m from the dripline, found only small effects, significant only over a number of seasons. These results demonstrate the resilience of the root system when faced with soil water stress and the ability of the vine to increase the resource allocation to the root system under these circumstances.

The mini-rhizotron system also demonstrated the remarkable longevity of fine roots in this vineyard, Ramsey rootstock in sandy soils in a hot climate. The data from the system also presents a resource whereby further in-depth analysis could look at active (white) roots separately from the entire root system, timing of root growth and other factors. Similarly, the soil core data set retains information on size distribution, which could be used to compare specific classes of root with the mini-rhizotron data.

References

Anderson, L.J., L.H. Comas, A.N. Lakso, and D.M. Eissenstat (2003) Multiple risk factors in root survivorship: a 4-year study in Concord grape. New Phytologist 158, 489-501. doi: 10.1046/j.1469-8137.2003.00757.x.

Bauerle, T.L., D.R. Smart, W.L. Bauerle, C. Stockert, and D.M. Eissenstat (2008) Root foraging in response to heterogeneous soil moisture in two grapevines that differ in potential growth rate. New Phytologist 179, 857-866. doi: 10.1111/j.1469-8137.2008.02489.x.

Burton, A.J., K.S. Pregitzer, G.P. Zogg, and D.R. Zak (1998) Drought reduces root respiration in sugar maple forests. Ecological Applications 8, 771-778. doi: 10.2307/2641265.

Chaves, M.M., J.S. Pereira, J. Maroco, M.L. Rodrigues, C.P.P. Ricardo, M.L. Osorio, I. Carvalho, T. Faria, and C. Pinheiro (2002) How plants cope with water stress in the field. Photosynthesis and growth. Annals of Botany 89, 907-916. doi: 10.1093/aob/mcf105.

Comas, L.H., L.J. Anderson, R.M. Dunst, A.N. Lakso, and D.M. Eissenstat (2005) Canopy and environmental control of root dynamics in a long-term study of Concord grape. New Phytologist 167, 829-840. doi: 10.1111/j.1469-8137.2005.01456.x.

Comas, L.H., T.L. Bauerle, and D.M. Eissenstat (2010) Biological and environmental factors controlling root dynamics and function: effects of root ageing and soil moisture. Australian Journal of Grape and Wine Research 16, 131-137. doi: 10.1111/j.1755-0238.2009.00078.x.

Comas, L.H., D.M. Eissenstat, and A.N. Lakso (2000) Assessing root death and root system dynamics in a study of grape canopy pruning. New Phytologist 147, 171-178. doi: 10.1046/j.1469-8137.2000.00679.x.

Edwards, E.J. and P.R. Clingeleffer (2013) Interseasonal effects of regulated deficit irrigation on growth, yield, water use, berry composition and wine attributes of Cabernet Sauvignon grapevines. Australian Journal of Grape and Wine Research 19, 261-276. doi: 10.1111/ajgw.12027.

Eissenstat, D.M., T.L. Bauerle, L.H. Comas, A.N. Lakso, D. Neilsen, G.H. Neilsen, and D.R. Smart (2006) Seasonal patterns of root growth in relation to shoot phenology in grape and apple. In: Proceedings of the Vth International Symposium on Mineral Nutrition of Fruit Plants, Ed. J.B. Retamales pp. 21-26.

Kato, Y. and M. Okami (2011) Root morphology, hydraulic conductivity and plant water relations of high-yielding rice grown under aerobic conditions. Annals of Botany 108, 575-583. doi: 10.1093/aob/mcr184.

Kidman, C.M., S.O. Mantilla, P.R. Dry, M.G. Mccarthy, and C. Collins (2014) Effect of Water Stress on the Reproductive Performance of Shiraz (Vitis vinifera L.) Grafted to Rootstocks. American Journal of Enology and Viticulture 65, 96-108. doi: 10.5344/ajev.2013.13069.

Lehnart, R., H. Michel, O. Loehnertz, and A. Linsenmeier (2008) Root dynamics and pattern of 'Riesling' on 5C rootstock using minirhizotrons. Vitis 47, 197-200.
Mainiero, R. and M. Kazda (2006) Depth-related fine root dynamics of Fagus sylvatica during exceptional drought. Forest Ecology and Management 237, 135-142. doi: 10.1016/j.foreco.2006.09.034.
Mapfumo, E., D. Aspinall, and T.W. Hancock (1994) Growth and development of roots of grapevine (vitis-vinifera l) in relation to water-uptake from soil. Annals of Botany 74, 75-85. doi: 10.1006/anbo.1994.1096.
Nagarajah, S. (1987) Effects of soil texture on the rooting patterns of thompson seedless vines on own roots and on ramsey rootstock in irrigated vineyards. American Journal of Enology and Viticulture 38, 54-59.
Soar, C.J. and B.R. Loveys (2007) The effect of changing patterns in soil-moisture availability on grapevine root distribution, and viticultural implications for converting full-cover irrigation into a point-source irrigation system. Australian Journal of Grape and Wine Research 13, 2-13. doi: 10.1111/j.1755-0238.2007.tb00066.x.

6.6 Measurement of carbohydrate concentration in grapevine trunk and leaf tissues using Near Infrared Spectroscopy

Introduction

Total non-structural carbohydrate concentration is normally assessed by wet chemistry methods such as simple colorimetric analyses or more sophisticated high performance liquid chromatography (HPLC) or gas chromatography mass spectrometry (GC-MS) methods. (Edwards, et al. 2011) reviewed and reported a technical brief describing an adaptation of the anthrone method (Dreywood 1946) to be applied to the determination of soluble carbohydrate concentration in grapevine tissues. However, even the latter method could be time consuming and costly when studying carbohydrate dynamics in grapevines over seasons. Therefore a rapid method for analysing carbohydrate concentration would be advantageous to study the relationships between carbohydrate accumulation and dynamics as affected by treatments imposed. Despite the large number of published methods, until recently there has been a lack of a simple, rapid and low cost procedure to be applied to a large number of samples.

Near infrared (NIR) is the region of the electromagnetic spectrum between 750 nm and 2500 nm and it is often used to gather information on the relative proportions of C-H, N-H and O-H bonds of the organic molecules (Murray and Kurtz 1993). NIR spectroscopy has been applied for grapevine tissues analysis in the past, demonstrating its ability to determine the following: concentration of anthocyanins, soluble solids and pH in red grape homogenates (Cozzolino, et al. 2006, Cozzolino, et al. 2004, Dambergs, et al. 2006, Gishen, et al. 2005), to measure wine composition (Cozzolino, et al. 2007,Smyth, et al. 2008) and more recently to estimate vine water potential (De Bei, et al. 2011). (Schmidtke, et al. 2012) have developed a rapid method for monitoring grapevine reserves (carbohydrate and nitrogen content) using attenuated total reflectance (ATR) coupled with mid infrared (MIR) in trunk and root samples. The main advantages of these techniques (NIR and MIR) over traditional methods are the rapidity and the ease of use in routine analysis (Cozzolino 2009), which allow a considerable reduction of costs and time.

In this project we combined NIR spectra of ground grapevine trunk and leaf tissues, the measure of carbohydrates concentration measured by applying the (Edwards, et al. 2011) method and multivariate data analysis to develop a rapid procedure for the estimation of carbohydrates concentration in grapevine tissues.

Methods

Trunk and leaf samples
Grapevine trunk and leaf tissues used for the development of the calibration models were sourced from the SDI and recovery trial Chardonnay vineyard as described in Chapter 5. Wood and leaf samples were taken from the trunks at key phenological stages during the seasons 2008-09 and 2009-10 as described in Chapter 6.5.

Chemical analysis
All samples (trunk and leaves) were freeze-dried using a Telstar LyoQuest freeze-drier (AVT Services Pty Ltd., Seven Hills, NSW, Australia) and then ground to a fine powder (particle size ~ 50μm) using a Labtech Essa LM1-P mill (Labtech Essa Pty Ltd., Bassendea, WA, Australia). The freeze-dried and ground samples were analysed for starch and sugar concentration according to

the adaptation of the anthrone method proposed by (Edwards, et al. 2011). Further details are in Chapter 6.4.

Visible/Near Infrared scanning

The freeze-dried and ground leaf and trunk samples were scanned with a NIRSystems 6500 (FOSS NIRSystems, Silver Spring, MD, USA), from 400–2500 nm, in transmittance mode with a 1 mm path length. The spectrum of each sample was the average of 32 successive scans (1050 data points per scan). Samples were not rotated when spectra collection was made. Two pairs of lead sulphide detectors collected the reflectance spectra. Reflectance energy readings were referenced to corresponding readings from a ceramic disk. Spectral data were collected using Vision software (Version 1.0, FOSS NIRSystems, Silver Spring, MD, USA) and stored as the logarithm of the reciprocal of reflectance (R) (i.e. as absorbance=log(1/*R*)) at 2 nm intervals.

Chemometrics and data analysis

Chemometric analysis was performed using The UnscramblerX software package (Version 10.2, CAMO ASA, Norway). The spectral region from 400 to 1099nm (visible and short wavelength near infrared) was not used for the analysis since it is mostly related to absorptions by pigments. Principal component analysis (PCA) was performed before partial least squares regression (PLS) models were developed. PCA was used to identify the dominant patterns in the spectral data and for outliers detection. The Unscrambler software detects outliers based on the Hotteling T^2 test. However, for the purpose of this study a spectral outlier was defined as any samples falling outside the 95% of the cloud of data in the PCA score plots. Calibrations were developed using partial least square regression (PLS) with test set validation. To perform the test set validation, the data set was firstly sorted ascending based on the values of starch (for starch and NSC calibrations) and on the values of sugar (for sugar calibrations) concentration and then divided into two groups. The first group, corresponding to 2/3 of the whole data set selected by choosing two samples every three was used to develop the calibration. The second group, formed by the remaining 1/3 of the data set, was kept as the validation set to test the model. For the trunk material dataset, 177 samples were used for the calibration set and 84 as the validation set for testing the model. For the leaf samples, the overall data set was split in two sets following the same procedure described above. In this case, 149 samples were used for the calibration set and 73 for the validation. PLS models were developed using the raw spectra and pre-processed data. The pre-processing performed were the standard normal variate (SNV) and second derivative transformation using the Savitzky-Golay second derivative with 20 points smoothing. The optimum number of terms in the PLS calibration models was determined as indicated by the lowest number of factors that gave the closest to minimum value of the PRESS (prediction residual error sum of squares). Statistical parameters calculated for the calibrations included: the standard error in cross validation (SECV), the coefficient of determination in calibration (R_{cal}^2), and the standard error of prediction (SEP). The optimum calibrations were selected based on minimising the SECV.

To evaluate how well the calibration model could predict compositional data, the residual predictive deviation (RPD) was used. The RPD is defined as the standard deviation (SD) of the population reference values divided by the SEP for the NIRS calibrations. If the SEP for estimating a constituent is large compared to the spread of that compound in all samples (SD), a relatively small RPD is calculated, thereby demonstrating that the NIRS calibration model is not robust. In contrast, relatively high RPD values indicate that models have greater power to predict the chemical composition of the samples. Generally, an RPD greater than three is recommended for screening purposes (Fearn 2002; Williams, 2001).

Results and Discussion

The descriptive statistics (average, range, standard deviation (SD) and coefficient of variation (CV)) of the concentration of starch ([St]), sugar ([Su]) and NSC ([NSC]) (starch + sugar) in trunk and leaf tissues measured with the reference method for the calibration and the validation data sets are shown in Table 1. For both trunk and leaf samples the values of [St] were well spread over the range. The CV value was higher for [St] compared to [Su] and [NSC] in both trunk and leaf samples. The CV value was particularly large for the [St] in the leaf samples (58.75% and 58.86% for calibration and validation set respectively). The CV values for the [Su] in trunks and leaves were small, ranging from 11.07% to 14.04%. Since NSC is the sum of [St] and [Su], the resulting CV value for this parameter was large as it was more influenced by the higher variation in the [St] than [Su]. Similar mean values and SD for [St], [Su] and [NSC] were observed for the calibration and validation sets for both trunks and leaves.

Table 1 Descriptive statistic of the starch [St], sugar [Su] and total non-structural carbohydrate (starch+sugar) [NSC] concentration in the trunk and leaf tissues analysed by reference method.

	Mean (mg/g)	Maximum (mg/g)	Minimum (mg/g)	SD (mg/g)	CV (%)
Trunk tissues					
Calibration set (n=177)					
[St] (mg/g)	133.84	194.07	62.46	26.65	19.91
[Su] (mg/g)	37.16	51.90	26.01	5.21	14.04
[NSC] (mg/g)	170.95	236.51	101.36	27.63	16.16
Validation set (n=82)					
[St] (mg/g)	133.33	187.72	63.88	26.88	20.16
[Su] (mg/g)	37.18	51.93	25.53	5.13	13.82
[NSC] (mg/g)	169.75	227.19	102.20	27.74	16.34
Leaf tissues					
Calibration set (n=149)					
[St] (mg/g)	102.76	222.64	8.13	60.37	58.75
[Su] (mg/g)	71.46	91.49	58.02	7.91	11.07
[NSC] (mg/g)	174.22	297.28	75.80	62.09	35.64
Validation set (n=73)					
[St] (mg/g)	103.31	229.50	10.45	60.81	58.86
[Su] (mg/g)	70.24	95.98	53.42	8.12	11.57
[NSC] (mg/g)	173.55	298.09	69.67	63.15	36.39

SD, standard deviation; CV, coefficient of variation [(SD/mean)*100]

The average absorbance spectra appeared similar for both trunk and leaf samples showing three main peaks, in the regions 1430, 1910 and 2300 nm (Figure 1a). Spectra collected from leaf tissues presented one additional absorption band in the region at 1700 nm (Figure 1a). The second derivative transformation of the spectra, which resolves the raw spectra in finer scale features, showed differences between the leaf and trunk tissues where the leaves present some additional peaks as compared to the trunks (Figure 1b). The common absorption bands in the NIR region were found around 1430, 1920 and 2300 nm as shown in the raw spectra. Additional peaks in the leaf tissues spectra were found at around 1200, 1500, 1700 and 2050 nm (Figure 1b).

Statistics for the PLS models developed using raw spectra, SNV transformation and Savitzky-Golay transformation are presented in Table 2. The calibration models for the prediction of [St] showed an R^2_{cal} ranging from 0.80 to 0.84, SECV values from 10.60 to 11.80 mg/g using 11 to 14 PLS loadings. Similar results were obtained for the prediction of [NSC]. The most robust (higher R^2_{cal}, lowest SECV/SEP and PCs number) model for the prediction of [St] was obtained using the second derivative transformation of the spectra. The RPD value for this model was 2.51.

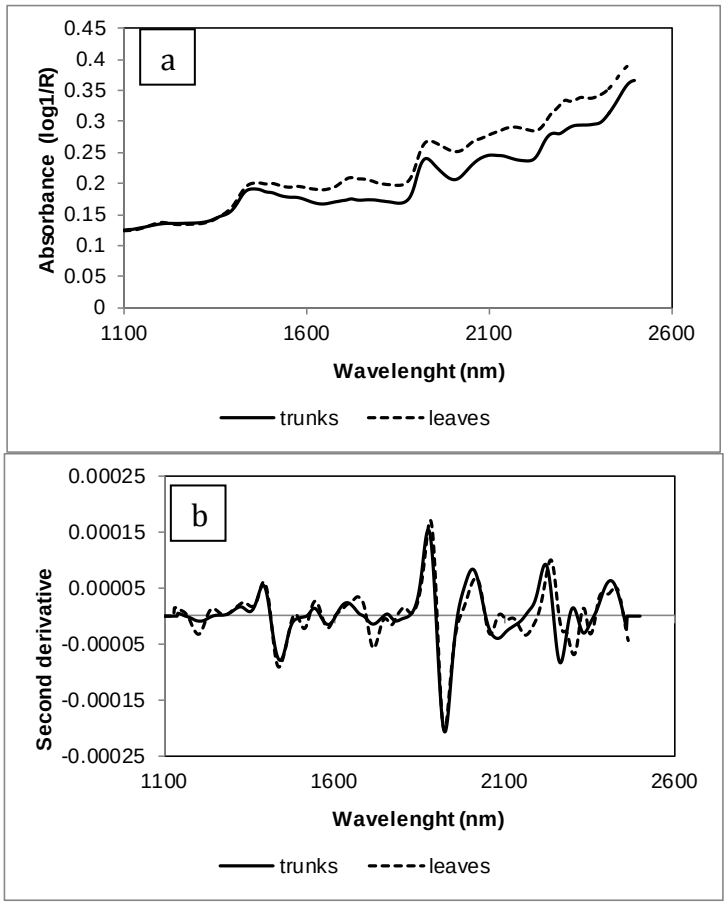

Figure 1 Mean Near infrared spectra (NIR) (1100-2500nm) (a) and Savitzky-Golay second derivative transformed spectra (b) of the ground trunk (continuous line) and leaf (dashed line) samples.

Table 2 Partial least square (PLS) calibration statistics for starch [St], sugar [Su] and total non-structural carbohydrate (starch + sugar) [NSC] concentration in trunk tissues using the raw spectra and with the application of SNV and Savitzky-Golay second derivative transformations.

	R^2		SECV/SEP (mg/g)		Slope		Bias		PCs	RPD
	Cal	Val	Cal	Val	Cal	Val	Cal	Val		
Raw spectra										
[St]	0.80	0.79	11.80	12.89	0.80	0.78	0.14e-04	0.11	14	2.23
[Su]	0.69	0.58	2.76	4.37	0.69	0.44	-2.4e-05	0.36	18	1.88
[NSC]	0.81	0.82	12.03	12.78	0.81	0.77	7.2e-05	-0.59	14	2.30
SNV transformed spectra										
[St]	0.81	0.80	11.51	12.51	0.81	0.78	7.65 e-06	0.26	13	2.32
[Su]	0.67	0.32	2.82	4.27	0.67	0.59	-2.01e-06	0.31	16	1.85
[NSC]	0.80	0.80	12.74	12.52	0.80	0.79	-6.64e-06	0.69	13	2.17
Savitzky-Golay transformed spectra										
[St]	0.84	0.80	10.60	12.51	0.84	0.78	3.72e-06	-0.45	11	2.51
[Su]	0.53	0.28	3.39	4.55	0.53	0.39	-3.54e-07	0.34	9	1.54
[NSC]	0.84	0.82	10.92	12.65	0.84	0.79	3.6e-06	-0.89	11	2.17

R^2, coefficient of determination, SECV, standard error in cross validation, SEP, standard error of the prediction, PC, number of partial least squares terms in calibration , RPD= SD/SEP, residual predictive deviation

Table 3 Partial least square calibration statistics for starch [St], sugar [Su] and total non-structural carbohydrate (starch + sugar) [NSC] concentration in leaf tissues using the raw spectra and with the application of SNV and Savitzky-Golay second derivative transformations.

	R^2		SECV/SEP (mg/g)		Slope		Bias		PCs	RPD
	Cal	Val	Cal	Val	Cal	Val	Cal	Val		
Raw spectra										
[St]	0.92	0.83	17.41	24.92	0.92	0.84	3.62 e-05	2.11	10	3.47
[Su]	0.46	0.39	5.99	6.22	0.46	0.42	1.66 e-05	-0.15	8	1.32
[NSC]	0.92	0.84	17.40	25.12	0.92	0.85	5.19 e-05	1.86	10	3.57
SNV transformed spectra										
[St]	0.92	0.85	16.78	23.77	0.92	0.86	-3.97 e-06	2.16	8	3.60
[Su]	0.28	0.42	6.88	6.25	0.28	0.35	-3.63 e-06	0.46	4	1.15
[NSC]	0.93	0.85	16.80	24.19	0.93	0.86	-7.63 e-06	1.76	8	3.70
Savitzky-Golay transformed spectra										
[St]	0.93	0.88	16.18	21.13	0.93	0.87	6.69 e-06	1.72	7	3.73
[Su]	0.43	0.43	6.11	5.99	0.43	0.45	-4.60 e-07	1.27	5	1.30
[NSC]	0.92	0.86	17.83	22.86	0.92	0.86	-2.71 e-06	0.18	5	3.48

R^2, coefficient of determination, SECV, standard error in cross validation, SEP, standard error of the prediction, PC, number of partial least squares terms in calibration , RPD= SD/SEP, residual predictive deviation

Table 4 Partial least square (PLS) calibration statistics for the universal model for total non-structural [NSC] concentration in both trunk and leaf tissues using the Savitzky-Golay second derivative transformations.

	R^2		SECV/SEP (mg/g)		Slope		Bias		PCs	RPD
	Cal	Val	Cal	Val	Cal	Val	Cal	Val		
[NSC]	0.86	0.84	17.75	19.80	0.86	0.84	-4.26 e-06	2.2	9	

R^2, coefficient of determination, SECV, standard error in cross validation, SEP, standard error of the prediction, PC, number of partial least squares terms in calibration , RPD= SD/SEP, residual predictive deviation

The PCA scores plot for the spectra collected from the trunk samples and transformed using the Savitzky-Golay second derivative, showed a clear separation of the samples along both the first two PCs associated with the phenological stage in which the samples were collected (Figure 2a). The first PC explained 66% of the variation in the NIR spectra while the second explained 25%. Examination of the eigenvectors derived from the first PC revealed that the specific region at 1900 nm mostly explains the separation between samples that could therefore be related to [St]. Three main loadings associated with the second PC were found around 1420nm, 2220 nm and 2240 nm associated with water and starch (Figure 2b). For all the models developed no spectral outliers were removed from the dataset. However, Figure 2a shows that three samples, at the top-right corner of the scores plot fell outside the 95% of the data cloud and could have been removed.

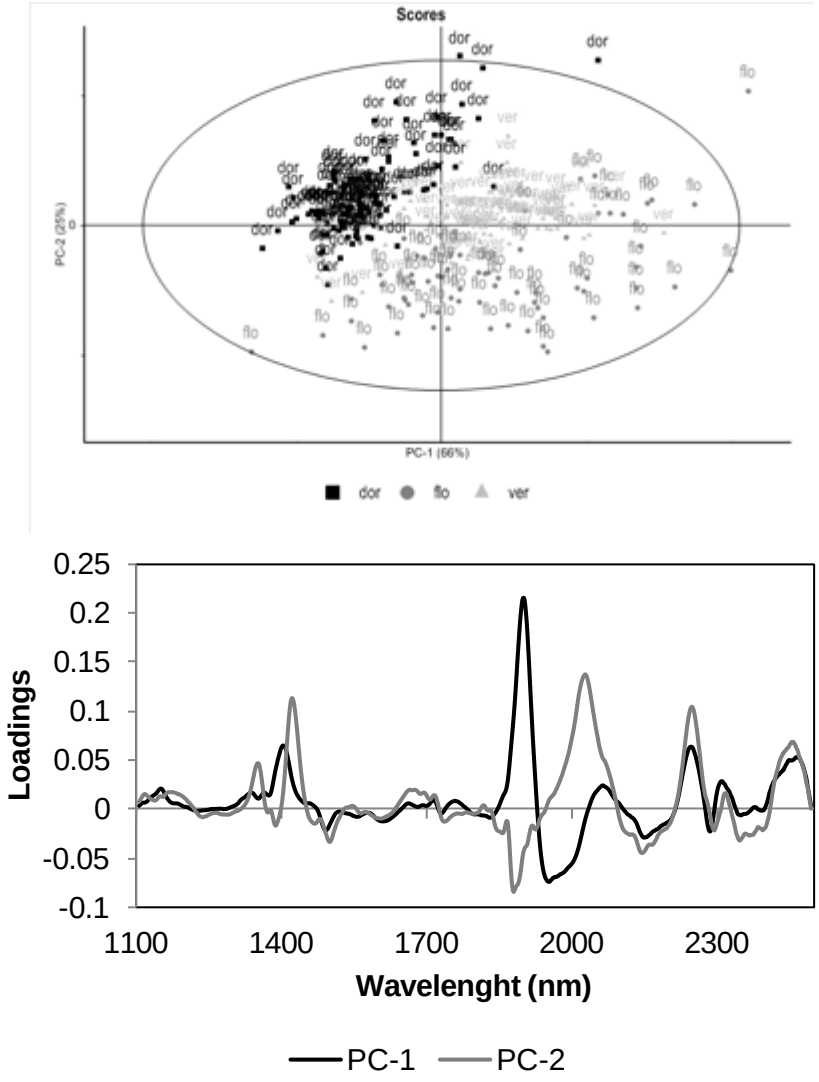

Figure 2 Score plot of the first and second principal components (PCs) of the Savitzky-Golay transformed near infrared spectra collected from the freeze-dried and ground trunk samples at three different phenological stages: dormancy (dor ■), flowering (flo ●) and veraison (ver ▲).

Similar results were obtained for the prediction of [NSC] when building the models using the second derivative of the spectrum ($R^2 = 0.84$). The low CV observed for the sugar concentration

in trunk samples might explain the poor PLS calibration obtained, with R^2 ranging from 0.53 to 0.69 (Table 2).

The calibration and validation models representing the correlation between the [NSC] measured with the reference method and predicted by NIR are shown in Figure 3 (a and b). For this model the first three principal components explained 96% of the variation in the dataset. The first PC explained 66% of the variation and the highest loadings were found at wavelengths around 1450 nm and 1900 nm. The highest loadings for the second PC, which accounts for 22% of the variation, were observed in the NIR regions around 1450, 2020 and 2250 nm (Figure 4 a, b).

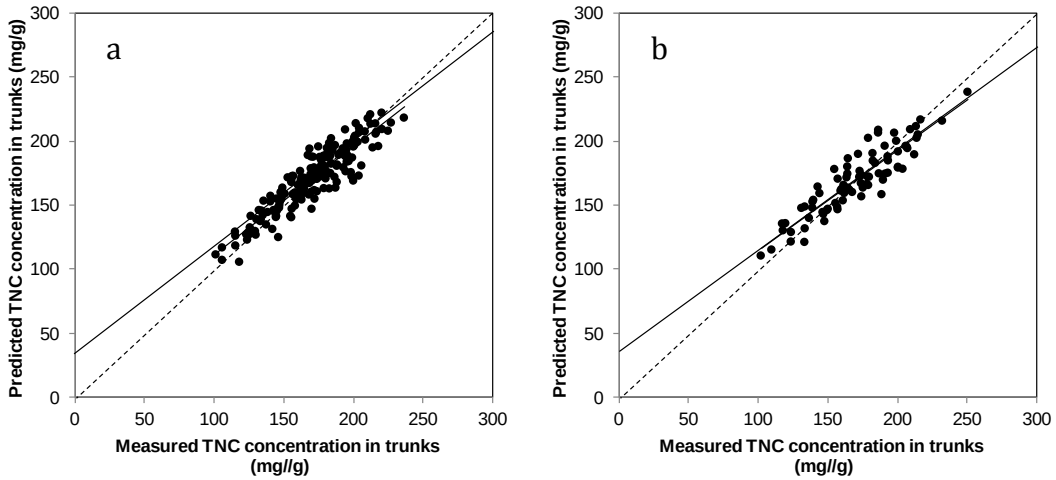

Figure 3 Comparison of the concentration of NSC (mg/g) determined by the anthrone method and the concentration predicted by NIR using PLS regression in trunk samples for both the calibration (a) and validation (b) data sets

Similarly to what was observed for the trunk samples, in leaf samples the second derivative transformation of the spectrum gave the best modelling results for the prediction of both [St] and [NSC] (Table 3). Very high RPD values were also observed for all the models related to starch and NSC (all RPDs are higher than 3) however very low values were obtained for sugar prediction. The model for the prediction of [NSC] in leaves samples achieved an R^2 of 0.92 and 0.86 in calibration and validation respectively and it required five PCs. The SECV resulted 17.83 mg/g, SEP 22.86 mg/g and the RPD was 3.48. This model is represented in Figure 5a and b for the calibration and validation respectively. For the leaf models the first three PCs explain 90% of the variation with PC 1, 2 and 3 accounting for a 47%, 23% and 20% of the variation respectively (Figure 5 a,b). The highest loadings for all the three PCs were found in similar regions of the spectrum: 1400 nm, 1900 nm and 2200 nm. Considering the similarities between the models created for the prediction of [NSC] in both trunk and leaf tissues, a universal model was also built (Figure 7 and Table 4). The results for the calibration set were: R^2_{cal}=0.86 with a SECV of 17.75 mg/g requiring nine PCs.

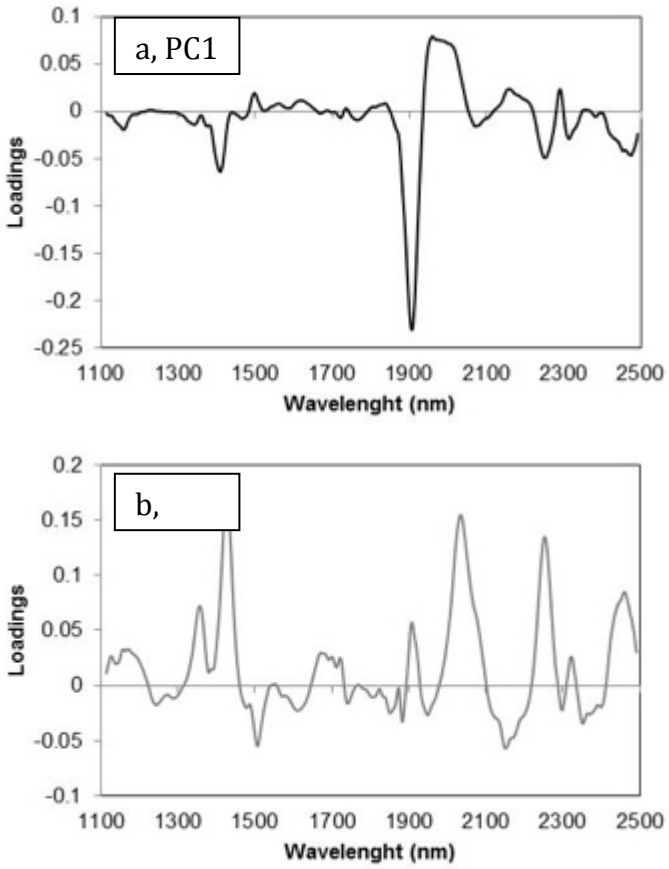

Figure 4 First two partial least square regression loadings (a= PC1, b=PC2) for the partial least square models developed to predict total non-structural carbohydrate concentration [NSC] using the Savitzky-Golay transformed near infrared spectrum collected on freeze dried and ground trunk samples .

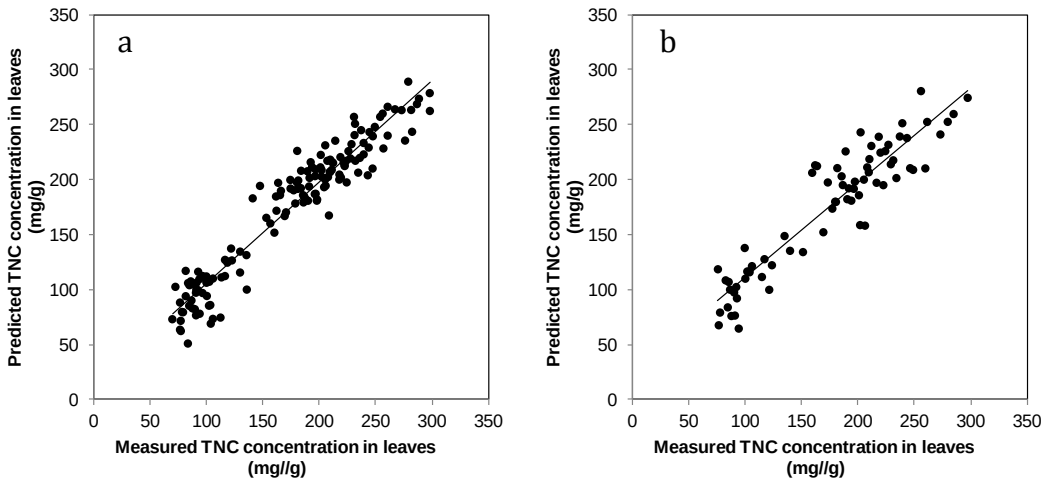

Figure 5 Comparison of the concentration of NSC (mg/g) determined by the anthrone method and the concentration predicted by NIR using PLS regression in leaf samples for both the calibration (a) and validation (b) data sets

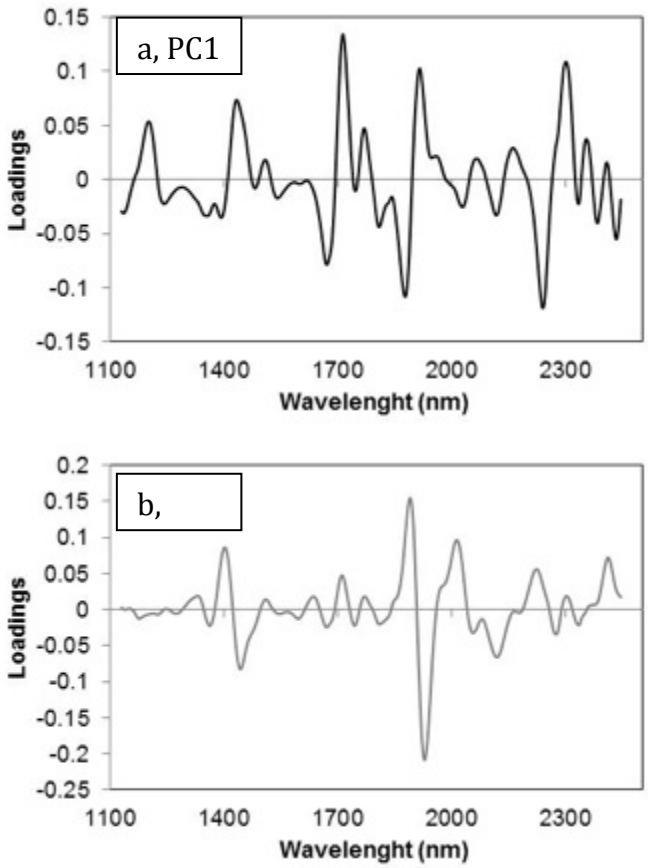

Figure 6 First two partial least square regression loadings (a= PC1, b=PC2) for the partial least square models developed to predict total non-structural carbohydrate concentration [NSC] using the Savitzky-Golay transformed near infrared spectrum collected on freeze dried and ground leaf samples

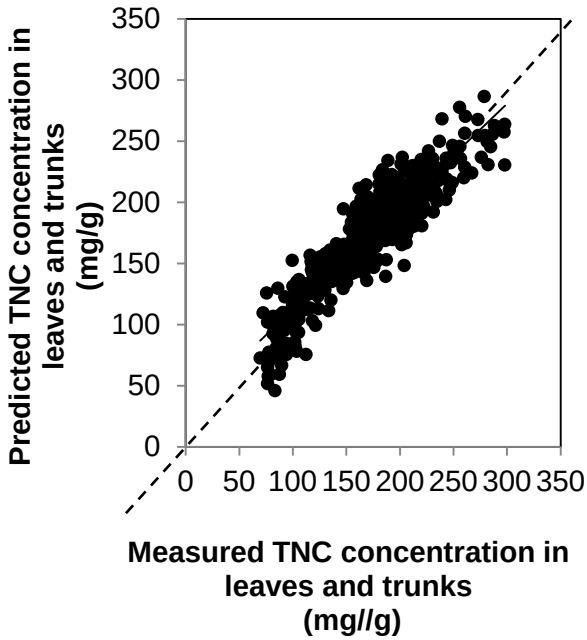

Figure 7 Near infrared predicted total non-structural carbohydrate concentration [NSC] versus measured concentrations obtained using the reference method proposed by Edwards et al. (2010) for freeze dried and ground leaf and trunk samples

Carbohydrate dynamics as affected by irrigation treatments

The high CV values obtained for [St] for the two datasets of tissue samples (leaf and trunk) could be attributed to both phenology and experimental design. According to (Holzapfel and Smith 2012), starch is the main form of CHO storage during the growing season while sugars decline rapidly after budburst. In this study, irrigation treatments were applied, therefore they are likely responsible for the changes in reserve capacity of the treated vines thus creating the high variability in the data set. Irrigation is often used as a practice to manipulate vine growth and photosynthetic capacity. (Holzapfel, et al. 2010) showed that regulated deficit irrigation reduced reserve starch in roots and wood tissues. The CV value was higher for the leaf samples and this could be attributed to higher and faster dynamics of remobilisation and usage according to water supply. Leaves [NSC] in particular can be influenced by the seasonal irrigation regime since it is dependent on the instantaneous photosynthetic processes happening in the leaf at the time of sampling and irrigation and/or water stress has a strong effect on the leaf transpiration and photosynthesis.

Spectral analysis and modelling

According to Table 5 the absorption bands observed in the spectra at 1450 and 1930 nm correspond to the OH first overtone and O-H stretch/HOH deformation combination respectively. These peaks are normally related to water but are also associated with starch and sugar (Curran 1989). The peaks at 2100 nm and 2280 nm are associated with C-O stretch combination and asymmetric C-O-O stretch third overtone. According to (Curran 1989) the absorption band at 2020 nm could be related to protein and nitrogen while at 2250 nm can be associated with both protein and starch. The extra absorption at 1700 nm in the leaf spectrum could be related to protein and nitrogen (Curran 1989). These spectral features are similar to those shown by other authors for other species (Richardson, et al. 2003). (Curran 1989) reported that similar wavelengths in the near infrared spectrum can be associated with different organic compounds since, for example, the O-H bond is present in multiple compounds such as water, cellulose, lignin, starch and sugar. Moreover, in the present study, since the tissues were freeze-dried, absorption by free water can be considered almost insignificant. Other authors have previously reported that on dried leaf material the absorption by free water was reduced (Curran, et al. 1992) and minor absorption peaks appear (Elvidge 1990). When the spectra are better resolved by the second derivative transformation, additional peaks became evident especially in the leaf tissues average spectrum. According to (Curran 1989), the peak at 1180 could be related to water but also cellulose and starch, while the other three minor absorption bands at 1500, 1700 and 2050 nm are likely to be associated with the presence of protein and nitrogen in the leaf material.

Table 5 Important absorption bands associated with starch and sugars as C-H and O-H related bands for the trunk and leaf samples (adapted from: Curran, 1989).

Calculated wavelength	Bond vibration	Functional grouping/Structure	Observed wavelength
Trunk samples			
1450	O-H stretch first overtone	Starch	1454
1930	O-H stretch/HOH deformation combination	Starch	1928
2100	O-H bend/C-O stretch combination Asym C-O-O stretch third overtone	Starch Starch or Cellulose	2106
2280	CH stretch/CH_2 deformation	Starch	2286
2300	C-H bend second overtone	Protein	2300
Leaf samples			
1215	C-H second overtone	CH_2	1208
1471	N-H stretch first overtone	CONHR	1468
1725	C-H stretch first overtone	CH_2	1728
1930	O-H stretch/HOH deformation combination	Starch	1936
2170	Asym CH-H stretch/ C-H deformation combination	HC= CH	2160
2310	C-H bend second overtone	Oil	2312

The best NIR models were obtained when the data set included samples representing the maximum variation of the parameter of interest and hence, the higher CV value. The CV value for the [Su] in trunk and leaf tissues was small and this could have affected the robustness of the calibrations. Since [NSC] is the sum of [St] and [Su], the resulting CV value for this parameter was large. According to the descriptive statistics and given the large CV values for [St] and [NSC] in the two data sets, these parameters were expected to produce more robust NIR calibrations while the variability in the [Su], especially for the leaf samples, was too small for the purpose of building a reliable calibration model. Another factor that could be causing the poor calibration for [Su] might be the error associated with the reference method. The reference method used in this study, proposed by (Edwards, et al. 2011), has been reported to overestimate the glucose by 10% in the trunk samples and up to 25% in leaves; the authors did not report the error for NSC.

The models for [St] prediction using the second derivative of the spectra showed the highest RPD values for both trunk and leaf samples. High RPD values are associated to models with higher prediction ability (Smyth, et al. 2008). It is generally recognised that RPD values greater than 3 are required in order to use the model for screening purposes (reference). In this study RPDs values higher than 3 were observed for all the models related to starch and NSC in leaves making them applicable for screening purposes. On the other hand, very low values were obtained for sugar prediction confirming the inadequacy of the available sugar dataset to build robust NIR models.

Considering the models developed for the prediction of [NSC] using the second derivative of the spectra, the SEP was 12.65 mg/g and 22.86 mg/g in trunks and leaves respectively. These errors could be considered acceptable if the benefits of using the NIR technique over the traditional method are taken into account. However, the reference method by (Edwards, et al. 2011) that was applied in this study has been reported to overestimate the glucose by 10% in the trunk

samples and up to 25% in leaves; the authors did not report the error for NSC. Nevertheless the authors in this same study discussed that this method is still acceptable when it is more important to know the difference between samples rather than having an absolute value.

For viticulture practices, the main objectives of knowing [NSC] are related to: i) determining the effect of particular treatments applied to the vines (such as irrigation, fertilisation, leaf removal or general canopy management), ii) compare varieties and growing regions and, on a larger scale, iii) study the effect of climate change (higher temperature, heat waves and increased atmospheric CO_2), on the vine reserves. In all these cases the knowledge of the relative variation of reserves is more important than the absolute value. Moreover, the NIR method more than halves the time required for the analysis and considering the potential of portability in the newly develop NIR instruments.

Conclusions

Results from this study showed that NIR can be used to predict starch and total non-structural carbohydrate concentration in freeze-dried and ground grapevine trunk and leaf tissues. Moreover it has been demonstrated that a robust universal model could be applied to the prediction of NSC in both leaves and trunks, making it a practical tool for a rapid screening of CHO concentration in grapevine tissues at given phenological stages.

The advantages of this method are the speed of the analysis (less than 30 seconds required for the spectrum to be collected) and the elimination of the use of chemical reagents. Models could be improved by calibrating against a reference method with a lesser error compared to the one that was used in this study.

More research needs to be conducted in order to apply the technique to intact samples so that the steps of freeze-drying and grinding the samples could be avoided/eliminated. Achieving the latter would enable using portable NIR spectroradiometers so that CHO concentration could be assessed in-field on both leaves and trunks. Monitoring the spatio-temporal distribution of CHO concentration in the vineyard will help growers in management decision making based on an objective plant measurement.

References

Cozzolino, D. (2009) Near Infrared Spectroscopy in Natural Products Analysis. Planta Medica 75, 746-756. doi: 10.1055/s-0028-1112220.

Cozzolino, D., R.G. Dambergs, L. Janik, W.U. Cynkar, and M. Gishen (2006) Analysis of grapes and wine by near infrared spectroscopy. Journal of near Infrared Spectroscopy 14, 279-289.

Cozzolino, D., M.B. Esler, R.G. Dambergs, W.U. Cynkar, D.R. Boehm, I.L. Francis, and M. Gishen (2004) Prediction of colour and pH in grapes using a diode array spectrophotometer (400-1100 nm). Journal of near Infrared Spectroscopy 12, 105-111.

Cozzolino, D., L. Liu, W.U. Cynkar, R.G. Dambergs, L. Janik, C.B. Colby, and M. Gishen (2007) Effect of temperature variation on the visible and near infrared spectra of wine and the consequences on the partial least square calibrations developed to measure chemical composition. Analytica Chimica Acta 588, 224-230. doi: 10.1016/j.aca.2007.01.079.

Curran, P.J. (1989) Remote-sensing of foliar chemistry. Remote Sensing of Environment 30, 271-278. doi: 10.1016/0034-4257(89)90069-2.

Curran, P.J., J.L. Dungan, B.A. Macler, S.E. Plummer, and D.L. Peterson (1992) Reflectance spectroscopy of fresh whole leaves for the estimation of chemical concentration. Remote Sensing of Environment 39, 153-166. doi: 10.1016/0034-4257(92)90133-5.

Dambergs, R.G., D. Cozzolino, W.U. Cynkar, L. Janik, and M. Gishen (2006) The determination of red grape quality parameters using the LOCAL algorithm. Journal of near Infrared Spectroscopy 14, 71-79.

De Bei, R., D. Cozzolino, W. Sullivan, W. Cynkar, S. Fuentes, R. Dambergs, J. Pech, and S. Tyerman (2011) Non-destructive measurement of grapevine water potential using near infrared spectroscopy. Australian Journal of Grape and Wine Research 17, 62-71. doi: 10.1111/j.1755-0238.2010.00117.x.

Dreywood, R. (1946) Qualitative test for carbohydrate material. Industrial and Engineering Chemistry-Analytical Edition 18, 499-499. doi: 10.1021/i560156a015.

Edwards, E.J., A.F. Downie, and P.R. Clingeleffer (2011) A Simple Microplate Assay to Quantify Nonstructural Carbohydrates of Grapevine Tissues. American Journal of Enology and Viticulture 62, 133-137. doi: 10.5344/ajev.2010.10051.

Elvidge, C.D. (1990) Visible and near-infrared reflectance characteristics of dry plant materials. International Journal of Remote Sensing 11, 1775-1795.

Gishen, M., R.G. Dambergs, and D. Cozzolino (2005) Grape and wine analysis - enhancing the power of spectroscopy with chemometrics. A review of some applications in the Australian wine industry. Australian Journal of Grape and Wine Research 11, 296-305. doi: 10.1111/j.1755-0238.2005.tb00029.x.

Holzapfel, B.P. and J.P. Smith (2012) Developmental Stage and Climatic Factors Impact More on Carbohydrate Reserve Dynamics of Shiraz than Cultural Practice. American Journal of Enology and Viticulture 63, 333-342. doi: 10.5344/ajev.2012.11071.

Holzapfel, B.P., J.P. Smith, S.K. Field, and W.J. Hardie (2010) Dynamics of carbohydrate reserves in cultivated grapevines. Horticultural Reviews 37, 143-211.

Murray, M. and J. Kurtz (1993) Near-infrared absorptions of monomethylhydrazine. Journal of Quantitative Spectroscopy & Radiative Transfer 50, 585-590. doi: 10.1016/0022-4073(93)90025-d.

Richardson, A.D., G.P. Berlyn, and S.P. Duigan (2003) Reflectance of Alaskan black spruce and white spruce foliage in relation to elevation and latitude. Tree Physiology 23, 537-544.

Schmidtke, L.M., J.P. Smith, M.C. Muller, and B.P. Holzapfel (2012) Rapid monitoring of grapevine reserves using ATR-FT-IR and chemometrics. Analytica Chimica Acta 732, 16-25. doi: 10.1016/j.aca.2011.10.055.

Smyth, H.E., D. Cozzolino, W.U. Cynkar, R.G. Dambergs, M. Sefton, and M. Gishen (2008) Near infrared spectroscopy as a rapid tool to measure volatile aroma compounds in Riesling wine: possibilities and limits. Analytical and Bioanalytical Chemistry 390, 1911-1916. doi: 10.1007/s00216-008-1940-0.

6.7 Non-destructive measurement of grapevine water potential using near infrared spectroscopy.

Non-destructive measurement of grapevine water potential using near infrared spectroscopy

R. DE BEI[1], D. COZZOLINO[2], W. SULLIVAN[1], W. CYNKAR[2], S. FUENTES[1], R. DAMBERGS[2], J. PECH[4] and S. TYERMAN[1]

[1] The University of Adelaide, School of Agriculture, Food and Wine, Plant Research Centre, Waite Campus, Glen Osmond, SA 5064, Australia
[2] The Australian Wine Research Institute. Waite Road, Urrbrae. PO Box 197, Glen Osmond, SA 5064, Australia
[3] The Australian Wine Research Institute, Tasmanian Institute of Agricultural Research, University of Tasmania, Private Bag 98, Hobart, Tasmania, 7001, Australia
[4] South Australian Research and Development Institute (SARDI), GPO Box 397, Adelaide SA 5001, Australia
Corresponding author: Professor Stephen D. Tyerman, fax +61 8 8313 0431, email steve.tyerman@adelaide.edu.au

Abstract

Background and Aims: Near infrared (NIR) spectroscopy techniques are not only used for a variety of physical and chemical analyses in the food industry, but also in remote sensing studies as tools to predict plant water status. In this study, NIR spectroscopy was evaluated as a method to estimate water potential of grapevines.

Methods and Results: Cabernet Sauvignon, Chardonnay and Shiraz leaves were scanned using an Integrated Spectronic (300–1100 nm) or an ASD FieldSpec® 3 (Analytical Spectral Devices, Boulder, Colorado, USA) (350–1850 nm) spectrophotometer and then measured to obtain midday leaf water potential using a pressure chamber. On the same shoot, the leaf adjacent the one used for midday leaf water potential measurement was used to measure midday stem water potential. Calibrations were built and NIR showed good prediction ability (standard error in cross validation (SECV) <0.24 MPa) for stem water potential for each of the three grapevine varieties. The best calibration was obtained for the prediction of stem water potential in Shiraz ($R = 0.92$ and a SECV = 0.09 MPa).

Conclusion: Differences in the NIR spectra were related to the leaf surface from which the spectra were collected, and this had an effect on the accuracy of the calibration results for water potential. We demonstrated that NIR can be used as a simple and rapid method to detect grapevine water status.

Significance of the Study: Grapevine water potential can be measured using NIR spectroscopy. The advantages of this new approach are speed and low cost of analysis. It may be possible for NIR to be used as a non-destructive, in-field tool for irrigation scheduling.

Abbreviations

Ψ_{leaf} midday leaf water potential; Ψ_{stem} midday stem water potential; **g** leaf conductance; **NIR** near infrared; **PC** principal component; **PCA** principal component analysis; **PLS** partial least squares regression; **PRESS** prediction residual error sum of squares; **R** coefficient of correlation; **RWC** relative water content; **SECV** standard error in cross validation; **SD** standard deviation; **WUE** water use efficiency.

Keywords: abaxial, adaxial, NIR, optical property

Introduction

The amount of water available for irrigation is declining worldwide because of a quantitative and qualitative deterioration of water resources (Eastham and Gray 1998). The Australian wine industry, in particular, is facing an unprecedented challenge to maintain international competitiveness in the current drought. The increasing shortages of water and costs of irrigation are leading to an emphasis on the development of new methods of irrigation and irrigation scheduling that minimise water use and maximise water use efficiency (WUE) (Jones 2004). According to Al-Kaisi and Yin (2003) WUE maximisation should be considered as a key subject for research because of water scarcity issues. Grapevines are an intensive crop in semi-arid regions, so irrigation would be more effective if scheduled appropriately and if dosages and timing are applied to maximise WUE. In order to achieve this, the crop water status must be monitored accurately and reliably (Jones 2007).

Irrigation scheduling in vineyards is conventionally based on direct measures of soil moisture status and/or on soil water balance calculations (Jones 2004, 2007). Soil water measurements rely on the availability of many commercial systems and are relatively easy to apply; however, these approaches are prone to cumulative errors, require many sensors and may not be representative because of soil heterogeneity (Jones 2004). Alternative approaches are based on the physiological knowledge of grapevine response to water stress, thus sensing the plant response to water deficits rather than sensing the soil moisture status directly.

doi: 10.1111/j.1755-0238.2010.00117.x
© 2010 Australian Society of Viticulture and Oenology Inc.

The most common direct sensing methods are the measures of midday leaf water potential (Ψ_{leaf}), and leaf conductance to water vapor (g) largely dependent on stomatal conductance (Flexas et al. 2010). The pressure chamber technique of measuring Ψ_{leaf}, which is a destructive method, has been assessed in several cases for grapevine as a relatively simple and rapid measurement (Naor et al. 1997, Trégoat et al. 2002, Williams and Araujo 2002, Sibille et al. 2007). A good correlation between Ψ_{leaf} and g has been found for many grapevine varieties, but not for those showing near-isohydric behaviour (Schultz 2003, Cifre et al. 2005). This may reduce the utility of Ψ_{leaf} as an indicator of water stress for the latter varieties (Cifre et al. 2005).

Leaf water status within a canopy is variable because it depends on the transpiration rate that a particular leaf has at the moment of measurement (Choné et al. 2001). As a partial solution to this variability, the measurement of midday stem water potential (Ψ_{stem}) was proposed because it is a more integrative indicator of whole-vine water status (Choné et al. 2001). Nevertheless, traditional methods for measuring Ψ_{stem} require destructive sampling and pretreatment for up to 1 h.

Near infrared (NIR) spectroscopy has been used as a non-destructive method to analyse components of several agricultural products (Osborne et al. 1993, Batten 1998, Cozzolino et al. 2006). The NIR region of the electromagnetic spectrum (730–2300 nm) contains several wavelengths that are strongly influenced by the presence of water, and the state of water in the measured sample. The NIR spectral region is dominated by weak overtones and combinations of vibration bands from molecular bonds of hydrogen attached to atoms such as nitrogen, oxygen and carbon (Murray 1993, Batten 1998). Strong NIR absorption bands of water are found around 1400–1440 nm and between 1900 to 1950 nm and have often been applied to quantitative analysis of water content in food (Murray 1993, Batten 1998, Williams 2001, Büning-Pfaue 2003, Cozzolino et al. 2006).

Wavelength bands related to water have also been utilised in NIR reflectance with remote sensing applications to determine water content and water status of plants (Hunt et al. 1987, Bowman 1989, Hunt and Rock 1989, Peñuelas et al. 1993, 1997a,b, Ceccato et al. 2001, Maki et al. 2004). Recently, Santos and Kaye (2009) attempted to use NIR spectroscopy to assess Ψ_{leaf} in grapevines. However, their measurements of Ψ_{leaf} using the pressure chamber (Boyer 1967) were not made in the field at the time of the NIR measurements in some experiments, potentially compromising the accuracy of Ψ_{leaf} determinations. Nevertheless, in a laboratory experiment, they obtained good calibrations ($R = 0.84$) for the prediction of Ψ_{leaf} in Cabernet Sauvignon and Thompson Seedless. Rodríguez-Pérez et al. (2007) obtained significant correlations for Ψ_{stem} and Ψ_{stem}-$\Psi_{pre\text{-}dawn}$ for grapevines using the ratio of leaf reflectance at specific wavelengths when measured at the canopy level, but correlation coefficients were generally low. They asserted that measurements of leaf reflectance may provide a better approach to standardise water status measurement for specific grapevine varieties and they identified several vegetation indices that may be useful for remote sensing of grapevine water stress.

In NIR spectroscopy, calibration is a key mathematical process, which uses multivariate regression techniques relating NIR optical measurements (absorbance values) at selected wavelengths to reference values measured by conventional chemical or physical methods (Murray 1993, Batten 1998, Williams 2001). Once calibrated, the advantages of NIR spectroscopy are the speed of the analysis, simplicity in sample preparation, multiplicity of analysis, and the non-requirement for the use of chemical reagents (Murray 1993, Batten 1998, Williams 2001). In contrast, water potential measurements can be restrictive, because they are slow, labour intensive, and are therefore expensive (Jones 2004).

This study reports the results of a multivariate analysis of the NIR absorption spectrum and physiological measures of water potential in pot and field grown Shiraz, Cabernet Sauvignon and Chardonnay grapevines.

Materials and methods

Field experiment 1 – Cabernet Sauvignon and Shiraz

The experiment was carried out in the Coombe vineyard at the Waite Campus of the University of Adelaide, South Australia (34°58'3.47"S; 138°38'0.43"E), during the season 2006–07. Measurements were made on own-rooted Cabernet Sauvignon and Shiraz vines, planted in 1991 with a vine spacing of 1.8 m in the row and 3 m between rows. Rows were oriented North-South. The training system was a bilateral spur-pruned cordon with the shoots vertically positioned. Vines were drip irrigated by in-line drippers discharging 1.5 L/h. Drippers spacing within the row was 0.8 m. Six plants for each variety were selected and Ψ_{leaf}, Ψ_{stem} and g were measured on six occasions for Cabernet Sauvignon and eight occasions for Shiraz, at approximately 7-day intervals, from February to March 2007. A Scholander pressure chamber (Scholander et al. 1965) was used to measure Ψ_{leaf} as described by Meron et al. (1987). Measurements were made at midday (1200 to 1400 hours, solar time) on two fully expanded and undamaged leaves for each plant chosen from the mid-upper part of the canopy. One leaf was collected from the midday sunlit side of the canopy and one from the shadowed side. Measurements on both the sunlit and shaded sides of the canopy were used to build the calibration. No leaves from secondary shoots were used. Ψ_{stem} was measured immediately after Ψ_{leaf} on the same shoot using the leaf below the one used to measure Ψ_{leaf}. For Ψ_{stem} measurements, leaves were covered for 60 min with a ziplock aluminium foil-coated plastic bag before the measure, in order to allow Ψ_{leaf} to equilibrate with Ψ_{stem} (Begg and Turner 1970). After the equilibration period, the leaves were cut and Ψ_{stem} was measured following the same procedure already described for Ψ_{leaf}. A maximum of 30 s elapsed between cutting the leaves and the measurements. The same pressure chamber operator did all measurements with the objective of normalising interpretation of the moment that sap emerges from the petiole. Leaf conductance (g) was measured using a diffusion porometer (AP4, Delta-T Devices, Cambridge, UK) before the leaf was cut for Ψ_{leaf} measurement.

A reflectance spectrum was acquired on the adaxial surface using the same leaf where g and Ψ_{leaf} were measured. The time elapsed between the spectra acquisition and the water potential measurements was about 30 s for Ψ_{leaf}, and 120 s for Ψ_{stem}. No spectra were acquired from the leaf used for Ψ_{stem} measurement. The spectrophotometer (custom made, Integrated Spectronics, Sydney, Australia) was equipped with a 10 W halogen lamp as the light source and a silicon diode array detector able to collect spectra from the visible and NIR regions of the spectrum to give a total range of 300 to 1100 nm at 3.2 nm wavelength resolution, producing a total of 220 data points. Leaf samples were placed in front of the lens (diameter approximately 40 mm) for scanning. A spectrally black surface was put on the underside of the leaf to minimise differences in background reflectance. Lab View software (Version 5.1, National Instruments, Austin, Texas, USA) was used to control the spectrophotometer and to acquire the NIR spectra.

© 2010 Australian Society of Viticulture and Oenology Inc.

Field experiment 2 – Chardonnay

The experiment was carried out during January (7th–8th) and February (12th) 2009 in a commercial Chardonnay vineyard at Qualco, South Australia (34°6′0.76″S; 139°50′55.76″E). The vines were 5 years old and grafted on Ramsey rootstock. The vines were trained on a two-wire vertical trellis system with a row spacing of 1.8 m between vines and 3.05 m between rows. Five irrigation strategies were used for this study: full irrigation (Control), and reductions to 50, 30, 20 and 10% of the control. The control treatment represented the amount of water that is normally applied in the vineyard (5 ML/ha/year). The trial was a randomised block design with four blocks and was established in 60 rows made of 90 vines each, covering a total area of 3.69 ha. In the block, each treatment was made of three rows and the rows were divided in three sections of 30 plants each. In the middle row of each treatment, the middle plant in each section was selected for measurements.

All treatments were irrigated with Netafim Dripmaster® (Netafim Australia, Laverton North, Australia) pressure compensated in-line drippers, spaced 0.5 m apart along the drip line and discharging 2.3 L/h. All irrigation events to the Control were scheduled to apply 6 mm using the Irrigated Crop Management Service (ICMS) Water Budgeting Tool (Irrigated Crop Management Service (2007) ICMS Water Budgeting Tool. http://www.pir.sa.gov.au/pirsa/drought/irrigation__and__water_management/irrigators_toolkit; 03/04/2010). To apply the reductions in irrigation volume, the interval between irrigations was increased.

Determinations of water potentials were performed with a pressure chamber on two leaves from each of the three vines per plot. Ψ_{leaf} and Ψ_{stem} measurements were made at midday (1200 to 1400 hours, solar time) using the method previously described. Ψ_{stem} was measured immediately after the Ψ_{leaf} on the same shoot using the leaf below the one used to measure Ψ_{leaf}. Diffuse reflectance spectra were acquired from both leaf surfaces (adaxial and abaxial) on the same leaves before Ψ_{leaf} was determined. No spectra were acquired from the leaf used for Ψ_{stem} measurement. The diffuse reflectance spectra of the leaf surfaces were recorded using a purpose-built contact probe attached by fibre optic cable to a spectrophotometer (ASD FieldSpec® 3, Analytical Spectral Devices, Boulder, Colorado, USA). The time elapsed between the spectra acquisition and the water potential measurements was about 30 s for Ψ_{leaf} and 120 s for Ψ_{stem}. The instrument records spectra with resolution of 1.4 nm for the region 350–1000 nm and 2 nm for the region 1000–1850 nm. The instrument was used in reflectance mode. The data processing software associated with the ASD spectrophotometer interpolates the 1.4 and 2 nm-spaced data to produce 1 nm-spaced data. The saved spectrum of each sample was the average of ten successive scans. A reference tile (Spectralon®, Analytical Spectral Devices, Boulder, Colorado, USA) was used as a white reference, for scatter correction. Software RS$_3$™ (Analytical Spectral Devices, Boulder, Colorado, USA) was used to control the spectrophotometer and to acquire the NIR spectra.

Glasshouse experiment

The experiment was carried out in a glasshouse at the Waite Campus of the University of Adelaide, South Australia (34°58′3.47″S; 138°38′0.43″E), during May and September 2009, on pot-grown Cabernet Sauvignon and Shiraz vines. The water potential measurements were conducted on ten plants per variety. The same 20 plants were measured in four occasions in May and five occasions in September at about 7-day intervals. One shoot for each plant was chosen and Ψ_{leaf} was measured on a fully expanded leaf using a pressure chamber as described before. The adjacent leaf was bagged for 1 h prior to measurement and Ψ_{stem} was measured immediately after Ψ_{leaf} as previously described. Six NIR spectra were acquired for each leaf on six different positions evenly distributed over the abaxial leaf surface; two distal along the mid vein and four proximal (two on each half of the leaf, halfway between the mid vein and leaf margin) using the ASD spectrophotometer. No spectra were acquired from the leaf used for Ψ_{stem} measurement. The time elapsed between the spectra acquisition and the water potential measurements was about 30 s for Ψ_{leaf} and 120 s for Ψ_{stem}.

Data analysis and interpretation

Spectral and associated laboratory reference data were exported to The Unscrambler® software (version 9.2 CAMO, Oslo, Norway) for chemometric analysis and calibration development. Principal component analysis (PCA) was used to examine any relevant and interpretable pattern in the data (Otto 1999, Naes et al. 2002). PCA was also used to explore the spectral data set for outliers. Calibration models were developed using partial least squares regression (PLS) with full cross validation. The NIR region 750–1050 nm was used to develop the calibration with the spectra obtained from the Integrated Spectronics spectrophotometer while for the ASD FieldSpec® 3 the range 1100–1830 nm was selected. The cross validation was performed using six segments, with 19 samples for each segment. The coefficients of correlation in validation (R) and the standard error in cross validation (SECV) were calculated. The optimum number of terms in the PLS calibration models was determined as indicated by the lowest number of factors that gave the closest to minimum value of the PRESS (prediction residual error sum of squares) function in cross validation, in order to avoid over fitting of the models (Naes et al. 2002).

Water potential and g data collected from the Chardonnay field experiment were analysed using analysis of variance (ANOVA) with Cohort Costat software (Version 6.2, CoHort Software, Monterey, CA, USA). Mean separations were determined using the Student-Newman-Keuls test.

Results

Spectra interpretation

Figure 1 shows averaged NIR spectra obtained during the 2006–07 season with the Integrated Spectronic spectrophotometer from the adaxial surface of leaves of field grown Cabernet

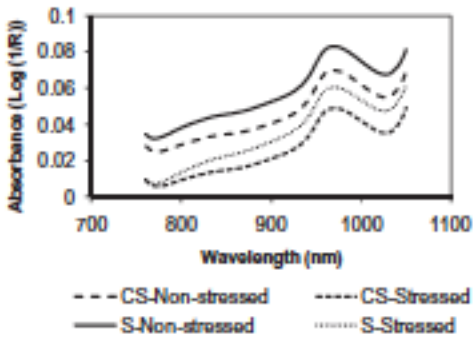

Figure 1. Near infrared spectra collected from Shiraz (S) and Cabernet Sauvignon (CS) leaves of stressed ($\Psi_{stem} < -1.2$ MPa) and non-stressed ($\Psi_{stem} > -1$ MPa) plants. Spectra were taken from the adaxial leaf surface using the Integrated Spectronic spectrophotometer during the season 2006–07. *R*, reflectance.

Sauvignon and Shiraz vines under non water stressed (Ψ_{stem} > –1 MPa) and water stressed (Ψ_{stem} < –1.2 MPa) conditions (Lampinen et al. 2001, Trégoat et al. 2002, Williams and Araujo 2002, Ferreyra et al. 2003, Cifre et al. 2005, Sibille et al. 2007). The main features of the spectra are absorption bands in the 970 nm region. Non-stressed vine leaves showed a higher absorbance in the whole spectrum compared with the stressed vines for both varieties.

The spectra collected with the ASD spectrophotometer from the adaxial and abaxial surfaces of stressed (Ψ_{stem} < –1.2 MPa) and non-stressed (Ψ_{stem} > –1 MPa) Chardonnay leaves (Figure 2a,b), show absorption bands in the region between 1400–1450 nm. Overall, leaves of non-stressed plants gave a higher absorbance in the whole spectrum (1100–1830 nm) compared with stressed plants (Figure 2a). Interpretation of the average spectra of adaxial and abaxial surfaces of the leaves at 1445 nm showed a higher absorbance in the adaxial (0.83 a.u.) compared with the abaxial (0.75 a.u.) (Figure 2b).

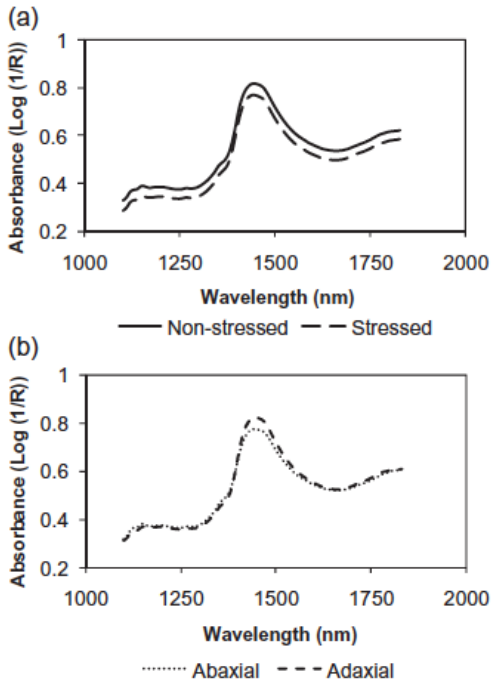

Figure 2. Near infrared spectra of leaves taken from stressed (Ψ_{stem} < –1.2 MPa) and non-stressed (Ψ_{stem} > –1 MPa) (a) and from the adaxial and abaxial leaf surface (b) of Chardonnay vines using the ASD FieldSpec ® 3 spectrophotometer during the 2008–09 season. *R*, reflectance.

NIR calibrations

Cabernet Sauvignon and Shiraz. Table 1 shows the NIR calibration statistics for the prediction of Ψ_{leaf}, Ψ_{stem} and g of grapevine leaves obtained using the samples from the 2006–07 season. The R obtained for the prediction of Ψ_{stem} using NIR was 0.87 (SECV = 0.23 MPa) for Cabernet Sauvignon and 0.67 (SECV = 0.11 MPa) for Shiraz. The NIR calibrations for Ψ_{leaf} yielded an $R = 0.74$ (SECV = 0.29 MPa) for Cabernet Sauvignon; however, a poor correlation ($R = 0.24$; SECV = 0.19 MPa) was found for Shiraz. The poorest calibration statistics were found for NIR and g in both varieties.

When all field samples of Cabernet Sauvignon and Shiraz were used to develop a global calibration for the prediction of Ψ_{stem}, the obtained correlation coefficient was 0.84 and a low SECV (0.18 MPa) was observed (Figure 3).

Chardonnay. The descriptive statistics for water potential measurements conducted on the commercial Chardonnay vineyard showed significant differences between irrigation treatments (Table 2). Based on Ψ_{stem} values, it was observed that plants experienced water deficits in January, but not in February, mostly because of the hot weather conditions in the first month (maximum temperatures: 7 January, 40.7°C, 12 February, 24.5°C). Moreover, in February, the measurements were made on a day when the irrigation was turned on and this could have influenced the measurements.

Control plants presented the highest water potentials in both months. The Ψ_{stem} measurements showed the biggest differences between treatments. In January, only the 10% treatment exceeded a Ψ_{stem} of –1.2 MPa, which was considered indicative of water stress. The 30 and 20% treatments reached a Ψ_{stem} lower than –1 MPa, meaning that those plants were experiencing moderate water restrictions (Lampinen et al. 2001, Trégoat et al. 2002, Williams and Araujo 2002, Ferreyra et al. 2003, Cifre et al. 2005, Sibille et al. 2007). In February, Ψ_{stem}

Table 1. Calibration statistics for midday stem water potential (Ψ_{stem}), midday leaf water potential (Ψ_{leaf}), and leaf conductance (g) calibrations prepared with NIR spectra collected on the adaxial surfaces of fully expanded attached leaves of field grown Cabernet Sauvignon and Shiraz vines.

	n	SD (MPa)	Range (MPa)	SECV (MPa)	R
Ψ_{stem} calibration					
Cabernet Sauvignon	84	0.29	–0.72, –1.65	0.23	0.87
Shiraz	71	0.14	–0.93, –1.52	0.11	0.67
Ψ_{leaf} calibration					
Cabernet Sauvignon	84	0.30	–0.9, –2.13	0.29	0.74
Shiraz	71	0.19	–0.51, –1.92	0.19	0.24
g_s calibration					
Cabernet Sauvignon	84	49.3	18–286	31.7	0.58
Shiraz	71	81.2	27–375	78.7	0.18

Data were obtained during the season 2006–07. *n*, number of samples used in calibration; R, coefficient of correlation; SD, standard deviation; SECV, standard error of cross validation.

© 2010 Australian Society of Viticulture and Oenology Inc.

differences between treatments were small. Only the 10% treatment was significantly different from the rest, and did not represent a water stress level for the plants.

The g was measured in January and results show only significant differences between the control and the rest of treatments, which is in contrast with the significant differences observed for Ψ_{stem} among treatments (Table 2).

Table 3 summarises the NIR calibration statistics obtained for the prediction of water potentials in Chardonnay. Similar correlation coefficients were obtained for both Ψ_{leaf} ($R = 0.67$; SECV = 0.26 MPa) and Ψ_{stem} ($R = 0.67$; SECV = 0.24 MPa) when spectra were collected on the adaxial leaf surface.

Effect of adaxial and abaxial leaf surface on the NIR spectra. A visual analysis of the score plot of the second and third principal components (PCs) of the leaf samples analysed using NIR spectroscopy (Figure 4) reveals a clear separation between the two leaf surfaces. The cluster or separation indicates differences in the NIR spectra between the two sides of a leaf. The first three PCs explain more than 95% of the variation in the NIR spectra related to surface. Overall, similar loading weights were observed for the calibrations built using the adaxial surface, with a dominant peak at 1415 nm corresponding to that expected for water. Similarly, the calibration for the prediction of Ψ_{leaf} using the abaxial leaf surface showed a dominant peak at 1415 nm. In contrast, the calibration for Ψ_{stem} using the abaxial surface had a less dominant negative peak at 1418 nm and a more even distribution of the loading weights with wavelength (Figure 5).

Table 3 shows the NIR calibration statistics for the water potential of Chardonnay grapevine leaves obtained from the abaxial leaf surface. The R for Ψ_{stem} was 0.84 (SECV 0.18 MPa), a poorer calibration was obtained for Ψ_{leaf} ($R = 0.80$, SECV 0.21 MPa). The best calibration was between NIR spectra collected from the abaxial surface and Ψ_{stem}.

Glasshouse experiment. The calibrations built for Ψ_{stem} and Ψ_{leaf}, when more than one spectrum was collected for each Shiraz leaf, yielded the same and high correlation coefficient ($R = 0.92$) and low SECV (0.09 MPa for Ψ_{stem} and 0.11 MPa for Ψ_{leaf}) (Table 4). Similarly, for Cabernet Sauvignon, no differences were observed between the R in the two calibrations but

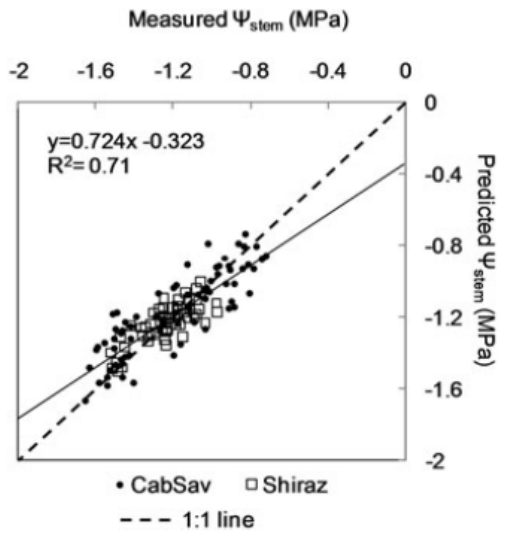

Figure 3. Near infrared predicted midday stem water potential (Ψ_{stem}) versus reference data obtained using a pressure chamber in Cabernet Sauvignon and Shiraz vines during the field experiment using cross validation. The measurements from both varieties were used to generate a global calibration. *n* (number of samples used in calibration) = 127, *R* (coefficient of correlation) = 0.84, SECV (standard error in cross validation) = 0.18 MPa.

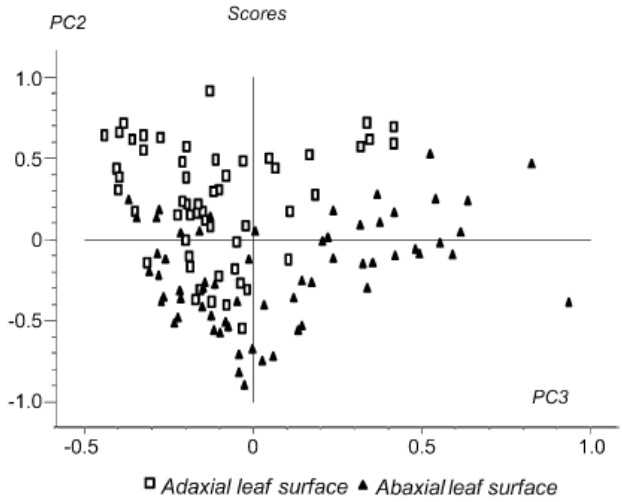

Figure 4. Score plot of the second and third principal components (PCs) of the near infrared spectra collected from the adaxial (□) and abaxial (▲) leaf surfaces of Chardonnay vines during the season 2008–09.

Table 2. Midday leaf water potential (Ψ_{leaf}), midday stem water potential (Ψ_{stem}) and leaf conductance (g) measured in a commercial Chardonnay vineyard with five irrigation treatments: control (fully irrigated), and 50, 30, 20 and 10% of the control.

Treatment	7–8 January			12 February	
	Ψ_{stem}(MPa)	Ψ_{leaf}(MPa)	g(mmol m^{-2} s^{-1})	Ψ_{stem}(MPa)	Ψ_{leaf}(MPa)
Control	–0.59^{a}	–0.90^{a}	353.08^{a}	–0.44^{a}	–0.59^{a}
50%	–0.96^{ab}	–1.24^{b}	230.92^{b}	–0.62^{b}	–0.67^{a}
30%	–1.07^{b}	–1.32^{b}	217.33^{b}	–0.57^{ab}	–0.67^{a}
20%	–1.14^{c}	–1.44^{c}	231.42^{b}	–0.54^{ab}	–0.66^{a}
10%	–1.27^{d}	–1.49^{c}	199.88^{b}	–0.94^{c}	–1.05^{b}

Measurements were made on the 7–8 January and 12 February 2009. Means followed by different letters are different at $P \leq 0.05$ (Newman-Keuls test).

© 2010 Australian Society of Viticulture and Oenology Inc.

this variety yielded lower R and lower SECV compared with Shiraz. Results in Table 4 show that all the calibrations built with only one random spectrum per leaf had a lower R and a higher SECV compared with those obtained including multiple spectra in the analysis. Moreover, better calibrations were obtained for Ψ_{stem} compared with Ψ_{leaf} for one spectrum per leaf.

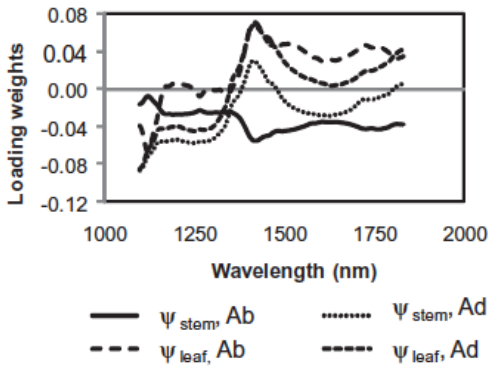

Figure 5. The first partial least square regression loading weights for the four calibrations performed in Chardonnay using leaf and stem water potential (Ψ_{leaf} and Ψ_{stem}) and the adaxial (Ad) and abaxial (Ab) leaf surfaces, during the season 2008–09.

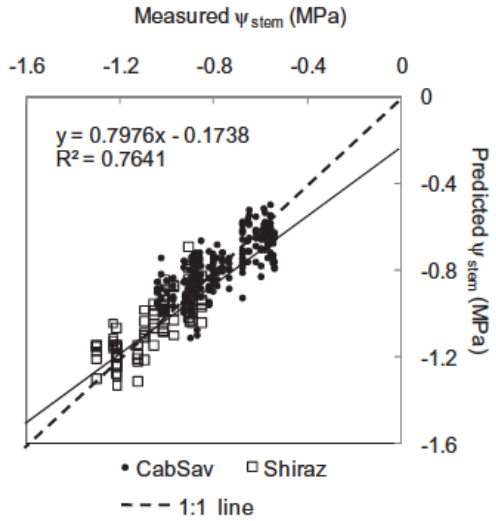

Figure 6. Near infrared predicted midday stem water potential (Ψ_{stem}) versus reference data obtained using a pressure chamber in Cabernet Sauvignon and Shiraz vines during the glasshouse experiment using cross validation. The measurements from both varieties were used to generate a global calibration. *n* (number of samples used in calibration) = 306, *R* (coefficient of correlation) = 0.87, SECV (standard error in cross validation) = 0.1 MPa.

Table 3. Calibration statistics for stem water potential (Ψ_{stem}) and leaf water potential (Ψ_{leaf}) calibrations prepared with near infrared spectra collected on the adaxial and abaxial surfaces of fully expanded attached leaves of field grown Chardonnay vines, during the season 2008–09.

	n	SD (MPa)	Range (MPa)	SECV (MPa)	R
Ψ_{stem} calibration					
Adaxial leaf surface	102	0.32	–0.25, –1.56	0.24	0.67
Abaxial leaf surface	102	0.32	–0.25, –1.56	0.18	0.84
Ψ_{leaf} calibration					
Adaxial leaf surface	101	0.35	–0.35, –1.8	0.26	0.67
Abaxial leaf surface	102	0.35	–0.35, –1.8	0.21	0.80

n, number of samples used in calibration; R, coefficient of correlation; SD, standard deviation; SECV, standard error of cross validation.

Table 4. Calibration statistics for stem water potential (Ψ_{stem}) and leaf water potential (Ψ_{leaf}) calibrations prepared with near infrared spectra collected on six spots and one spot (spot size 20 mm^2) on the abaxial surface of fully expanded attached leaves of potted Cabernet Sauvignon and Shiraz vines.

	SD (MPa)	Range (MPa)	Six spectra/leaf			One spectrum/leaf		
			n	SECV (MPa)	R	*n*	SECV (MPa)	R
Ψ_{stem} calibration								
Cabernet Sauvignon	0.15	–0.54, –1.05	419	0.08	0.83	72	0.10	0.73
Shiraz	0.22	–0.48, –1.15	385	0.09	0.92	107	0.10	0.88
Ψ_{leaf} calibration								
Cabernet Sauvignon	0.14	–0.69, –1.20	415	0.07	0.84	72	0.11	0.66
Shiraz	0.29	–0.45, –1.55	386	0.11	0.92	107	0.14	0.86

n, number of samples used in calibration; R, coefficient of correlation; SD, standard deviation; SECV, standard error of cross validation.

© 2010 Australian Society of Viticulture and Oenology Inc.

When all glasshouse samples of Cabernet Sauvignon and Shiraz were used to develop a global calibration for the prediction of Ψ_{stem}, a high correlation coefficient ($R = 0.87$) and a low SECV (0.1 MPa) were observed (Figure 6).

Discussion

NIR reflectance spectroscopy may be used to predict Ψ_{stem} and Ψ_{leaf} in grapevine because we have demonstrated that regions of the NIR spectrum are highly correlated with the water potential in three varieties of *Vitis vinifera* L. using different NIR spectrophotometers and over different ranges of wavelengths. A higher absorbance in the whole NIR spectrum was consistently associated with non-stressed vine leaves for the three varieties, with both types of spectrophotometers used. Peñuelas and Inoue (1999) observed an increase in the reflectance at all wavelengths with decreasing leaf water content in peanut and wheat leaves. These observations are in general agreement with previous studies showing that the NIR reflectance of a dried leaf is greater than that of a fresh leaf at all wavelengths (Thomas et al. 1966, Knipling 1970, Woolley 1971, Gausman 1974, Peñuelas et al. 1994, Jones et al. 2004). It is well known that water is a strong absorber in the NIR region of the electromagnetic spectrum, therefore non-stressed plants will have higher absorbance values in the NIR spectrum compared with stressed plants.

According to Carter (1991), when scanning single leaves, the water absorption bands that show the highest sensitivity to leaf water concentration are those in the 1300–2500 nm range. Peñuelas et al. (1993, 1997b) and Peñuelas and Filella (1998) showed that the weaker water absorption band between 950 and 970 nm is also effective and they defined a water index, initially as the ratio between the reflectance at 970 nm and that at 900 nm (R970/R900) (Peñuelas et al. 1993) and later as the inverse (R900/R970) (Peñuelas et al. 1997b). The latter ratio was highly correlated with the plant relative water content (RWC) in several trees, shrubs, crops and grasses. Combinations of wavelength bands sensitive to water (760, 970, 1450 and 1940 nm) have been used to generate other indices related to plant water status and soil water availability (Thomas et al. 1971, Hunt and Rock 1989, Danson et al. 1992, Mogensen et al. 1996, Bahrun et al. 2003, Rodríguez-Pérez et al. 2007). Some of these indices have been used to estimate crop water status (Peñuelas et al. 1993, 1997b, Jones et al. 2004, Rodríguez-Pérez et al. 2007) and in remote sensing studies aimed to asses vineyard conditions (Tucker 1980, Broge and Leblanc 2001, Zarco-Tejada et al. 2005a,b). Furthermore, Eitel et al. (2006) found a correlation ($r^2 = 0.34$) between Ψ_{leaf} and their proposed maximum difference water index (MDWI) when spectra were collected at leaf level for poplar trees. They defined MDWI as the spectral response at the leaf level to water status calculated from the maximum and minimum reflectance located between 1500 and 1750 nm.

In this study, spectra were obtained at the leaf level and it was found that the most relevant water absorption peaks were in the regions of 970 and 1400–1450 nm for the Integrated Spectronics and the ASD FieldSpec® 3 spectrophotometers, respectively. The absorption bands at 970 nm are related to the second overtone of the O-H stretch vibration of water (Murray 1986, Osborne et al. 1993, Williams 2001). Bands in the 1400–1450 nm are related to the first overtone of the OH stretch of water (Murray 1986, Osborne et al. 1993, Williams 2001). According to Eitel et al. (2006) the advantage of taking spectra at the leaf level is that the effect of background variables or atmospheric noise is eliminated so that variations in the spectra are only caused by leaf properties. However, we did not find correlations between Ψ_{leaf} or Ψ_{stem} and some of the above mentioned indices (WI, MDWI) (data not shown). Nevertheless, water potential was used in this study rather than other measures related to plant water status, such as the RWC and equivalent water thickness (EWT), which is the hypothetical thickness of a single layer of water averaged over the whole leaf (Danson et al. 1992). Water potential provides information about the water status of the plant and the soil as an integrated soil–plant-atmosphere system (Kozlowski et al. 1991), compared with RWC and EWT, which may vary with cell elasticity and leaf development for equivalent water potentials. In this study, rather than using any specific wavelength, a multivariate analysis of the whole spectrum in the range 1100–1830 nm was used to build the calibrations. Previously, Santos and Kaye (2009) obtained good calibrations for the prediction of Ψ_{leaf} in Cabernet Sauvignon and Thompson Seedless in a laboratory experiment, using the whole spectral range 1100–2300 nm. Therefore, the higher correlations obtained in this study and by Santos and Kaye (2009) compared with those obtained by Rodríguez-Pérez et al. (2007) using various vegetation indices ($0.55 < R < 0.67$), might be related to: (i) the use of a larger range of wavelengths rather than ratios of specific wavelengths; (ii) including regions known to be related to water content, and (iii) the collection of spectra at the leaf level instead of the canopy level.

As suggested by Eitel et al. (2006), variations in leaf properties are influenced by factors other than plant water status and these factors complicate the development of a direct relationship between plant water status and spectral indices. Varietal differences in leaf structure, such as the presence or absence of a thick cuticle or waxes, might negatively influence the amount of light transmitted or reflected from the adaxial leaf surface, hampering the penetration of the NIR light through the leaf. These variations might explain the differences in performance of the NIR calibration statistics obtained for the analysed samples. Additionally, factors such as the closely packed palisade tissue in the adaxial surface, compared with the air-filled spongy tissue in the abaxial surface, might play a role in the amount of light transmitted or reflected, as reported by Woolley (1971) and Gausman and Allen (1973). Sinclair et al. (1971) asserted that the spectral response of leaves depends on their surface and internal chemical and structural characteristics.

In this study, NIR calibration statistics from spectra collected using the abaxial surface of the Chardonnay leaves yielded better correlations with water potential compared with those collected on the adaxial surface. In particular, the collection of the NIR spectra in Shiraz samples from the abaxial surface might be one of the reasons why better calibrations were obtained for this variety in the glasshouse experiment compared with the results obtained in the field trial for the season 2006–07. However, this could be the result of factors other than the leaf surface, considering that different instruments and wavelength ranges were used in the two experiments. Differences have been observed previously between adaxial and abaxial surfaces of leaves (Woolley 1971, Walter-Shea et al. 1991, Slaton et al. 2001). The results from this study, in relation to the importance of leaf surface on the collection of the NIR spectra, have some practical implications in the way that canopy reflectance is used to predict plant water status in remote sensing studies.

The PLS loading weights as a function of wavelength were examined to determine if particular NIR wavelengths tended to dominate the PLS calibrations obtained for Ψ_{leaf} and Ψ_{stem} on the

© 2010 Australian Society of Viticulture and Oenology Inc.

two leaf surfaces (abaxial and adaxial). The similarities between the PLS loading weights for the calibrations obtained using the adaxial leaf surface suggested that wavelengths, in the region around 1400 nm, were important. In contrast, the differences between the loading weights for the two calibrations (Ψ_{leaf} and Ψ_{stem}) developed using the abaxial surface indicate a greater variability in reflectance when collecting spectra from this surface. Because these two calibrations yielded better R and SECV compared with those built using the adaxial surface, this may indicate that the spectra contain more information when collected from the abaxial surface, making them more suitable for the purpose of water potential calibrations. Interestingly, the calibration that gave highest R and SECV (Ψ_{stem} on the abaxial surface) also had the lowest absolute value of loading at 1400 nm relative to other wavelengths. This indicates that other wavelengths in the range 1100–1830 nm gave extra information that improved the calibrations relative to those that might be obtained from selection of only a few wavelengths known to be related to water.

Choné et al. (2001) suggested that ψ_{stem} might be used, instead of ψ_{leaf}, for vine irrigation management. Given that ψ_{stem} is generally considered to be a more integrated and stable measure of plant water status compared with ψ_{leaf}, this might explain better NIR calibration statistics obtained for the measurement of ψ_{stem}. In most cases, there was greater variation in ψ_{leaf} than ψ_{stem}. Furthermore, there may be differences in tissue water potential for different positions of a leaf, perhaps because of patchiness in stomatal conductance (Downton et al. 1988). Water status measurements made on Chardonnay during this study showed that ψ_{stem} reflects more the imposed water stress treatments than ψ_{leaf} or g. These results are in agreement with those reported by other authors (Choné et al. 2001). These authors suggested that ψ_{stem} might be used, instead of ψ_{leaf}, for vine irrigation management. Given that ψ_{stem} is generally considered to be a more integrated and stable measure of plant water status compared with ψ_{leaf}, this might explain better NIR calibration statistics obtained for the measurement of ψ_{stem}. It was shown that there was greater variation in ψ_{leaf} than ψ_{stem} and furthermore, there may be differences in tissue water potential and water content for different positions of a leaf, perhaps because of patchiness in stomatal conductance (Downton et al. 1988). This variation appears to be the reason why a single measured spectrum per leaf (spot size 20 mm^2) correlated less well with ψ_{leaf} than with ψ_{stem}. Taking the average of six spectra uniformly distributed over the lamina surface of a single leaf, resulted in equivalent correlations with ψ_{leaf} and ψ_{stem} (Table 4). However, Santos and Kaye (2009), found that repeated NIR scanning on the same leaf (15–20 spectra per leaf) may contribute to high levels of background noise in the spectra, requiring the use of the first derivative of the absorbance values to compute the best calibration.

Precision irrigation can be achieved in grapevines using Ψ_{stem} as a measure of vine water status, because it responds quickly and accurately to (i) vine water restriction; (ii) soil water availability; (iii) soil hydraulic conductivity; and (iv) the capacity of the vine to transport water from the soil to the atmosphere (Choné et al. 2000, 2001). Because NIR can be used as a surrogate and non-destructive measure of Ψ_{stem}, this technique can be used to accurately control water deficits imposed on vines with the objective of obtaining better WUE and high quality grapes for wine production (Ojeda et al. 2002, Coombe and Iland 2005, Pellegrino et al. 2005). NIR can be used as a physiological indicator for irrigation scheduling based on vine water demand, rather than relying on weather and/or soil moisture measurements, which do not consider the plant in the assessment.

For irrigation scheduling purposes, NIR has the potential to be used within the same general guidelines for vineyard water management as for Ψ_{stem}, which are: above –1.0 MPa (non-stress), between –1.0 to –1.2 MPa (moderate water restriction) and from –1.2 to –1.5 MPa (severe water restrictions) (Lampinen et al. 2001, Trégoat et al. 2002, Williams and Araujo 2002, Ferreyra et al. 2003, Cifre et al. 2005, Sibille et al. 2007). However, these thresholds may vary depending on the yield and quality aims and the climatic conditions. From our irrigation trial on Chardonnay, it was evident that even at 50% of the normally applied irrigation the vines would not be classified as stressed according to the values indicated above. The link between Ψ_{stem} and berry quality attributes was shown by Trégoat et al. (2002), who found a strong correlation between this parameter and anthocyanins, phenols and malic acid content in berries. These authors also found good correlations between midday Ψ_{stem} and grape berry weight and yield.

Conclusions

This study showed that grapevine Ψ_{leaf} and Ψ_{stem} can be measured non-destructively using NIR spectroscopy using appropriate calibrations. Observed differences in the NIR spectra were related to the leaf surface in which the spectra were collected, and this had an effect on the accuracy of the calibration statistics for water potential. The global calibrations built using data obtained from glasshouse and field studies on two varieties are indicative that, in the future, a universal calibration, able to predict water potential for all varieties in different environments can be built. Further studies will be carried out in order to address the physiological implications of different leaf surfaces and morphology on the accuracy of NIR calibrations for water potential and in order to build a universal calibration able to predict field water potential for all varieties in all environments.

Acknowledgements

This project is supported by Australia's grape growers and winemakers through their investment body the Grape and Wine Research and Development Corporation, with matching funds from the Australian government.

The four organisations, involved in this research project, UoA, CSIRO, SARDI, AWRI, are all part of the Wine Innovation Cluster (http://www.wineinnovationcluster.com). The authors would like to thank Yalumba Nurseries, particularly Ashleay Ratcliff, Adam Hall and Fred Strachan who co-designed, converted and managed the trial site and Chris Dyson for trial design.

The work of Roberta De Bei during the season 2006–07 was part of the research activities of the 'Dottorato in Viticoltura, Enologia and Marketing delle Imprese Vitivinicole' supported by the Provincia di Treviso and partially supported by the Fondazione 'Ing. Aldo Gini', Italy.

References

Al-Kaisi, M.M. and Yin, X. (2003) Effects of nitrogen rate, irrigation rate, and plant population on corn yield and water use efficiency. Agronomy Journal **95**, 1475–1482.

Bahrun, A., Mogensen, V.O. and Jensen, C.R. (2003) Water stress detection in field-grown maize by using spectral vegetation index. Communications in Soil Science and Plant Analysis **34**, 65–79.

Batten, G.D. (1998) Plant analysis using near infrared reflectance spectroscopy: the potential and the limitations. Australian Journal of Experimental Agriculture **38**, 697–706.

Begg, J.E. and Turner, N.C. (1970) Water potential gradients in field tobacco. Plant Physiology **46**, 343–346.

© 2010 Australian Society of Viticulture and Oenology Inc.

Bowman, W. (1989) The relationship between leaf water status, gas exchange, and spectral reflectance in cotton leaves. Remote Sensing of Environment **30**, 249–255.
Boyer, J.S. (1967) Leaf water potential measured with a pressure chamber. Plant Physiology **42**, 133–137.
Broge, N.H. and Leblanc, E. (2001) Comparing prediction power and stability of broadband and hyperspectral vegetation indices for estimation of green leaf area index and canopy chlorophyll density. Remote Sensing of Environment **76**, 156–172.
Büning-Pfaue, H. (2003) Analysis of water in food by near infrared spectroscopy. Food Chemistry **82**, 107–115.
Carter, G.A. (1991) Primary and secondary effects of water content on the spectral reflectance of leaves. American Journal of Botany **78**, 916–924.
Ceccato, P., Flasse, S., Tarantola, S., Jacquemoud, S. and Grégoire, J.M. (2001) Detecting vegetation leaf water content using reflectance in the optical domain. Remote Sensing of Environment **77**, 22–33.
Choné, X., Trégoat, O., Van Leeuwen, C. and Dubourdieu, D. (2000) Vine water deficit: among the three applications of pressure chamber, stem water potential is the most sensitive indicator. Journal International des Sciences de la Vigne et du Vin **34**, 169–176.
Choné, X., Van Leeuwen, C., Dubourdieu, D. and Gaudillère, J.P. (2001) Stem water potential is a sensitive indicator of grapevine water status. Annals of Botany **87**, 477–483.
Cifre, J., Bota, J., Escalona, J.M., Medrano, H. and Flexas, J. (2005) Physiological tools for irrigation scheduling in grapevine (*Vitis vinifera* L.): an open gate to improve water-use efficiency? Agriculture, Ecosystems Environment **106**, 159–170.
Coombe, B.G. and Iland, P. (2005) Grapevine phenology. In: Viticulture, Vol. 1: resources, Chapter 11. Eds. P.R. Dry and B.G. Coombe (Winetitles: Ashford, Australia) pp. 210–248.
Cozzolino, D., Dambergs, R.G., Janik, L., Cynkar, W.U. and Gishen, M. (2006) Analysis of grape and wine by near infrared spectroscopy – a review. Journal of Near Infrared Spectroscopy **14**, 279–289.
Danson, F.M., Steven, M.D., Malthus, T.J. and Clark, J.A. (1992) High-spectral resolution data for determining leaf water content. International Journal of Remote Sensing **13**, 461–470.
Downton, W.J.S., Loveys, B.R. and Grant, W.J.R. (1988) Non-uniform stomatal closure induced by water stress causes putative non-stomatal inhibition of photosynthesis. New Phytologist **110**, 503–509.
Eastham, J. and Gray, S.A. (1998) A preliminary evaluation of the suitability of sap flow sensors for use in scheduling vineyard irrigation. American Journal of Enology and Viticulture **49**, 171–176.
Eitel, J.U.H., Gessler, P.E., Smith, A.M.S. and Robberecht, R. (2006) Suitability of existing and novel spectral indices to remotely detect water stress in Populus spp. Forest Ecology and Management **229**, 170–182.
Ferreyra, R., Sellés, G., Ruiz, R. and Sellés, I. (2003) Efecto del estrés hídrico aplicado en distintos períodos de desarrollo de la vid cv. Chardonnay en la producción y calidad del vino. Chilean Journal of Agricultural Research **63**, 277–286.
Flexas, J., Galmés, J., Gallé, A., Gulías, J., Pou, A., Ribas-Carbo, M., Tomàs, M. and Medrano, H. (2010) Improving water-use-efficiency in grapevines: potential physiological targets for biotechnological improvement. Australian Journal of Grape and Wine Research **16**, 106–121.
Gausman, H.W. (1974) Leaf reflectance of near-infrared. Photogrammetric Engineering **10**, 183–191.
Gausman, H.W. and Allen, W.A. (1973) Optical parameters of leaves of 30 plant species. Plant Physiology **52**, 57–62.
Hunt, E.R., Jr and Rock, B.N. (1989) Detection of changes in leaf water content using near- and middle-infrared reflectances. Remote Sensing of Environment **30**, 43–54.
Hunt, E.R., Jr, Rock, B.N. and Nobel, P.S. (1987) Measurement of leaf relative water content by infrared reflectance. Remote Sensing of Environment **22**, 429–435.
Jones, H.G. (2004) Irrigation scheduling: advantages and pitfalls of plant-based methods. Journal of Experimental Botany **55**, 2427–2436.
Jones, H.G. (2007) Monitoring plant and soil water status: established and novel methods revisited and their relevance to studies of drought tolerance. Journal of Experimental Botany **58**, 119–130.
Jones, C.L., Weckler, P.R., Maness, N.O., Stone, M.L. and Jayasekara, R.J. (2004) Estimating water stress in plants using hyperspectral sensing. *Proceedings for the ASAE/CSAE Annual International Meeting*, pp. 2–11. Paper 043065. Montreal.
Knipling, E.B. (1970) Physical and physiological basis for the reflectance of visible and near-infrared radiation from vegetation. Remote Sensing of Environment **1**, 155–159.
Kozlowski, T.T., Kramer, P.J. and Pallardy, S.G. (1991) The physiological ecology of woody plants: water stress (Academic Press, Inc.: San Diego).
Lampinen, B.D., Shackel, K.A., Southwick, S.M. and Olson, W.H. (2001) Deficit irrigation strategies using midday stem water potential in prune. Irrigation Science **20**, 47–54.
Maki, M., Ishiahra, M. and Tamura, M. (2004) Estimation of leaf water status to monitor the risk of forest fires by using remotely sensed data. Remote Sensing of Environment **90**, 441–450.
Meron, M., Grimes, D.W., Phene, C.J. and Davis, K.R. (1987) Pressure chamber procedures for leaf water potential measurements of cotton. Irrigation Science **8**, 215–222.
Mogensen, V.O., Jensen, C., Mortensen, G., Thage, J.H., Koribidis, J. and Ahmed, A. (1996) Spectral reflectance index as an indicator of drought of field grown oilseed rape (*Brassica napus* L. European Journal of Agronomy **5**, 125–135.
Murray, I. (1986) The NIR spectra of homologous series of organic compounds. In: Proceedings of the International NIR/NIT Conference. Eds. J. Hollo, K.J. Kaffka and J.L. Gonczy (Akademiai Kiado: Budapest) pp. 13–28.
Murray, I. (1993) Forage analysis by near infrared spectroscopy. In: Sward Measurement Handbook. Eds. A. Davies, R.D. Baker, S.A. Grant and A.S. Laidlaw (British Grassland Society: Reading, UK) pp. 285–312.
Naes, T., Isaksson, T., Fearn, T. and Davies, A.M.C. (2002) A user-friendly guide to multivariate calibration and classification (NIR Publications: Chichester, UK).
Naor, A., Gal, Y. and Bravdo, B. (1997) Crop load affects assimilation rate, stomatal conductance, stem water potential and water relations of field-grown Sauvignon Blanc grapevines. Journal of Experimental Botany **48**, 1675–1680.
Ojeda, H., Andary, C., Kraeva, E., Carbonneau, A. and Deloire, A. (2002) Influence of pre- and postveraison water deficit on synthesis and concentration of skin phenolic compounds during berry growth of *Vitis vinifera* cv. Shiraz. American Journal of Enology and Viticulture **53**, 261–267.
Osborne, B.G., Fearn, T. and Hindle, P.H. (1993) Practical NIR spectroscopy with applications in food and beverage analysis, 2nd edn (Longman Scientific and Technical: Harlow, UK).
Otto, M. (1999) Chemometrics: statistics and computer application in analytical chemistry (Wiley-VCH: Chichester, UK).
Pellegrino, A., Lebon, E., Simonneau, T. and Wery, J. (2005) Towards a simple indicator of water stress in grapevine (*Vitis vinifera* L.) based on the differential sensitivities of vegetative growth components. Australian Journal of Grape and Wine Research **11**, 306–315.
Peñuelas, J. and Filella, I. (1998) Visible and near-infrared reflectance techniques for diagnosing plant physiological status. Trends in Plant Science **3**, 151–156.
Peñuelas, J. and Inoue, Y. (1999) Reflectance indices indicative of changes in water and pigment contents of peanut and wheat leaves. Photosynthetica **36**, 355–360.
Peñuelas, J., Filella, I., Biel, C., Serrano, L. and Save, R. (1993) The reflectance at the 950–970 nm region as an indicator of plant water status. International Journal of Remote Sensing **14**, 1887–1905.
Peñuelas, J., Gamon, J.A., Fredeen, A.L., Merino, J. and Field, C.B. (1994) Reflectance indices associated with physiological changes in nitrogen- and water-limited sunflower leaves. Remote Sensing of Environment **48**, 135–146.
Peñuelas, J., Llusia, J., Piñol, J. and Filella, I. (1997a) Photochemical reflectance index and leaf photosynthetic radiation-use-efficiency assessment in Mediterranean trees. International Journal of Remote Sensing **18**, 2863–2868.
Peñuelas, J., Piñol, J., Ogaya, R. and Filella, I. (1997b) Estimation of plant water concentration by the reflectance water index WI (R900/R970). International Journal of Remote Sensing **18**, 2869–2875.
Rodríguez-Pérez, J.R., Riaño, D., Carlisle, E., Ustin, S. and Smart, D.R. (2007) Evaluation of hyperspectral reflectance indices to detect grapevine water status in vineyards. American Journal of Enology and Viticulture **58**, 302–317.
Santos, A.O. and Kaye, O. (2009) Grapevine leaf water potential based upon near infrared spectroscopy. Scientia Agricola **66**, 287–292.
Scholander, P.F., Bradstreet, E.D., Hemmingsen, E.A. and Hammel, H.T. (1965) Sap pressure in vascular plants, negative hydrostatic pressure can be measured in plants. Science **148**, 339–346.
Schultz, H.R. (2003) Differences in hydraulic architecture account for near-isohydric and anisohydric behaviour of two field-grown *Vitis vinifera* L. cultivars during drought. Plant, Cell & Environment **26**, 1393–1405.
Sibille, I., Ojeda, H., Prieto, J., Maldonado, S., Lacapere, J.N. and Carbonneau, A. (2007) Relation between the values of three pressure chamber modalities (midday leaf, midday stem and predawn water potential) of 4 grapevine cultivars in drought situation of the southern of France. Applications for the irrigation control. Proceedings of the 15th International

© 2010 Australian Society of Viticulture and Oenology Inc.

6.8 Computational water stress indices obtained from thermal image analysis of grapevine canopies.

Irrig Sci (2012) 30:523–536
DOI 10.1007/s00271-012-0375-8

ORIGINAL PAPER

Computational water stress indices obtained from thermal image analysis of grapevine canopies

Sigfredo Fuentes · Roberta De Bei · Joanne Pech · Stephen Tyerman

Received: 14 August 2011 / Accepted: 12 April 2012 / Published online: 22 August 2012
© Springer-Verlag 2012

Abstract Thermal imaging of crop canopies has been proposed more than a decade ago as a sensitive methodology to determine the water status of different crops. This paper describes the development of a semi-automated and automated methodology using MATLAB® programming techniques to analyse the infrared thermal images taking into consideration the pitfalls pointed out previously in the literature. The proposed method was tested in an irrigation reduction and recovery trial for Chardonnay in the 2010–2011 season and in the 2009–2010 season from seven varieties in field conditions. There was a clear separation (assessed by principal component analysis) between control and recovery compared to stress treatments using leaf area index (LAI), stomatal conductance, stem water potential and indices derived from canopy temperatures measured by infrared imaging. High and significant correlations were found between canopy temperature indices and other measures of water stress obtained in the same vines that were independent of LAI. Furthermore, a fully automated analysis method has been proposed using ancillary weather information obtained from the same locations of infrared thermal images. This paper is a first step towards automation of infrared thermography acquisition and analysis in the field for grapevines and other crops.

Communicated by E. Fereres.

S. Fuentes (✉) · R. De Bei · S. Tyerman
School of Agriculture, Food and Wine, Plant Research Centre, The University of Adelaide, PMB 1, Glen Osmond, SA 5064, Australia
e-mail: sigfredo.fuentes@adelaide.edu.au

J. Pech
South Australia Research and Development Institute (SARDI), GPO Box 397, Adelaide, SA 5001, Australia

Introduction

Canopy conductance (g_c), taken as the averaged leaf conductance (g_L) for the whole canopy, is one of the most sensitive parameters to water stress. This parameter can be estimated from leaf-based measurements of stomatal conductance (g_s), after scaling to the whole canopy using leaf area index (LAI) to obtain g_c. However, this method of estimating canopy conductance has disadvantages that limit its practical use for irrigation scheduling (Lu et al. 2003). These include: (1) spatial variability of g_s within the leaf, canopy, irrigation block or the whole vineyard (Jones and Vaughan 2010); (2) time consuming, depending on the number of measurements per leaf and leaves per canopy; and (3) instrumentation required can be cost prohibitive.

Canopy conductance can also be estimated from infrared thermal imaging providing "snapshots" of the whole canopy, or several rows of grapevines when taken from a height above the canopy, making this method a more integrative approach (Moller et al. 2007; Wang et al. 2010). Furthermore, besides still thermal images, currently there are cameras available that can record infrared videos, allowing the incorporation of an in-built geographic positioning system (GPS) that can be used to produce spatial maps with canopy temperature distributions and potential distribution of crop water stress indices (CWSI) within a field (i.e. SC series cameras, FLIR Systems, Portland, USA).

Canopy temperature has been proposed as an indicator of plant water stress since the 1960s (Tanner 1963) based on the cooling effect of the transpiration process. Since

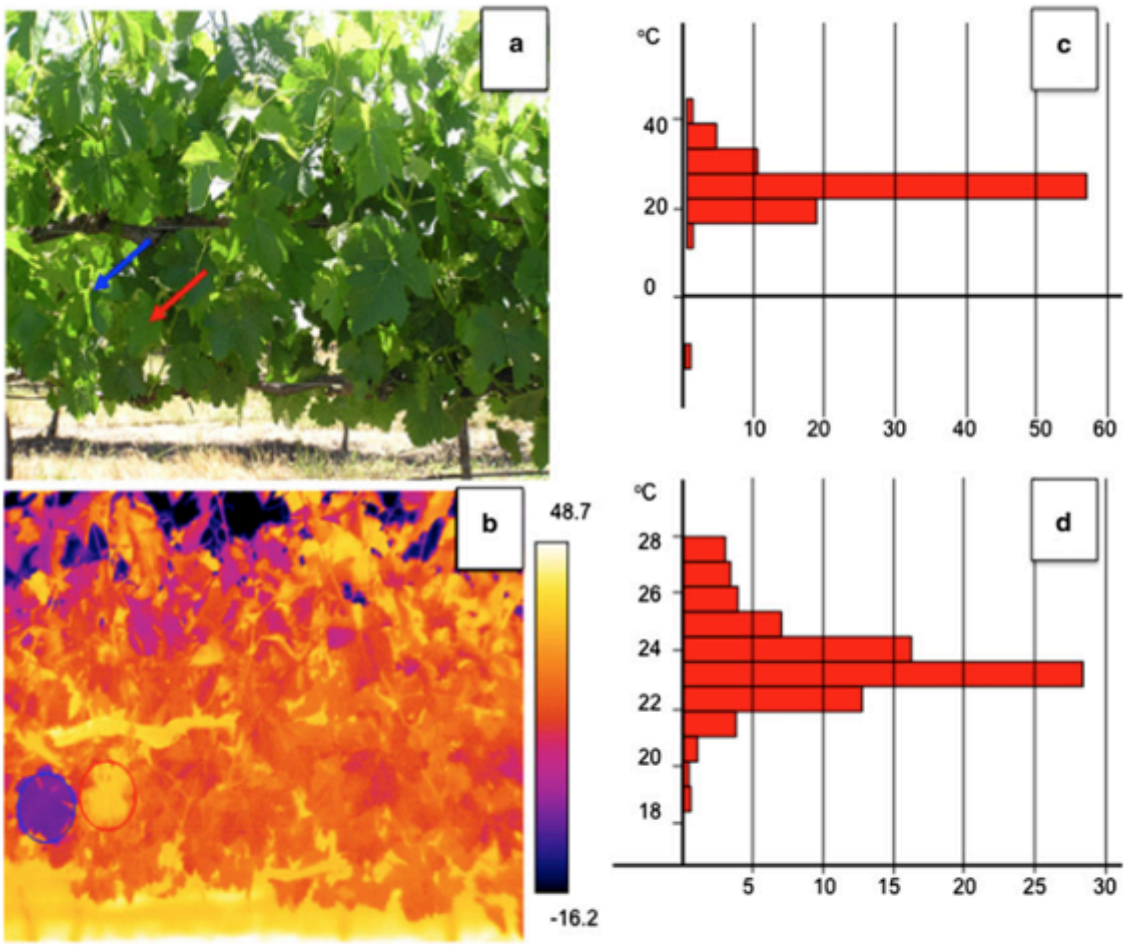

Fig. 1 **a** Example of digital image from a grapevine canopy depicting the dry and wet reference leaves with a *red* and *blue arrow*, respectively, **b** corresponding infrared thermal image, **c** temperature frequency distributions considering the whole thermal image and **d** considering only the range between T_{dry} and T_{wet}. Dry and wet reference leaves can be seen in the *bottom left corner* of Fig. 1b. From Fuentes et al. (2005)

then, technological advances have allowed improved applications in agriculture from temperature sensors clamped on leaves to short range remote sensing, such as infrared thermometry and thermal imaging. The latter has been recognised as a more suitable method to assess variability of thermal properties within grapevine canopies (Cifre et al. 2005; Jones 2004; Jones et al. 2002). Since thermal images are effectively snapshots, they can include non-leaf material within the image of canopies, such as branches, wires from training systems, bunches, sky and soil (Fig. 1a), which need to be excluded from the analysis (Fuentes et al. 2005; Jones 1999a; b; Jones et al. 2002). Non-leaf material can be excluded from thermal images using a variety of methods, such as (1) manual selection of leaf material using polygonal or user-defined shapes, (2) the use of "wet" and "dry" reference materials (or leaves) "painted" with petroleum jelly and water within the thermal image (Fig. 1b) in order to obtain the maximum (T_{dry}) and minimum (T_{wet}) canopy temperatures, respectively, to exclude non-leaf material outside this range (Fuentes et al. 2005; Guilioni et al. 2008; Jones 1999b; Jones et al. 2002; Lindenthal et al. 2005) and (3) other studies have proposed estimating T_{dry} and T_{wet} using ancillary weather variables to derive these parameters using energy balance algorithms (Moller et al. 2007).

A wide range of research has been done recently in grapevines to obtain CWSI based on thermal image analysis, which correlate with other well-established plant water stress parameters, such as g_s and leaf or stem water potential (Ψ_s) (Ferrini et al. 1995; Grant et al. 2007; Guilioni et al. 2008; Jones 1999a; b; Jones et al. 2002; Moller et al. 2007; Stoll et al. 2008c). Furthermore, the use of thermal images has been proposed for pathogen detection, which can also affect thermal and water transference dynamics of leaves or sections of the canopy with the atmosphere (Lindenthal et al. 2005; Stoll et al. 2008a, b, c).

Though the potential of infrared imaging for irrigation scheduling has been highlighted (Jones 2004), there are

some disadvantages and specific considerations that need to be taken into account, such as (1) windy conditions that can complicate the accuracy of the grapevine water status assessment due to rapid changes in g_s within a single canopy (Guilioni et al. 2008); (2) inclusion of non-leaf material in the analysis; (3) difficulty in the analysis of large volumes of data, since every pixel from each image is effectively a temperature reading (usually 5 megapixels per image) (Wang et al. 2010); and (4) grapevines offer an extra complication due to the heterogeneity of their canopies compared to broad acre crops with more homogeneous canopies and closed canopies or cover (Grant et al. 2007; Jones 1999b; Jones et al. 2002). To minimise thermal variability within grapevine canopies, it has been proposed the shaded side rather than the sunny side be used to obtain thermal images (Jones et al. 2002); and finally, (5) Guilioni et al. (2008) identified a problem of consistency in previous studies related to the way that reference leaves were treated with both petroleum jelly and water to obtain T_{dry} and T_{wet}, respectively. Some studies obtained reference leaves by painting only one side, while others were applying on both sides of the reference leaves.

Initial analyses of infrared thermal images were achieved using specialised computer programs from the IR camera providers, such as FLIR QuickReport® and Reporter Pro® (FLIR Systems, Portland, USA) (Cohen et al. 2005). These software packages offer basic computations of mean, maximum and minimum temperature from regions of interest (ROI) obtained by drawing ROIs by hand using square, polygonal or user-defined shape selections. This technique is time consuming considering that a considerable number of thermal images are required to have a representative assessment of the spatial variability of plant water status of an irrigation block or a complete vineyard.

A combined approach using visible and thermal images has been proposed by pre-analysing the visible red, blue and green (RGB) components of each image to separate leaf and non-leaf material by colour discrimination (Leinonen and Jones 2004) using a custom-made code in C+ (Moller et al. 2007). However, this method requires further steps in the analysis and an extra threefold data volume to be analysed, considering visible (RGB) and infrared data per canopy. This approach also lacks the option of batch analysis for large quantities of images. An automated method has been proposed by Wang et al. (2010), using a similar approach that consists of analysing visible and thermal images through a combination of colour identification and Gaussian mixture distribution extraction techniques to obtain CWSI. However, this work only offered comparisons of results (CWSI) with Ψ_s as a physiological parameter with low and statistically non-significant correlations.

Considering previous research, a simple and robust automated imaging analysis technique is required for a rapid and effective assessment of water status of grapevines. This system would allow the implementation of thermal image analysis to schedule irrigation using a plant-based technique. In this paper, we have focused on the problems identified in previous work to develop an automated methodology for thermal image analysis using the T_{dry} and T_{wet} reference leaves and calculated T_{dry} and T_{wet} using leaf energy balance models and matrix analysis techniques. Furthermore, this methodology can be applied to analyse thermal images and thermal videos automatically using the versatility offered by MATLAB® programming to manage very large matrices of data as indexed images in an efficient and rapid way. A spatial data analysis technique is also proposed to assess data quality within thermal images and to identify potential sources of temperature variability within canopies, which can be associated with windy conditions, thermal influence of bare soils (in the case of low canopies), pathogen or insect attacks, or any other biotic and abiotic factors affecting the g_L and, therefore, the index obtained from infrared thermal image analysis (I_G), which is proportional to g_L (Jones et al. 2002) and CWSI within canopies.

Materials and methods

Thermal images and physiological data were collected during the seasons 2009–2010 and 2010–2011 in Australia. A detailed study, incorporating leaf area index, was conducted on the variety Chardonnay within an irrigation reduction and recovery trial (Chardonnay trial). The automated system was also tested on infrared thermal images from a fully irrigated variety trial (variety trial). Infrared thermal images and physiological data acquisition were from 12:00 to 14:00 h (LST), which coincides with the maximum atmospheric demand recorded at the field sites. These data are regarded as "midday" in this paper.

Experimental sites and plant material

Chardonnay trial

The experiment was carried out during February 2011 in an irrigation reduction and recovery after water restrictions have been applied trial within a commercial Chardonnay vineyard at Qualco (SA), (Yalumba Nurseries). This trial was started in the 2008–2009 season using a total area of 3.69 ha with a randomised block design considering four blocks (Fig. 2). The vines in the trial are 8 years old grafted on Ramsey rootstock and trained on a two-wire vertical trellis system with row spacing of 1.8 m between vines and

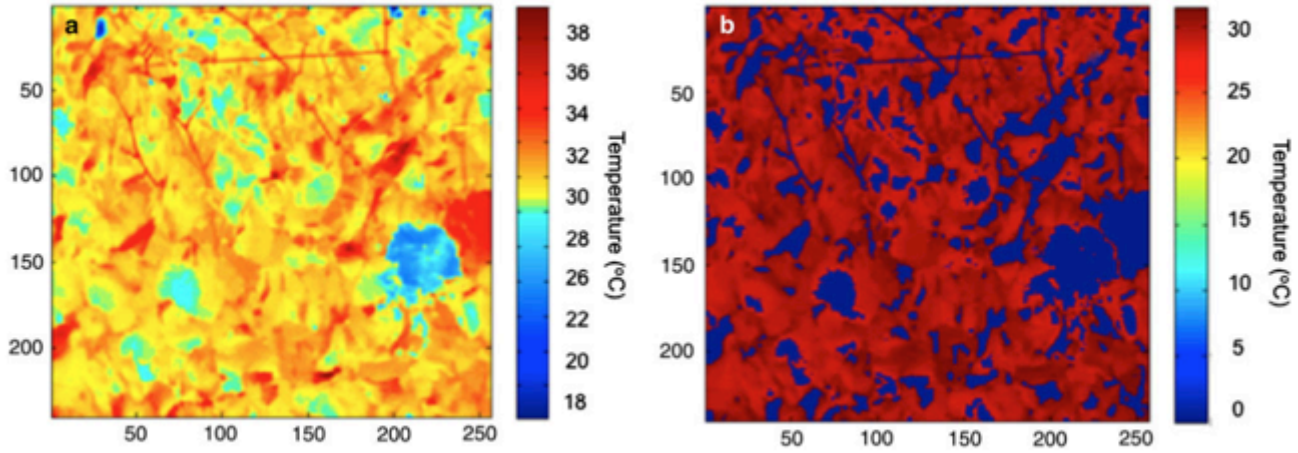

Fig. 2 **a** Example of infrared thermal images obtained using reference leaves (*middle right*) and **b** filtered thermal image using T_{wet} and T_{dry} as thresholds. *Dark blue colour* in the filtered image corresponds to non-leaf or exposed leaf material exclusion. *Colour bar* shows temperatures in °C for the Chardonnay trial

3 m between rows. From this trial, three irrigation strategies were considered for this study: full irrigation or control (C), and reductions to 30 % (30S) and 10 % (10S) of the control. The control treatment represented the amount of irrigation that is normally applied to the vines in a season (5 ML ha^{-1} $year^{-1}$). Each treatment consisted of three rows divided into three sections of 30 vines each. In the 2009–2010 season, one of these three sections for each treatment was changed to the control irrigation level in order to study the physiological changes of vines in recovery from irrigation reduction. Thus, two recovery treatments were added that were 30 % (30R) and 10 % (10R). All treatments were irrigated with Netafim Dripmaster pressure compensated in-line drippers with a 2.3 L h^{-1} of flow. All irrigation events were scheduled to apply 6 mm in 4 h. To apply the reductions in irrigation volume, the interval between irrigations was increased using the Irrigated Crop Management Service (ICMS) Water Budgeting Tool (SARDI). Infrared imaging acquisition and physiological measurements were made in parallel on the same vines at midday for three consecutive days in the trial site at the post-veraison stage (17th, 18th and 19th of February 2011).

Variety trial

The variety experiment was carried out in the Coombe vineyard at the Waite Campus of the University of Adelaide, South Australia, during the 2009–2010 season. Infrared thermal images were acquired in two consecutive dates, the 19th and 20th of January 2010. Three red and three white wine varieties were selected for the study. The varieties were as follows: Shiraz, Merlot, Pinot Noir, Chardonnay, Pinot Gris and Sauvignon Blanc. All varieties are own-rooted, planted in 1991 with a vine spacing of 1.8 m in the row and 3 m between rows. The training system for all varieties is a bilateral spur-pruned cordon with the shoots vertically positioned. All vines were drip irrigated twice per week by in-line drippers discharging 1.5 L/h. Infrared imaging acquisition and physiological measurements were performed in parallel on the same vines at midday for the 2 days of measurements.

Infrared thermal image acquisition

Thermal images were acquired from canopies using an infrared camera FLIR T-series (Model B360) (FLIR Systems, Portland USA), with a resolution of 320 × 240 pixels. The camera measures temperature in the range of −20–1,200 °C. The thermal sensitivity of the camera is <0.08 °C @ +30 °C/80 mK with a spatial resolution of 1.36 milliradians. Each pixel is considered an effective temperature reading in degrees Celsius (°C). Infrared images were acquired from the shaded side of the canopy to reduce variability in the estimation of I_G and CWSI to be compared with other plant water status indicators, such as g_L and Ψ_s (Fuentes et al. 2005a; Jones et al. 2002). One thermal image from the canopy, from each of the four plants per treatment (Chardonnay trial) and per variety (variety trial), was obtained from a constant distance of 2.5 m perpendicular to the row direction (distance between rows is 3 m). Infrared thermography parameters (I_G and CWSI) were compared with physiological measurements acquired immediately after obtaining each thermal image from the same vines. All thermal images were acquired on clear days with minimal wind conditions, which were assessed visually by leaf movement at the top of canopies previous thermal image acquisition, to avoid the influence

of air movement on temperature variability within the canopy and reference leaves. Reference temperatures (T_{wet} and T_{dry}) were obtained by selecting two non-detached mature and representative leaves from a reference plant per treatment. These leaves were "painted" on the abaxial and adaxial sides 2 min before taking the thermal images. One leaf was painted with a solution of water and detergent (dishwashing soap) 0.01 % (v/v) to obtain the T_{wet} reference and the second leaf with liquid petroleum jelly (Vaseline) to obtain the T_{dry} reference.

Algorithms used

Crop water stress index (CWSI) was calculated using the following equation, proposed by Jones (1992) modified from Idso (1982) after determining T_{dry} and T_{wet}:

$$\mathrm{CWSI} = \frac{T_{canopy} - T_{wet}}{T_{dry} - T_{wet}} \quad (1)$$

where T_{canopy} is the actual canopy temperature obtained from the thermal image, and T_{dry} and T_{wet} are the reference temperatures (°C), obtained using the method of painting both sides of reference leaves with petroleum jelly and water, respectively (Idso 1982; Jones 1992).

An index, proportional to leaf conductance to water vapour transfer (g_L), can be obtained using the relationship proposed by Jones et al. (2002) as follows:

$$I_G = \frac{T_{dry} - T_{canopy}}{T_{canopy} - T_{wet}} = g_L\left(r_{aw} + \left(\frac{s}{\gamma}\right)r_{HR}\right) \quad (2)$$

where r_{aw} = boundary layer resistance to water vapour, r_{RH} = the parallel resistance to heat and radiative transfer (Jones 1992), γ = psychrometric constant and s = slope of the curve relating saturation vapour pressure to temperature (Jones 2004; Jones et al. 2002).

Thermal image analysis

Thermal images were analysed using custom code written in MATLAB® 2010b (Mathworks Inc., Natick, MA, USA) and the Image Analysis Toolbox®. The use of the automated code requires that all thermal images (JPEG) are saved in a Microsoft Excel® file, in which each image is stored as a separate worksheet. To change the file formatting, thermal images were loaded firstly using the FLIR QuickReport® (FLIR Systems, Portland USA) software and exported to Excel® (FLIR Systems, Portland, USA). This process can be automated using the FLIR ThermaCAM™ Researcher software (FLIR Systems, Portland USA).

Thermal images are imported by the code and stored in matrix variables automatically, which can be treated in MATLAB as 8-bit indexed images. Therefore, each variable assigned in MATLAB corresponds to an indexed image represented by a matrix $A_{(m,n)}$ with the pixel position (m, n) as indices and temperature (T) in °C as the values:

$$A(m,n) = \begin{pmatrix} T_{1,1} & \cdots & T_{1,n} \\ \vdots & \ddots & \vdots \\ T_{m,1} & \cdots & T_{m,n} \end{pmatrix}. \quad (3)$$

Since (m, n) represents pixels in the thermal image, the maximum thermal image dimension is constant and corresponds to $m = 320$ and $n = 240$ pixels.

Analysis of thermal images from reference leaves to obtain T_{dry} and T_{wet}

As a first step, the code asks which spreadsheets correspond to thermal images containing the reference leaves (T_{wet} and T_{dry}). The user inputs are numerical and correspond to the number of the specific spreadsheets from 1 to n. Once the reference images are specified, the data are uploaded to obtain T_{dry} and T_{wet} as an average of the region of interest (ROI) delimited by the user on the image. For this purpose, a selector is displayed on the image to obtain T_{wet} on the cooled leaf and T_{dry} on the heated leaf. Once these thresholds are calculated as the average T (°C) value of the specific ROI, the code asks for the images to be analysed in batch.

Analysis of thermal images from ancillary information to obtain T_{dry} and T_{wet}

Ancillary information can be obtained using sensors at the same time and position from which the infrared thermography images are obtained. Micro-meteorological data were used from the LiCOR 6,400 readings that were made in the same canopies from which infrared thermal images were obtained (see "Physiological measurements"). Further, meteorological data were obtained from a nearby automatic meteorological station (Measurement Engineering Australia, Adelaide). Ancillary meteorological measurements were used to calculate local T_{dry} and T_{wet} reference temperatures using the basic leaf balance approach (Jones 1999a; Jones et al. 2002). The algorithms used to compute T_{dry} and T_{wet} were as follows:

$$T_{dry} - T_a = \frac{r_{HR}R_{ni}}{\rho c_p} \quad (4)$$

where Ta is the air temperature measured at the same positions and time as infrared thermography acquisition, r_{HR} is the parallel resistance to heat and radiative transfer, R_{ni} is the net isothermal radiation (the net radiation that would be received by an equivalent surface at air temperature), ρ is the density of air, and c_p is the specific heat capacity of air. This formula uses the concept of

isothermal radiation and assumes a dry surface with the same aerodynamic and radiative properties, in which the sensible heat loss will equal the net radiation absorbed (Jones 1992).

$$T_{wet} - T_a = \frac{r_{HR} r_{aW} \gamma R_{ni}}{\rho c_p [\gamma(r_{aW}) + s r_{HR}]} - \frac{r_{HR} \delta e}{\gamma(r_{aW}) + s r_{HR}} \quad (5)$$

where r_{aW} is the boundary layer resistance to water vapour transfer (assumed to be largely determined by the stomatal resistance), γ is the psychrometric constant, s is the slope of the curve relating saturation vapour pressure to temperature, and δe is the water vapour pressure deficit in the air.

Automated subdivision of thermal images

Based on the hypothesis that wind velocity will affect primarily the upper part of canopies, due to architectural arrangement of rows in a vineyard configuration, the code subdivides each thermal image to assess wind velocity on spatial variability of canopy temperatures. For this purpose, each image ($A_{(m,n)}$) is automatically divided into three (d) horizontal sections corresponding to the top (A_t), middle (A_m) and bottom (A_b) for differential analysis.

$$A_t = \begin{pmatrix} T_{1,1} & \cdots & T_{1,n} \\ \vdots & \ddots & \vdots \\ T_{\left(\frac{m}{d}\right),1} & \cdots & T_{\left(\frac{m}{d}\right),n} \end{pmatrix};$$

$$A_m = \begin{pmatrix} T_{\left(\frac{m}{d}+1\right),1} & \cdots & T_{\left(\frac{m}{d}+1\right),n} \\ \vdots & \ddots & \vdots \\ T_{2\left(\frac{m}{d}\right),1} & \cdots & T_{2\left(\frac{m}{d}\right),n} \end{pmatrix};$$

$$A_b = \begin{pmatrix} T_{2\left(\frac{m}{d}+1\right),1} & \cdots & T_{2\left(\frac{m}{d}+1\right),n} \\ \vdots & \ddots & \vdots \\ T_{m,1} & \cdots & T_{m,n} \end{pmatrix}$$

Equations 1 and 2 are used to analyse separately each sub-matrix to obtain CWSI and I_G for the top, middle and bottom sections of each canopy.

Customised subdivision

For a more detailed spatial analysis of canopies, a second tool was developed to divide each image ($A_{(m,n)}$) in a number of sub-images defined by the user (d). This algorithm was previously used for LAI estimation using gap analysis and image subdivision (Fuentes et al. 2008). This tool divides each thermal image in $n \times m$ subdivisions, where $n = m$ and corresponds to the user input (i.e. a subdivision input $d = 5$ will divide the image in $5 \times 5 = 25$ subdivisions). For each subdivision, the I_G index can be calculated (Eq. 2), which allows generating a 2D image to discriminate sections of the canopy that could be influenced by biotic and abiotic factors that can explain variability within a single canopy. This analysis can be visual or statistical based on the analysis of variability of means for I_G values.

To test the customised subdivision tool, a 30 cm (diameter) fan was located facing the top of canopies from a distance of 2 m of well-irrigated vines (control) in the Chardonnay trial. The wind speed was measured using a portable watch with wind sensor (WindMaster® Swiss-made Sensor, Swiss). The wind speed (u) was maintained approximately constant at 1.39 ms^{-1}. Infrared images were obtained after 2 min of applying wind. From these thermal images, the I_G index was calculated using the subdivision (top, middle and bottom) to obtain any statistical differences in these three sections of the canopy. For the customised subdivision tool, a d value of $d = 12$ was used, giving a total number of subdivisions of 144.

Automated filtering of non-leaf material from sub-images

For each thermal image, a simple filter rule was used to exclude all T values above T_{dry} and below T_{wet}, which were considered non-leaf material or sun-exposed leaf material as follows:

$$A_{if} = T_{wet} \geq A_{(t,m,b)} \geq T_{dry}; (A_{(t,m,b)} \neq A_{if}) \notin A_{if} \quad (6)$$

where A_{if} is a sub-image filtered matrix with values of T that meet the rule set in Eq. 4 and "0" values replacing T that does not meet the filter rule (Fig. 3b). After filtering, calculations of mean temperatures, standard deviation of the mean, I_G and CWSI can be obtained for each sub-matrix.

Outputs handling

Numerical outputs from thermal images analysis are automatically saved in an Excel® file containing relevant data, such as T_{dry}, T_{wet}, mean canopy temperature (T_c), maximum canopy temperature (T_{max}), minimum canopy temperature (T_{min}), standard deviation of temperatures in the canopy (SD_T), I_G and CWSI for the entire thermal image, for the three main subdivisions or for the customised subdivision methods. The programme has also an option to obtain frequency distribution of temperatures for determined thermal images (Fig. 1c and d).

Physiological measurements

Stem water potential (Ψ_s)

Measurements of Ψ_s were performed on each plant studied using a Scholander type pressure chamber (PMS

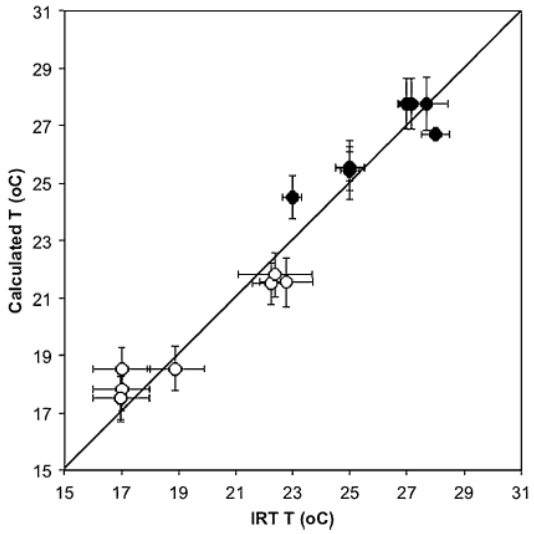

Fig. 3 Comparison between temperature thresholds obtained from reference leaves (IRT T in °C) and calculated using energy balance algorithms (Eqs. 4 and 5). T_{dry} (*filled circles*) and T_{wet} (*clear circles*) corresponded to two days of measurements (18th and 19th of February 2011)

Instruments, Model 1005, Albany, OR. USA). For this purpose, a fully expanded mature leaf was selected from each plant and bagged for at least 30 min before each measurement with a plastic bag coated with aluminium foil ($n = 24$). No more than 30 s elapsed between the leaf cutting and measurement of bagged leaves.

Gas exchange and leaf conductance measurements

Leaf conductance (g_L), transpiration rate (E) and photosynthesis (A) were obtained using a portable LI-COR 6400 gas exchange system (LI-COR Environmental, Lincoln, Nebraska, USA). All LI-COR measurements were obtained from three mature and fully expanded leaves from each plant per replicate, per treatment at the same time as infrared thermal images and Ψ_s measurements ($n = 72$). For the variety trial, leaf conductance (g_L) was measured on five mature and fully expanded leaves per plant and per variety ($n = 120$) using a non-steady state porometer (AP4, Delta-T Devices, Cambridge, UK). All physiological measurements were performed immediately after thermal imaging acquisition and from the same plants at midday.

Canopy size measurements

Leaf area index (LAI) was obtained in February 2010 using a LAI-2000 plant canopy analyser (Licor Inc., Lincoln, Nebraska, USA). Canopy measurements were performed the day before of physiological and thermal image data acquisition using the same plants.

Statistical analysis

Principal component analysis (PCA) with full cross-validation was used to obtain a hierarchy of variables analysed, to find patterns in the data, detection of outliers and to classify any combination of variables that could explain links between I_G, CWSI and physiological and growth parameters measured. For PCA, the Unscrambler® software (version X 10.1 CAMO, Oslo, Norway) was used. The data set used for PCA contained the following variables: I_G, CWSI, Ψ_s and LAI.

Correlation analysis was used to compare: (1) reference temperatures obtained using reference leaves from infrared thermal images (IRT leaves) and calculated using energy balance models (Eqs. 4 and 5), and (2) CWSI and I_G calculated from thermal images and physiological variables obtained from the same canopies. The correlation analysis was performed using the Curve Fitting Toolbox® (MATLAB® 2010b, Mathworks, Natick, MA, USA). Significance of correlations and separation of means between (1) treatments, (2) infrared indices and (3) spatial distribution of indices within thermal images were obtained using the CoStat statistical software (CoHort, Monterrey, CA, USA) and using the Student–Newman–Keuls test with a significance level of $P \leq 0.05$.

Results

Outputs from the automated thermal image analysis

The semi-automated method was able to discriminate leaf material from sunny exposed leaves and non-leaf material using the threshold temperatures obtained from reference leaves. The example presented in Fig. 2a shows a thermal image with considerable amount of branches, a few small gaps with very low temperature, located in the upper section of the canopy, corresponding to sky and a training system wire running horizontally in the upper half of the thermal image. Figure 2b shows the filtered image in which it can be clearly seen the exclusion of non-leaf and sun-exposed material in dark blue by using the T_{wet} and T_{dry} thresholds.

Reference temperatures and statistical analyses of automated outputs are presented in Tables 1 and 2, respectively. Table 1 shows the reference temperatures obtained for different treatments from the Chardonnay trial with non-significant differences between reference leaves. Table 2 shows the averaged outputs for thermal images obtained at midday (maximum atmospheric demand) at the Chardonnay trial. The data did not show significant differences for temperatures and indices shown in Table 2 from top, middle and bottom sections for each canopy.

Table 1 Infrared reference temperatures (T_{dry} and T_{wet}) and canopy temperatures (T_c) obtained from reference thermal images

Treatment	T_{dry}	SD T_{dry}	T_{wet}	SD T_{wet}	T_c	SD T_c
10R; 10S	27.1	0.42	22.8	0.94	25.2	0.48
30R; 30S	27.7	0.72	22.4	1.29	25.9	0.64
Control	27.0	0.34	22.2	0.67	23.6	0.54

Standard deviations (SD) correspond to the ROI selected for the Chardonnay trial. All values are in °C

There were significant differences for temperatures and indices between treatments (Table 2). The control treatment showed the lowest T_c (23.7 °C), T_{max} (24.2 °C), T_{min} (22.4 °C) and minimal difference between T_{max} and T_{min}. T_{max}, T_{min} and T_c varied in the rest of the treatments with averaged T_{max} of 27.4 °C and T_{min} of 23.4 °C and T_c of 25.9 °C. The control treatment was significantly different from other treatments for all the parameters obtained and calculated from thermal images, with exception of T_{min}. The I_G and CWSI values for the control treatment were in average 2.3 and 0.31, respectively. The treatment with reduced water applied (10S) also differentiated statistically from the rest of the treatments for T_c, I_G and CWSI with averaged values of 26.4 °C, 0.24 and 0.81, respectively. Moreover, the I_G indices were not statistically different for the recovery treatments and 30S.

Calculated versus reference leaves temperatures

Figure 3 shows the relationship between the calculated T_{dry} and T_{wet} reference temperatures using Eqs. 4 and 5, compared to the reference leaves temperatures obtained using the analysis proposed and manual ROI analysis in MATLAB® (IRT leaves). There was a strong and significant correlation between IRT and calculated T for 2 days of measurements (SEE = 10.16; $R^2 = 0.95$; RMSE = 0.85; $P < 0.001$).

Physiological and canopy growth response to water application

Physiological responses of irrigation treatments and relationships between the variables measured (Ψ_s and LAI) and indices calculated from thermal images (CWSI and I_G) are presented in Fig. 4 as a PCA score plot (Fig. 4a) and a correlation loading plot (Fig. 4b). The I_G and CWSI best differentiated and separated the control and 30R from other treatments, which are associated with values of g_L of 278 mmol m^{-2} s^{-1} (control) and 178 mmol m^{-2} s^{-1} (30R) in average, compared to 161 mmol m^{-2} s^{-1} (10R) and 121 mmol m^{-2} s^{-1} (10S). Recovery treatments showed values of Ψ_s of −0.45 MPa on average. The 30S and 10S treatments reached values of $\Psi_s = -0.61$ MPa and −0.75 MPa, which can be considered as non-water-stressed and mild water-stressed conditions, respectively, for the experiment (Acevedo-Opazo et al. 2010). Canopy growth also responded to water applications. LAI ranged from 3.87 corresponding to the 30R treatment to 2.15 corresponding to the 10S treatment (Table 3). There were no significant differences between the control, 30R and 30S treatments, but they differentiated from the 10S and 10R treatments. Canopy leaf area was reduced 35 % for the 10S and 10R treatments compared to control, 30S and 30R. The PCA in Fig. 4a shows positive correlations between I_G, Ψ_s and LAI. An inverse correlation was found for the previous variables and CWSI. The two factors shown in the PCA are factor 1 and factor 2, which explained 81 and 17 % of the variability in the data, respectively. The two factors

Table 2 Averaged values of temperatures in °C for canopy (T_c), maximum canopy temperature (T_{max}), minimum canopy temperature (T_{min}), I_G and CWSI from infrared thermal images (Chardonnay trial)

Position	Treatment	T_c	T_{max}	T_{min}	I_G	CWSI
Top^{ns}	10R	26.6^{ab}	27.2^{b}	23.5^{ab}	0.57^{bc}	0.65^{b}
	10S	26.4^{a}	27.2^{b}	23.9^{a}	0.22^{c}	0.82^{a}
	30R	25.2^{b}	27.5^{a}	22.9^{ab}	0.95^{b}	0.52^{b}
	30S	25.6^{ab}	27.7^{a}	23.1^{ab}	0.65^{bc}	0.61^{b}
	Control	23.7^{c}	24.2^{c}	22.5^{b}	2.22^{a}	0.32^{c}
Middle^{ns}	10R	25.7^{b}	27.2^{b}	23.5^{ab}	0.51^{bc}	0.67^{b}
	10S	26.4^{a}	27.2^{b}	24.1^{a}	0.23^{c}	0.82^{a}
	30R	25.1^{c}	27.6^{a}	22.9^{b}	1.01^{b}	0.51^{c}
	30S	25.7^{b}	27.7^{a}	23.1^{ab}	0.63^{bc}	0.62^{b}
	Control	23.7^{d}	24.2^{c}	22.4^{b}	2.21^{a}	0.32^{d}
Bottom^{ns}	10R	25.5^{b}	27.2^{b}	23.1^{ns}	0.67^{bc}	0.62^{b}
	10S	26.3^{a}	27.2^{b}	23.7^{ns}	0.27^{c}	0.80^{a}
	30R	25.0^{b}	27.6^{ab}	23.3^{ns}	1.12^{b}	0.49^{c}
	30S	25.6^{b}	27.7^{a}	23.4^{ns}	0.66^{bc}	0.61^{bc}
	Control	23.6^{c}	24.2^{c}	22.2^{ns}	2.46^{a}	0.30^{d}

Means followed by different letters are different at $P \leq 0.05$ and ns correspond to non-significant differences

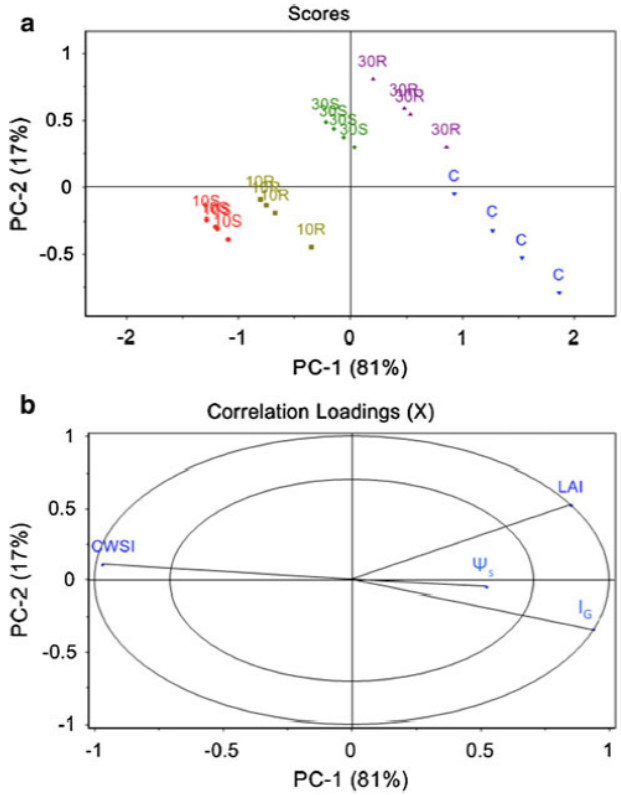

Fig. 4 **a** Principal component analysis (PCA) showing the separation of treatments for the Chardonnay trial by the *score plot* and **b** the correlation loadings showing the relationship between the physiological variables measured: leaf conductance (g_L) and stem water potential (Ψ_s), the thermal indices calculated: infrared index (I_G), crop water stress indices (CWSI) and canopy growth (LAI)

Table 3 Canopy size results (LAI) measured in February 2011 per irrigation treatments (Chardonnay trial)

Means followed by different letters are different at $P \leq 0.05$ and ns correspond to non-significant differences

Treatment	LAI
10R	2.54[b]
10S	2.15[b]
30R	3.87[a]
30S	3.37[a]
Control	3.62[a]

combined explained 98 % of the data variability. Factor 1 was identified as vine water status and factor 2 as vegetative growth in response to water availability.

Thermal imaging and physiological responses to irrigation

Highly significant correlations were obtained between g_L measured and I_G and CWSI obtained using the semi-automated thermal image analysis method proposed in this paper for the Chardonnay and the variety trial (Table 4). Positive linear correlations were found, considering all treatments for the Chardonnay trial, between g_L and I_G at midday

Table 4 Results of correlations between leaf conductance (g_L), the infrared index (I_G) and crop water stress indices (CWSI) calculated by infrared thermal image analysis for the Chardonnay and the variety trials

Trial	Data set	R^2	SEE	RMSE	Significance (P)
Chardonnay	g_L versus I_G	0.92	0.56	0.18	<0.001
	g_L versus CWSI	0.86	0.03	0.04	<0.001
Varieties	g_L versus I_G	0.87	0.14	0.12	<0.001
	g_L versus CWSI	0.83	0.04	0.06	<0.001

($R^2 = 0.92$; Fig. 5a), and for the variety trial ($R^2 = 0.81$; Fig. 6a). Negative linear correlations were found between g_L and CWSI at midday for the Chardonnay trial ($R^2 = 0.87$; Fig. 5b) and the variety trial ($R^2 = 0.83$; Fig. 6b). These results are in agreement with studies by Grant et al. (2007), Leinonen et al. (2006) and Jones et al. (2002), which found that I_G is proportional to g_L for grapevines. Results for the relationship between g_L and CWSI also are in accordance with studies by Moller et al. (2007).

Discrimination of wind influence in thermal images

Mean values and statistical analysis obtained from the top, middle and bottom sections of the canopy submitted to wind are shown in Table 5. A statistically significant higher value of $I_G = 3.30$ was found for the top section of the canopy. There were no statistically significant differences for the mean values of I_G found for the middle ($I_G = 1.16$) compared to the bottom sections of the canopy ($I_G = 1.09$). Furthermore, a significantly higher standard deviation of means was found also for the top section of the canopy (SD = 2.97) compared to the middle and bottom sections (SD = 0.54 and 0.61, respectively).

Figure 7 shows the original thermal image submitted to windy conditions (Fig. 7a). A more visible blue colour can be seen at the top part of the canopy (dashed square) compared to the bottom section, corresponding to higher I_G. Figure 7b shows the filtered I_G image in which all values above $I_G = 3.0$ were forced to a light blue colour (top part) and all I_G values below $I_G = 0.3$ were forced to a red colour (bottom part). Higher and lower criteria were obtained from physiological data presented in Fig. 5a.

Discussion

Reference leaves compared to leaf energy balance calculations

Results from comparisons between calculated T_{dry} and T_{wet} using ancillary information and those obtained using the

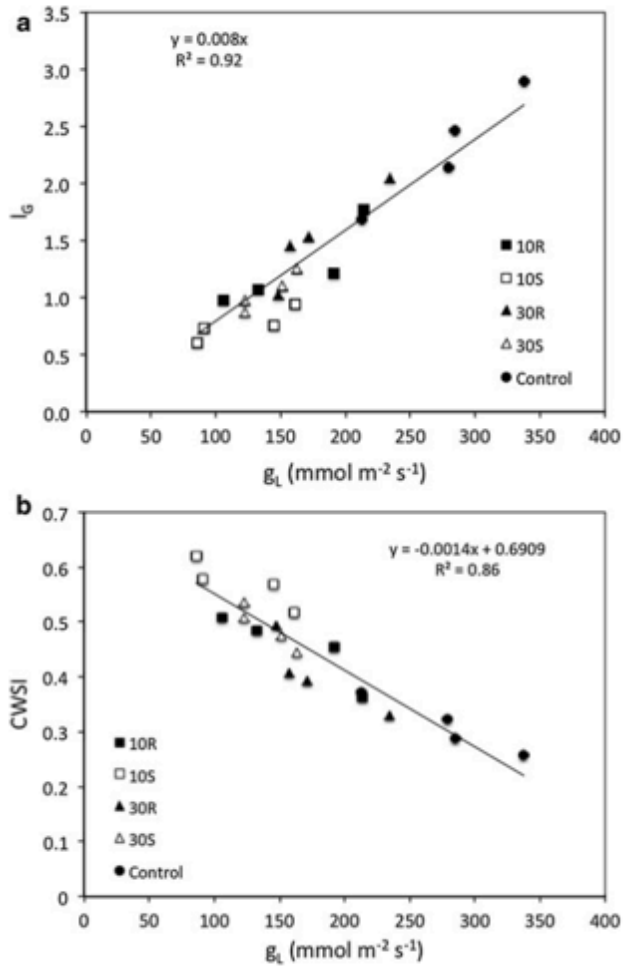

Fig. 5 **a** Relationship between leaf conductance (g_L) and infrared index calculated for thermal images and **b** with crop water stress index (CWSI) for the Chardonnay trial

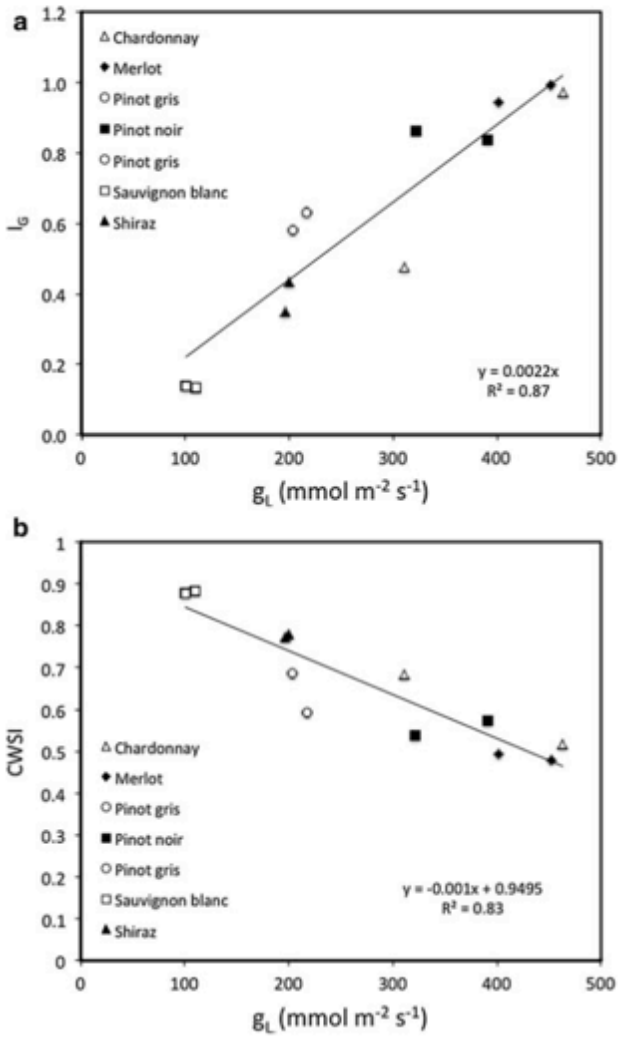

Fig. 6 **a** Relationship between leaf conductance (g_L) and infrared index calculated for thermal images and **b** with crop water stress index (CWSI) for the variety trial. Each point corresponds to the averaged values of four plants per variety measured in 2, 6 days apart

reference leaves are in accordance with those obtained in previous studies (Leinonen et al. 2006). Even though Leinonen et al. (2006) found good correlations between IRT reference temperatures with calculated temperatures, the latter were more stable than those obtained using reference leaves. Furthermore, the calculated temperatures did not reflect the canopy-to-canopy variability of T_{dry} and T_{wet} as accurately as the painting method and reference leaves. This can be explained by the single estimation of reference temperatures from an automatic meteorological station located close to the vineyard site where the experiment was conducted. In our study, we obtained micrometeorological data from the Licor 6400 to compute calculated T_{dry} and T_{wet}, and the results were higher correlations between reference temperatures from reference leaves (IRT) compared to calculated reference temperatures. Therefore, having microclimatic ancillary information helps to improve the estimation of T_{dry} and T_{wet}, making possible a higher degree of automation in the use of thermal images to obtain grapevine water status.

Table 5 Results of the subdivision tool on a thermal image from a canopy submitted to wind velocities of 1.39 ms^{-1} on the top section

Trial	Section	I_G	SD	Significance (P)
Chardonnay	Top	3.30[a]	2.97	<0.001
	Middle	1.16[b]	0.54	
	Bottom	1.09[b]	0.61	

Means followed by different letters are different at $P \leq 0.05$ and ns correspond to non-significant differences. *SD* standard deviation of the mean

I_G values correspond to the mean from a particular section of the infrared thermal image

Further studies are required to acquire parallel microclimatic data using a customised mini-meteorological station along with the infrared thermal images to improve

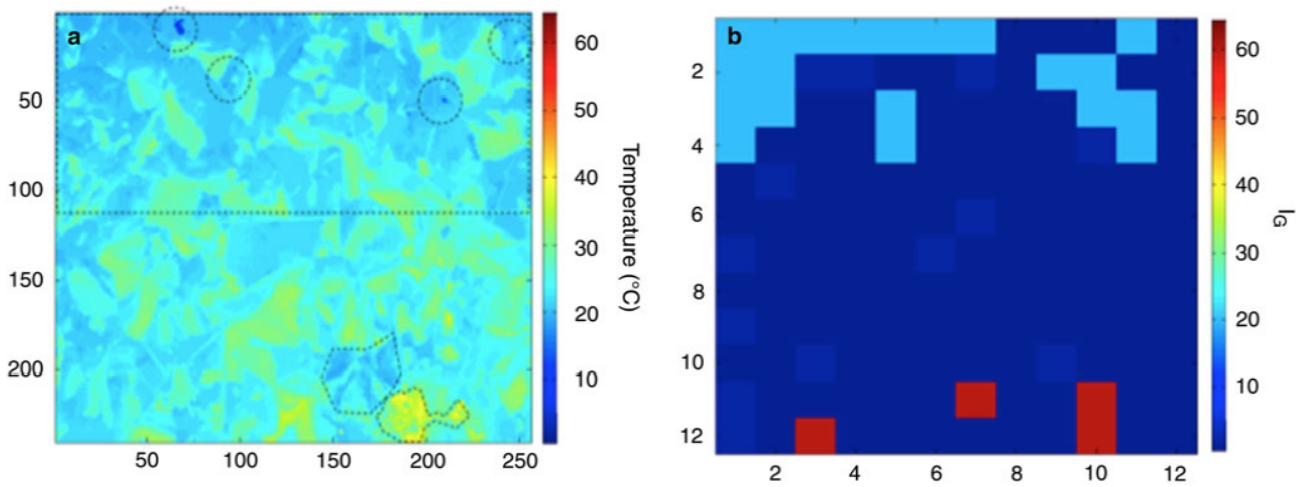

Fig. 7 **a** Thermal image from a control canopy submitted to wind at the top section. *Dashed rectangle* shows roughly the area where wind was applied. *Dashed circles* indicate gaps in the canopy with low temperatures. User-defined polygons at the bottom right are the wet and dry reference leaves. **b** Filtered I_G image obtained using the customised subdivision tool with a $d = 12$ corresponding to 144 subdivisions. Values of $I_G \geq 3$ were coloured light blue and $I_G \leq 0.3$ were coloured red to denote areas influenced by wind or consistent temperatures close to the T_{dry} threshold, respectively

accuracy of the T_{dry} and T_{wet} estimates, specifically to obtain the net isothermal radiation (R_{ni}), which for the purpose of this study was assumed to be equal to the absorbed short-wave radiation. This assumption was based on studies made by Jones (1992) and Leinonen et al. (2006). Consecutive data acquisition and processing its possible using MATLAB® and the Instrument Control Toolbox® making the collection of infrared thermal images, ancillary weather information and calculations of T_{dry}, T_{wet}, I_G and CWSI automatic. This integrated system will be tested in following seasons for grapevines and will be available as freeware to interested researchers in a beta version.

Thermal indices and physiological measurements

Results from the Chardonnay trial were consistent with previous physiological studies (season 2006–2007) obtained from the same trial site for Ψ_s and g_L (season 2009–2010) (De Bei et al. 2011). Therefore, it can be said that physiological responses found for the period used for the Chardonnay trial were representative of the seasonal treatment response to irrigation. Our study on six varieties using a normalised stabilisation time of 2 min for the wet and dry leaves gave similar correlation values and significance compared to the Chardonnay trial. Variations observed in g_L, I_G and CWSI can be attributed to: (1) differences in stomatal response due to differences in phenological stage and water requirements of the different varieties and (2) spatial variability within the irrigation block (water application), which was assessed through a drip uniformity test ($du = 81$ %, data not shown).

The PCA in Fig. 4a separated the irrigation treatments explaining a higher percentage of variability (81 %) due to plant water status (Factor 1). Statistical analysis showed that the 10S, 10R and 30S were the treatments that presented mild water stress (higher CWSI and lower Ψ_s and g_L and I_G) compared to control and 30R for the days of the experiment. There was higher variability for data from the control and 30R treatments compared to 30S, 10R and 10S along the I_G vector, which has been shown to be proportional to g_L (Leinonen et al. 2006; Leinonen and Jones 2004). This effect on water stress treatments can be explained by higher stomatal regulation due to reductions in water supplied to the vines. It has been shown that chemical signals from root-to-shoot, mainly abscisic acid (ABA), increase stomatal sensitivity to VPD due to soil moisture depletion and roots exposed to drying soil (Collins et al. 2009; Fuentes et al. 2005). A strong and significant inverse correlation between Ψ_s and CWSI found in this study ($R^2 = 0.75$; SSE = 0.034; RMSE = 0.11) is in accordance with studies made by Moller et al. (2007). Factor 2 on the PCA was related to vigour, which was affected by long-term levels of water supply by irrigation (Fig. 4a and b).

Leaf area index

Canopy growth and architecture can affect the amount of sun-exposed leaf material and, therefore, the amount of filtering required per thermal image. Control treatments, with a higher LAI, will present more shading and bigger canopy walls. On the contrary, water stress treatments will present significantly smaller canopies with a higher gap

fraction, which will result in more sun-exposed leaf material.

Canopy growth, measured as LAI, did not affect significantly the thermal properties of reference leaves. Even though there were non-significant differences among reference leaves, the control treatment registered the lowest averaged temperature compared to the rest of the treatments (Table 1). Factors such as canopy growth, structure, leaf area and thickness and their influence in thermal properties of reference leaves and canopy temperature need to be studied in more detail for different varieties under water stress treatments.

Automated differential analysis of I_G within the canopy

The separation of thermal image analysis between top, middle and bottom regions allowed the detection of wind velocity influence on the spatial variability of canopy thermal signature, which according to the training system used in the Chardonnay trial (Scott Henry) is expected to be more influential in the top sections of canopies for transversal winds in relation to row orientation. According to Jones et al. (2002), canopy temperatures, and hence reference temperatures and calculated indices, start to change considerably at wind velocities (u) of around 1 ms^{-1}. This effect is mainly due to the removal of the boundary layer resistance to water vapour from the surface of leaves, which increases leaf transpiration, and, therefore, I_G, in non-water stress conditions. In our study, infrared thermal images were always obtained in very calm wind conditions to minimise this effect for validation purposes of the infrared technique.

The spatial analysis tools proposed in this study can be used as a data quality assessment for data obtained from sites with moderate wind conditions. In the example presented in this paper (Table 5 and Fig. 7), mild wind conditions were forced upon the top part of the canopies of well-irrigated Chardonnay vines. The customised subdivision tool and analysis allowed detecting the changes of canopy temperature in the top section by statistically analysing changes on the calculated I_G index spatially within the canopies. In regard to the analysis time, it did not vary considerably when changing the d value from 10 to 250, the latter corresponding to the subdivision of an image to the maximum possible value, or pixel-by-pixel (approximately 3–6 s per image using a Mac Book Pro®, 8 Gb RAM, 2.7 GHz, core i7). However, this small difference in analysis time could become important when batch analyses several images.

Since the automatic division (top, middle and bottom) and the customised subdivision tools filter each sub-image using T_{dry} and T_{wet}, non-leaf material is generally excluded from the differential analysis. Therefore, gaps that show sky, which are below zero due to the lack of reflection, will not be included as possible wind effect. Furthermore, leaves that are too damaged by senescence, insect or disease attacks will lose their capacity of thermal regulation through transpiration (presenting temperatures closer or higher than T_{dry}), which could fall into the non-leaf material thermal range. This effect can be seen in Fig. 7, where the dry and wet reference leaves (bottom right) were left with petroleum jelly and the water solution for more than 10 min after application. After this time, T_{wet} increased temperature and was not included as "anomalous" low temperature in the analysis, since the specific I_G value for this leaf was $I_G = 2.0$. Three leaves were included in the criteria of $I_G \leq 0.3$ (from Fig. 5a), which were located in the bottom part of the image. These leaves corresponded to the T_{dry} and two leaves that showed signs of senescence assessed visually (red and yellow colours).

Further development of the code has been started to incorporate direct statistical analysis tools to assess spatial differences within canopies that can explain variability of data from single infrared thermal images.

Use of thermal indices for irrigation scheduling

For a potential application of infrared thermography in irrigation scheduling, it would be recommended to use the I_G data obtained in the period of maximum atmospheric demand to assess plant water status (Flexas et al. 2002). This is the same time of the day and conditions that have been commonly used to measure midday Ψ_s, which is considered one of the most integrative plant water status parameters since it integrates the soil–plant–atmosphere conditions at the time of measurement (Acevedo-Opazo et al. 2010; Chone et al. 2001). Other researchers have shown correlations between I_G and Ψ_s using manual thermal image analysis techniques (Moller et al. 2007) and lower correlations using other automated methods (Wang et al. 2010).

Furthermore, a more automated procedure of acquiring thermal images and relevant data for analysis can be achieved by using microclimatic ancillary information obtained at the same time and locations of thermal imaging data. The extra cost of implementing this method will not be significant due to the low price of reliable sensors that can be integrated in thermal camera system. Further research has been started by our group to automatically integrate infrared imagery collection from the field, ancillary microclimatic data and data processing using the method proposed in this paper to obtain real-time plant water status assessment. The latter method will allow obtaining and analysing a higher volume of data for a more representative spatial and temporal assessment of grapevine water status within the canopy and field scales.

Conclusions

This paper has proposed the use of a semi-automated and automated infrared image analysis technique to obtain accurate plant water status indicators using MATLAB® programming tools. Results can be acquired in a rapid form to be statistically analysed and be applied for experimental research or potential irrigation scheduling management and decision-making. Further studies will be conducted to automate the data acquisition and analysis for real-time assessment. Since this methodology considers the automated separation of top, middle and bottom sections of the canopy, plus a customised subdivision of thermal image for variability analysis within a canopy, data quality techniques can be implemented to assess the influence of wind speed on the variability of estimation of I_G and CWSI or potentially the detection of biotic and abiotic stresses from sections of the canopy. These tools can be of great help for other experimental trials that are more specific in the study of these stresses. The use of these automated tools could allow the implementation of precision irrigation scheduling according to the specific physiological behaviour of different grapevine varieties and their responses to water application. Due to the sensitivity of infrared thermography, this technique can be used to implement irrigation techniques such as regulated deficit irrigation (RDI) or partial root-zone drying (PRD), which require narrow plant water status thresholds to maximise quality of grapes, water use efficiency and minimise detrimental effects on yield.

Acknowledgments This project is supported by Australia's grape growers and winemakers through their investment body the Grape and Wine Research and Development Corporation, with matching funds from the Australian Government. The four organisations, involved in this research project, UoA, CSIRO, SARDI, AWRI, are all part of the Wine Innovation Cluster (www.wineinnovationcluster.com). This project is being undertaken on a collaborative basis by the parties. The authors thank staff from Yalumba Nurseries whose in-kind contributions have included irrigation supplies, irrigation system conversion and management of the vineyard, staff from the Irrigated Crop Management Service (ICMS) who designed the irrigation system conversion and have provided ongoing irrigation system advice, staff at Measurement Engineering Australia (MEA) for in-kind contribution of field monitoring equipment.

References

Acevedo-Opazo C, Ortega-Farias S, Fuentes S (2010) Effects of grapevine (Vitis vinifera L.) water status on water consumption, vegetative growth and grape quality: an irrigation scheduling application to achieve regulated deficit irrigation. Agric Water Manag 97(7):956–964

Chone X, Van Leeuwen C, Dubourdieu D, Gaudillere J-P (2001) Stem water potential is a sensitive indicator of grapevine water status. Ann Bot 87:477–483

Cifre J, Bota J, Escalona JM, Medrano H, Flexas J (2005) Physiological tools for irrigation scheduling in grapevine (Vitis vinifera L.): an open gate to improve water-use efficiency? Agric Ecosyst Environ 106(2/3):159–170

Cohen Y, Alchanatis V, Meron M, Saranga Y, Tsipris J (2005) Estimation of leaf water potential by thermal imagery and spatial analysis. J Exp Bot 56(417):1843–1852

Collins MJ, Fuentes S, Barlow EWR (2009) Partial rootzone drying and deficit irrigation increase stomatal sensitivity to vapour pressure deficit in anisohydric grapevines. Funct Plant Biol, in press

De Bei R, Cozzolino D, Sullivan W, Cynkar W, Fuentes S, Dambergs R, Pech J, Tyerman S (2011) Non-destructive measurement of grapevine water potential using near infrared spectroscopy. Aust J Grape Wine Res 17(1):62–71

Ferrini F, Mattii GB, Nicese FP (1995) Effect of temperature on key physiological responses of grapevine leaf. Am J Enol Vitic 46(3):375–379

Flexas J, Bota J, Escalona JM, Sampol B, Medrano H (2002) Effects of drought on photosynthesis in grapevines under field conditions: an evaluation of stomatal and mesophyll limitations. Funct Plant Biol 29(4):461–471

Fuentes S, Collins M, Rogers G, Kelley G, Conroy J (2005) Use of infrared thermography to assess spatial and temporal variability of stomatal conductance of grapevines under partial root zone drying: an irrigation scheduling application. Acta Hortic 689:309–316

Fuentes S, Palmer AR, Taylor D, Zeppel M, Whitley R, Eamus D (2008) An automated procedure for estimating the leaf area index (LAI) of woodland ecosystems using digital imagery, MATLAB programming and its application to an examination of the relationship between remotely sensed and field measurements of LAI. Funct Plant Biol 35(10):1070–1079

Grant OM, Tronina L, Jones HG, Chaves MM (2007) Exploring thermal imaging variables for the detection of stress responses in grapevine under different irrigation regimes. J Exp Bot 58(4):815–825

Guilioni L, Jones HG, Leinonen I, Lhomme JP (2008) On the relationships between stomatal resistance and leaf temperatures in thermography. Agric For Meteorol 148(11):1908–1912

Idso SB (1982) Non-water-stressed baselines: a key to measuring and interpreting plant water stress. Agric Meteorol 27(1–2):59–70

Jones HG (1992) Plants and microclimate: a quantitative approach to environmental plant physiology. Cambridge University Press, Cambridge

Jones HG (1999a) Use of infra red thermometry for estimation of stomatal conductance as a possible aid to irrigation scheduling. Agric Forest Meterol 95:139–149

Jones HG (1999b) Use of thermography for quantitative studies of spatial and temporal variation of stomatal conductance over leaf surfaces. Plant, Cell Environ 22:1043–1055

Jones HG (2004) Irrigation scheduling: advantages and pitfalls of plant-based methods. J Exp Bot 55(407):2427–2436

Jones HG, Vaughan RA (2010) Remote sensing of vegetation. Principles, practices and applications. Oxford University Press, New York, p 353

Jones HG, Stoll M, Santos T, de Sousa C, Chaves MM, Grant OM (2002) Use of infrared thermography for monitoring stomatal closure in the field: application to grapevine. J Exp Bot 53(378):2249–2260

Leinonen I, Jones HG (2004) Combining thermal and visible imagery for estimating canopy temperature and identifying plant stress. J Exp Bot 55(401):1423–1431

Leinonen I, Grant OM, Tagliavia CPP, Chaves MM, Jones HG (2006) Estimating stomatal conductance with thermal imagery. Plant, Cell Environ 29(8):1508–1518

Lindenthal M, Steiner U, Dehne H-W, Oerke E-C (2005) Effect of downy mildew development on transpiration of cucumber leaves visualized by digital infrared thermography. Phytopathology 95(3):233–240

Lu P, Yunusa IAM, Walker RR, Muller WJ (2003) Regulation of canopy conductance and transpiration and their modelling in irrigated grapevines. Funct Plant Biol 30(6):689–698

Moller M, Alchanatis V, Cohen Y, Meron M, Tsipris J, Naor A, Ostrovsky V, Sprintsin M, Cohen S (2007) Use of thermal and visible imagery for estimating crop water status of irrigated grapevine. J Exp Bot 58(4):827–838

Stoll M, Schultz H, Baecker G, Berkelmann-Loehnertz B (2008a) Early pathogen detection under different water status and the assessment of spray application in vineyards through the use of thermal imagery. Precision Agric 9(6):407–417

Stoll M, Schultz HR, Berkelmann-Loehnertz B (2008b) Exploring the sensitivity of thermal imaging for Plasmopara viticola pathogen detection in grapevines under different water status. Funct Plant Biol 35(4):281–288

Stoll M, Schultz HR, Berkelmann-Loehnertz B (2008c) Thermal sensitivity of grapevine leaves affected by Plasmopora viticola and water stress. Vitis 2:133–134

Tanner CB (1963) Plant temperatures. Agron J 55:210–211

Wang X, Yang W, Wheaton A, Cooley N, Moran B (2010) Automated canopy temperature estimation via infrared thermography: a first step towards automated plant water stress monitoring. Comput Electron Agric 73(1):74–83

6.9 Automated estimation of leaf area index from grapevine canopies using cover photography, video and computational analysis methods.

Automated estimation of leaf area index from grapevine canopies using cover photography, video and computational analysis methods

S. FUENTES[1], C. POBLETE-ECHEVERRÍA[2], S. ORTEGA-FARIAS[2], S. TYERMAN[1] and R. DE BEI[1]

[1] Plant Research Centre, The University of Adelaide, Waite Campus, PMB 1, Glen Osmond, SA 5064, Australia
[2] Research and Extension Center for Irrigation and Agroclimatology (CITRA), Universidad de Talca, Avenida Lircay S/N, Talca, Chile
Corresponding author: Dr Carlos Poblete-Echeverría, email cpoblete@utalca.cl

Abstract

Background and Aims: Monitoring of canopy vigour is an important tool in vineyard management to obtain balanced vines (vegetative vs reproductive organs). Leaf area index is the main parameter representing canopy vigour. Our aim was to test an automated computational method to obtain leaf area index and canopy vigour parameters from grapevines with digital photography and video analysis using MATLAB programming techniques for rapid data uptake and gap size analysis.

Methods and Results: The proposed method was tested against allometry at a Chilean experimental site planted with cv. Merlot. A temporal and spatial assessment of the method was also tested in a drought and drought/recovery experiment with cv. Chardonnay in the Riverland, South Australia. These data were geo-referenced and compared to the normalised difference vegetation index extracted from the WorldView-2 satellite images at a 2 m^2 per pixel resolution.

Conclusions: The maximum leaf area index data obtained with cover digital photography and video analysis are an accurate, cost-effective and easy-to-use method to estimate spatial and temporal canopy LAI and structure when compared to standard measurements (allometry and plant canopy analyser).

Significance of the Study: This study has demonstrated that the method proposed is an accurate and inexpensive tool for application in experiments and by the industry to monitor spatio-temporal distribution of vigour.

Keywords: canopy cover, digital image analysis, MATLAB programming, porosity, satellite imagery

Introduction

Leaf area index (LAI) has been defined as the total one-sided area of leaf tissue per unit ground surface area (Watson 1947). Most of the currently available methods for monitoring LAI are based on manual measurement points, which have low spatial resolution and are time consuming. Thus, it is difficult to assess efficiently the spatial and temporal variability of LAI from vineyards, usually caused by differences in soil characteristics and management.

Studies based on remote sensing have shown that monitoring variation in LAI could be a good spatial indicator of canopy vigour for grapevines using airborne platforms (Johnson et al. 2003b, Hall et al. 2008) and satellite platforms (Johnson 2003a, Zarco-Tejada et al. 2005, Martin et al. 2007). These same studies, however, pointed out that the canopy discontinuity from vineyards posed an analysis problem for accurate LAI estimation due to the inter-row component, especially when a cover crop is present.

Measuring leaf area index and canopy structure as vigour indicators for management purposes

Canopy vigour can be managed with different training systems to regulate the microclimate of canopies to affect yield and grape composition (Smart 1985). Adjusting canopy vigour to decrease disease incidence can be also achieved by removing leaves (English et al. 1989) or by summer pruning (Wermelinger and Koblet 1990, Guidoni et al. 1997, Rügner et al. 2002).

It is well known that canopy structure and size can also be altered, as a management strategy, by reducing the amount of water applied to control vigour. Increments in irrigation have resulted in increased LAI, indicative of a more vigorous vine (Esteban et al. 1999, 2001, Acevedo-Opazo et al. 2010). Another effect sought by reducing LAI is to obtain greater light penetration to bunches and the renewal zone (area where the fruiting canes originate) to improve fruit composition and productivity for the next season (Dokoozlian and Kliewer 1995). Berries with increased sun exposure are generally higher in phenolic substances along with decreased acidity when compared to that of non-exposed fruit (Bergqvist et al. 2001). Therefore, there is an inverse relationship between vigour and gap fraction that affects fruit composition. This effect needs to be taken into account for optimal management purposes and has been the main subject for many experimental trials in the past.

Monitoring canopy cover and LAI has been also proposed as a way to estimate accurately crop coefficients (Kc) for grapevines to assess water requirements for irrigation scheduling purposes (Williams and Ayars 2005). In general, the Kc value for grapevines can be obtained from the literature (Allen et al.

doi: 10.1111/ajgw.12098
© 2014 Australian Society of Viticulture and Oenology Inc.

1998). These values, however, are generic, developed in different agroclimatic conditions and do not account for differences between canopy size, row orientation, training system and vine spacing, among other factors (Martin et al. 2007, Poblete-Echeverría et al. 2012, Poblete-Echeverría and Ortega-Farias 2013).

Measuring leaf area index as an indicator of vigour for experimental purposes

For experimental purposes, LAI is a critical parameter widely used for: (i) experiments that involve the estimation of growth and development of plants (Fuentes et al. 2008); (ii) modelling growth and water use (Williams and Ayars 2005); (iii) functional plant modelling (Whitley et al. 2008); and (iv) scaling up leaf-based physiological measurements to the whole plant or tree (Ewert 2004) and tree-based measurements (e.g. sap flow) that can also be upscaled to the whole field or region (Zeppel et al. 2008). The magnitude of LAI in a vineyard depends on environmental and management factors, such as training systems, water and nutrient supply and the use of cover crops, among others (Oliveira and Santos 1995). Therefore, there is the requirement to determine accurately spatio-temporal variations of LAI for scientific experiments to verify the effect of treatments on canopy vigour and, from the management perspective, to assess precision irrigation strategies, such as regulated deficit irrigation and partial root-zone drying, to maximise yield and quality of grapes.

Current methodologies to estimate leaf area index

Leaf area index can be directly measured using destructive methods or indirectly estimated with a variety of instrumentation. Direct measurement of LAI (allometry), by either scanning every single leaf from the canopy or generating empirical shoot length versus leaf area per shoot, is difficult and time consuming to perform (Cutini et al. 1998). Furthermore, these methods do not easily allow a representative spatial and temporal resolution of LAI, which is required in grapevine research experiments and/or for management purposes. There are also non-destructive direct methods to estimate LAI, such as the Li-Cor-3000 portable area meter (LI-3000C, Li-Cor Inc., Lincoln, NE, USA), which requires scanning of individual leaves from canopies. This method can be used as an in situ calibration for indirect LAI estimation methodologies, such as the one proposed in this paper.

Consequently, non-destructive, ground-based or indirect methods have been developed and are more commonly used to estimate LAI in practical terms. Typically, these are based on measurement of radiation transmission through the canopy, for example, the LAI-2000 and 2200 (Plant canopy analyser; Li-Cor Inc.) (Villalobos et al. 1995, Cutini et al. 1998, Bréda 2003, Arias et al. 2007). The cost of these instruments, however, can be prohibitive, and it has been reported that they can underestimate LAI by between 10–40% in forests and crop trees (Macfarlane et al. 2000).

Indirect estimation of LAI by digital or cover photography and gap fraction analysis has been developed recently and provides an accurate and rapid estimation of LAI (Macfarlane et al. 2007a,b, Fuentes et al. 2008). One disadvantage of the cover photography method was that it could not be automated using the available analysis software (Macfarlane et al. 2007a,b,c). An automated and semi-automated method, however, has been developed for trees and crops using MATLAB (The Mathworks Inc., Natick, MA, USA) programming techniques (Fuentes et al. 2008). This study aims at testing a modified automated and semi-automated method using digital imaging and MATLAB programming on grapevines compared to destructive and non-destructive techniques applied in Chile and Australia from downward-looking and upward-looking images, respectively. The technique has been developed further to allow the automated analysis of zenith-orientated videos of grapevine canopies taken from moving vehicles, such as tractors, quad bikes, remote controlled vehicles and robotic vehicles. By geo-referencing these data, the new analysis module allows data mapping to assess spatial distribution of LAI and canopy vigour parameters within the vineyard. Furthermore, in this paper, we contrast geo-referenced LAI data obtained using the cover photography method against the Normalised Difference Vegetation Index (NDVI) from satellites.

Materials and methods

Description of the Chilean site

Data were collected from a drip-irrigated Merlot vineyard located in the Talca Valley, Maule Region, Chile (35° 25′ LS; 71° 32′ LW; 125 m.a.s.l.) during the 2009/10 and 2010/11 growing seasons. The climate of the study area is classified as Mediterranean semi-arid with an average daily temperature of 17.1°C and an average annual rainfall of 679 mm. The summer period is usually dry and hot (2.2% of annual rainfall), while the spring is wet (16% of annual rainfall). The soil at the vineyard is classified as Talca series (Fine family, mixed, thermic Ultic Haploxeralfs) with a clay loam texture and average bulk density of 1.5 g/cm^3. The vineyard was irrigated daily using 4 L/h drippers spaced at intervals of 1.5 m. The vines were planted in 1999 in north-south oriented rows, 2.5 m apart, with 1.5 m within-row spacing and were trained on a vertical shoot-positioned system with the main wire 1 m above the soil surface. The shoots were maintained on a vertical plane by three wires, the highest one located 2 m above the soil surface.

Description of the Australian site

Data were collected during November 2010 and January 2011 in a drought and drought-recovery experiment (DDRE) within a commercial Chardonnay vineyard at Qualco, South Australia, (Yalumba Nurseries: 37° 25.8′ N; 122 ° 05.4′ W). This experiment started in the 2008/09 season using a total area of 3.69 ha with a split-plot randomised complete block design with four replicates. Main plots consisted of three adjacent rows of 30 vines per row that were split into three sub-plots of three adjacent rows of 10 vines per row. The vines in the trial were 8 years old grafted on Ramsey rootstock and trained on a two-wire vertical trellis system with row spacing of 1.8 m between vines and 3 m between rows. The experiment consisted of five main deficit irrigation treatments split into three recovery treatments. The deficit irrigation treatments were: full irrigation or control (C), and reduction to 50 (50S), 30 (30S), 20 (20S) and 10% (10S) of the control. The C treatment represented the amount of irrigation that is normally applied to the vineyard (5 ML/ha in year 1). Recovery treatments consisted of continued deficit irrigation, reverting back to C in 2009/10 (RR) and reverting back to C in 2010/11 (R). All measurements were made on a panel of three vines in the middle of each sub-plot. All treatments were irrigated for 4 h with Netafim Dripmaster pressure compensated in-line drippers with a 2.3 L/h of flow. To apply the reduction in irrigation volume, the interval between irrigations was increased using the Irrigated Crop Management Service (ICMS) Water Budgeting Tool (South Australian Research and Development Institute).

Leaf area index of grapevine canopies measured by allometry

At the Chilean site, LAI was estimated using an allometric relationship between total leaf area per shoot and shoot length as ground truth. Total leaf area per shoot was calculated using scanned images of leaves and total leaf number per shoot. A customised MATLAB code was created to obtain automatically total leaf area per scanned image. Finally, the length of shoots was measured manually with a flexible measuring tape to generate the following empirical equations:

$$LA_{shoot} = -634.86 + 3543.92(SL) \quad (1)$$

$$LAI_a = \frac{\sum_{1}^{j} LA_{shoot}}{A_V} \quad (2)$$

where LAI_a corresponds to LAI by allometry, LA_{shoot} corresponds to the total leaf area per shoot (m^2), A_v was the area designated to the vine (m^2), SL was the shoot length (m), and j was the total shoot number per vine (Poblete-Echeverría and Ortega-Farias 2013).

To follow the development of LAI_a from plants during the two seasons, total shoot length per vine was measured once per week on three representative vines. Digital images from these same plants were captured at the same dates to obtain maximum leaf area index (LAI_M). This allometric procedure is a semi-direct method that relates canopy parameters, such as shoot diameter, shoot length and leaf length, to total leaf area per vine. Allometric equations are widely used in the calculation of LAI_a in vineyards (Montero et al. 2000, Johnson et al. 2003b, Williams and Martinson 2003, Poblete-Echeverria and Ortega-Farias 2009). Because of their accuracy, allometric equations are commonly used as a standard way to validate other methods of LAI estimation (Gower et al. 1999). But allometric equations are site specific and vary with the canopy and climatic conditions (Mencuccini and Grace 1995, Le Dantec et al. 2000).

Measurement of leaf area index of grapevines by plant canopy analyser

At the DDRE, LAI_{2000} was measured with the Li-Cor LAI2000 plant canopy analyser (Li-Cor Inc.); measurements were made at the same time and locations as the digital image acquisition per irrigation treatments following the manufacturer's protocol. Measurements were made in triplicate around the middle plant per irrigation replicate to generate an averaged LAI_{2000} value per replicate ($n = 12$ averaged values per treatment) (Dokoozlian and Kliewer 1995).

Digital image and video acquisition

At the Chilean site, a Samsung camera with a resolution of 5.2 megapixels (Digimax A503, Samsung Group, Seoul, South Korea) mounted on a pole with a bubble level was used to acquire downward looking digital images (at nadir angle) from canopies using the Joint Photographic Experts Group format. Digital images were collected at 3.9 m from the ground covering the area assigned to the vine. Camera settings were configured following the methodology proposed by Fuentes et al. (2008).

For the DDRE, a Nikon SLR D90 (Resolution 12.9 megapixels) with an AFS-Nikon 18–55 mm f/3.5–5.6 G lens (Nikon Corporation, Chiyoda, Tokyo, Japan) was mounted on a flat wooden platform with a bubble level at the zenith angle to acquire upward-looking digital images from approximately 20 cm from the soil surface (Figure 1). Images were acquired and measured LAI_{2000} data collected in November 2010 and January 2011. The camera was set to automatic exposure using F16 lens with the zoom adjusted to cover the whole canopy. Settings were the same for all the pictures taken. Three digital images were obtained from around the middle plant on every replicate per irrigation treatment ($n = 120$ per date). Video was acquired with a high definition (640 × 480 resolution) sport video camera (DVR-460, Swann, Melbourne, Australia) mounted on top of a remote control car.

Figure 1. Typical digital image taken at zenith angle from grapevine canopies. The automated system can deal with clear, cloudy or partially cloudy days as described by Fuentes et al. (2008).

MATLAB script to analyse cover photography

A code developed using MATLAB (version 2011b) and the Image Processing Toolbox (The Mathworks Inc.) was modified and tested to generate a script specific for grapevine canopies to batch process numerous upward-looking digital images taken from vineyards. This methodology has been explained in depth in Fuentes et al. (2008). The image subdivisions used for grapevines was five (total subdivisions = 25) and the big gap criteria = 0.75.

The algorithms used were: the fractions of foliage projective cover (f_f), crown cover (f_c) and crown porosity (Φ), which were calculated from Macfarlane et al. (2007a) as:

$$f_f = 1 - \frac{tg}{tp} \quad (3)$$

$$f_c = 1 - \frac{lg}{tp} \quad (4)$$

$$\Phi = 1 - \frac{f_f}{f_c} \quad (5)$$

where lg = large gap pixels; tg = total pixels in all gaps and tp = total pixels in images.

LAI_M is calculated from Beer's Law.

$$LAI_M = -f_c \frac{\ln \Phi}{k} \quad (6)$$

where k corresponds to the light extinction coefficient k used = 0.7 (Herwitz et al. 2004) and the clumping index at the zenith, $\Omega(0)$, was calculated as follows:

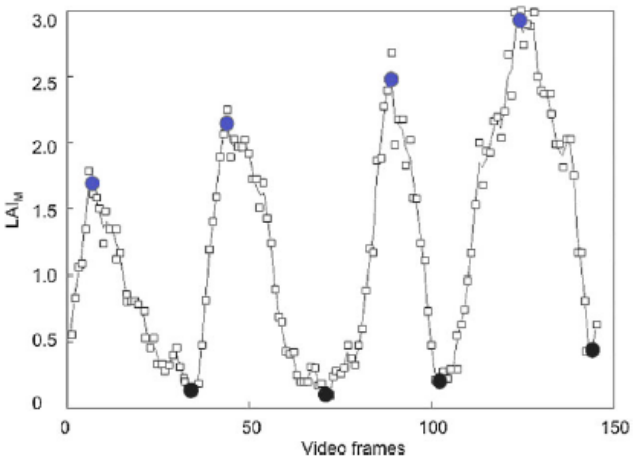

Figure 2. Maximum leaf area index (LAI_M) from automated analysis of video frames (□) using the code developed in MATLAB. Maxima [LAI_M (●)] and minima [LAI_{IrowM} (●)] correspond to LAI from the canopy and contribution from the inter-row, respectively.

$$\Omega(0) = \frac{(1-\Phi)\ln(1-f_f)}{\ln(\Phi)/f_f} \quad (7)$$

The clumping index is a correction factor to obtain effective LAI (LAI_e), which is the product of:

$$\mathrm{LAI}_e = LAI_M\ \Omega(0) \quad (8)$$

Equation 7 describes the non-random distribution of canopy elements. If $\Omega(0) = 1$, means that the canopy displays random dispersion; for $\Omega(0) < 1$, the canopy is defined as clumped.

Automated module to analyse leaf area index from videos

An automated module was added to the original code presented in Fuentes et al. (2008) to analyse upward-looking videos taken from grapevine canopies. The module uses commands from the Image Analysis Toolbox to extract frames (images) from videos that are automatically batch analysed by the original code to obtain LAI_M and canopy vigour parameters (Fuentes et al. 2008). Calculated LAI_M data were obtained per video frame automatically, which were treated as individual images, represented as small open squares in Figure 2. These data were later interpolated using a smooth spline technique (continuous line) and automatically filtered to obtain LAI_M from the row (blue circles) and from the inter-row (LAI_{IrowM}). The latter values correspond to the minima values (black circles). This module allows the use of video cameras mounted on small vehicles that can travel under the canopies transversally through the rows. Videos can also be obtained with a camera mounted on a quad bike along the row. This code was tested on the DDRE.

Satellite remote sensing data

Remote sensing data were obtained from the WorldView-2 satellite (DigitalGlobe, Longmont, CO, USA). Images were acquired for the DDRE on the 7 and 21 November 2011. WorldView-2 is the first commercial high-resolution satellite to provide eight spectral sensors in the visible to near-infrared range. WorldView-2 provides the only high-resolution eight-band multispectral commercial satellite imagery currently available. Along with the four typical multispectral bands: blue (450–510 nm), green (510–580 nm), red (630–690 nm) and near infrared (NIR) (770–895 nm), each sensor is narrowly focused on a particular range of the electromagnetic spectrum that is sensitive to a particular feature from the ground, or a property of the atmosphere. In this study, the values of red NIR_1 were extracted from a fusion image for each grid sample points from the DDRE using the geo-statistical software package ArcGIS version 9.0 (ESRI, Redlands, CA. USA), giving a resolution of 2 m² per pixel. Subsequently, these values were used to calculate the classical normalised vegetation index (NDVI) (Rouse et al. 1974) using the following equations:

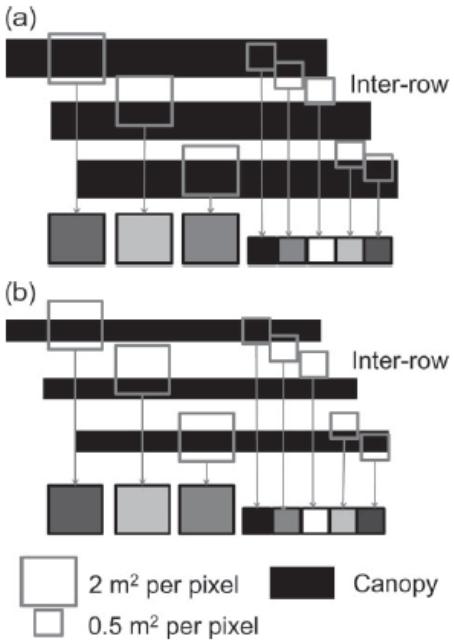

Figure 3. Representation of different pixel resolution obtained at low (0.5 m² per pixel) and high resolution (2 m² per pixel) from the WorldView-2 satellite near-infrared bands for (a) vigorous canopies and (b) less vigorous canopies.

$$NDVI = \frac{NIR - Red}{NIR + Red} \quad (9)$$

The resolution of images obtained from WorldView-2 can be increased to 0.5 m² using a fused WorldView-2 image and the panchromatic image. Data obtained using Equation 9 were compared to geo-referenced LAI_M obtained using the photographic method proposed in this paper. For this, the NDVI data corresponding to geo-referenced positions of ground-truth measurements (LAI_M) per treatment were extracted from the 2 m² image using a customised code developed in MATLAB. A linear model was obtained from the NDVI versus LAI_M. This model was used to generate a LAI_{sat} model from the Australian experimental site.

The image resolution of 2 m² gave more representative results to be compared to ground-measured LAI_M according to the irrigation treatments and canopy sizes within the experiment. This pixel size corresponds to the integrative values of the canopies and inter-row for grapevines (Figure 3). Using the maximum resolution possible of 0.5 m² (by a fusion between NIR and panchromatic bands) resulted in an overestimation of NDVI for the water stressed treatments (<30% full irrigation), since pixels falling inside the area of canopies corresponding to

vigorous and less vigorous canopies which can both present values of NDVI = 1 (Figure 3a,b).

Statistical analysis

The performance of the measured LAI values was compared by linear regression analysis against the estimated values: (i) LAI_M with LAI_a; (ii) LAI_M with LAI_{2000}; and (iii) NDVI with LAI_M. The statistical analysis was performed with MATLAB R2011b Statistical Toolbox and the Curve Fitting Toolbox (The Mathworks, Inc.). The slope and intercepts for each linear regression analysis was tested with a *t*-test using Statgraphics Centurion (Statpoint Technologies Inc., Warrenton, VA, USA). The root mean squared error (RMSE), mean bias error (MBE) and the mean absolute error (MAE) were calculated with the same program following standard methodologies of analysis (English et al. 1989, Wermelinger and Koblet 1990, Haselgrove et al. 2000).

Results

Temporal estimation using LAI_M compared to LAI_a and LAI_{2000}

The allometric model, developed for the cultivar Merlot at the Chilean site, has been previously presented in Poblete-Echeverria and Ortega-Farias (2009). A strong and significant correlation was obtained between LAI_a and LAI_M for both seasons measured at the Chilean site ($r^2 = 0.96$ with $P < 0.05$). The mean absolute error obtained was 8.9% (Figure 4a) and the RMSE = 11.5%. In the same figure, it can be seen that LAI_M values consistently overestimated LAI_a. This overestimation, however, corresponded only to 3% (Table 1). Figure 4b shows the temporal evolution of LAI_a within the 2009/10 and 2010/11 seasons. Both seasons showed a gradual increment in LAI_a from basal values of $LAI_a = 0.2$, at the beginning of the season (budburst), to flowering for the 2009/10 season (DOY = 345), which was 10 days earlier for the 2010/11 season compared to that for the 2009/10 season. Values of LAI_a at flowering corresponded to $LAI_a = 0.92$ and $LAI_a = 0.65$ for the 2009/10 and 2010/11 seasons, respectively. The maximum LA_a value for both seasons was found in pre-veraison (DOY = 14) for the 2009/10 season and DOY = 362 for the 2010/11 season. The first season showed a maximum LAI_a value of 1.71 (reached at DOY = 5, 2010/11 season), which was higher than the second season with LAI_a value of 1.22 (reached at DOY = 14, 2010/11 season) corresponding to a decrease of 29% for cv. Merlot. The clumping index for the Chilean site was close to 1 [$\Omega(0) = 0.986$, data not shown]. Therefore LAI_M and LAI_e were considered equivalent.

For the DDRE, a strong and significant linear correlation across all treatments (Figure 5) was found for LAI_{2000} compared to LAI_M ($r^2 = 0.92$ with $P < 0.05$) for the months of November 2010 and January 2011. The MAE obtained was 6% and RMSE = 7.39% (Table 1). Minimum LAI_M and LAI_{2000} values of around 2.0 were found in November 2010, and maximum values of around 5.5 were found in the month of January 2011 for cv. Chardonnay. January 2011 corresponded to the maximum LAI_M found for this particular site and season, which corresponded to pre-veraison. The clumping index for the DDRE was close to 1 [$\Omega(0) = 0.976$, data not shown]. Therefore LAI_M and LAI_e were considered equivalent.

Spatial estimation of LAI_M compared to NDVI and LAI_{sat}

A linear correlation was obtained from the relationship between NDVI, extracted from the WorldView-2 image and LAI_M (Figure 6). The r^2 was equal to 0.93, which corresponded to a strong and statistically significant correlation ($P < 0.05$) with an MAE = 13%. The model obtained, considering the linear regression passing through the origin, was $LAI_M = 4.44 * NDVI$.

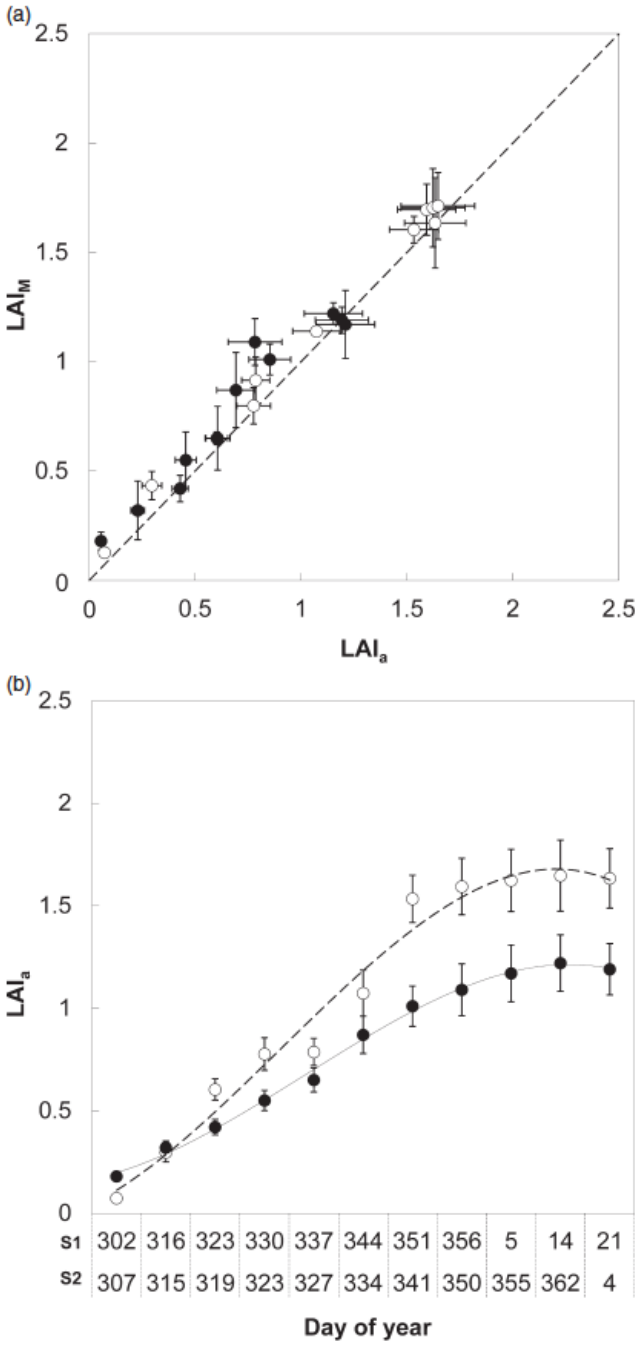

Figure 4. (a) Relationship between the leaf area index measured by allometry (LAI_a) and by the cover photography method (LAI_M) for the cv. Merlot during the seasons 2009/10 (○) and 2010/11 (●) for the Chilean site and (b) seasonal evolution of LAI_a for the two growing seasons studied at the Chilean site. Error bars correspond to the standard deviation of measurements for the LAI_a and LAI_M methods.

Minima values obtained from videos and automated analysis proposed in Figure 2 (LAI_{IrowM}) show the contribution of the inter-row for different irrigation treatments (Figure 7). Stressed treatments showed values close to zero (10 and 20%, and 10R). The highest contribution was found for 30%, 30RR, 30R, 50RR, 50R and C, with values of LAI_{IrowM} of around 0.35. The

Table 1. Statistical analysis for relationships obtained between (i) LAI_M and LAI_a and (ii) LAI_{2000} and LAI_a:

Approach	RMSE	MAE	MBE	r^2	d	a	*n*
LAI_M versus LAI_a	11.5%	8.9%	−8.4%	0.97	0.99	0.11	22
LAI_a versus LAI_{2000}	7.39%	6.01%	−0.34%	0.91	0.98	0.01	25

a, intercept; b, slope; LAI_a, leaf area index measured with allometric procedure; LAI_{2000}, leaf area index measured with the Li-Cor LAI2000 plant canopy analyser; LAI_M, leaf area index estimated with digital photographs; MAE, mean absolute error; MBE, mean bias error; *n*, total number of observations; r^2, coefficient of determination; RMSE, root mean square error.

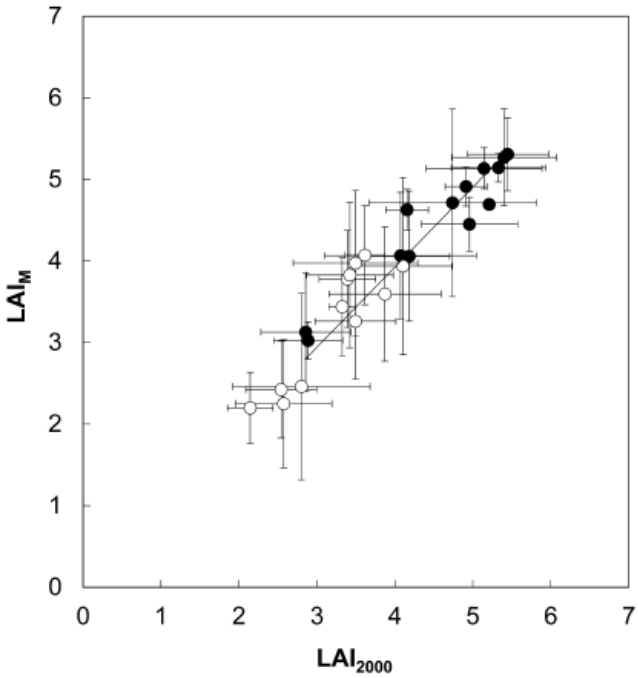

Figure 5. Relationship between the leaf area index measured using the LAI2000 PCA instrument (LAI_{2000}) and the cover photography method (LAI_M) for Chardonnay at the drought and drought-recovery experiment for the months of November 2010 and January 2011. Error bars correspond to the standard deviation of measurements for the LAI_{2000} and LAI_M methods.

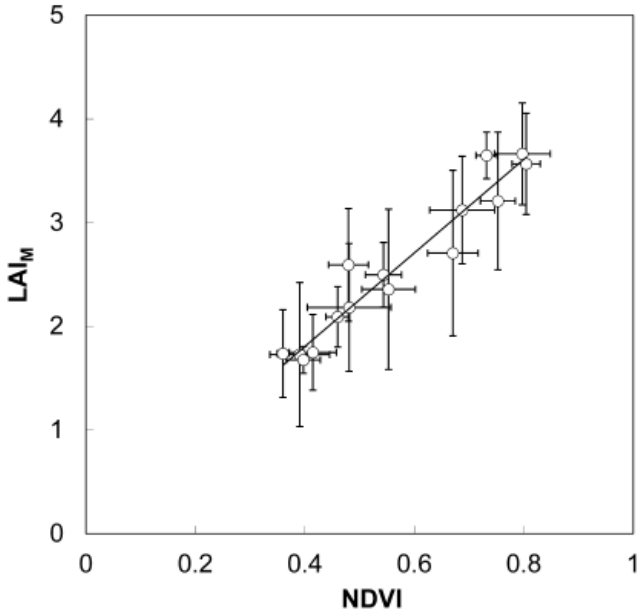

Figure 6. Relationship between the normalised differential vegetation index (NDVI) obtained from WorldView-2 satellite imagery (resolution of 2 m^2 per pixel) and the cover photography method (LAI_M) for Chardonnay at the drought and drought-recovery experiment in November 2010. Error bars correspond to the standard deviation of measurements for the NDVI and LAI_M methods.

stabilisation of the camera needs to be improved for future research to obtain stable videos from irregular terrain.

Discussion

The robustness of the digital image method to estimate LAI of grapevines presented in this paper allows monitoring of LAI through the season. It has been shown that there is a strong and significant correlation between LAI measured in the field and the Kc for grapevines obtained by weighing lysimeters (Williams and Ayars 2005) and by using the micrometeorological approach combined with sap flow sensors (Martin et al. 2007). Usually, Kc can be obtained from tables available from a variety of sources such as FAO paper 56 (Allen et al. 1998). These Kc values, however, were obtained from different agroclimatic conditions than those in which they were intended to be used. Therefore, errors in this factor can result in over or underestimation of crop evapotranspiration within the season (Poblete-Echeverria and Ortega-Farias 2009). Such under or overestimations can result in excessive stress and reduced yield, or overirrigation, which could increase canopy vigour, yield and alter berry composition (Acevedo-Opazo et al. 2010). Therefore, our method could contribute to obtaining specific Kc values adjusted by LAI (Allen et al. 1998).

A clear seasonal effect in canopy growth can be seen in Figure 4b for the Chilean site. Season 2010/11 corresponded mainly to a warmer season (data not shown), which resulted in an advance of phenological stages of around 1 week for flowering and fruitset and 2 weeks for veraison.

Temporal assessment of canopy vigour can be determined by a variety of instrumentation available in the market, such as the Li-Cor LAI-2000 (or LAI-2200) plant canopy analyser as shown in Figure 4 (Li-Cor Inc.), or the AccuPAR LP-80 (Decagon Devices, Pullman, WA, USA). For practical applications, however, these instruments can be cost prohibitive. The method proposed was developed using a digital camera for the Chilean site and a semi-professional camera for the DDRE. Similar results and comparisons with allometric and indirect LAI measurements were obtained. These results are consistent with LAI studies using cover photography and comparisons between low-cost digital cameras with single-lens reflex (SLR) cameras (Nikon D80) (Fuentes et al. 2012). Therefore, the cover photography method is an accurate and cost-effective method for

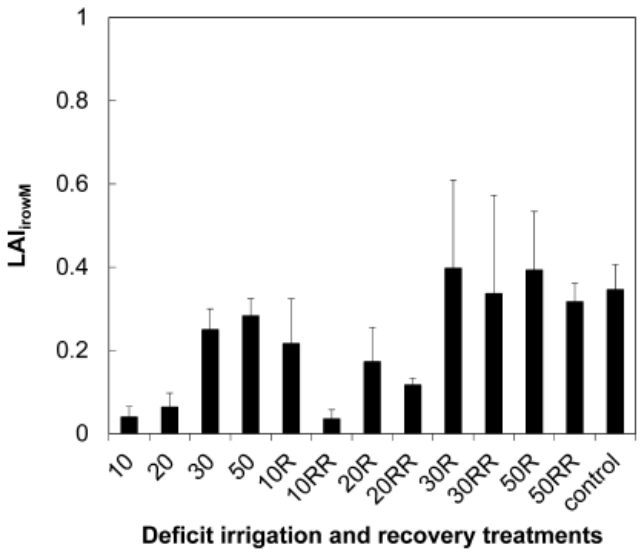

Figure 7. Effect of irrigation treatment on the vegetative inter-row contribution (LAI_{IrowM}) obtained by analysing minima values from video outputs at the drought and drought-recovery experiment for Chardonnay in November 2010. Error bars correspond to the standard deviation of measurements for the LAI_{IrowM} method. The deficit irrigation and recovery treatments were: full irrigation or control (C), and reduction to 50 (50S), 30 (30S), 20 (20S) and 10% (10S) of C. The C treatment represented the amount of irrigation that is normally applied to the vineyard (5 ML/ha in year 1). Recovery treatments consisted of continued deficit irrigation, reverting back to C in 2009/10 (RR) and reverting back to C in 2010/11 (R).

practical applications and scientific research involving canopy size assessments.

For practical reasons, the upward-looking images (Australia) are easier to obtain compared to the downward-looking images (Chile). The latter was only possible due to the absence of green material in the inter-row (bare soils). This method will not work with the inclusion of weeds or cover crops in the inter-row, since it will make difficult the discrimination between the canopy and the background for an automated method.

It is important to note that according to data presented in Figure 4a, the overestimation of LAI_M compared to that of LAI_a can be explained by the inclusion of cordons and shoots in the images obtained to calculate LAI_M, which were not considered in the development of the LAI_a model. The non-leaf material included can be assessed early in the season (budbreak), in which most of the LAI_M registered corresponds to the contribution of grapevine cordons and pruned shoots (Figure 4a, $LAI < 1$).

Spatial assessment of LAI_M and geo-referenced LAI_M compared to NDVI

Temporal and spatial assessment of LAI and canopy cover obtained using satellite platforms (downward-looking images) has been reported as a suitable method compared to upward-looking digital images as ground truth for forestry environments (Fuentes et al. 2008, Palmer et al. 2008, 2010). Some of these environments, however, showed an overestimation up to 17% approximately of LAI due to the incorporation of the understorey component from satellite imagery (Fuentes et al. 2008). The latter will pose a problem for the use of satellite imagery for vineyards in Australian growing regions, since the use of cover crops could introduce an overestimation of real LAI, especially at early and mid-season.

Satellite-based imagery has limited application in crop management in general due to the low spatial and temporal resolution of these platforms (Herwitz et al. 2004, Torres-Sánchez et al. 2013). Spatial and temporal resolution has been improved in new commercial satellites, such as Ikonos, Quickbird, WorldView (1 and 2), GeoEye, RapidEye and Pleyades; however, images from these new satellites images are expensive. They also require a high level of know-how to treat and analyse images to obtain meaningful results that can be transferable to growers. Currently, free satellite images are limited to medium-resolution sensors, such as Landsat 7ETM+ providing 60 m pixel size images and Moderate Resolution Imaging Spectroradiometer (MODIS) providing 500 m pixel size images, which are impractical for site-specific agricultural applications, since a significant level of spatial variability of vegetative growth can be commonly found in vineyard blocks (Hall et al. 2008) and for extensive experimental trials. These differences will probably result in variability of fruit composition, yield and grapevine physiology among other factors, because of the modification of light interception by the fruit zone and the renewal zone of grapevines.

The method proposed in this paper using cover photography and a rapid method of data acquisition and analysis, with still and video cameras mounted on robotic vehicles, can result in inexpensive and accurate growth and LAI maps, offering a valuable tool for scientific experiments and viticultural management in general. Furthermore, results comparing the LAI_M and NDVI from this study indicate that the method proposed is highly correlated to high-resolution satellite data.

In previous studies, it has been shown that NDVI may be a poor indicator of vegetation index for vineyard canopy characteristics (Zarco-Tejada et al. 2005). The main problem of NDVI as a vegetation index for grapevine canopies is that vineyards present a non-continuous canopy consisting of grapevine rows and inter-row space, which are different for those found in broad-acre crops, such as cereals and legumes. Furthermore, grapevine canopies are distributed in a three-dimensional wall array, the shape of which will depend on the training system. The cover photography method showed a high correlation with NDVI obtained from high-resolution satellite data; therefore, it can be a suitable tool to obtain spatial two-dimensional maps of vineyards or of research experiments of grapevines without considering the cover crop contribution (used in the inter-row to take up excessive soil moisture from winter time and heavy rainfalls) (Barbeau et al. 2005a,b). The advantage of satellite or airborne NDVI maps is that they are instant snapshots of spatial distribution of vegetative cover in a large area. Remote sensed imagery, however, can also be cost prohibitive to achieve a temporal assessment of canopy growth within a season.

The versatility of the analysis method described by using MATLAB computations and cover image analysis allows the handling of large data sets, such as those acquired with digital cameras or videos. By either geo-referencing a large number of digital images obtained spatially, it is possible to compare LAI_M with airborne or satellite NDVI data from vineyards. Such comparisons have been previously done for LAI_M obtained in different Australian forests and LAI_{MODIS} obtained from satellite at low-spatial resolution (250 m^2 per pixel) (Fuentes et al. 2008). Analysis of satellite imagery at low-spatial-resolution (Ikonos with 4 m^2 resolution per pixel) has resulted in a significant correlation between LAI and NDVI for multiple vineyards (Johnson et al. 2001, Johnson 2003a). Our study selected the 2 m^2 per pixel resolution, since it integrates the proportion of canopy to inter-row space, which is independent of pixel

location relative to grapevines and inter-row (Figure 3a). Imagery from the WorldView-2 satellite allows a maximum resolution of 0.5 m^2 (using a fusion between NIR and panchromatic bands). Using the latter to compare LAI_M and NDVI could present a problem in the pixel extraction method, which can be a source of bias due to the high NDVI values (NDVI = 0.75–0.95) from pixels that fall covering just the top canopies without inter-row inclusion (Figure 2).

The video analysis capabilities from the code developed in MATLAB allow the extraction of LAI_M from videos obtained from a vehicle travelling under the canopies transversally to the rows (continuous data using robots). Values exactly below the canopy (maxima) and values in the middle of the inter-row (minima) can be automatically extracted (Figure 2). LAI_M from the inter-row may not be necessarily zero for vigorous canopies (i.e. 50% and C treatments), in which shoots can grow towards the middle of the inter-row and in extreme cases touch with shoots from the following row (partial canopy closure) (Figure 7).

Conclusions

This work has demonstrated the strong relationships that exist between the proposed method (LAI_M) and allometry (LAI_a), specialised LAI instrumentation (LAI_{2000}) and spatial assessment using satellite platforms (NDVI). Digital image and video acquisition, coupled with MATLAB image data analysis, provides a rapid, robust, cheap and simple method to obtain LAI of grapevine canopies. This method can be applied for managerial purposes on commercial vineyards to assess the spatial variability of canopy growth within a field and for experimental research of the effect of treatments on canopy growth and vigour. Finally, the LAI_M method can be used to develop models to calibrate indices obtained by remote sensed data (airborne or satellite). Through application of the latter method it will be possible to obtain more accurate and representative spatial maps for larger spatial scales.

Aknowledgements

This project is supported by Australia's grape growers and winemakers through their investment body the Grape and Wine Research and Development Corporation, with matching funds from the Australian government. The four organisations, involved in this research project, The University of Adelaide, Commonwealth Scientific and Industrial Organisation, South Australian Research and Development Institute, The Australian Research Institute, are all part of the Wine Innovation Cluster (www.wineinnovationcluster.com).

The authors thank staff from Yalumba Nurseries whose in-kind contribution has included irrigation supplies, irrigation system conversion and management of the vineyard, staff from the Irrigated Crop Management Service (ICMS) who designed the irrigation system conversion and have provided ongoing irrigation system advice, staff at Measurement Engineering Australia for in-kind contribution of field monitoring equipment. This project has been also undertaken on a collaborative basis with Universidad de Talca through the research program 'Adaptation of Agriculture to Climate Change (A2C2)' and Chilean projects CONICYT (No 79090035) and FONDECYT (No 3100128 and 11130601). Finally, we acknowledge the support given by Digital Globe Geospatial Industries for the WorldView-2 images.

References

Acevedo-Opazo, C., Ortega-Farias, S. and Fuentes, S. (2010) Effects of grapevine (*Vitis vinifera* L.) water status on water consumption, vegetative growth and grape quality: an irrigation scheduling application to achieve regulated deficit irrigation. Agricultural Water Management **97**, 956–964.

Allen, R.G., Pereira, L.S., Raes, D. and Smith, M. (1998) Crop evapotranspiration: guidelines for computing crop water requirements. FAO irrigation and drainage paper No. 56 (Food and Agriculture Organization: Rome, Italy).

Arias, D., Calvo-Alvarado, J. and Dohrenbusch, A. (2007) Calibration of LAI-2000 to estimate leaf area index (LAI) and assessment of its relationship with stand productivity in six native and introduced tree species in Costa Rica. Forest Ecology and Management **247**, 185–193.

Barbeau, G., Goulet, E., Ramillon, D., Rioux, D., Blin, A. and Marsault, J. (2005a) Effects of the interaction between rootstock and grass sward on the agronomic behaviour of the grapevine (*Vitis vinifera* L., cv. Cabernet Franc et Chenin) (GESCO: Geisenheim, Germany) pp. 103–108. XIV International GESCO viticulture congress; 23–27 August 2005; Geisenheim, Germany.

Barbeau, G., Ramillon, D., Blin, A., Marsault, J. and Landure, J. (2005b) Combined effects of the grass sward and rootstock on the agronomic behaviour of Cabernet Franc and Chenin. Role of the annual climate (GESCO: Geisenheim, Germany) pp. 155–160. XIV International GESCO viticulture congress; 23–27 August 2005; Geisenheim, Germany.

Bergqvist, J., Dokoozlian, N. and Ebisuda, N. (2001) Sunlight exposure and temperature effects on berry growth and composition of Cabernet Sauvignon and Grenache in the Central San Joaquin Valley of California. American Journal of Enology and Viticulture **52**, 1–7.

Bréda, N.J.J. (2003) Ground-based measurements of leaf area index: a review of methods, instruments and current controversies. Journal of Experimental Botany **54**, 2403–2417.

Cutini, A., Matteucci, G. and Mugnozza, G.S. (1998) Estimation of leaf area index with the Li-Cor LAI 2000 in deciduous forests. Forest Ecology and Management **105**, 55–65.

Dokoozlian, N. and Kliewer, W. (1995) The light environment within grapevine canopies. II. Influence of leaf area density on fruit zone light environment and some canopy assessment parameters. American Journal of Enology and Viticulture **46**, 219–226.

English, J., Thomas, C., Marois, J. and Gubler, W. (1989) Microclimates of grapevine canopies associated with leaf removal and control of Botrytis bunch rot. Phytopathology **79**, 395–401.

Esteban, M.A., Villanueva, M.J. and Lissarrague, J.R. (1999) Effect of irrigation on changes in berry composition of Tempranillo during maturation. Sugars, organic acids and mineral elements. American Journal of Enology and Viticulture **50**, 418–434.

Esteban, M.A., Villanueva, M.J. and Lissarrague, J.R. (2001) Effect of irrigation on changes in the anthocyanin composition of the skin of cv Tempranillo (*Vitis vinifera* L.) grape berries during ripening. Journal of the Science of Food and Agriculture **81**, 409–420.

Ewert, F. (2004) Modelling plant responses to elevated CO_2: how important is leaf area index? Annals of Botany **93**, 619–627.

Fuentes, S., Palmer, A.R., Taylor, D., Zeppel, M., Whitley, R. and Eamus, D. (2008) An automated procedure for estimating the leaf area index (LAI) of woodland ecosystems using digital imagery, MATLAB programming and its application to an examination of the relationship between remotely sensed and field measurements of LAI. Functional Plant Biology **35**, 1070–1079.

Fuentes, S., De Bei, R., Pozo, C. and Tyerman, S.D. (2012) Development of a smartphone application to characterise temporal and spatial canopy architecture and leaf area index for grapevines. Wine & Viticulture Journal **27** (6), 56–60.

Gower, S.T., Kucharik, C.J. and Norman, J.M. (1999) Direct and indirect estimation of leaf area index, fAPAR, and net primary production of terrestrial ecosystems. Remote Sensing of Environment **70**, 29–51.

Guidoni, S., Mannini, F., Ferrandino, A., Argamante, N. and Di Stefano, R. (1997) The effect of grapevine leafroll and rugose wood sanitation on agronomic performance and berry and leaf phenolic content of a Nebbiolo clone (*Vitis vinifera* L. American Journal of Enology and Viticulture **48**, 438–442.

Hall, A., Louis, J. and Lamb, D.W. (2008) Low-resolution remotely sensed images of winegrape vineyards map spatial variability in planimetric canopy area instead of leaf area index. Australian Journal of Grape and Wine Research **14**, 9–17.

Haselgrove, L., Botting, D., van Heeswijck, R., Høj, P.B., Dry, P.R., Ford, C. and Land, P. (2000) Canopy microclimate and berry composition: the effect of bunch exposure on the phenolic composition of *Vitis vinifera* L cv. Shiraz grape berries. Australian Journal of Grape and Wine Research **6**, 141–149.

Herwitz, S.R., Johnson, L.F., Dunagan, S.E., Higgins, R.G., Sullivan, D.V., Zheng, J., Lobitz, B.M., Leung, J.G., Gallmeyer, B.A., Aoyagi, M., Slye, R.E. and Brass, J.A. (2004) Imaging from an unmanned aerial vehicle:

agricultural surveillance and decision support. Computers and Electronics in Agriculture **44**, 49–61.
Johnson, L., Roczen, D. and Youkhana, S. (2001) Vineyard canopy density mapping with IKONOS satellite imagery. van Henken, E.J., Goense, D. and Lokhorst, C., eds. Proceedings of the 3rd international conference on geospatial information in agriculture and forestry; 5–7 November 2001; Denver, CO, USA (Wageningen Academic Publishers: Wageningen, The Netherlands) 1–10.
Johnson, L.F. (2003a) Temporal stability of an NDVI-LAI relationship in a Napa Valley vineyard. Australian Journal of Grape and Wine Research **9**, 96–101.
Johnson, L.F., Roczen, D.E., Youkhana, S.K., Nemani, R.R. and Bosch, D.F. (2003b) Mapping vineyard leaf area with multispectral satellite imagery. Computers and Electronics in Agriculture **38**, 33–44.
Le Dantec, V., Dufrêne, E. and Saugier, B. (2000) Interannual and spatial variation in maximum leaf area index of temperate deciduous stands. Forest Ecology and Management **134**, 71–81.
Macfarlane, C., Coote, M., White, D.A. and Adams, M.A. (2000) Photographic exposure affects indirect estimation of leaf area in plantations of *Eucalyptus globulus* Labill. Agricultural and Forest Meteorology **100**, 155–168.
Macfarlane, C., Grigg, A. and Evangelista, C. (2007a) Estimating forest leaf area using cover and fullframe fisheye photography: thinking inside the circle. Agricultural and Forest Meteorology **146**, 1–12.
Macfarlane, C., Arndt, S.K., Livesley, S.J., Edgar, A.C., White, D.A., Adams, M.A. and Eamus, D. (2007b) Estimation of leaf area index in eucalypt forest with vertical foliage, using cover and fullframe fisheye photography. Forest Ecology and Management **242**, 756–763.
Macfarlane, C., Hoffman, M., Eamus, D., Kerp, N., Higginson, S., McMurtrie, R. and Adams, M. (2007c) Estimation of leaf area index in eucalypt forest using digital photography. Agricultural and Forest Meteorology **143**, 176–188.
Martin, P., Zarco-Tejada, P., Gonzalez, M. and Berjon, A. (2007) Using hyperspectral remote sensing to map grape quality in Tempranillo vineyards affected by iron deficiency chlorosis. Vitis **46**, 7–14.
Mencuccini, M. and Grace, J. (1995) Climate influences the leaf area/sapwood area ratio in Scots pine. Tree Physiology **15**, 1–10.
Montero, F.J., de Juan, J.A., Cuesta, A. and Brasa, A. (2000) Nondestructive methods to estimate leaf area in *Vitis vinifera* L. Hortscience: A Publication of the American Society for Horticultural Science **35**, 696–698.
Oliveira, M. and Santos, M. (1995) A semi-empirical method to estimate canopy leaf area of vineyards. American Journal of Enology and Viticulture **46**, 389–391.
Palmer, A.R., Fuentes, S., Taylor, D., Macinnis-Ng, C., Zeppel, M., Yunusa, I., February, E. and Eamus, D. (2008) The use of pre-dawn leaf water potential and MODIS LAI to explore seasonal trends in the phenology of Australian and southern African woodlands and savannas. Australian Journal of Botany **56**, 557–563.
Palmer, A.R., Fuentes, S., Taylor, D., Macinnis-Ng, C., Zeppel, M., Yunusa, I. and Eamus, D. (2010) Towards a spatial understanding of water use of several land-cover classes: an examination of relationships amongst pre-dawn leaf water potential, vegetation water use, aridity and MODIS LAI. Ecohydrology **3**, 1–10.
Poblete-Echeverría, C., Ortega-Farias, S., Zuñiga, M. and Fuentes, S. (2012) Evaluation of compensated heat-pulse velocity method to determine vine transpiration using combined measurements of eddy covariance system and microlysimeters. Agricultural Water Management **109**, 11–19.
Poblete-Echeverría, C. and Ortega-Farias, S. (2009) Estimation of actual evapotranspiration for a drip-irrigated Merlot vineyard using a three-source model. Irrigation Science **28**, 65–78.
Poblete-Echeverría, C.A. and Ortega-Farias, S.O. (2013) Evaluation of single and dual crop coefficients over a drip-irrigated Merlot vineyard (*Vitis vinifera*L.) using combined measurements of sap flow sensors and an eddy covariance system. Australian Journal of Grape and Wine Research **19**, 249–260.
Rouse, J.W., Haas, R.H., Schell, J.A. and Deering, D.W. (1974) Monitoring vegetation systems in the Great Plains with ERTS. Third ERTS symposium (NASA: Washington, DC, USA) pp. 309–317. 10–14 December 1973; Washington, DC, USA.
Rügner, A., Rumbolz, J., Huber, B., Bleyer, G., Gisi, U., Kassemeyer, H.H. and Guggenheim, R. (2002) Formation of overwintering structures of Uncinula necator and colonization of grapevine under field conditions. Plant pathology **5**, 322–330.
Smart, R.E. (1985) Principles of grapevine canopy microclimate manipulation with implications for yield and quality. A review. American Journal of Enology and Viticulture **36**, 230–239.
Torres-Sánchez, J., López-Granados, F., De Castro, A. and Peña-Barragán, J. (2013) Configuration and specifications of an unmanned aerial vehicle (UAV) for early site specific weed management. PLoS ONE **8** (3), e58210.
Villalobos, F.J., Orgaz, F. and Mateos, L. (1995) Non-destructive measurement of leaf area in olive (Olea europaea L.) trees using a gap inversion method. Agricultural and Forest Meteorology **73**, 29–42.
Watson, D.J. (1947) Comparative physiological studies on the growth of field crops: I. Variation in net assimilation rate and leaf area between species and varieties, and within and between years. Annals of Botany **11**, 41–76.
Wermelinger, B. and Koblet, W. (1990) Seasonal growth and nitrogen distribution in grapevine leaves, shoots and grapes. Vitis **29**, 15–26.
Whitley, R., Zeppel, M., Armstrong, N., Macinnis-Ng, C., Yunusa, I. and Eamus, D. (2008) A modified Jarvis-Stewart model for predicting stand-scale transpiration of an Australian native forest. Plant and Soil **305**, 35–47.
Williams, L. and Martinson, T.E. (2003) Nondestructive leaf area estimation of 'Niagara' and 'DeChaunac' grapevines. Scientia Horticulturae **98**, 493–498.
Williams, L.E. and Ayars, J.E. (2005) Grapevine water use and the crop coefficient are linear functions of the shaded area measured beneath the canopy. Agricultural and Forest Meteorology **132**, 201–211.
Zarco-Tejada, P.J., Berjón, A., López-Lozano, R., Miller, J.R., Martín, P., Cachorro, V., González, M.R. and de Frutos, A. (2005) Assessing vineyard condition with hyperspectral indices: leaf and canopy reflectance simulation in a row-structured discontinuous canopy. Remote Sensing of Environment **99**, 271–287.
Zeppel, M., Macinnis-Ng, C., Ford, C. and Eamus, D. (2008) The response of sap flow to pulses of rain in a temperate Australian woodland. Plant and Soil **305**, 121–130.

Manuscript received: 22 October 2012
Revised manuscript received: 24 October 2013
Accepted: 15 March 2014

7. Outcome/Conclusion

7.1 Comparison of project performance against planned outputs.

All anticipated earlier year outputs were largely met from the project except for *Wine made from 2 –year stressed vines* in 2009-10. Yalumba made wines from the treatments from year 1 and commercial sized ferments from year 2: 10% irrigation (plus recovery), 50% irrigation (plus recovery) and control; a total of five wines, 2-3 tonnes per treatment were made. These were not replicated and assessment data are not available at the time of writing this report. Replicated wine making and sensory assessment were not achieved because of resource limitations in terms of personnel available to make a set of fully replicated wines from across the trial, and funding limitation that prevented outsourcing of winemaking and sensory analysis.

The broader outputs of the project as listed in the original agreement for the final two years of the project are listed below with a short description of each that have occurred or that are pending.

Integration of 4 years of field data during water stress and various periods of recovery.

Chapters 6.1, 6.2, 6.3, 6.4, 6.5 provide integration of field data over 4 years of sustained deficit irrigation and up to three years of recovery. Each of these chapters forms the basis of a future publication.

Near Infrared Reflectance Spectroscopy methods to rapidly measure vine water stress and carbohydrate allocation.

Chapters 6.6 and 6.7 describe the methods, with Chapter 6.7 already published. The advantages of these methods are the speed of the analysis (less than 30 seconds required for the NIR spectrum to be collected), the elimination of the use of chemical reagents in the case of carbohydrate analysis, and the elimination of bulky pressurised equipment in the case of water potential measurements.

Industry update on trial outcomes from 4 years.

Industry uptake, mainly by Treasury Wine Estates, Wynns Coonawarra, has occurred for the NIR measurement of vine water potential and the development of an iPhone app for leaf area index both of which were developed in this project (Chapter 6.7 & 6.9).

Knowledge on long-term effects of water deficit and 2 yr recovery on vine physiology.

This is fully described in Chapter 6.1 and represents the first ever trial of this kind. The work will be submitted for a full publication in the near future.

Knowledge on long-term effects of water deficit and 2 yr recovery on growth and production.

This is fully described in Chapter 6.2, 6.3, 6.4 and 6.5 and again represents the first ever trial of this kind. Each of these Chapters will be submitted as full publications in the near future.

Integration of 5 years of field data during water stress and various periods of recovery.

This is presented in each of the Chapters described above.

Industry update on final trial outcomes from 5 years.
The last industry update occurred with a publication in August 2011 in the Wine and Viticulture Journal (see publication list, Appendix 1. We intend to submit another for the full trial in the near future to summarise the main outcomes and industry implications as detailed in this report.

Innovators Network material developed.

This has yet to be done, but it is anticipated that a series of fact sheets can now be developed from the total analysis of the trial that is detailed in this report.

Final report to GWRDC

This report was late as a result of time-pressure on the PI due to teaching commitments and loss of staff at UA, and loss of staff from the R&D sector placing more onus on the PI for data analysis.

7.2 Practical implications of the research results for the Australian grape and wine industry.

Each chapter from this report contains outcomes that have practical implications, particularly in relation to how to manage vines under sustained deficit irrigation (SDI) and how to more efficiently measure vine water stress and leaf area development. These are outlined below, but the reader is also referred to the detailed discussions and conclusions in each Chapter.

Chapter 6.1 Effect of SDI and recovery on vine water relations and gas exchange.

Methods that are used to monitor vine water stress include measures of vine water potential using the pressure chamber, or consequences of vine transpiration that include: sap flow, stomatal conductance or canopy temperature. We showed that midday stem water potential was a good indicator of vine water stress over long-term SDI and furthermore that this could be calibrated against a near infrared reflectance spectral pattern to rapidly monitor vine water stress (Chapter 6.7). NIR instruments are now available in a price range that makes it feasible for companies to invest in this technology and this has been trialled by Wynns Coonawarra. We also showed that stomatal conductance was the most sensitive parameter in terms of assessment of physiological recovery after SDI. The canopy temperature reflects the stomatal conductance and can be used to measure the degree of water stress, integrated over a whole canopy, quite accurately as described in Chapter 6.8 using IR thermal imaging. Thermal cameras have greatly reduced in price and are now within the price range that may make them feasible for use in viticulture using the methods described in Chapter 6.8.

In respect of the levels of SDI and their absolute effects on vine physiology, the 50% treatment showed only small reductions in leaf water potential or leaf gas exchange. This would indicate that this level of reduction in irrigation would have only minimal effects on vine physiology, yet the reductions in amount of water applied are substantial. Of all the SDI treatments the 20% appeared to give the optimum g_s and A suggested from the literature, but leaf water potentials

were often more negative than observed in the other treatments, suggesting that the 30% treatment may be a safer option as a target based on leaf physiology. However it would not be recommended to reduce the depth of irrigation since this option resulted in greater vine stress and greater reduction in vine productivity compared to the equivalent (30%) amount of irrigation but at reduced frequency.

Chapter 6.2 Vine productivity, water productivity and vine balance.

It is very likely that the Australian wine industry will face water shortages as experienced in the millennium drought more frequently into the future. We are currently experiencing one of the most intense *El Nino* events since 1998 that will also lead to drought conditions in SE Australia. Thus it is likely that future water shortages will require long-term SDI in some irrigated areas. The following points are critical for planning of SDI strategies, but it must be noted that this only applies to Chardonnay on Ramsey rootstock and may not be relevant for other varieties on own roots or different rootstocks:

- Yield was reduced in proportion to irrigation plus effective rain and we provide the quantitative descriptors of total yield and yield components of the relationship that may be used to predict future productivity under SDI. The relationship was unaltered by length of time under SDI, but was more dependent on seasonal impacts on yield potential.
- There is a trend in SDI for vines to compensate yield towards higher levels resulting in the yield-to-pruning weight increasing. This puts more stress on carbohydrate reserves. Thus the impact of SDI may be reduced by altering vine balance (i.e. reduce buds per metre, or bunch thinning). Clusters per vine were not reduced by SDI.
- As a conservative estimate for complete recovery of yield after one year of deficit this would be in the third season of full irrigation, but can occur earlier for less extreme reductions in irrigation (i.e. 30% or 50%).
- After recovery there may be an over compensation effect with higher yields in the fourth season of recovery.

Chapter 6.3 Berry composition and ripening.

As for yield we provide important information that may be used to predict the impacts of SDI on productivity and grape quality in drought years. The main practical implications of the work pertaining to Chardonnay on Ramsey are:

- Only for the more extreme SDI were there consistent increases in TSS across seasons.
- Solutes per berry were reduced by deficit in proportion to the degree of deficit and generally gave more significant responses than TSS.
- Juice pH increased proportionally with SDI severity and was the most sensitive of the berry composition parameters measured.
- Titratable acidity decreased with severity of SDI.
- Recovery in berry composition after one year of deficit was complete, but there was a carry-over into the recovery season after two years of continuous deficit. This was more obvious at more extreme SDI and with juice pH.
- There was a trend for overshoot in solutes per berry in subsequent recovery years after a deficit year that was more obvious for the more extreme SDI.

- Successive seasons of SDI gave the same characteristics of the effects of total water applied on pH, indicating that if carry-over occurred from previous deficits this did not change significantly the response in pH to total water received by the vines.

Chapter 6.4 Carbohydrate dynamics

There are important practical implications uncovered by our investigation of carbohydrate dynamics, mainly in the trunk wood, that may also be used to better manage SDI in drought years. The main practical implications of the work pertaining to Chardonnay on Ramsey are:

- At dormancy there were no significant differences between any SDI treatments, suggesting that post-harvest leaf photosynthesis in stressed vines was adequate to replenish the non-structural carbohydrate (NSC) in trunks to control levels, despite lower leaf area in SDI and lower assimilation rates. This implies that good management of vines post-harvest is critical in allowing them to replenish stored carbohydrate for spring growth under SDI and also suggests that management of vine balance (reducing yield to canopy size ratio) may reduce the impact of SDI in the long term.
- A measure of budburst trunk NSC concentrations could be used to predict final harvest yield in that season. The correlation we observed not only explained variation caused by SDI but also differences between seasons and in particular the large difference in yield between the 2009-10 season (low yield) and the other seasons.
- For the most extreme reduction in irrigation (10%) there appeared to be a longer lag for recovery for trunk starch at harvest, but complete recovery of starch concentration after one year of reduced irrigation occurred at the end of the second season.
- Trunk capacity to store NSC is also dependent on total wood volume and after four years of SDI there were significant (50%) reductions in storage capacity for the 10%, 20% and 30% SDI, but not for the 50% treatment. Recovery in trunk capacity is slower than recovery in concentration of NSC since it requires a growth response to compensate for reduced growth over previous seasons of deficit.

Chapter 6.5 Root growth dynamics

This Chapter revealed some unexpected results in terms of resilience of roots to SDI.

- Despite up to four seasons of SDI as low as 10% of control irrigation, only very limited effects were seen on vine root growth.
- There were no effects of deficit irrigation in the dripper-wetting zone. Soil coring at 0.2 m from the dripline, found only small effects, significant only over a number of seasons.
- These results demonstrate the resilience of the root system when faced with soil water stress and the ability of the vine to increase the resource allocation to the root system under these circumstances.
- We also demonstrated the remarkable longevity of fine roots of Ramsey rootstock under the conditions of the experiment.

Chapter 6.6 Measurement of carbohydrate concentration in grapevine trunk or leaf tissues using near infrared spectroscopy.

- Results from this study showed that NIR can be used to predict starch and total non-structural carbohydrate concentration in freeze-dried and ground grapevine trunk and leaf tissues.
- It was demonstrated that a robust universal model could be applied to the prediction of TNC in both leaves and trunks, making it a practical tool for a rapid screening of CHO concentration in grapevine tissues.

Chapter 6.7 Non-destructive measurement of grapevine water potential using near infrared spectroscopy.

- This study showed that grapevine leaf water potential can be measured non-destructively and rapidly using NIR spectroscopy using appropriate calibrations.
- Observed differences in the NIR spectra were related to the leaf surface in which the spectra were collected, and this had an effect on the accuracy of the calibration statistics for water potential. Therefore calibrations need to be checked for different varieties.
- However, the global calibrations built using data obtained from glasshouse and field studies on two varieties are indicative that, in the future, a universal calibration, able to predict water potential for all varieties in different environments can be built.

Chapter 6.8 Computational water stress indices obtained from thermal image analysis of grapevine canopies.

- We showed the use of semi-automated and automated infrared image analysis techniques to obtain accurate plant water status indicators using MATLAB programming tools.
- Results can be acquired in a rapid form and applied for irrigation scheduling.
- Due to the sensitivity of infrared thermography, this technique can be used to implement irrigation techniques such as regulated deficit irrigation (RDI) or partial root-zone drying (PRD), which require narrow plant water status thresholds to maximise grape quality and water use efficiency, and minimise detrimental effects on yield.

Chapter 6.9 Automated estimation of leaf area index from grapevine canopies using cover photography, video and computational analysis methods.

- This work has demonstrated the strong positive correlations that exist between our method of measuring leaf area index (LAI) using cover photography and image analysis, and that obtained from allometry, specialised LAI instrumentation (LAI2000) and spatial assessment using satellite platforms (NDVI).
- Digital image and video acquisition, coupled with MATLAB image data analysis, provides a rapid, robust, cheap and simple method to obtain LAI of grapevine canopies.
- This method can be applied for managerial purposes on commercial vineyards to assess the spatial variability of canopy growth within a field and for experimental research of the effect of treatments on canopy growth and vigour.
- Our method can be used to develop models to calibrate indices obtained by remotely sensed data (airborne or satellite).

- Our method has been applied to an iPhone app that is now released on iTunes (VitiCanopy).

8. Recommendations

8.1 Identification of future research directions.

Chapter 6.1 Effect of SDI and recovery on vine water relations and gas exchange.

Vine hydraulic conductivity was identified as a potential limitation to recovery of vines after SDI. This is largely a result of changes to the root system, yet only small effects occurred in root density under SDI (Chapter 6.5). This indicates that physiological changes occurred in the water-carrying capacity of roots under SDI and this warrants further investigation and comparison between rootstocks.

Chapter 6.2 Vine productivity, water productivity and vine balance.

Further investigation is required to understand how vines are able to compensate yield towards higher levels under SDI resulting in the yield-to-pruning weight increasing. The link between vine balance and tolerance to long-term SDI and recovery rates is worthy of further investigation. It is likely that there will be effects of rootstock and scion on this capacity.

The recovery information may suggest a strategy for handling reduced irrigation allocations, i.e. one year at 10% SDI followed by one year at 50%, potentially allowing reasonable yields and quality over a several-year time frame. This "year-to-year pulsed-SDI" strategy may also condition vines for SDI in the future and it would be a worthy area for future research.

Chapter 6.3 Berry composition and ripening.

It is not clear why juice pH increased proportionally with SDI severity and was the most sensitive of the berry composition parameters measured. This may be the result of inorganic ion accumulation in berries with SDI, and potassium would be the obvious target ion to investigate. Considering the close correlation between sugar accumulation and potassium accumulation in berries it would be worthwhile investigating the effects of SDI on K accumulation as a way to prevent increase in juice pH under SDI and to lessen this detrimental impact on wine.

Chapter 6.4 Carbohydrate dynamics

Trunk capacity to store NSC is also dependent on total wood volume and after four years of SDI there were significant (50%) reductions in storage capacity. Recovery in trunk capacity is slower than recovery in concentration of NSC since it requires a growth response to compensate for reduced growth over previous seasons of deficit. If a "year-to-year pulsed-SDI" strategy were used this may reduce the impact on total trunk capacity to store carbohydrate and may lessen the long-term impacts of SDI for a substantial savings in irrigation water.

It would be interesting to follow up the observation of asymmetric trunk development under the more extreme SDI, perhaps indicative of altered root distribution, though this was not so evident in the transect results presented in Chapter 6.5.

Chapter 6.5 Root growth dynamics

Determining dynamics of root growth and density profiles in the field is hampered by methodology, since this is currently labour intensive and time consuming. Methodological advances are urgently needed to more efficiently and accurately determine root behaviour, particularly if many genotypes are to be assessed. Further research is required to understand the remarkable longevity of fine roots of Ramsey rootstock under the SDI conditions of the experiment and whether this pertains more generally to other rootstocks and environments.

Chapter 6.6 Measurement of carbohydrate concentration in grapevine trunk or leaf tissues using near infrared spectroscopy.

This technique could be further developed to be applied on intact tissue rather than freeze dried samples.

Chapter 6.7 Non-destructive measurement of grapevine water potential using near infrared spectroscopy.

This work needs to be developed so that global calibrations can be built across multiple varieties and environments.

Chapter 6.8 Computational water stress indices obtained from thermal image analysis of grapevine canopies.

With the advent of cheaper IR imaging and even the prospect of using smart phones for this purpose (i.e. the *Seek* thermal camera for iPhone) it could be possible to develop an App for iPhone or Android to rapidly measure a vine water stress index.

Chapter 6.9 Automated estimation of leaf area index from grapevine canopies using cover photography, video and computational analysis methods.

This work has been developed to an iPhone app and Android app that is now released on iTunes (VitiCanopy). It should be possible using the same or similar algorithms to develop an app to measure total perennial wood in the dormant vine before or after pruning, which could be used in conjunction with VitiCanopy to determine vine balance.

8.2 Research outcomes related to broader industry practices and priorities for further R&D, extension and policy.

Depending on the cultivar, rootstock and the soil type, it may be possible to lower irrigation rates in warm climate conditions and markedly improve water use efficiency as shown by this study for Chardonnay on Ramsey rootstock. This project has shown that 50% of normal industry rates of irrigation (about 40% of ETc) for Chardonnay on Ramsey on a deep loamy sand had very small, if any, effects on vine physiology and productivity compared to 100%, but with substantial savings in water. The small and largely insignificant effect on productivity is largely attributed to a small reduction in leaf assimilation and no effect on carbohydrate storage or root density. It should be noted that SDI treatments in this trial were fully irrigated until fruit set and early season irrigation could diminish the effects of SDI at the very low rates and more so over an increasing number of seasons of SDI.

When a water-saving strategy is required, it would be recommended not to use reduced depth of irrigation, rather a reduced frequency but to the same depth, since this was less stressful and had less effect on vine productivity. Very low rates of irrigation down to 10% are tolerated over four seasons by Chardonnay on Ramsey, but time to recovery of full production can be three seasons or more after just one season in SDI. However, better management of vine balance may reduce the longer-term impacts of reduced irrigation.

For future R&D the suggested priority would be to continue such long-term SDI trials to prepare the industry for the inevitable increased frequency of water shortage and drought. Future trials should consider variations in vine balance in conjunction with SDI, perhaps with a lesser number of SDI options, for example 20%, 30% and 50% or equivalent fractions of ET. Also it would be important to investigate the impact of early season irrigation with an overall SDI strategy. Another option would be to investigate a "year-to-year pulsed-SDI" strategy alternating between say 20% (or lower) and 50% from year to year, but with due consideration of soil type, extreme weather events and rainfall. Irrigation management guidelines will need to include a sensitivity analysis using water cost, yield impacts, recovery times, grape value and vineyard redevelopment costs. The applicability of the results reported here to other sites will need to be assessed.

Research on how roots respond to deficit irrigation in the field may give better insight on the impacts of different rootstock tolerance to SDI, but there needs to be either a large investment or substantial methodological breakthroughs to allow efficient R&D to occur.

Extension activities should involve discussion of the implications above for reduced irrigation and to demonstrate to growers some of the newer technologies for vine monitoring that have arisen from this project.

Appendix 1: Communication

Journal Publications

Riverland SA – Large scale Irrigation Cutback and Grapevine Recovery, Season 1. Joanne Pech Adam Hall, Marisa Collins, Roberta Debei, Sigfredo Fuentes, Daniel Cozzolino, Steve Tyerman, Michael McCarthy, Ashley Ratcliff, & Robert Strachan *Technical Issue of Grapegrower and Winemaker*

De Bei R, Cozzolino D, Sullivan W, Cynkar W, Fuentes S, Dambergs R, Pech J and Tyerman S (2011). Non Destructive Measurement of Grapevine Water Potential Using Near Infrared Spectroscopy. Australian Journal of Grape and Wine Research. 17(1): 62-71

McCarthy M., Pech J., Ratcliff A., Hall A. and Strachan R. From Drought to flooding rains – how have vines responded? Wine & Viticulture Journal July/August 2011 p 49-52.

Fuentes S., De Bei R., Pech J., Tyerman S. 2012. Computational water stress indices obtained from thermal image analysis of grapevine canopies *Irrigation Science.* DOI: 10.1007/s00271-012-0375-8

Fuentes S, De Bei R, Pozo C, Tyerman SD. 2012. Development of a smartphone application to characterise temporal and spatial canopy architecture and leaf area index for grapevines. Wine and Viticulture Journal. Nov-Dec 2012: 56-60.

Fuentes S, De Bei R, Tyerman SD (2013) New and emerging technologies for the vineyard: the vineyard of the future initiative. Wine and Viticulture Journal 28: 38-45.

Fuentes S, Poblete-Echeverría C, Ortega-Farias S, Tyerman SD, and De Bei R (2014) Automated estimation of leaf area index from grapevine canopies using cover photography, video and computational analysis methods. Australian Journal of Grape and Wine Research 20: 465-473.

Book

Iland P, Dry P, Proffit T and Tyerman S (2011) The Grapevine: from the science to the practice of growing vines for wine, 310 pp, ISBN: 978-0-9581605-5-1

Book Chapter

Webb LB, Clingerleffer PR and Tyerman SD 2010. The genetic envelope of winegrape vines: potential for adaptation to future climate challenges. *In*: Crop Adaptation to Climate Change, Yadav R, Hatfield, Lotze-Campen, ed. Vol. In press. Iowa, USA: John Wiley & Sons, Inc. 25 pp

Published conference proceedings

De Bei R, Fuentes S., Sullivan W., Pech J., Edwards E., McCarthy M., Tyerman S. 2011. Carbohydrate dynamics of Chardonnay grapevine affected by irrigation reduction and recovering regimes. Proceedings 17th International Symposium GiESCO, Aug28-Sept02 Asti-Alba (Italy).

Tyerman SD, De Bei R, Fuentes S, Vandeleur R, Shelden M, Sullivan W, Pech J, Edwards E, Wilkinson C, Cozzolino D, Cynkar W, Dambergs R, Loveys B, McCarthy M (2011) The future of irrigation scheduling:emerging technologies linked to vine physiology. In: Proceedings of the fourteenth Australian Wine Industry Technical Conference, pp. 108–12.

Seminars including to the grape and wine industry*

*Pech J, McCarthy M, De Bei R & Tyerman S (2011) Response & recovery of grapevines to severe irrigation reduction in the SA Riverland, Year Two 2009-10. Annual report to industry collaborators.

*McCarthy, M, (10/5/2011) PIRSA Executive Group Presentation, Qualco, SA, 25min

*McCarthy, M, (30/6/2011) Mudgee Growers Association, Adelaide, SA, 15min

*Pech J M, McCarthy M G, Ayres M, Crocker J, Orlando Wines & Skewes M A, Recovery of Cabernet Sauvignon Grapevines at Langhorne Creek after 3years of severe irrigation cutback. (Presented at: The 14th AWITC, Adelaide, SA, 5-9/7/2010, The Australian Irrigation Conference, Sydney, NSW, 8-11/6/2010, The Barossa Valley Viticulture Technical Group Seminar, Tanunda, SA 12/7/2010)

*Pech J M, Hall A P, Strachan R L, Ratcliff A M, McCarthy M G & Skewes M A (2010) Resuming irrigation after severe reductions – effects on grapevine productivity. (presented at: The 14th AWITC, Adelaide, SA, 5-9/7/2010, The Australian Irrigation Conference, Sydney, NSW, 8-11/6/2010, The Barossa Valley Viticulture Technical Group Seminar, Tanunda, SA 12/7/2010)

*Pech J, McCarthy M, Ratcliff A, Hall A, Strachan R and Skewes M, The value of increasing intra-property metering. The Regional Australian Irrigation Conference, Launceston, TAS, 22-26/8/2011.

*Pech J, Skewes M, Adams T and McCarthy M, Use of an irrigator software program to present research outcomes. The Regional Australian Irrigation Conference, Launceston, TAS, 22-26/8/2011.

*Fuentes S., De Bei R. and Tyerman S. Automated Infrared thermography and leaf area index data acquisition and analysis. Oregon Wine Industry Symposium, Portland Oregon USA. 22nd February 2011

Fuentes S., De Bei R. and Tyerman S. Near infrared (NIR) Spectroscopy used to monitor grapevine water status and carbohydrate content in leaves and trunks. Oregon State University Viticulture and Oenology Research Colloquium 24th February 2011

Fuentes S., De Bei R. and Tyerman S. Night-time response to diurnal anisohydric and isohydric behaviour of grapevines (*Vitis vinifera* L.) 8th – 12th of May 2011. 8th International Workshop on Sap Flow. Volterra, Italy.

Fuentes S., De Bei R. and Tyerman S. State of the art in sensor techniques to monitor water stress in grapevines 16th of May, lecture at the University of Padova.

Fuentes S., De Bei R. and Tyerman S. State of the art in sensor techniques to monitor water stress in grapevines 18th of May. The University of Padova, Conegliano Campus.

*De Bei R., Fuentes S., Tyerman S.: ADDRESSING WINE INDUSTRY CHALLENGES: fine-tuning irrigation using NIR spectroscopy. Wine 2030 Board meeting, May 2012.

*Fuentes S., De Bei R., Tyerman S.D. Wine 2030 Development of a novel canopy architecture-monitoring App for smartphones and tablet computers. Board meeting, August 2012.

De Bei R., S. Fuentes, M. Wirthensohn, D. Cozzolino and S.D. Tyerman. Advances in the use of NIR spectroscopy for water status monitoring in grapevine and almond trees. Presented at the 7th International Symposium on Irrigation of Horticultural Crops. July, 16-20, 2012, Geisenheim, Germany

Fuentes S., De Bei R. and S.D. Tyerman. The Vineyard of The Future. Presented at the 7th International Symposium on Irrigation of Horticultural Crops. July, 16-20, 2012, Geisenheim, Germany.

Fuentes S., De Bei R. and S.D. Tyerman. Use of Infrared Thermography in Viticulture and automated analysis techniques. Seminar presented at The University of La Rioja, Spain. 13th July 2012.

Fuentes S., De Bei R. and S.D. Tyerman. Image analysis techniques applied to canopies, berries, plant tissues and leaves. Presented at the International Conference of Agriculture Engineering. Section: Computer image analysis in Agriculture. 8th – 12th of July 2012.

Fuentes S., De Bei R. and S.D. Tyerman. New tools for monitoring and data analysis for Viticulture within a climate change scenario. Seminar presented at The University of Talca, Chile. 27th June 2012.

Fuentes S., De Bei R., Tyerman S. 2012. Image analysis techniques applied to canopies, berries, plant tissues and leaves. Paper presented for the proceedings of the International Conference of Agriculture Engineering. Section: Computer image analysis in Agriculture. 8th – 12th of July 2012.

The following papers were accepted as either oral or posters presentations at the 9th International Conference on Grapevine Physiology and Biotechnology to be held in La Serena, Chile, 21-26 April, 2013.

1. Fuentes S., De Bei R. and Tyerman S. Using smartphones and tablet PCs for canopy architecture assessment to upscale physiological parameters: LAICanopy© App.
2. Poblete-Echeverria C., Fuentes S., De Bei R., Diago MP., Ortega-Farias S. and Tardaguila J. Infrared Thermal Images Of Grapevines: From Manual to Complete Automated Analysis.
3. Fuentes S., De Bei R., Wilkinson K., Ristic R., and Tyerman S. Using Infrared Thermal Images To Detect Smoke Contamination For Different Grapevine Varieties.
4. Diago MP., De Bei R., Millan B., Poni S., Gatti M., Bernizzoni F., Tyerman S. and Tardaguila J. Assessment of grapevine water status by ground-based hyperspectral imaging.
5. Fuentes S., De Bei R. and Tyerman S. Night-time sap flow behaviour for grapevines (*Vitis vinifera* L.) under drought and recovery treatments in Australia
6. Tyerman S.D Regulation of hydraulic conductivity by aquaporins in roots and leaves

*The PI reported data from the trial at two workshops at the 15th AWITC: **Workshop 10** (New and emerging technologies for your vineyard): *The use of Near Infrared Spectroscopy for vine water status and carbohydrate monitoring.* **Workshop 21** (Practical applications of rapid analytical measurement tools for grapes and wine): *Measuring leaf water potential: fine-tuning irrigation using NIR spectroscopy*

Appendix 2: Intellectual Property

All IP resulting from this project has been, or will be published, and is in the public domain. A list of publications arising from this project is attached.

Appendix 3: References

References are provided at the end of each Results and Discussion section but are also reproduced here.

Bahar, E., A. Carbonneau, and I. Korkutal (2011) The effect of extreme water stress on leaf drying limits and possibilities of recovering in three grapevine (Vitis vinifera L.) cultivars. African Journal of Agricultural Research 6, 1151-1160.

Bauerle, T.L., D.R. Smart, W.L. Bauerle, C. Stockert, and D.M. Eissenstat (2008) Root foraging in response to heterogeneous soil moisture in two grapevines that differ in potential growth rate. New Phytologist 179, 857-866. doi: 10.1111/j.1469-8137.2008.02489.x.

Bennett, J., P. Jarvis, G.L. Creasy, and M.C.T. Trought (2005) Influence of defoliation on overwintering carbohydrate reserves, return bloom, and yield of mature Chardonnay grapevines. American Journal of Enology and Viticulture 56, 386-393.

Bonada, M., V. Sadras, M. Moran, and S. Fuentes (2013) Elevated temperature and water stress accelerate mesocarp cell death and shrivelling, and decouple sensory traits in Shiraz berries. Irrigation Science 31, 1317-1331. doi: 10.1007/s00271-013-0407-z.

Burton, A.J., K.S. Pregitzer, G.P. Zogg, and D.R. Zak (1998) Drought reduces root respiration in sugar maple forests. Ecological Applications 8, 771-778. doi: 10.2307/2641265.

Chaves, M.M., J.S. Pereira, J. Maroco, M.L. Rodrigues, C.P.P. Ricardo, M.L. Osorio, I. Carvalho, T. Faria, and C. Pinheiro (2002) How plants cope with water stress in the field. Photosynthesis and growth. Annals of Botany 89, 907-916. doi: 10.1093/aob/mcf105.

Chaves, M.M., O. Zarrouk, R. Francisco, J.M. Costa, T. Santos, A.P. Regalado, M.L. Rodrigues, and C.M. Lopes (2010) Grapevine under deficit irrigation: hints from physiological and molecular data. Annals of Botany 105, 661-676. doi: 10.1093/aob/mcq030.

Chaves, M.M., T.P. Santos, C.R. Souza, M.F. Ortuno, M.L. Rodrigues, C.M. Lopes, J.P. Maroco, and J.S. Pereira (2007) Deficit irrigation in grapevine improves water-use efficiency while controlling vigour and production quality. Annals of Applied Biology 150, 237-252. doi: 10.1111/j.1744-7348.2006.00123.x.

Cifre, J., J. Bota, J.M. Escalona, H. Medrano, and J. Flexas (2005) Physiological tools for irrigation scheduling in grapevine (Vitis vinifera L.): An open gate to improve water-use efficiency? Agriculture, Ecosystems & Environment 106, 159-170.

Comas, L.H., D.M. Eissenstat, and A.N. Lakso (2000) Assessing root death and root system dynamics in a study of grape canopy pruning. New Phytologist 147, 171-178. doi: 10.1046/j.1469-8137.2000.00679.x.

Comas, L.H., L.J. Anderson, R.M. Dunst, A.N. Lakso, and D.M. Eissenstat (2005) Canopy and environmental control of root dynamics in a long-term study of Concord grape. New Phytologist 167, 829-840. doi: 10.1111/j.1469-8137.2005.01456.x.

Comas, L.H., T.L. Bauerle, and D.M. Eissenstat (2010) Biological and environmental factors controlling root dynamics and function: effects of root ageing and soil moisture. Australian Journal of Grape and Wine Research 16, 131-137. doi: 10.1111/j.1755-0238.2009.00078.x.

Cozzolino, D. (2009) Near Infrared Spectroscopy in Natural Products Analysis. Planta Medica 75, 746-756. doi: 10.1055/s-0028-1112220.

Cozzolino, D., L. Liu, W.U. Cynkar, R.G. Dambergs, L. Janik, C.B. Colby, and M. Gishen (2007) Effect of temperature variation on the visible and near infrared spectra of wine and the consequences on the partial least square calibrations developed to measure chemical composition. Analytica Chimica Acta 588, 224-230. doi: 10.1016/j.aca.2007.01.079.

Cozzolino, D., M.B. Esler, R.G. Dambergs, W.U. Cynkar, D.R. Boehm, I.L. Francis, and M. Gishen (2004) Prediction of colour and pH in grapes using a diode array spectrophotometer (400-1100 nm). Journal of near Infrared Spectroscopy 12, 105-111.
Cozzolino, D., R.G. Dambergs, L. Janik, W.U. Cynkar, and M. Gishen (2006) Analysis of grapes and wine by near infrared spectroscopy. Journal of near Infrared Spectroscopy 14, 279-289.
Curran, P.J. (1989) Remote-sensing of foliar chemistry. Remote Sensing of Environment 30, 271-278. doi: 10.1016/0034-4257(89)90069-2.
Curran, P.J., J.L. Dungan, B.A. Macler, S.E. Plummer, and D.L. Peterson (1992) Reflectance spectroscopy of fresh whole leaves for the estimation of chemical concentration. Remote Sensing of Environment 39, 153-166. doi: 10.1016/0034-4257(92)90133-5.
Dambergs, R.G., D. Cozzolino, W.U. Cynkar, L. Janik, and M. Gishen (2006) The determination of red grape quality parameters using the LOCAL algorithm. Journal of near Infrared Spectroscopy 14, 71-79.
Dayer, S., J.A. Prieto, E. Galat, and J.P. Pena (2013) Carbohydrate reserve status of Malbec grapevines after several years of regulated deficit irrigation and crop load regulation. Australian Journal of Grape and Wine Research 19, 422-430. doi: 10.1111/ajgw.12044.
De Bei, R., D. Cozzolino, W. Sullivan, W. Cynkar, S. Fuentes, R. Dambergs, J. Pech, and S. Tyerman (2011) Non-destructive measurement of grapevine water potential using near infrared spectroscopy. Australian Journal of Grape and Wine Research 17, 62-71. doi: 10.1111/j.1755-0238.2010.00117.x.
Dreywood, R. (1946) Qualitative test for carbohydrate material. Industrial and Engineering Chemistry-Analytical Edition 18, 499-499. doi: 10.1021/i560156a015.
Dry, P. (2013) Can the production of flow alcohol wines start in the vineyard? Wine and Viticulture Journal 28, 40-43.
Edwards, E.J. and P.R. Clingeleffer (2013) Interseasonal effects of regulated deficit irrigation on growth, yield, water use, berry composition and wine attributes of Cabernet Sauvignon grapevines. Australian Journal of Grape and Wine Research 19, 261-276. doi: 10.1111/ajgw.12027.
Edwards, E.J., A.F. Downie, and P.R. Clingeleffer (2011) A Simple Microplate Assay to Quantify Nonstructural Carbohydrates of Grapevine Tissues. American Journal of Enology and Viticulture 62, 133-137. doi: 10.5344/ajev.2010.10051.
Eissenstat, D.M., T.L. Bauerle, L.H. Comas, A.N. Lakso, D. Neilsen, G.H. Neilsen, and D.R. Smart (2006) Seasonal patterns of root growth in relation to shoot phenology in grape and apple. In: Proceedings of the Vth International Symposium on Mineral Nutrition of Fruit Plants, Ed. J.B. Retamales pp. 21-26.
Elvidge, C.D. (1990) Visible and near-infrared reflectance characteristics of dry plant materials. International Journal of Remote Sensing 11, 1775-1795.
Esteban, M.A., M.J. Villanueva, and J.R. Lissarrague (1999) Effect of irrigation on changes in berry composition of Tempranillo during maturation. Sugars, organic acids, and mineral elements. American Journal of Enology and Viticulture 50, 418-434.
Etchebarne, F., H. Ojeda, and J.J. Hunter (2010) Leaf:Fruit Ratio and Vine Water Status Effects on Grenache Noir (Vitis vinifera L.) Berry Composition: Water, Sugar, Organic Acids and Cations. South African Journal of Enology and Viticulture 31, 106-115.
Flexas, J., J. Galmes, A. Galle, J. Gulias, A. Pou, M. Ribas-Carbo, M. Tomas, and H. Medrano (2010) Improving water use efficiency in grapevines: potential physiological targets for biotechnological improvement. Australian Journal of Grape and Wine Research 16, 106-121. doi: 10.1111/j.1755-0238.2009.00057.x.
Gishen, M., R.G. Dambergs, and D. Cozzolino (2005) Grape and wine analysis - enhancing the power of spectroscopy with chemometrics. A review of some applications in the

Australian wine industry. Australian Journal of Grape and Wine Research 11, 296-305. doi: 10.1111/j.1755-0238.2005.tb00029.x.
Greenspan, M.D., H.R. Schultz, and M.A. Matthews (1996) Field evaluation of water transport in grape berries during water deficits. Physiologia Plantarum 97, 55-62. doi: 10.1034/j.1399-3054.1996.970109.x.
Holzapfel, B.P. and J.P. Smith (2012) Developmental Stage and Climatic Factors Impact More on Carbohydrate Reserve Dynamics of Shiraz than Cultural Practice. American Journal of Enology and Viticulture 63, 333-342. doi: 10.5344/ajev.2012.11071.
Holzapfel, B.P., J.P. Smith, R.M. Mandel, and M. Keller (2006) Manipulating the postharvest period and its impact on vine productivity of Semillon grapevines. American Journal of Enology and Viticulture 57, 148-157.
Holzapfel, B.P., J.P. Smith, S.K. Field, and W.J. Hardie (2010) Dynamics of carbohydrate reserves in cultivated grapevines. Horticultural Reviews 37, 143-211.
Huglin, P. and C. Schneider (1998) Biology and ecology of the grapevine.
Intrigliolo, D.S. and J.R. Castel (2008) Effects of irrigation on the performance of grapevine cv. Tempranillo in Requena, Spain. American Journal of Enology and Viticulture 59, 30-38.
Intrigliolo, D.S. and J.R. Castel (2008) Effects of irrigation on the performance of grapevine cv. Tempranillo in Requena, Spain. American Journal of Enology and Viticulture 59, 30-38.
Intrigliolo, D.S., D. Perez, D. Risco, A. Yeves, and J.R. Castel (2012) Yield components and grape composition responses to seasonal water deficits in Tempranillo grapevines. Irrigation Science 30, 339-349. doi: 10.1007/s00271-012-0354-0.
Kato, Y. and M. Okami (2011) Root morphology, hydraulic conductivity and plant water relations of high-yielding rice grown under aerobic conditions. Annals of Botany 108, 575-583. doi: 10.1093/aob/mcr184.
Keller, M., R.P. Smithyman, and L.J. Mills (2008) Interactive effects of deficit irrigation and crop load on Cabernet Sauvignon in an arid climate. American Journal of Enology and Viticulture 59, 221-234.
Kidman, C.M., S.O. Mantilla, P.R. Dry, M.G. Mccarthy, and C. Collins (2014) Effect of Water Stress on the Reproductive Performance of Shiraz (Vitis vinifera L.) Grafted to Rootstocks. American Journal of Enology and Viticulture 65, 96-108. doi: 10.5344/ajev.2013.13069.
Koblet, W., M.C. Candolfivasconcelos, W. Zweifel, and G.S. Howell (1994) Influence of leaf removal, rootstock, and training system on yield and fruit composition of pinot-noir grapevines. American Journal of Enology and Viticulture 45, 181-187.
Lebon, G., G. Wojnarowiez, B. Holzapfel, F. Fontaine, N. Vaillant-Gaveau, and C. Clément (2008) Sugars and flowering in the grapevine (Vitis vinifera L.). Journal of Experimental Botany 59, 2565-2578. doi: 10.1093/jxb/ern135.
Lehnart, R., H. Michel, O. Loehnertz, and A. Linsenmeier (2008) Root dynamics and pattern of 'Riesling' on 5C rootstock using minirhizotrons. Vitis 47, 197-200.
Lopez, M.-I., M.-T. Sanchez, A. Diaz, P. Ramirez, and J. Morales (2007) Influence of a deficit irrigation regime during ripening on berry composition in grapevines (Vitis vinifera L.) grown in semi-arid areas. International Journal of Food Sciences and Nutrition 58, 491-507. doi: 10.1080/09637480701311801.
Lopez, M.I., M.T. Sanchez, A. Diaz, P. Ramirez, and J. Morales (2007) Influence of a deficit irrigation regime during ripening on berry composition in grapevines (Vitis vinifera L.) grown in semi-arid areas. International Journal of Food Sciences and Nutrition 58, 491-507. doi: 10.1080/09637480701311801.
Mainiero, R. and M. Kazda (2006) Depth-related fine root dynamics of Fagus sylvatica during exceptional drought. Forest Ecology and Management 237, 135-142. doi: 10.1016/j.foreco.2006.09.034.

Mapfumo, E., D. Aspinall, and T.W. Hancock (1994) Growth and development of roots of grapevine (vitis-vinifera l) in relation to water-uptake from soil. Annals of Botany 74, 75-85. doi: 10.1006/anbo.1994.1096.

Martorell, S., A. Diaz-Espejo, M. Tomas, A. Pou, H. El Aou-Ouad, J.M. Escalona, J. Vadell, M. Ribas-Carbo, J. Flexas, and H. Medrano (2015) Differences in water-use-efficiency between two Vitis vinifera cultivars (Grenache and Tempranillo) explained by the combined response of stomata to hydraulic and chemical signals during water stress. Agricultural Water Management 156, 1-9. doi: 10.1016/j.agwat.2015.03.011.

Matthews, M.A. and M.M. Anderson (1989) Reproductive development in grape (Vitis-vinifera l) - responses to seasonal water deficits. American Journal of Enology and Viticulture 40, 52-59.

Matthews, M.A. and M.M. Anderson (1989) Reproductive development in grape (Vitis-vinifera l) - responses to seasonal water deficits. American Journal of Enology and Viticulture 40, 52-59.

Mccarthy, M.G. (1997) The effect of transient water deficit on berry development of cv. Shiraz (Vitis vinifera L.). Australian Journal of Grape and Wine Research 3, 102-108.

Medrano, H., M. Tomas, S. Martorell, J. Flexas, E. Hernandez, J. Rossello, A. Pou, J.M. Escalona, and J. Bota (2015) From leaf to whole-plant water use efficiency (WUE) in complex canopies: Limitations of leaf WUE as a selection target. Crop Journal 3, 220-228. doi: 10.1016/j.cj.2015.04.002.

Murray, M. and J. Kurtz (1993) Near-infrared absorptions of monomethylhydrazine. Journal of Quantitative Spectroscopy & Radiative Transfer 50, 585-590. doi: 10.1016/0022-4073(93)90025-d.

Nagarajah, S. (1987) Effects of soil texture on the rooting patterns of thompson seedless vines on own roots and on ramsey rootstock in irrigated vineyards. American Journal of Enology and Viticulture 38, 54-59.

Naor, A., Y. Gal, and B. Bravdo (1997) Crop load affects assimilation rate, stomatal conductance, stem water potential and water relations of field-grown Sauvignon blanc grapevines. J. Exp. Bot. 48, 1675-1680. doi: 10.1093/jxb/48.9.1675.

Pastenes, C., L. Villalobos, N. Rios, F. Reyes, R. Turgeon, and N. Franck (2014) Carbon partitioning to berries in water stressed grapevines: The role of active transport in leaves and fruits. Environmental and Experimental Botany 107, 154-166. doi: 10.1016/j.envexpbot.2014.06.009.

Poni, S., M. Galbignani, E. Magnanini, F. Bernizzoni, A. Vercesi, M. Gatti, and M.C. Merli (2014) The isohydric cv. Montepulciano (Vitis vinifera L.) does not improve its whole-plant water use efficiency when subjected to pre-veraison water stress. Scientia Horticulturae 179, 103-111. doi: 10.1016/j.scienta.2014.09.021.

Pou, A., H. Medrano, M. Tomas, S. Martorell, M. Ribas-Carbo, and J. Flexas (2012) Anisohydric behaviour in grapevines results in better performance under moderate water stress and recovery than isohydric behaviour. Plant and Soil 359, 335-349. doi: 10.1007/s11104-012-1206-7.

Rebucci, B., S. Poni, C. Intrieri, E. Magnanini, and A.N. Lakso (1997) Effects of manipulated grape berry transpiration on post-veraison sugar accumulation. Australian Journal of Grape and Wine Research 3, 57-65. doi: 10.1111/j.1755-0238.1997.tb00116.x.

Reynolds, A.G., W.D. Lowrey, L. Tomek, J. Hakimi, and C. De Savigny (2007) Influence of irrigation on vine performance, fruit composition, and wine quality of Chardonnay in a cool, humid climate. American Journal of Enology and Viticulture 58, 217-228.

Richardson, A.D., G.P. Berlyn, and S.P. Duigan (2003) Reflectance of Alaskan black spruce and white spruce foliage in relation to elevation and latitude. Tree Physiology 23, 537-544.

Romero, P., J. Ignacio Fernandez-Fernandez, and A. Martinez-Cutillas (2010) Physiological Thresholds for Efficient Regulated Deficit-Irrigation Management in Winegrapes Grown under Semiarid Conditions. American Journal of Enology and Viticulture 61, 300-312.
Sadras, V.O. (2009) Does partial root-zone drying improve irrigation water productivity in the field? A meta-analysis. Irrigation Science 27, 183-190. doi: 10.1007/s00271-008-0141-0.
Sadras, V.O., M. Collins, and C.J. Soar (2008) Modelling variety-dependent dynamics of soluble solids and water in berries of Vitis vinifera. Australian Journal of Grape and Wine Research 14, 250-259. doi: 10.1111/j.1755-0238.2008.00025.x.
Schmidtke, L.M., J.P. Smith, M.C. Muller, and B.P. Holzapfel (2012) Rapid monitoring of grapevine reserves using ATR-FT-IR and chemometrics. Analytica Chimica Acta 732, 16-25. doi: 10.1016/j.aca.2011.10.055.
Scholefield, P.B., T.F. Neales, and P. May (1978) Carbon balance of sultana vine (vitis-vinifera l) and effects of autumn defoliation by harvest-pruning. Australian Journal of Plant Physiology 5, 561-570.
Schultz, H.R. and M.A. Matthews (1988) Vegetative growth distribution during water deficits in vitis-vinifera L. Australian Journal of Plant Physiology 15, 641-656.
Shellie, K.C. (2014) Water Productivity, Yield, and Berry Composition in Sustained versus Regulated Deficit Irrigation of Merlot Grapevines. American Journal of Enology and Viticulture 65, 197-205. doi: 10.5344/ajev.2014.13112.
Sibille, I., H. Ojeda, J. Prieto, S. Maldonado, J.-N. Lacapere, and A. Carbonneau (2007) Relation between the values of three pressure chamber modalities (midday leaf, midday stem and predawn water potential) of 4 grapevine cultivars in drought situation of the southern of France. Applications for the irrigation control. In Proceedings of XVth Conference GESCO. Porec, Croatia. p. 685-695.
Smith, J.P. and B.P. Holzapfel (2009) Cumulative Responses of Semillon Grapevines to Late Season Perturbation of Carbohydrate Reserve Status. American Journal of Enology and Viticulture 60, 461-470.
Smyth, H.E., D. Cozzolino, W.U. Cynkar, R.G. Dambergs, M. Sefton, and M. Gishen (2008) Near infrared spectroscopy as a rapid tool to measure volatile aroma compounds in Riesling wine: possibilities and limits. Analytical and Bioanalytical Chemistry 390, 1911-1916. doi: 10.1007/s00216-008-1940-0.
Soar, C.J. and B.R. Loveys (2007) The effect of changing patterns in soil-moisture availability on grapevine root distribution, and viticultural implications for converting full-cover irrigation into a point-source irrigation system. Australian Journal of Grape and Wine Research 13, 2-13. doi: 10.1111/j.1755-0238.2007.tb00066.x.
Stevens, R.M. and D.L. Partington (2013) Grapevine recovery from saline irrigation was incomplete after four seasons of non-saline irrigation. Agricultural Water Management 122, 39-45. doi: 10.1016/j.agwat.2013.02.003.
Stevens, R.M., J.M. Pech, M.R. Gibberd, R.R. Walker, J.A. Jones, J. Taylor, and P.R. Nicholas (2008) Effect of reduced irrigation on growth, yield, ripening rates and water relations of Chardonnay vines grafted to five rootstocks. Australian Journal of Grape and Wine Research 14, 177-190. doi: 10.1111/j.1755-0238.2008.00018.x.
Tarara, J.M., J.E.P. Pena, M. Keller, R.P. Schreiner, and R.P. Smithyman (2011) Net carbon exchange in grapevine canopies responds rapidly to timing and extent of regulated deficit irrigation. Functional Plant Biology 38, 386-400. doi: 10.1071/fp10221.
Tilbrook, J. and S.D. Tyerman (2008) Cell death in grape berries: varietal differences linked to xylem pressure and berry weight loss. Functional Plant Biology 35, 173-184. doi: 10.1071/fp07278.

Tilbrook, J. and S.D. Tyerman (2009) Hydraulic connection of grape berries to the vine: varietal differences in water conductance into and out of berries, and potential for backflow. Functional Plant Biology 36, 541-550. doi: 10.1071/fp09019.

Tomas, M., H. Medrano, E. Brugnoli, J.M. Escalona, S. Martorell, A. Pou, M. Ribas-Carbo, and J. Flexas (2014) Variability of mesophyll conductance in grapevine cultivars under water stress conditions in relation to leaf anatomy and water use efficiency. Australian Journal of Grape and Wine Research 20, 272-280. doi: 10.1111/ajgw.12069.

Tombesi, S., A. Nardini, T. Frioni, M. Soccolini, C. Zadra, D. Farinelli, S. Poni, and A. Palliotti (2015) Stomatal closure is induced by hydraulic signals and maintained by ABA in drought-stressed grapevine. Scientific Reports 5, 12. doi: 10.1038/srep12449.

Tregoat, O., Van Leeuwen C., Choné X., and G.J. P. (2002) Etude du régime hydrique et de la nutrition azotée de la vigne per des indicateurs physiologiques. Influence sur le comportement de la vigne et la maturation du raisin (Vitis vinifera L. cv. Merlot, 2000, Bordeaux). Journal International des Sciences de la Vigne et du Vin 36, 133-142.

Trigo-Cordoba, E., Y. Bouzas-Cid, I. Orriols-Fernandez, and J.M. Miras-Avalos (2015) Effects of deficit irrigation on the performance of grapevine (Vitis vinifera L.) cv. 'Godello' and 'Treixadura' in Ribeiro, NW Spain. Agricultural Water Management 161, 20-30. doi: 10.1016/j.agwat.2015.07.011.

Tsuda, M. and M.T. Tyree (2000) Plant hydraulic conductance measured by the high pressure flow meter in crop plants. Journal of Experimental Botany 51, 823-828. doi: 10.1093/jexbot/51.345.823.

Vandeleur, R.K., G. Mayo, M.C. Shelden, M. Gilliham, B.N. Kaiser, and S.D. Tyerman (2009) The Role of Plasma Membrane Intrinsic Protein Aquaporins in Water Transport through Roots: Diurnal and Drought Stress Responses Reveal Different Strategies between Isohydric and Anisohydric Cultivars of Grapevine. Plant Physiology 149, 445-460. doi: 10.1104/pp.108.128645.

Williams, L.E. (1996) Grape. In: Photoassimilate Distribution in Plants and Crops: Source-Sink Relationships, Eds. A.A. Schaffer and E. Zamski (Marcel Dekker: New York) pp. 851–883

Williams, L.E. (2012) Effects of applied water amounts at various fractions of evapotranspiration (ETc) on leaf gas exchange of Thompson Seedless grapevines. Australian Journal of Grape and Wine Research 18, 100-108. doi: 10.1111/j.1755-0238.2011.00176.x.

Williams, L.E. (2014) Effect of Applied Water Amounts at Various Fractions of Evapotranspiration on Productivity and Water Footprint of Chardonnay Grapevines. American Journal of Enology and Viticulture 65, 215-221. doi: 10.5344/ajev.2014.12105.

Williams, L.E. and F.J. Araujo (2002) Correlations among predawn leaf, midday leaf, and midday stem water potential and their correlations with other measures of soil and plant water status in Vitis vinifera. Journal of the American Society for Horticultural Science 127, 448-454.

Williams, L.E. and T.J. Trout (2005) Relationships among vine- and soil-based measures of water status in a Thompson Seedless vineyard in response to high-frequency drip irrigation. American Journal of Enology and Viticulture 56, 357-366.

Yang, Y.S., Y. Hori, and R. Ogata (1980) Studies on re translocation of accumulated assimilates in grapevines vitis-labruscana cultivar delaware 2. re translocation of assimilates accumulated during the previous growing season. Tohoku Journal of Agricultural Research 31, 109-119.

Appendix 4: Staff

Professor Stephen Tyerman (PI, UA)
Dr Sigfredo Fuentes (CI, UA, now University of Melbourne)
Dr Everard Edwards (CI, CSIRO)
Dr Michael McCarthy (CI, SARDI)
Dr Daniel Cozzolino (CI, AWRI, now Central Queensland University)
Dr Roberta De Bei (Postdoctoral employed on this project, UA)
Ms Joanne Pech (Research Assistant employed on this project, SARDI)
Ms Wendy Sullivan (Research Assistant employed on this project, UA)

Appendix 5: Acknowledgements

The four organisations, involved in this research project, UoA, CSIRO, SARDI, AWRI, are all part of the Wine Innovation Cluster (www.wineinnovationcluster.com). This project was undertaken on a collaborative basis by the parties.

The PI and CIs would like to thank Yalumba Nurseries, particularly Ashley Ratcliff, Adam Hall and Fred Strachan who co-designed, converted and managed the trial site and Chris Dyson for trial design.

Appendix 6: End of project financial statement

Statement provided separately